

UNIVERSIDADE DE LISBOA
FACULDADE DE CIÊNCIAS
DEPARTAMENTO DE QUÍMICA E BIOQUÍMICA



***p*-Cymene Based Ruthenium Complexes as Catalysts**

Joel David Avelino Fonseca

MESTRADO EM QUÍMICA TECNOLÓGICA
Especialização em Química Tecnológica e Qualidade

2011

UNIVERSIDADE DE LISBOA
FACULDADE DE CIÊNCIAS
DEPARTAMENTO DE QUÍMICA E BIOQUÍMICA



***p*-Cymene Based Ruthenium Complexes as Catalysts**

Joel David Avelino Fonseca

MESTRADO EM QUÍMICA TECNOLÓGICA
Especialização em Química Tecnológica e Qualidade

Dissertação de mestrado orientada pela
Professora Dra. Maria Helena Garcia

2011

This project took place in the School of Chemistry of the University of Leeds, United Kingdom, under the scope of Erasmus Placements. It was co-supervised by Dr. Patrick C. McGowan and Dr. John A. Blacker



UNIVERSITY OF LEEDS

Acknowledgements

First, I would like to express my deepest gratitude to Professor Patrick C. McGowan for giving me the opportunity of doing my master placement in his work group, also for his mentorship, guidance, insightful discussions, continuous support, patience and encouragements during ten months at the University of Leeds.

Then I would like to thank Professor John A. Blacker for his valuable discussions and suggestions during my research.

My special thanks to Professor Maria H. Garcia for being so supportive in the decision of going abroad, for making this placement possible, for her mentorship, guidance and carefully reviewing the dissertation.

I would like to thank the European Commission for providing financial support, namely by giving me an ERASMUS Placement scholarship.

I am thankful to all the colleagues with whom I have shared the laboratory, namely from the McGowan and Halcrow groups, who have made my work days so pleasant. Special thanks to Andrea for her guidance and patience, to Steph for being meticulous and giving valuable advices, to David for being funny and helpful all the time and acquiring a valuable X-ray structure, to Rufeida for providing a good laugh everyday and being so supportive. Big thanks also to Chris, which I could not forget, for the valuable spectra analysis, for the insightful discussions, for being there whenever I needed. Thank you also to Ben, Rianne, Jonathan, Sara, Laura, Lawrence, Adi, Tom, Aida, Andrew and Warka.

To all the friends that I have made in Leeds I want to say a big thank you because they made this period very enjoyable.

Finally I want to thank my family for their support and encouragement throughout my study and my daily life.

Joel Fonseca

Abstract

p-Cymene based ruthenium complexes were employed in the alkylation of *t*-butylamine with phenethyl alcohol by redox neutral alkylation and in the reduction of acetophenone and benzaldehyde by transfer hydrogenation. A range of *in situ* generated catalysts formed by $[\text{RuX}_2(\textit{p}\text{-cymene})]_2$ dimers (X=Cl or I) with dppf, DPEPhos, dppf or $\text{P}(\textit{i}\text{-Bu})_3$ and a range of *p*-cymene ruthenium monomers, namely $[\text{RuCl}(\text{dppf})(\textit{p}\text{-cymene})]\text{SbF}_6$, $[\text{RuI}(\text{dppf})(\textit{p}\text{-cymene})]\text{SbF}_6$, $[\text{RuCl}(\text{dppf})(\textit{p}\text{-cymene})]\text{BF}_4$, $[\text{RuCl}(\text{dppf})(\textit{p}\text{-cymene})]\text{Cl}$, $[\text{RuI}(\text{P}(\textit{n}\text{-Bu})_3)_2(\textit{p}\text{-cymene})]\text{SbF}_6$, $[\text{RuCl}(\text{P}(\textit{i}\text{-Bu})_3)_2(\textit{p}\text{-cymene})]\text{SbF}_6$, $[\text{RuCl}_2(\text{P}(\textit{n}\text{-Bu})_3)_2(\textit{p}\text{-cymene})]$, $[\text{RuCl}(\text{P}(\text{CH}_3)_3)_2(\textit{p}\text{-cymene})]\text{SbF}_6$ have been employed in these reactions. These monomers have been synthesised and characterized in this project and only $[\text{RuCl}_2(\text{P}(\textit{n}\text{-Bu})_3)_2(\textit{p}\text{-cymene})]$ has been already reported in the literature.

Results were compared in terms of conversions and the best ones for the redox neutral alkylation were with the *in situ* generated catalyst formed by $[\text{RuI}_2(\textit{p}\text{-cymene})]$ and DPEPhos, giving 96% conversion for a catalyst/substrate ratio of 20 and with $[\text{RuI}(\text{dppf})(\textit{p}\text{-cymene})]\text{SbF}_6$ which gave 85% conversion for a catalyst/substrate ratio of 40. These reactions have been run out in the open air without degassing or inert gas protection throughout which is not the typical approach found in the literature and that can be very appealing in the industrial point of view. The different halides incorporated in these complexes have been proved to have different effects in the catalytic activity, with iodine usually leading to more active catalysts. Some results and experiments that were performed allowed drawing some conclusions about the mechanism.

For the reduction of acetophenone and benzaldehyde by transfer hydrogenation it has been demonstrated that the dimers, the dimer-phosphine pairs and the ruthenium monomers mentioned before are not the most suitable pre-catalysts for these reactions. Overall, conversions up to 73% were obtained which lag far behind the 100% reported in the literature for several other complexes. Some conclusions were drawn about the mechanism and two catalytic cycles were proposed.

The brand new dimer $[\text{Ru}_2\text{Cl}_3(\text{DPEPhos})_2(\text{CH}_3\text{CN})_2]\text{SbF}_6$ has been serendipitously synthesised and has shown it forms catalytically active species in both the alkylation of *t*-butylamine and reduction of acetophenone giving moderate conversions.

Keywords: transfer hydrogenation, ruthenium, *p*-cymene, N-alkylation, catalyst.

Resumo

Neste projecto foram sintetizados complexos de ruténio e *p*-cimeno que foram posteriormente avaliados do ponto de vista catalítico em reacções de transferência de hidrogénio. Os complexos de ruténio e *p*-cimeno têm demonstrado ser catalisadores/pré-catalisadores eficientes em várias reacções envolvendo compostos orgânicos e foi inicialmente sugerido para este projecto pela empresa biofarmacêutica *Astra Zeneca* o estudo da actividade catalítica do dímero $[\text{RuCl}_2(\textit{p}\text{-cimeno})]_2$ na presença das fosfinas DPEPhos, dppf e $\text{P}(\textit{i}\text{-Bu})_3$ em reacções de transferência de hidrogénio. Esta empresa verificou que este dímero é extremamente activo na alquilação de morfolina com álcool benzílico na presença das fosfinas referidas (conversões acima de 97%).

No que respeita aos complexos sintetizados, levaram-se a cabo as sínteses dos dímeros de cloro e iodo de fórmula molecular $[\text{RuX}_2(\textit{p}\text{-cimeno})]_2$ em que X = Cl ou I e ainda de monómeros utilizando os dímeros referidos como compostos de partida. A síntese do dímero de bromo foi também tentada mas este revelou-se muito difícil de obter e portanto não foi utilizado em sínteses posteriores nem nas reacções catalíticas. Para obter os monómeros foram ainda utilizadas fosfinas mono ou bidentadas, nomeadamente dppf, DPEPhos, dppf, $\text{P}(\textit{i}\text{-Bu})_3$, $\text{P}(\textit{n}\text{-Bu})_3$, $\text{P}(\text{CH}_3)_3$ ou PhPCl_2 que originaram os seguintes complexos neutros ou mono catiónicos: $[\text{RuCl}(\text{dppf})(\textit{p}\text{-cimeno})]\text{SbF}_6$, $[\text{RuI}(\text{dppf})(\textit{p}\text{-cimeno})]\text{SbF}_6$, $[\text{RuCl}(\text{dppf})(\textit{p}\text{-cimeno})]\text{BF}_4$, $[\text{RuCl}(\text{dppf})(\textit{p}\text{-cimeno})]\text{Cl}$, $[\text{RuCl}(\text{P}(\textit{n}\text{-Bu})_3)_2(\textit{p}\text{-cimeno})]\text{SbF}_6$, $[\text{RuI}(\text{P}(\textit{n}\text{-Bu})_3)_2(\textit{p}\text{-cimeno})]\text{SbF}_6$, $[\text{RuCl}(\text{P}(\textit{i}\text{-Bu})_3)_2(\textit{p}\text{-cimeno})]\text{SbF}_6$, $[\text{RuCl}_2\text{P}(\textit{n}\text{-Bu})_3(\textit{p}\text{-cimeno})]$, $[\text{RuCl}_2\text{P}(\textit{i}\text{-Bu})_3(\textit{p}\text{-cimeno})]$, $[\text{RuCl}(\text{P}(\text{CH}_3)_3)_2(\textit{p}\text{-cymene})]\text{SbF}_6$ e $[\text{RuCl}_2\text{PPh}(\text{OCH}_3)_2(\textit{p}\text{-cymene})]$. Entretanto foi ainda sintetizado, por acaso, o dímero $[\text{Ru}_2\text{Cl}_3(\text{DPEPhos})_2(\text{CH}_3\text{CN})_2]\text{SbF}_6$ numa das tentativas de obter o monómero $[\text{RuCl}(\text{DPEPhos})(\textit{p}\text{-cymene})]\text{SbF}_6$. Estes compostos foram caracterizados por ^1H , ^{13}C e ^{31}P NMR, espectrometria de massa e análise elementar. Entre eles apenas os complexos neutros $[\text{RuCl}_2\text{P}(\textit{n}\text{-Bu})_3(\textit{p}\text{-cimeno})]$ e $[\text{RuCl}_2\text{P}(\textit{i}\text{-Bu})_3(\textit{p}\text{-cimeno})]$ já tinham sido referenciados na literatura.

As reacções aos quais foram submetidos os complexos sintetizados envolvem todas elas, como foi dito, transferência de hidrogénio. Este tipo de reacções envolve normalmente a redução de cetonas ou iminas e a oxidação de álcoois ou aminas em que um catalisador transfere hidrogénio entre o substrato e o dador ou aceitador de hidrogénio, respectivamente. As reacções de transferência de hidrogénio que aqui foram testadas foram

a alquilação da *t*-butilamina com álcool fenilético designada formalmente por “redox neutral alkylation” e a redução da acetofenona e do benzaldeído aos respectivos álcoois. O potencial catalítico dos complexos sintetizados para com as reacções mencionadas foi avaliado maioritariamente por ^1H NMR pela percentagem de álcool de partida convertido a produto e num dos casos foi avaliado por cromatografia gasosa pela monitorização da concentração de produto ao longo do tempo. Nomeadamente foi avaliado o potencial catalítico dos dímeros, dos dímeros na presença de fosfinas e dos monómeros.

Na alquilação da *t*-butilamina os dímeros por si mesmo revelaram-se inapropriados uma vez que não foram obtidas conversões acima de 3%. Já no caso dos dímeros na presença de fosfinas os resultados foram significativamente melhores com o par $[\text{RuCl}_2(\textit{p}\text{-cimeno})]_2\text{-DPEPhos}$ a merecer lugar de destaque uma vez que apresentou 96% de álcool de partida convertido a produto com uma proporção substrato/catalisador de 20. Este resultado foi mesmo o melhor de entre todas as reacções de alquilação levadas a cabo. Relativamente ao uso dos monómeros como pré-catalisadores, o monómero $[\text{Ru}(\text{dppf})(\textit{p}\text{-cimeno})]\text{SbF}_6$ apresentou o resultado mais promissor com 85% de conversão com uma proporção substrato/catalisador de 40. Estes resultados tornam-se ainda mais interessantes se levarmos em conta de que estas reacções foram levadas a cabo em contacto com a atmosfera, sem desarejamento ou uso de gás inerte durante a reacção o que não é a abordagem normalmente encontrada na literatura e que pode ser muito apelativa do ponto de vista industrial. De uma maneira geral as fosfinas bidentadas levaram a resultados promissores tanto quando usadas em combinação com os dímeros tanto quando foram incorporadas nos respectivos monómeros. O mesmo não pode ser dito das fosfinas monodentadas. A fosfina $\text{P}(\textit{i}\text{-Bu})_3$ quando na presença do dímero $[\text{RuCl}_2(\textit{p}\text{-cimeno})]_2$ levou a uma conversão de álcool a amina de apenas 28% e quando incorporada no respectivo monómero $[\text{RuCl}(\text{P}(\textit{i}\text{-Bu})_3)_2(\textit{p}\text{-cimeno})]\text{SbF}_6$ não foi além dos 9%. Os outros complexos contendo fosfinas monodentadas e que foram testados nesta reacção de alquilação, nomeadamente o $[\text{Ru}(\text{P}(\textit{n}\text{-Bu})_3)_2(\textit{p}\text{-cimeno})]\text{SbF}_6$, $[\text{RuCl}_2\text{P}(\textit{n}\text{-Bu})_3(\textit{p}\text{-cimeno})]$, e o $[\text{RuCl}(\text{P}(\text{CH}_3)_3)_2(\textit{p}\text{-cymene})]\text{SbF}_6$ não formaram qualquer espécie activa cataliticamente uma vez que não foi detectada a formação de qualquer amina. Nesta reacção, para além da análise do efeito da fosfina, foi analisado o efeito do halogeneto e de uma maneira geral a presença de iodo em vez de cloro tanto nos dímeros como nos monómeros levou à obtenção de maiores percentagens de produto e/ou redução na quantidade de álcool por

reagir. Foi ainda analisado o efeito do contra-íão, nomeadamente entre os monómeros $[\text{RuCl}(\text{dppf})(p\text{-cimeno})]\text{SbF}_6$, $[\text{RuCl}(\text{dppf})(p\text{-cimeno})]\text{BF}_4$ e $[\text{RuCl}(\text{dppf})(p\text{-cimeno})]\text{Cl}$ e o monómero $[\text{RuCl}(\text{dppf})(p\text{-cimeno})]\text{Cl}$ parece ser o melhor pré-catalisador apresentando 82% de amina obtida com uma proporção substrato/catalisador de 20. Os resultados sugerem ainda que os complexos de fórmula molecular $[\text{RuX}(\text{LL})(p\text{-cimeno})]^+$ onde X = halogeneto e LL = ligando bidentado são os precursores catalíticos nas reacções em que são empregues os dímeros $[\text{RuX}_2(p\text{-cimeno})]_2$ e fosfinas bidentadas.

Uma das reacções de alquilação, como dito anteriormente, foi monitorizada por cromatografia gasosa. Nesta reacção foi empregue o dímero $[\text{RuCl}_2(p\text{-cimeno})]_2$ na presença de dppf e a monitorização decorreu durante 24h, isto é, o tempo a que todas as alquilações foram submetidas. No entanto esta reacção apresentou concentrações de produto/conversões muito abaixo das esperadas comparativamente à conversão obtida por ^1H NMR para a mesma reacção. Apesar disso, o padrão de redução da concentração de álcool e o padrão de aumento da concentração de produto ao longo do tempo, corroboram uma das observações feitas acerca das conversões obtidas por ^1H NMR, nomeadamente de que durante a reacção se está a formar um produto secundário, nomeadamente o éster $\text{PhCH}_2\text{CH}_2\text{O}_2\text{CCH}_2\text{Ph}$ que resulta da reacção do aldeído formado cataliticamente com o álcool remanescente em solução que ainda não reagiu. No entanto, dadas as incoerências encontradas a nível das concentrações, da avaria do cromatógrafo gasoso durante um largo período de tempo e de algumas questões relacionadas com o método, a monitorização por cromatografia gasosa foi abandonada.

Relativamente às reduções por transferência de hidrogénio, nomeadamente a redução da acetofenona e do benzaldeído estas demonstraram padrões de conversão muito semelhantes, nomeadamente os pré-catalisadores que apresentaram percentagens de conversão maiores foram os dímeros sem qualquer adição de fosfina, ao contrário do que aconteceu nas reacções de alquilação, e a presença de iodo nos pré-catalisadores não levou ao aumento, na grande maioria dos casos, da percentagem de produto obtido. No geral, não foram obtidas conversões acima de 73% o que é um resultado que fica muito aquém dos 100% já referenciados na literatura para uma larga gama de complexos. Ainda, mais uma vez, as fosfinas monodentadas parecem não ser apropriadas para serem incorporadas nos pré-catalisadores nas reacções de transferência de hidrogénio uma vez que o monómero $[\text{Ru}(\text{P}(n\text{-Bu})_3)_2(p\text{-cimeno})]\text{SbF}_6$ não foi além dos 3% de acetofenona convertida ao respectivo

álcool ou além dos 12% no caso do benzaldeído. Apesar de tudo, os resultados obtidos permitiram especular um pouco acerca dos mecanismos reaccionais seguidos tendo sido propostos dois mecanismos, um para quando são empregues apenas os dímeros e outro para quando são empregues os dímeros na presença de fosfinas ou empregues os monómeros.

Quanto aos resultados obtidos pelo dímero $[\text{Ru}_2\text{Cl}_3(\text{DPEPhos})_2(\text{CH}_3\text{CN})_2]\text{SbF}_6$, este formou espécies activas cataliticamente tanto nas alquilações como nas reduções obtendo-se conversões moderadas em ambos os casos, o que não deixa de ser um resultado interessante uma vez que, tanto quanto se sabe, ainda não foi referenciado na literatura o uso de complexos com três pontes de cloro nas reacções em questão.

Palavras-chave: transferência de hidrogénio, ruténio, *p*-cimeno, N-alquilação, catalisador.

Contents

Acknowledgements.....	i
Abstract.....	ii
Contents.....	vii
List of Figures.....	xiv
List of Schemes.....	xvi
List of Tables.....	xviii
Abbreviations.....	xix
1. Introduction.....	1
1.1 Aims.....	1
1.2 Target molecules for catalysis.....	1
1.3 Ligand Effects in Catalysis.....	5
1.4 Ruthenium catalysts and Ruthenium Catalysed Reactions.....	7
1.5 Reactions of Interest for this Project.....	9
1.6 Mechanistic Features Common to the Reactions of Interest.....	13
2. Results and Discussion.....	18
2.1 Target Molecules with Regard to Catalytic Studies.....	18
2.2 Synthesis of the Ruthenium Precursors [RuX ₂ (<i>p</i> -cymene)] ₂ (X=Cl, Br, I).....	19
2.3 Synthesis of <i>p</i> -cymene ruthenium monomers.....	23
2.3.1 Synthesis of [RuCl(dppf)(<i>p</i> -cymene)]SbF ₆ (4).....	23
2.3.1.1 Method 1.....	24
2.3.1.1 Method 2.....	24
2.3.1.2 ¹ H, ¹³ C{ ¹ H} and ³¹ P{H} NMR characterization for [RuCl(dppf)(<i>p</i> -cymene)]SbF ₆ (4).....	25
2.3.2 Synthesis of [RuI(dppf)(<i>p</i> -cymene)]SbF ₆ (5).....	29
2.3.3 Synthesis of [RuCl(dppf)(<i>p</i> -cymene)]BF ₄ (6).....	30
2.3.4 Synthesis of [RuCl(dppf)(<i>p</i> -cymene)]Cl (7).....	30
2.3.5 Synthesis of [Ru ₂ (CH ₃ CN) ₂ (DPEPhos) ₂]SbF ₆ (8).....	32
2.3.5.1 X-ray crystal structure analysis of complex 8	32
2.3.6 Synthesis of [RuCl(P(<i>n</i> -Bu ₃)) ₂ (<i>p</i> -cymene)]SbF ₆ (9).....	33
2.3.7 Synthesis of [RuI(P(<i>n</i> -Bu ₃)) ₂ (<i>p</i> -cymene)]SbF ₆ (10).....	34

2.3.8	Synthesis of $[\text{RuCl}(\text{P}(i\text{-Bu}_3)_2)(p\text{-cymene})]\text{SbF}_6$ (11)	34
2.3.9	Synthesis of $[\text{RuCl}_2\text{P}(i\text{-Bu}_3)(p\text{-cymene})]$ (12)	35
2.3.10	Synthesis of $[\text{RuCl}_2\text{P}(n\text{-Bu}_3)(p\text{-cymene})]$ (13)	36
2.3.11	Synthesis of $[\text{RuCl}(\text{P}(\text{CH}_3)_3)_2(p\text{-cymene})]\text{SbF}_6$ (14)	36
2.3.12	Synthesis of $[\text{RuCl}_2\text{PPh}(\text{OCH}_3)_2(p\text{-cymene})]$ (15)	37
2.4	Catalytic Studies	37
2.4.1	Redox Neutral Alkylations (N-alkylations)	37
2.4.1.1	^1H NMR Results	40
2.4.1.2	Gas Chromatography Analysis	46
2.4.2	Transfer hydrogenations	48
2.4.2.1	Reduction of Acetophenone	49
2.4.2.2	Reduction of Benzaldehyde	55
3.	Conclusions	57
4.	Future Work	59
5.	Experimental Procedures	60
5.1	General Experimental Considerations	60
5.2	Synthesis of the complexes	61
5.2.1	Synthesis of $[\text{RuCl}_2(p\text{-cymene})]_2 - \text{C}_{20}\text{H}_{28}\text{Cl}_4\text{Ru}_2$ (1)	61
5.2.2	Synthesis of $[\text{RuI}_2(p\text{-cymene})]_2 - \text{C}_{20}\text{H}_{28}\text{I}_4\text{Ru}_2$ (2)	61
5.2.3	Synthesis of $[\text{RuBr}_2(p\text{-cymene})]_2 - \text{C}_{20}\text{H}_{28}\text{Br}_4\text{Ru}_2$ (3)	62
5.2.4	Synthesis of $[\text{RuCl}(\text{dppf})(p\text{-cymene})]\text{SbF}_6 - \text{C}_{44}\text{H}_{42}\text{P}_2\text{ClFeRu}(\text{SbF}_6)$ (4)	62
5.2.4.1	Method 1	62
5.2.4.2	Method 2	63
5.2.5	Synthesis of $[\text{RuI}(\text{dppf})(p\text{-cymene})]\text{SbF}_6 - \text{C}_{44}\text{H}_{42}\text{P}_2\text{FeRuI}(\text{SbF}_6)$ (5)	64
5.2.6	Synthesis of $[\text{RuCl}(\text{dppf})(p\text{-cymene})]\text{BF}_4 - \text{C}_{44}\text{H}_{42}\text{P}_2\text{ClFeRu}(\text{BF}_4)$ (6)	65
5.2.7	Synthesis of $[\text{RuCl}(\text{dppf})(p\text{-cymene})]\text{Cl} - \text{C}_{44}\text{H}_{42}\text{P}_2\text{ClFeRu}(\text{Cl})$ (7)	66
5.2.8	Synthesis of $[\text{Ru}_2\text{Cl}_3(\text{DPEPhos})_2(\text{CH}_3\text{CN})_2]\text{SbF}_6 - \text{C}_{76}\text{H}_{62}\text{O}_2\text{N}_2\text{P}_4\text{Cl}_3\text{Ru}_2(\text{SbF}_6)$ (8)	66
5.2.9	Synthesis of $[\text{RuCl}(\text{P}(n\text{-Bu})_3)_2(p\text{-cymene})]\text{SbF}_6 - \text{C}_{34}\text{H}_{68}\text{P}_2\text{ClRu}(\text{SbF}_6)$ (9)	67
5.2.10	Synthesis of $[\text{RuI}(\text{P}(n\text{-Bu})_3)_2(p\text{-cymene})]\text{SbF}_6 - \text{C}_{34}\text{H}_{68}\text{P}_2\text{IRu}(\text{SbF}_6)$ (10)	68
5.2.11	Synthesis of $[\text{RuCl}(\text{P}(i\text{-Bu})_3)_2(p\text{-cymene})]\text{SbF}_6 - \text{C}_{34}\text{H}_{68}\text{P}_2\text{ClRu}(\text{SbF}_6)$ (11)	69
5.2.12	Synthesis of $[\text{RuCl}_2\text{P}(i\text{-Bu})_3(p\text{-cymene})] - \text{C}_{22}\text{H}_{41}\text{PCL}_2\text{Ru}$ (12)	69
5.2.13	Synthesis of $[\text{RuCl}_2\text{P}(n\text{-Bu})_3(p\text{-cymene})] - \text{C}_{22}\text{H}_{41}\text{PCL}_2\text{Ru}$ (13)	70

5.2.14	Synthesis of $[\text{RuCl}(\text{P}(\text{CH}_3)_3)_2(\textit{p}\text{-cymene})]\text{SbF}_6 - \text{RuC}_{16}\text{H}_{32}\text{P}_2\text{Cl}(\text{SbF}_6)$ (14).....	70
5.2.15	Synthesis of $[\text{RuCl}_2\text{PPh}(\text{OCH}_3)_2(\textit{p}\text{-cymene})] - [\text{RuC}_{18}\text{H}_{25}\text{PO}_2\text{Cl}_2]$ (15)	71
5.3	Catalytic Reactions	72
5.3.1	Redox Neutral Alkylations	72
5.3.1.2	Gas Chromatography Analysis	73
5.3.2	Transfer Hydrogenations	75
6.	References	76

APPENDIX 1	^1H NMR spectrum of $[\text{RuCl}_2(\textit{p}\text{-cymene})]_2$ (1) in CDCl_3	a
APPENDIX 2	^1H NMR spectrum of $[\text{RuI}_2(\textit{p}\text{-cymene})]_2$ (2) in CDCl_3	b
APPENDIX 3	^1H NMR spectrum of $[\text{RuBr}_2(\textit{p}\text{-cymene})]_2$ (3) in CDCl_3	c
APPENDIX 4	^1H NMR spectrum of $[\text{RuCl}(\text{dppf})(\textit{p}\text{-cymene})]\text{SbF}_6$ (4) (method 1) in $(\text{CD}_3)_2\text{CO}$..d	
APPENDIX 4.1	^1H NMR spectrum of $[\text{RuCl}(\text{dppf})(\textit{p}\text{-cymene})]\text{SbF}_6$ (4) (method 1) in CDCl_3e	
APPENDIX 4.2	$^{13}\text{C}\{^1\text{H}\}$ NMR spectrum of $[\text{RuCl}(\text{dppf})(\textit{p}\text{-cymene})]\text{SbF}_6$ (4) (method 1) in $(\text{CD}_3)_2\text{CO}$	f
APPENDIX 4.3	DEPT $^{13}\text{C}\{^1\text{H}\}$ NMR spectrum of $[\text{RuCl}(\text{dppf})(\textit{p}\text{-cymene})]\text{SbF}_6$ (4) (method 1) in $(\text{CD}_3)_2\text{CO}$	g
APPENDIX 4.4	HMQC NMR spectrum of $[\text{RuCl}(\text{dppf})(\textit{p}\text{-cymene})]\text{SbF}_6$ (4) (method 1) in $(\text{CD}_3)_2\text{CO}$	h
APPENDIX 4.5	COSY NMR spectrum of $[\text{RuCl}(\text{dppf})(\textit{p}\text{-cymene})]\text{SbF}_6$ (4) (method 1) in $(\text{CD}_3)_2\text{CO}$	i
APPENDIX 4.6	$^{31}\text{P}\{^1\text{H}\}$ NMR spectrum of $[\text{RuCl}(\text{dppf})(\textit{p}\text{-cymene})]\text{SbF}_6$ (4) (method 1) in $(\text{CD}_3)_2\text{CO}$	j
APPENDIX 4.7	Mass spectrum of $[\text{RuCl}(\text{dppf})(\textit{p}\text{-cymene})]\text{SbF}_6$ (4) (method 1)	k
APPENDIX 4.8	^1H NMR spectrum of $[\text{RuCl}(\text{dppf})(\textit{p}\text{-cymene})]\text{SbF}_6$ (4) (method 2) in CDCl_3l	
APPENDIX 5	^1H NMR spectrum of $[\text{RuI}(\text{dppf})(\textit{p}\text{-cymene})]\text{SbF}_6$ (5) in CDCl_3	m
APPENDIX 5.1	$^{13}\text{C}\{^1\text{H}\}$ NMR spectrum of $[\text{RuI}(\text{dppf})(\textit{p}\text{-cymene})]\text{SbF}_6$ (5) in CDCl_3	n
APPENDIX 5.2	$^{31}\text{P}\{^1\text{H}\}$ NMR spectrum of $[\text{RuI}(\text{dppf})(\textit{p}\text{-cymene})]\text{SbF}_6$ (5) in CDCl_3	o
APPENDIX 5.3	Mass spectrum of $[\text{RuI}(\text{dppf})(\textit{p}\text{-cymene})]\text{SbF}_6$ (5)	p
APPENDIX 6	^1H NMR spectrum of $[\text{RuCl}(\text{dppf})(\textit{p}\text{-cymene})]\text{BF}_4$ (6) in CDCl_3	q
APPENDIX 6.1	$^{13}\text{C}\{^1\text{H}\}$ NMR spectrum of $[\text{RuCl}(\text{dppf})(\textit{p}\text{-cymene})]\text{BF}_4$ (6) in CDCl_3	r
APPENDIX 6.2	$^{31}\text{P}\{^1\text{H}\}$ NMR spectrum of $[\text{RuCl}(\text{dppf})(\textit{p}\text{-cymene})]\text{BF}_4$ (6) in CDCl_3	s

APPENDIX 6.3 – Mass spectrum of [RuCl(dppf)(<i>p</i> -cymene)]BF ₄ (6)	t
APPENDIX 7 – ¹ H NMR spectrum of [RuCl(dppf)(<i>p</i> -cymene)]Cl (7) in CDCl ₃	u
APPENDIX 7.1 – ³¹ P{ ¹ H} NMR spectrum of [RuCl(dppf)(<i>p</i> -cymene)]Cl (7) in CDCl ₃	v
APPENDIX 7.2 – Mass spectrum of [RuCl(dppf)(<i>p</i> -cymene)]Cl (7)	w
APPENDIX 8 – ¹ H NMR spectrum of [Ru ₂ Cl ₃ (DPEPhos) ₂ (CH ₃ CN) ₂]SbF ₆ (8) in CDCl ₃	x
APPENDIX 8.1 – ¹³ C{ ¹ H} NMR spectrum of [Ru ₂ Cl ₃ (DPEPhos) ₂ (CH ₃ CN) ₂]SbF ₆ (8) in CDCl ₃	y
APPENDIX 8.2 – Mass spectrum of [Ru ₂ Cl ₃ (DPEPhos) ₂ (CH ₃ CN) ₂]SbF ₆ (8)	z
APPENDIX 9 – ¹ H NMR spectrum of [RuCl(P(<i>n</i> -Bu) ₃) ₂ (<i>p</i> -cymene)]SbF ₆ (9) in CDCl ₃	aa
APPENDIX 9.1 – ¹³ C{ ¹ H} NMR spectrum of [RuCl(P(<i>n</i> -Bu) ₃) ₂ (<i>p</i> -cymene)]SbF ₆ (9) in CDCl ₃	bb
APPENDIX 9.2 – ³¹ P{ ¹ H} NMR spectrum of [RuCl(P(<i>n</i> -Bu) ₃) ₂ (<i>p</i> -cymene)]SbF ₆ (9) in CDCl ₃	cc
APPENDIX 9.3 – Mass spectrum of [RuCl(P(<i>n</i> -Bu) ₃) ₂ (<i>p</i> -cymene)]SbF ₆ (9)	dd
APPENDIX 10 – ¹ H NMR spectrum of [RuI(P(<i>n</i> -Bu) ₃) ₂ (<i>p</i> -cymene)]SbF ₆ (10) in CDCl ₃	ee
APPENDIX 10.1 – ¹³ C{ ¹ H} NMR spectrum of [RuI(P(<i>n</i> -Bu) ₃) ₂ (<i>p</i> -cymene)]SbF ₆ (10) in CDCl ₃	ff
APPENDIX 10.2 – Mass spectrum of [RuI(P(<i>n</i> -Bu) ₃) ₂ (<i>p</i> -cymene)]SbF ₆ (10)	gg
APPENDIX 11 – ¹ H NMR spectrum of [RuCl(P(<i>i</i> -Bu) ₃) ₂ (<i>p</i> -cymene)]SbF ₆ (11) in CDCl ₃	hh
APPENDIX 11.1 – ¹³ C{ ¹ H} NMR spectrum of [RuCl(P(<i>i</i> -Bu) ₃) ₂ (<i>p</i> -cymene)]SbF ₆ (11) in CDCl ₃	ii
APPENDIX 11.2 – ³¹ P{ ¹ H} NMR spectrum of [RuCl(P(<i>i</i> -Bu) ₃) ₂ (<i>p</i> -cymene)]SbF ₆ (11) in CDCl ₃	jj
APPENDIX 11.3 – Mass spectrum of [RuCl(P(<i>i</i> -Bu) ₃) ₂ (<i>p</i> -cymene)]SbF ₆ (11)	kk
APPENDIX 12 – ¹ H NMR spectrum of [RuCl ₂ P(<i>i</i> -Bu) ₃ (<i>p</i> -cymene)] (12) in CDCl ₃	ll
APPENDIX 12.1 – Mass spectrum of [RuCl ₂ P(<i>i</i> -Bu) ₃ (<i>p</i> -cymene)] (12)	mm
APPENDIX 13 – ¹ H NMR spectrum of [RuCl ₂ P(<i>n</i> -Bu) ₃ (<i>p</i> -cymene)] (13) in CDCl ₃	nn
APPENDIX 13.1 – Mass spectrum of [RuCl ₂ P(<i>n</i> -Bu) ₃ (<i>p</i> -cymene)] (13)	oo
APPENDIX 14 – ¹ H NMR spectrum of [RuCl(P(CH ₃) ₃) ₂ (<i>p</i> -cymene)]SbF ₆ (14) in CDCl ₃	pp
APPENDIX 14.1 – ³¹ P{ ¹ H} NMR spectrum of [RuCl(P(CH ₃) ₃) ₂ (<i>p</i> -cymene)]SbF ₆ (14) in CDCl ₃	qq
APPENDIX 14.2 – Mass spectrum of [RuCl(P(CH ₃) ₃) ₂ (<i>p</i> -cymene)]SbF ₆ (14)	rr
APPENDIX 15 – ¹ H NMR spectrum of [RuCl ₂ PhP(OCH ₃) ₂ (<i>p</i> -cymene)] (15) in CDCl ₃	ss
APPENDIX 15.1 – Mass spectrum of [RuCl ₂ PhP(OCH ₃) ₂ (<i>p</i> -cymene)] (15)	tt
APPENDIX 16 – [Ru ₂ Cl ₃ (DPEPhos) ₂ (CH ₃ CN) ₂]SbF ₆ (8) Crystal Data	uu
APPENDIX 17 – Labelled molecular structure of [Ru ₂ Cl ₃ (DPEPhos) ₂ (CH ₃ CN) ₂]SbF ₆ (8)	vv
APPENDIX 18 – Selected Bond Lengths (Å) and Angles (deg) for [Ru ₂ Cl ₃ (DPEPhos) ₂ (CH ₃ CN) ₂]SbF ₆ (8) obtained by X-ray crystallography.	vv

APPENDIX 19 – ¹ H NMR spectrum of the product from the N-alkylation of <i>t</i> -butylamine using [RuCl ₂ (<i>p</i> -cymene)] ₂ (1)-dppf as pre-catalyst (S/C=20), in CDCl ₃	ww
APPENDIX 20 – ¹ H NMR spectrum of the product from the N-alkylation of <i>t</i> -butylamine using [RuCl ₂ (<i>p</i> -cymene)] ₂ (1)-DPEPhos as pre-catalyst (S/C=20), in CDCl ₃	ww
APPENDIX 21 – ¹ H NMR spectrum of the product from the N-alkylation of <i>t</i> -butylamine using [RuCl ₂ (<i>p</i> -cymene)] ₂ (1)-dippf as pre-catalyst (S/C=20), in CDCl ₃	xx
APPENDIX 22 – ¹ H NMR spectrum of the product from the N-alkylation of <i>t</i> -butylamine using [RuCl ₂ (<i>p</i> -cymene)] ₂ (1)-P(<i>i</i> -Bu) ₃ as pre-catalyst (S/C=20), in CDCl ₃	xx
APPENDIX 23 – ¹ H NMR spectrum of the product from the N-alkylation of <i>t</i> -butylamine using [RuI ₂ (<i>p</i> -cymene)] ₂ (2)-dppf as pre-catalyst (S/C=20), in CDCl ₃	yy
APPENDIX 24 – ¹ H NMR spectrum of the product from the N-alkylation of <i>t</i> -butylamine using [RuI ₂ (<i>p</i> -cymene)] ₂ (2)-DPEPhos as pre-catalyst (S/C=20), in CDCl ₃	yy
APPENDIX 25 – ¹ H NMR spectrum of the product from the N-alkylation of <i>t</i> -butylamine using [RuI ₂ (<i>p</i> -cymene)] ₂ (2)-dippf as pre-catalyst (S/C=20), in CDCl ₃	zz
APPENDIX 26 – ¹ H NMR spectrum of the product from the N-alkylation of <i>t</i> -butylamine using [RuCl(dppf)(<i>p</i> -cymene)]SbF ₆ (4) as pre-catalyst (S/C=40), in CDCl ₃	zz
APPENDIX 27 – ¹ H NMR spectrum of the product from the N-alkylation of <i>t</i> -butylamine using [RuCl(dppf)(<i>p</i> -cymene)]BF ₄ (6) as pre-catalyst (S/C=40), in CDCl ₃	aaa
APPENDIX 28 – ¹ H NMR spectrum of the product from the N-alkylation of <i>t</i> -butylamine using [RuCl(dppf)(<i>p</i> -cymene)]BF ₄ (6) as pre-catalyst (S/C=20), in CDCl ₃	aaa
APPENDIX 29 – ¹ H NMR spectrum of the product from the N-alkylation of <i>t</i> -butylamine using [RuCl(dppf)(<i>p</i> -cymene)]Cl (7) as pre-catalyst (S/C=40), in CDCl ₃	bbb
APPENDIX 30 – ¹ H NMR spectrum of the product from the N-alkylation of <i>t</i> -butylamine using [RuCl(dppf)(<i>p</i> -cymene)]Cl (7) as pre-catalyst (S/C=20), in CDCl ₃	bbb
APPENDIX 31 – ¹ H NMR spectrum of the product from the N-alkylation of <i>t</i> -butylamine using [RuI(dppf)(<i>p</i> -cymene)]SbF ₆ (5) as pre-catalyst (S/C=40), in CDCl ₃	ccc
APPENDIX 32 – ¹ H NMR spectrum of the product from the N-alkylation of <i>t</i> -butylamine using [Ru ₂ Cl ₃ (DPEPhos) ₂ (CH ₃ CN) ₂]SbF ₆ (8) as pre-catalyst (S/C=40), in CDCl ₃	ccc
APPENDIX 33 – ¹ H NMR spectrum of the product from the N-alkylation of <i>t</i> -butylamine using [RuI(P(<i>n</i> -Bu) ₃) ₂ (<i>p</i> -cymene)]SbF ₆ (10) as pre-catalyst (S/C=40), in CDCl ₃	ddd
APPENDIX 34 – ¹ H NMR spectrum of the product from the N-alkylation of <i>t</i> -butylamine using [RuCl(P(<i>i</i> -Bu) ₃) ₂ (<i>p</i> -cymene)]SbF ₆ (11) as pre-catalyst (S/C=40), in CDCl ₃	ddd

APPENDIX 35 – ¹ H NMR spectrum of the product from the N-alkylation of <i>t</i> -butylamine using [RuCl ₂ (P(<i>n</i> -Bu) ₃) ₂ (<i>p</i> -cymene)] (13) as pre-catalyst (S/C=40), in CDCl ₃	eee
APPENDIX 36 – ¹ H NMR spectrum of the product from the N-alkylation of <i>t</i> -butylamine using [RuCl(P(CH ₃) ₃) ₂ (<i>p</i> -cymene)]SbF ₆ (14) as pre-catalyst (S/C=40), in CDCl ₃	eee
APPENDIX 37 – ¹ H NMR spectrum of the product from the reduction of acetophenone using [RuCl ₂ (<i>p</i> -cymene)] ₂ (1) as pre-catalyst, in CDCl ₃	fff
APPENDIX 38 – ¹ H NMR spectrum of the product from the reduction of acetophenone using [RuCl ₂ (<i>p</i> -cymene)] ₂ (1)-dppf as pre-catalyst, in CDCl ₃	fff
APPENDIX 39 – ¹ H NMR spectrum of the product from the reduction of acetophenone using [RuCl ₂ (<i>p</i> -cymene)] ₂ (1)-DPEPhos as pre-catalyst, in CDCl ₃	ggg
APPENDIX 40 – ¹ H NMR spectrum of the product from the reduction of acetophenone using [RuCl ₂ (<i>p</i> -cymene)] ₂ (1)-dippf as pre-catalyst, in CDCl ₃	ggg
APPENDIX 41 – ¹ H NMR spectrum of the product from the reduction of acetophenone using [Ru ₂ (<i>p</i> -cymene)] ₂ (2) as pre-catalyst, in CDCl ₃	hhh
APPENDIX 42 – ¹ H NMR spectrum of the product from the reduction of acetophenone using [Ru ₂ (<i>p</i> -cymene)] ₂ (2)-dppf as pre-catalyst, in CDCl ₃	hhh
APPENDIX 43 – ¹ H NMR spectrum of the product from the reduction of acetophenone using [Ru ₂ (<i>p</i> -cymene)] ₂ (2)-DPEPhos as pre-catalyst, in CDCl ₃	iii
APPENDIX 44 – ¹ H NMR spectrum of the product from the reduction of acetophenone using [Ru ₂ (<i>p</i> -cymene)] ₂ (2)-dippf as pre-catalyst, in CDCl ₃	iii
APPENDIX 45 – ¹ H NMR spectrum of the product from the reduction of acetophenone using [RuCl(dppf)(<i>p</i> -cymene)]Cl (7) as pre-catalyst, in CDCl ₃	jjj
APPENDIX 46 – ¹ H NMR spectrum of the product from the reduction of acetophenone using [Ru(P(<i>n</i> -Bu) ₃) ₂ (<i>p</i> -cymene)]SbF ₆ (10) as pre-catalyst, in CDCl ₃	jjj
APPENDIX 47 – ¹ H NMR spectrum of the product from the reduction of acetophenone using [Ru ₂ Cl ₃ (DPEPhos) ₂ (CH ₃ CN) ₂]SbF ₆ (8) as pre-catalyst, in CDCl ₃	kkk
APPENDIX 48 – ¹ H NMR spectrum of the product from the reduction of benzaldehyde using [RuCl ₂ (<i>p</i> -cymene)] ₂ (1) as pre-catalyst, in CDCl ₃	kkk
APPENDIX 49 – ¹ H NMR spectrum of the product from the reduction of benzaldehyde using [RuCl ₂ (<i>p</i> -cymene)] ₂ (1)-dppf as pre-catalyst, in CDCl ₃	lll
APPENDIX 50 – ¹ H NMR spectrum of the product from the reduction of benzaldehyde using [RuCl ₂ (<i>p</i> -cymene)] ₂ (1)-DPEPhos as pre-catalyst, in CDCl ₃	lll

APPENDIX 51 – ¹ H NMR spectrum of the product from the reduction of benzaldehyde using [RuCl ₂ (<i>p</i> -cymene)] ₂ (1)-dippf as pre-catalyst, in CDCl ₃	mmm
APPENDIX 52 – ¹ H NMR spectrum of the product from the reduction of benzaldehyde using [RuI ₂ (<i>p</i> -cymene)] ₂ (2) as pre-catalyst, in CDCl ₃	mmm
APPENDIX 53 – ¹ H NMR spectrum of the product from the reduction of benzaldehyde using [RuI ₂ (<i>p</i> -cymene)] ₂ (2)-dppf as pre-catalyst, in CDCl ₃	nnn
APPENDIX 54 – ¹ H NMR spectrum of the product from the reduction of benzaldehyde using [RuI ₂ (<i>p</i> -cymene)] ₂ (2)-DPEPhos as pre-catalyst, in CDCl ₃	nnn
APPENDIX 55 – ¹ H NMR spectrum of the product from the reduction of benzaldehyde using [RuCl(dppf)(<i>p</i> -cymene)]Cl (7) as pre-catalyst, in CDCl ₃	ooo
APPENDIX 56 – ¹ H NMR spectrum of the product from the reduction of benzaldehyde using [RuI(P(<i>n</i> -Bu) ₃) ₂ (<i>p</i> -cymene)]SbF ₆ (10) as pre-catalyst, in CDCl ₃	ooo

List of Figures

Figure 1.1 – Coordination sites for ligands in piano-stool complexes.....	2
Figure 1.2 – Components of bonding in phosphine ligands.....	3
Figure 1.3 – Electronic properties of halide ligands.....	4
Figure 1.4 – Stabilization and destabilization arising from molecular orbital interactions for an octahedral coordination geometry.	5
Figure 1.5 – Ruthenium complexes with different catalytic effects.	6
Figure 1.6 – “Privileged” phosphine ligands in catalysis.....	7
Figure 1.7 – Examples of metal hydrides that have been isolated or proven to take place in hydrogen transfer reactions.....	14
Figure 1.8 – Original version of the MPV reduction. Direct hydrogen transfer through an aluminium alkoxide using isopropanol reported in the early XX century. ²	14
Figure 2.1 – ¹ H NMR spectra of [RuCl ₂ (<i>p</i> -cymene)] ₂ (1), [RuI ₂ (<i>p</i> -cymene)] ₂ (2) and [RuBr ₂ (<i>p</i> -cymene)] ₂ (3) in CDCl ₃	21
Figure 2.2 – Labelled diagram of [RuCl ₂ (<i>p</i> -cymene)] ₂ (1) for ¹ H NMR purposes.....	22
Figure 2.3 – Labelled diagram of [RuCl(dppf)(<i>p</i> -cymene)]SbF ₆ (4) for NMR purposes.....	25
Figure 2.4 – Crystal structure of [RuCl(dppf)(<i>p</i> -cymene)]PF ₆ reported by M. Spicer <i>et. al.</i> ⁴³ The ligand phenyl protons and PF ₆ are omitted for clarity.....	27
Figure 2.5 – ¹ H NMR spectrum of [RuCl(dppf)(<i>p</i> -cymene)]SbF ₆ (4) in (CD ₃) ₂ CO with expansions of the Cp and <i>p</i> -cymene peaks.....	28
Figure 2.6 – ¹³ C{ ¹ H} NMR spectrum of [RuCl(dppf)(<i>p</i> -cymene)]SbF ₆ (4) in (CD ₃) ₂ CO with expansions of the phenyl, Cp and <i>p</i> -cymene peaks. <i>o</i> = ortho, <i>p</i> = para, <i>m</i> = meta, <i>q</i> = quaternary carbon.....	28
Figure 2.7 – Expansions of HMQC NMR spectrum of [RuCl(dppf)(<i>p</i> -cymene)]SbF ₆ (4) in (CD ₃) ₂ CO. a) phenyl protons region. b) Cp and aromatic <i>p</i> -cymene protons region.	29
Figure 2.8 – ¹ H NMR spectra of compounds [RuCl(dppf)(<i>p</i> -cymene)]SbF ₆ (4), [RuCl(dppf)(<i>p</i> -cymene)]BF ₄ (6) and [RuCl(dppf)(<i>p</i> -cymene)]Cl (7) in CDCl ₃ . X = <i>p</i> -cymene peak that undergoes shifting according to the different counter-ion of the complex.	31
Figure 2.9 – Molecular structure of [Ru ₂ (NCCH ₃) ₂ (DPEPhos) ₂]SbF ₆ (8) obtained by X-ray crystallography in this project.....	33
Figure 2.10 – Molecular structure of [RuCl(P(<i>i</i> -Bu ₃)) ₂ (<i>p</i> -cymene)]SbF ₆ (11).....	35

Figure 2.11 – Molecular structure of $[\text{RuCl}_2\text{PPh}(\text{OCH}_3)_2(p\text{-cymene})]$ (15).....	37
Figure 2.12 – ^1H NMR spectrum of the oily residue obtained after filtration of the reaction mixture through celite of the N-alkylation of tert-butylamine with phenethyl alcohol by $[\text{RuCl}(\text{dppf})(p\text{-cymene})]\text{Cl}$ (7). Substrate:catalyst ratio of 40:1. (a), (b) and (c) are the peaks which integrals were used to calculate the product conversion.	40
Figure 2.13 – Variation of the product and alcohol concentration in an n-alkylation catalysed by $[\text{RuCl}_2(p\text{-cymene})]_2$ in the presence of dppf ligand.	47
Figure 2.14 – Schematic for the Radley’s carousel used for batch reactions. Adapted from J. Williams and co-workers. ²⁷	49
Figure 2.15 – ^1H NMR spectrum of the oily residue obtained after evaporation of the reaction mixture of the conversion of acetophenone to 1-phenylethanol by transfer hydrogenation using $[\text{RuCl}_2(p\text{-cymene})]_2(\mathbf{1})\text{-dppf}$ as pre-catalyst. The reaction scheme is also depicted. (a) and (b) are the peaks which integrals were used to calculate the product conversion.	50
Figure 2.16 – BINOL-derived diphosphonites which have proven to be excellent ligands for asymmetric olefin hydrogenation and other reactions. ⁶² A = 1,1'-Bis[(11bR)-dinaphtho[2,1-d:1', 2'-f][1,3,2]dioxaphosphepin-4-yl]ferrocene; B = (11bR, 11'bR)-4,4'-(Oxydi-2,1-phenylene)bis-dinaphtho[2,1-d: 1', 2'-f][1,3,2]dioxaphosphepin.....	51
Figure 2.17 – ^1H NMR spectrum of the oily residue obtained after evaporation of the reaction mixture of the conversion of benzaldehyde to benzyl alcohol by transfer hydrogenation using $[\text{RuCl}_2(p\text{-cymene})]_2(\mathbf{1})\text{-DPEPhos}$ as pre-catalyst. The reaction scheme is also depicted. (a) and (b) are the peaks which integrals were used to calculate the product conversion.	55
Figure 2.18 – Comparison of the catalytic activities according to the substrate in the reduction of acetophenone and benzaldehyde by transfer hydrogenation.....	57

List of Schemes

Scheme 1.1 – Enantioselective synthesis employing a ruthenium catalyst with a chiral ligand.	8
Scheme 1.2 – Oxidation of an alcohol to an ester employing a ruthenium catalyst.	8
Scheme 1.3 – Oxidation of an alcohol employing a ruthenium catalyst and an oxidant.	9
Scheme 1.4 – Hydrogenation and transfer hydrogenation of carbonyl compounds using either the formic acid/triethylamine or isopropanol as hydrogen source.	10
Scheme 1.5 – General scheme for the asymmetric transfer hydrogenation of ketones using isopropanol as hydrogen donor. The resulting by-product is a molecule of acetone.	11
Scheme 1.6 – Borrowing Hydrogen Strategy in the alkylation of amines with alcohols. ²⁷	12
Scheme 1.7 – Ruthenium-catalyzed N-alkylation of amines with primary alcohols by J. Williams <i>et. al.</i> showing the reaction yields. ¹	13
Scheme 1.8 – Racemisation of an α -deuterated chiral alcohol in the dihydride mechanism. ²	15
Scheme 1.9 – Racemisation of an α -deuterated chiral alcohol in the monohydride mechanism. ²	15
Scheme 1.10 – Inner-sphere pathway for monohydride mechanisms. ²	15
Scheme 1.11 – Outer-sphere concerted pathway for monohydride mechanisms. ²	16
Scheme 1.12 – ATH of ketones by isopropanol via Noyori's metal–ligand bifunctional catalysis. ¹⁹	17
Scheme 1.13 – Mechanism for the hydride formation in the catalytic transfer hydrogenation of ketones under base-free conditions proposed by Carrión <i>et. al.</i> ⁴¹	18
Scheme 2.1 – Synthesis of $[\text{RuCl}_2(p\text{-cymene})]_2$ (1).	19
Scheme 2.2 – Synthesis carried out to obtain $[\text{RuI}_2(p\text{-cymene})]_2$ (2) and $[\text{RuBr}_2(p\text{-cymene})]_2$ (3).	20
Scheme 2.3 – Synthesis of $[\text{RuCl}(\text{dppf})(p\text{-cymene})]\text{SbF}_6$ (4).	24
Scheme 2.4 – Synthesis $[\text{RuCl}(\text{dppf})(p\text{-cymene})]\text{Cl}$ (7).	31
Scheme 2.5 – Synthesis of $[\text{RuCl}(\text{P}(n\text{-Bu}_3))_2(p\text{-cymene})]\text{SbF}_6$ (9).	34
Scheme 2.6 – Synthesis of $[\text{RuCl}_2\text{P}(i\text{-Bu}_3)(p\text{-cymene})]$ (12).	36
Scheme 2.7 – N-alkylation of phenethyl alcohol with tert-butylamine.	38
Scheme 2.8 – Catalytic synthesis of 4-(phenylmethyl)morpholine by N-alkylation.	39
Scheme 2.9 – Proposed mechanism by J. Williams and co-workers ¹ of N-Alkylation Reactions Involving Enantiomerically Pure Substrates.	44

Scheme 2.10 – Hydrogen/Deuterium crossover study in Morpholine Alkylation by J. Williams and co-workers. ¹	44
Scheme 2.11 – Reaction between [RuCl(dppf)(<i>p</i> -cymene)]SbF ₆ (4) and pyridine (top left) and between [RuCl ₂ (<i>p</i> -cymene)(NC ₅ H ₅)] and dppf (bottom left).....	45
Scheme 2.12 – Proposed catalytic cycle in the present study for the reduction of acetophenone (R=CH ₃) and benzaldehyde (R=H) employing ruthenium dimers in the absence of any additional ligands. X = halide.....	52
Scheme 2.13 – Proposed catalytic cycle in the present study for the reduction of acetophenone (R=CH ₃) and benzaldehyde (R=H) employing ruthenium dimers in the presence of biphosphine ligands or just employing diphosphine ruthenium monomers (33). X = halide.	54

List of Tables

Table 2.1 – ¹ H NMR chemical shift assignment of [RuCl ₂ (<i>p</i> -cymene)] ₂ (1).	22
Table 2.2 – ¹ H and ¹³ C{ ¹ H} NMR chemical shift assignment of [RuCl(dppf)(<i>p</i> -cymene)]SbF ₆ (4) in (CD ₃) ₂ CO.....	26
Table 2.3 – Results for the N-alkylation of tert-butylamine with phenethyl alcohol. Catalyst/ligand evaluation.....	41
Table 2.4 – Alcohol and product concentrations over time in the N-alkylation catalysed by [RuCl ₂ (<i>p</i> -cymene)] ₂ (1) in the presence of dppf.	47
Table 2.5 – Results for the reduction of acetophenone to 1-phenylethanol by transfer hydrogenation. The base employed is <i>t</i> -BuOK and the hydrogen source is isopropanol unless otherwise stated.....	50
Table 2.6 – Results for the reduction of benzaldehyde to benzyl alcohol by transfer hydrogenation. The base employed is <i>t</i> -BuOK and the hydrogen source is isopropanol.....	56

Abbreviations

<i>p</i> -cymene	1-Methyl-4-(1-methylethyl)benzene
dppf	1,1'-Bis(diphenylphosphino)ferrocene
dippf	Bis(diisopropylphosphino)ferrocene
DPEPhos	(Oxydi-2,1-phenylene)bis(diphenylphosphine)
dppb	Diphenylphosphino butane
dppp	1,3-Bis(diphenylphosphino)propane
dcypb	1,4-bis(dicyclohexylphosphino)butane
P(<i>i</i> -Bu ₃)	Triisobutylphosphine
P(<i>n</i> -Bu ₃)	Trinbutylphosphine
BINOL	1,1'-Bi-2-naphthol
BINAP	2,2'-bis(diphenylphosphino)-1,1'-binaphthyl
TsDPEN	N-(<i>p</i> -toluenesulfonyl)-1,2-diphenylethylenediamine
BINAP	2,2'-bis(diphenylphosphino)-1,1'-binaphthyl
DIPAMP	Ethane-1,2-diylbis[(2-methoxyphenyl)phenylphosphane]
Tetralin	1,2,3,4-tetrahydronaphthalene
Me-DuPhos	1,2-Bis(2,5-dimethylphospholano)benzene
Et-DuPhos	1,2-Bis(2,5-diethylphospholano)benzene
PHOX	Phosphinooxazoline
Bpz	2,2'-Bipyrazine
ATH	Asymmetric Transfer Hydrogenation
GC	Gas chromatography
NMR	Nuclear Magnetic Resonance
¹ H NMR	Proton Nuclear Magnetic Resonance
¹³ C NMR	Carbon Nuclear Magnetic Resonance
³¹ P NMR	Phosphorus Nuclear Magnetic Resonance
COSY	Correlation Spectroscopy
DEPT	Distortionless Enhancement by Polarization Transfer
HMQC	Heteronuclear Multiple Quantum Correlation
ESMS	Electrospray Mass Spectrometry
br.	Broad (NMR)

p-Cymene Based Ruthenium Complexes as Catalysts

s	Singlet (NMR)
d	Duplet (NMR)
t	Triplet (NMR)
m	Multiplet (NMR)
sept	Septet (NMR)
Et	Ethyl
Me	Methyl
δ	Chemical Shift Relative to Tetramethylsilane
<i>J</i>	Coupling Constant
ppm	parts per million
ee	Enantiomeric excess
r.t.	Room temperature
MHz	Megahertz
<i>t</i> -Bu	Tert-butyl
Ph	Phenyl
THF	Tetrahydrofuran
K	Kelvin
Cp	η^5 -Cyclopentadienyl
Cp*	Pentamethylcyclopentadienyl
<i>m</i>	Meta
<i>p</i>	Para
<i>o</i>	Orto
Ac	Acetyl
S/C	Substrate/Catalyst
COD	1,5-Cyclooctadiene

1. Introduction

1.1 Aims

This project is concerned about the synthesis and evaluation of the catalytic properties of *p*-cymene ruthenium (II) complexes towards a series of organic and pharmaceutical reactions of great industrial interest. These reactions are redox neutral alkylations and transfer hydrogenations. Both of them are applications of the transfer dehydrogenation/hydrogenation methodology. Hydrogen transfer reactions are mild methodologies for reduction of ketones or imines and oxidation of alcohols or amines in which a substrate-selective catalyst transfers hydrogen between the substrate and a hydrogen donor or acceptor, respectively.² This methodology is increasing its importance and growing rapidly since it is contributing to more selective chemical processes with a minimum amount of waste (“green chemistry”). Unlike typical hydrogenations, it does not involve the use of molecular hydrogen which is explosive and the handling requires expensive and specialized equipment. Also, hydrogen gas is highly reactive, therefore showing low chemoselectivity towards other functional groups.³

The organometallic approach of using a molecular catalyst consisting of a metal atom or ion, phosphorus or nitrogen donor ligands and η^6 -arenes is the general approach for the purpose of the reactions mentioned above and it was the approach followed herein. These complexes are believed to have catalytic potential due to spectator benzene-substituted ring which provides steric protection for the ruthenium centre by blocking three adjacent coordination sites in an octahedral Ru coordination environment, leaving three sites with a *fac* relationship for other functions.⁴ The ligands employed in this project were η^6 -arenes, phosphines and halides. The ruthenium chemistry is based on previous work in the McGowan’s research group.

1.2 Target molecules for catalysis

The complexes used/synthesized in this project were η^6 -arenes ruthenium derivatives, where the ruthenium centre adopts a half-sandwich structure. Complexes with

such structure are widely known as piano-stool complexes and are, without doubt, the most studied ones within the large family of η^6 -arene ruthenium complexes. This family of complexes possess a pseudo-octahedral geometry at the ruthenium (II) atom where the arene ligand occupies three coordinating sites (the seat) and the other ligands (the legs) occupies the other three places (figure 1.1). The coordinated aromatic ring introduces steric

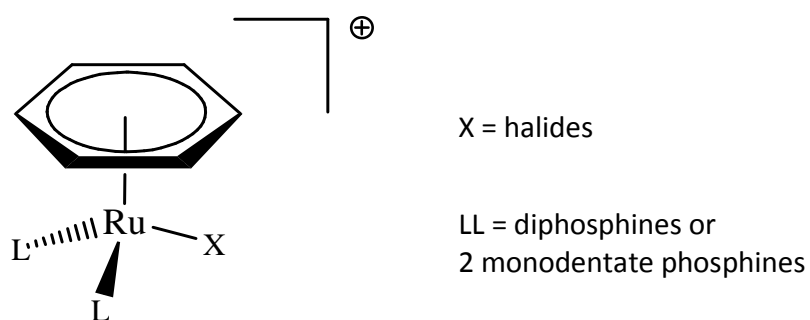


Figure 1.1 – Coordination sites for ligands in piano-stool complexes.

and electronic properties, for instance it prevents the metal centre from being rapidly oxidised to ruthenium (III).⁵ These properties linked to those of the corresponding co-ligands, affect reactivity and if the one of the ligands is chiral, it affects mainly the enantioselectivity, and this is higher with substituted arenes, for example, than with simple benzene.⁶ Modifications in the arene moiety, for instance the introduction of different substituents, provide ruthenium complexes with different solubility, reactivity, biological activity, immobilization potential, among others. These modifications can be achieved since the complexation of aromatic ligands by transition metal has a great effect on the reactivity of the arene. One major feature is the enhancement of the acidity of benzylic protons, which could lead to the alkylation and functionalisation of the methylated aromatic compounds. Arene ligands are relatively inert towards substitution reactions and consequently are often considered as spectator ligands.⁵

The other three coordinating sites available in the ruthenium complexes and are opposite to the arene ligands can be used to introduce a wide variety of ligands with N-, O-, S- or P-donor atoms.⁷ The resulting complexes are neutral, mono- or dicationic, and often these ligands are labile. In this project some monodentate and bidentate P-donor ligands (phosphines) were studied in catalytic reactions. Phosphine ligands have the general formula

PR_3 where R = alkyl, aryl, H, halide etc., and are neutral two electron donors that bind to transition metals through their lone pairs. A variety of chiral phosphine transition metal complexes have been reported in the literature;⁸ these phosphine-metal complexes are stereogenic and can function as stereospecific catalysts. Phosphines are easy to synthesise and are considered as excellent ligands for transition metals. As a consequence, the steric attributes of the phosphine ligand are easily controlled. This ability to control the bulk of the ligand permits one to tune the reactivity of the metal complex. For example, if the dissociation of a phosphine ligand is the first step in a reaction, the reaction can be accelerated by utilizing a larger phosphine ligand. Likewise, if dissociation is a problem, then a smaller phosphine can be used. The bonding in phosphine ligands, like that of carbonyls can be thought of as having two important components. The primary component is sigma donation of the phosphine lone pair to an empty orbital on the metal. The second component is backdonation from a filled metal orbital to an empty orbital on the phosphine ligand (figure 1.2). This empty phosphorous orbital has been described as being either a d-orbital or an antibonding sigma orbital; current consensus is that the latter is more

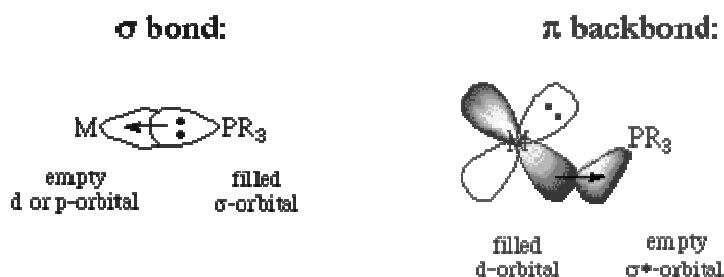


Figure 1.2 – Components of bonding in phosphine ligands.

appropriate given the relatively high energy of a phosphorous d-orbital. As electron-withdrawing (electronegative) groups are placed on the phosphorous atom, the sigma-donating capacity of the phosphine ligand tends to decrease. At the same time, the energy of the pi-acceptor (sigma-*) on phosphorous is lowered in energy, providing an increase in backbonding ability. Therefore, phosphines can exhibit a range of sigma donor and pi-acceptor capabilities, and the electronic properties of a metal centre can be tuned by the substitution of electronically different but isosteric phosphines.

Besides the coordinate phosphines, a third coordination position still available in the piano-stool complexes can be filled with halides. Indeed, halide ions are among the most common ligands found on transition metal catalysts and most of the available catalysts or pre-catalysts that can be found in the market are halo-complexes.⁹ Halides play the role of spectator or ancillary ligands in transition metal ligand-substitution reactions. Since most of the reactions with halo-complexes involve the removal of halides from the coordination sphere and replacement with weakly coordinating anions, halide ligands are often regarded as being of limited importance. Although, through a wise choice of the ancillary ligands it is often possible to alter the steric and electronic properties (influence both reactivity and selectivity) of the metal and therefore influence the course of many catalytic reactions.

In reactions where the halide is *cis* to the reaction, the relative size of the halide can influence the easiness of the process. For example, as the steric bulk of a ligand increases, oxidative addition process can be slowed while reductive elimination may be favoured as means of reducing the steric interactions. The steric bulk of halide ligands increase down the group in terms of ionic radii, covalent radii, and cone angle. On the other hand, electronegativity increases up the group. Due to this electronegativity profile and availability of the *s* electrons, the ability to form σ bonds increases down the group (figure 1.3). In the

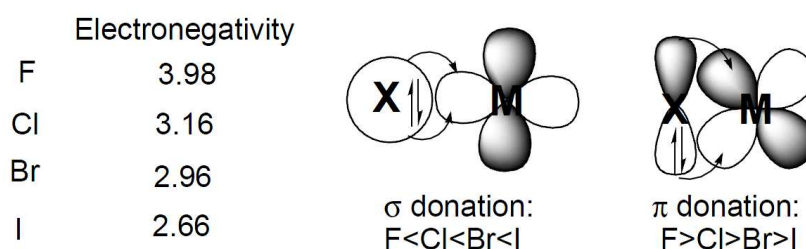


Figure 1.3 – Electronic properties of halide ligands.

absence of other interactions, iodide is expected to form the strongest bonds and donate the most electron density to the metal. This is rarely the case, however, since π interactions commonly occur between the halide lone-pair electrons and the metal *d* orbitals. When π interactions predominate, the opposite trend in electron donation to that predicted by electronegativity can be observed, and fluorine is the strongest π donor. π interactions occur when there is a metal orbital of appropriate symmetry available to interact with halide lone

pairs. If this orbital is empty, a net stabilization can result. If the *d* orbital is fully occupied, a net destabilization termed “filled-filled” interactions will occur (figure 1.4).

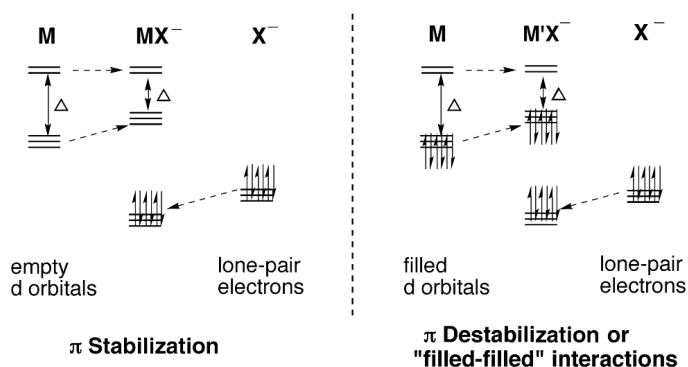


Figure 1.4 – Stabilization and destabilization arising from molecular orbital interactions for an octahedral coordination geometry.

Another halide feature that should be mentioned is the polarizability. Halides relative polarizability or softness is expected to increase down the group. It can be expected that as a transition metal becomes softer in character it will increasingly prefer to bind the heavier halides (other ligands present in the complex can influence this trend). Transition metals will become softer in character as its oxidation state is lowered, the further down the group it lies, and the further to the right in the transition metal series it is found.

1.3 Ligand Effects in Catalysis

Arene ruthenium complexes were shown to be catalytically active in hydrogenation, transfer-hydrogenation, Diels-Alder reactions, olefin metathesis, olefin cyclopropanation, atom-transfer radical polymerisation and kinetic resolutions.⁵ In most cases, the ruthenium catalyst precursor possesses a hydrocarbon η^6 -arene ligand with nitrogen or phosphorus donor ligands. In general, the catalytic activities and selectivity are good and are strongly affected by the nature of the arene ligand.¹⁰ In most cases the mechanism of these catalytic reactions remains a debatable point, and the role of the arene ligand is unclear. For instance, in the transfer hydrogenation of ketones, the arene moiety is assumed to be a spectator ligand, while for olefin metathesis and atom-transfer radical polymerisation, the catalytic activity results from arene displacement. Therefore, in some cases it is crucial to form a

robust molecular arene ruthenium catalyst to avoid arene exchange, while in other cases arene displacement is an essential step in the catalytic cycle.

Arene ruthenium compounds were employed as catalysts in asymmetric synthesis. The three-legged piano-stool complexes with three different ligands possess metal-centred chirality and some research groups are using the arene ligand to introduce a second element of chirality, thus giving rise to diastereoisomers instead of enantiomers which are difficult to resolve. The first strategy is to use planar chirality as a second element of chirality while the second possibility is to introduce an enantiomerically pure auxiliary group tethered to the arene ligand.

Apart from the aromatic ring, also halides have been reported as playing a significant role in some catalytic reactions. For example, D. Gillingham *et. al.* reported that the ruthenium iodide complex shown in figure 1.5 promotes ring-opening metathesis with significantly higher asymmetric induction than the chloride analogue, although being less active.¹¹ They attempted the reaction with the chiral iodide complex depicted in figure 1.5 in order to obtain higher optical purity, what came to be true. They were inspired by a disclosure by Grubbs who reported that addition of NaI to a solution of a chiral Ru-dichloride phosphine complex in certain cases leads to enhancement in enantioselectivity of ringclosing metathesis.

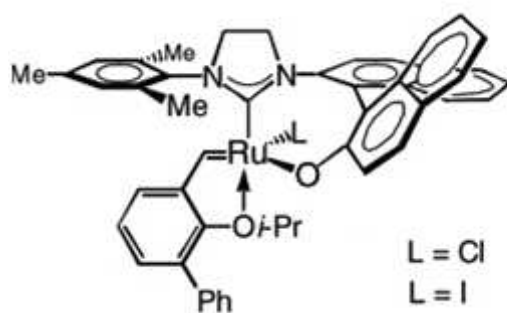


Figure 1.5 – Ruthenium complexes with different catalytic effects.

Phosphine ligands complexes of late transition metals have been widely used in almost every kind of C–H, C–C, and C–X bond-forming reactions, most notably asymmetric hydrogenation (Ru, Rh, Ir) and palladium catalysed processes.¹² Many of the phosphine ligands developed for hydrogenation reactions also generate high selectivity over a broad

canvas of mechanistic unrelated reactions, and were subsequently termed as “privileged” ligands (figure 1.6). This has stimulated further development of ligands that contain similar structure elements.

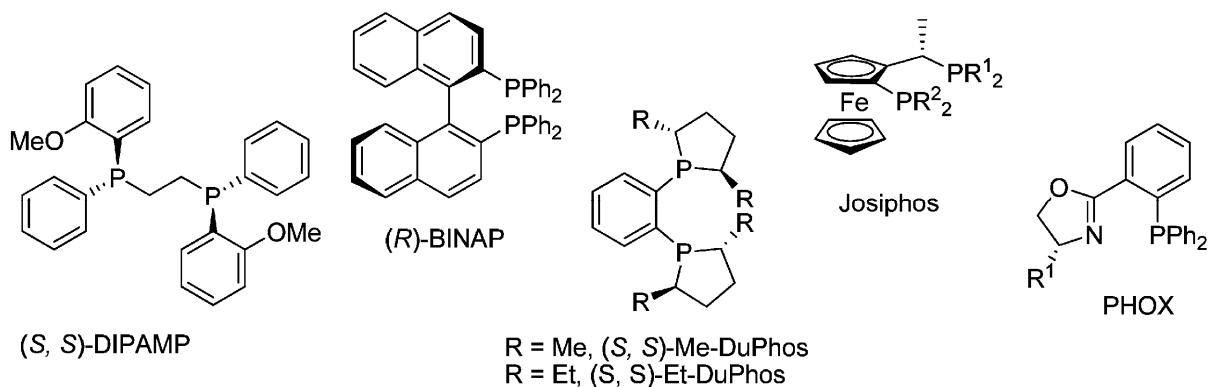


Figure 1.6 – “Privileged” phosphine ligands in catalysis.

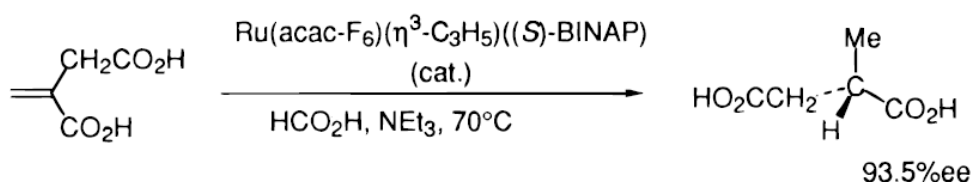
1.4 Ruthenium catalysts and Ruthenium Catalysed Reactions

Ruthenium has been playing a crucial role in catalysis. It is a widely used metal centre for catalytic complexes, employed in many different types of catalytic reactions at small and industrial scales. The reason for this is the large number of advantages that this metal presents. Since it has $4d^75s^1$ electron configuration, it has the widest scope of oxidation states of all elements of the periodic table, varying from -2 in complexes like $\text{Ru}(\text{CO})_4^{2-}$ to +8 in, for example, RuO_4 , and each of these oxidation states has a preferred coordination geometry, like trigonal-bipyramidal or octahedral for Ru(0), (II) and (III) respectively.¹³

Ruthenium complexes have a variety of useful characteristics including high electron transfer ability, high Lewis acidity, low redox potentials and stabilities of reactive metallic species such as oxometals, metallacycles, and metal carbene complexes. Since many of them are air and moisture stable, they can be prepared easily at ambient conditions, frequently using $\text{RuCl}_3 \cdot n\text{H}_2\text{O}$ as the starting material. Thus, a large number of novel, useful reactions have begun to be developed using both stoichiometric and catalytic amounts of ruthenium complexes.

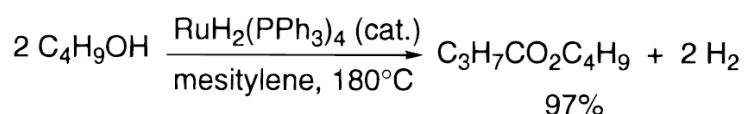
Ruthenium complexes have increased their importance in organic synthesis over the years. They have been used in reduction, oxidation, isomerisation and carbon-carbon bond formation. Some examples of reduction and oxidation reactions are shown below.

In reductions, ruthenium complexes have been used successfully in hydrogenations employing or not molecular hydrogen. Low-valent ruthenium complexes are excellent catalysts for these reactions because of their low redox potential and higher affinity toward heteroatom compounds. Ru-BINAP complexes serve as efficient catalysts for the asymmetric hydrogen transfer reactions of α,β -unsaturated carboxylic acids with formic acid (scheme 1.1). Combined use of ruthenium complexes with chiral amine ligands is proven to be highly effective for enantioselective synthesis.



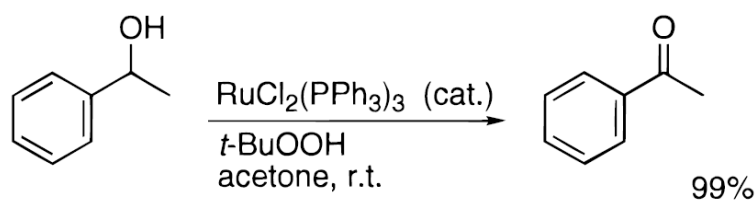
Scheme 1.1 – Enantioselective synthesis employing a ruthenium catalyst with a chiral ligand.

Ruthenium complexes have also been successfully employed in oxidations. One of the typical oxidations is the transformation of primary alcohols to the corresponding esters (scheme 1.2). These reactions are initiated by the oxidative addition of O-H bond of alcohols to low-valent ruthenium complexes and the subsequent β -hydrogen elimination.



Scheme 1.2 – Oxidation of an alcohol to an ester employing a ruthenium catalyst.

Low-valent ruthenium complexes also catalyze the oxidation of alcohols and the related hydroxy compounds in combination with various oxidants such as *t*-BuOOH, AcOOH, H₂O₂ etc. (scheme 1.3).



Scheme 1.3 – Oxidation of an alcohol employing a ruthenium catalyst and an oxidant.

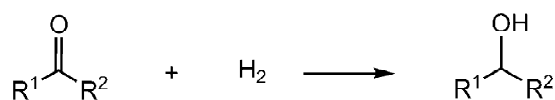
1.5 Reactions of Interest for this Project

The target catalytic reactions of this project are transfer hydrogenations and redox neutral alkylations. These reactions are of great interest to the pharmaceutical industry and to the chemical industry in general because they allow: the obtainment of compounds otherwise not possible to obtain synthetically; an easiest (cheaper) way to obtain compounds already available in the market; and, on the other hand, they are considered as “green” technology since, usually, the by-products are harmless to the environment (e. g. water).

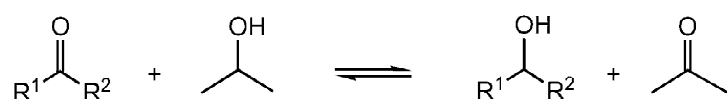
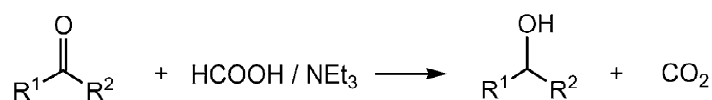
All the reactions that are being considered have several features in common, like all of them use similar transition metal catalysts composed by the metal and coordinating ligands and all of them proceed, in principle, through hydrogenations/dehydrogenations of ketones-alcohols, imines-amines or both, without the use of molecular hydrogen.¹⁴ These reactions are known as transfer hydrogenations where hydrogen atoms are transferred between an organic substrate and a hydrogen acceptor or donor. This occurs upon coordination of these molecules to the metal catalysts employed and they can proceed through different pathways. Bäckvall and co-workers² conclude that for transition metals, routes involving the formation of a hydride intermediate are by far the most common. In some of these reactions, hydride intermediates have already been isolated.

Transfer hydrogenation using alcohol as the hydrogen source is a convenient method to reduce ketones and imines because of the simplicity in experimental aspects. In this project were studied the reductive transfer hydrogenation of acetophenone and aldehyde. The advantages of hydrogen transfer over other methods of hydrogenation comprise the use of readily available hydrogen donors such as isopropanol, the very mild reaction conditions, and the high selectivity¹⁵ (scheme 1.4).

Hydrogenation



Transfer hydrogenation



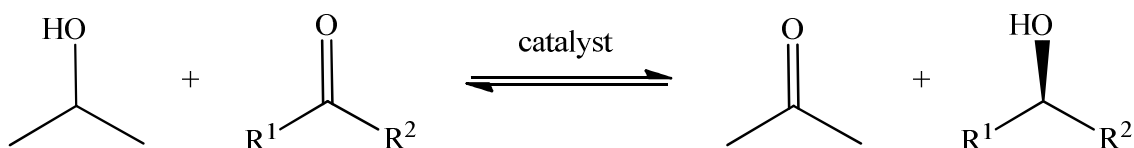
Scheme 1.4 – Hydrogenation and transfer hydrogenation of carbonyl compounds using either the formic acid/triethylamine or isopropanol as hydrogen source.

In fact, isopropanol has been widely used in transfer hydrogenations. Employment of this solvent which is not toxic and is easy to handle requires an excess of alcohol to shift the equilibrium to the desired product.¹⁶ This alcohol has been chosen instead of primary alcohols like ethanol or methanol since it has a more favourable redox potential. Furthermore, the aldehydes resulting from primary alcohols are susceptible in basic media to deprotonation of the hydrogens of the α -CH group which leads to aldol condensation and may also undergo decarbonylation reactions with deactivation of the catalysts.¹⁵ It is well-documented that the presence of a strong base as a cocatalyst enhances the rate of these reactions.¹⁷

Hydrogen transfer reactions have been used together with other reactions. Due to their reversibility, they have been exploited extensively in racemisation reactions in combination with kinetic resolutions of racemic alcohols.¹⁵ This resulted in the so called dynamic kinetic resolutions, kinetic resolutions of 100% yield of the desired enantiopure compound. Hydrogen transfer reactions were also incorporated in reactions called redox neutral alkylations which were also studied in this project and are described later.

The interest over transfer hydrogenations has increased over time. The fact that contributed the most to this was the application of this methodology together with chiral catalysts in the dehydrogenation of prochiral ketones which allowed the obtainment of alcohols in high enantiopure form. This transformation is known as asymmetric transfer

hydrogenation (ATH) and has recently been the subject of intense study by a number of groups worldwide.¹⁸ It is among the most important transformations to prepare alcohols in high enantiopure form from ketones (scheme 1.5). Among small chiral molecules, chiral alcohols occupy a central place in the synthesis of pharmaceuticals, flavour, aroma and agricultural chemicals, and speciality materials.¹⁹



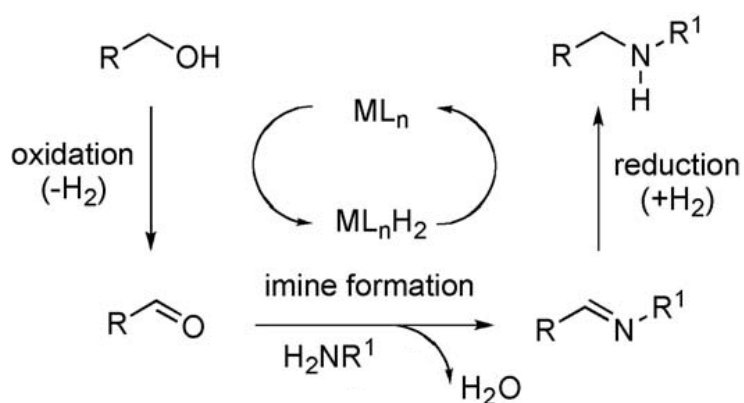
Scheme 1.5 – General scheme for the asymmetric transfer hydrogenation of ketones using isopropanol as hydrogen donor. The resulting by-product is a molecule of acetone.

The major contribution to ATH was provided by Noyori *et. al.*,²⁰ who reported highly active and robust Ru(II) catalysts based on complexes of monotosylated diamines and amino alcohols in the decade of 90. Generally, the reaction rate and the enantioselectivity are dependent on the electronic properties of the substituents on the aromatic ring as well as the steric environment of the carbonyl group²¹. It has also been reported that reactions proceed faster with electron-withdrawing groups in the substrates, and this has been explained in terms of molecular orbitals, with lower LUMO values giving faster reactions.^{22, 23} Since ATH is an operational simple and versatile reaction, it has become one of the best reduction systems for both academia and industry.¹⁸

Redox neutral alkylations or N-alkylations are reactions that convert primary amines into secondary or tertiary amines using alcohols as alkylating agents.²⁴ Amines are of significant importance for the bulk and fine chemical industry as building blocks for polymers, dyes, but also for the synthesis of new pharmaceuticals and agrochemicals.²⁵ Previous methodology used alkyl halides as alkylating agent but it can give rise to poly-alkylation products and is unpleasant for the environment because alkyl halides can be toxic and generate wasteful salts as by-products.²⁶ Another well-known method which has been developed as the most useful tool in the synthesis of various amines is the reductive amination of aldehydes and ketones. But, because it requires the use of strong reducing

agents or dangerous hydrogen gas, is not the best one to follow. Also this method is not always selective for monoalkylation of primary amines. The *N*-alkylation of amines with alcohols proceeds via a hydrogen borrowing strategy²⁴ (scheme 1.6). This strategy combines the advantages of transfer hydrogenation with additional transformations. The hydrogen donor compound is not a waste compound such as isopropanol. Initially the alcohol borrows the hydroxilic proton to the catalyst and forms a carbonyl compound (oxidation by transfer hydrogenation), then the carbonyl compound reacts with the primary amine to give an imine, which is then converted to the final amine by reductive amination with the hydrogens borrowed by the alcohol through the catalyst.

The alkylation of amines by alcohol occurs with loss of water and has been proved to be a thermodynamically favored process where the loss of a C-O bond for a C-N bond is compensated by the gain of an O-H bond for an N-H bond.¹



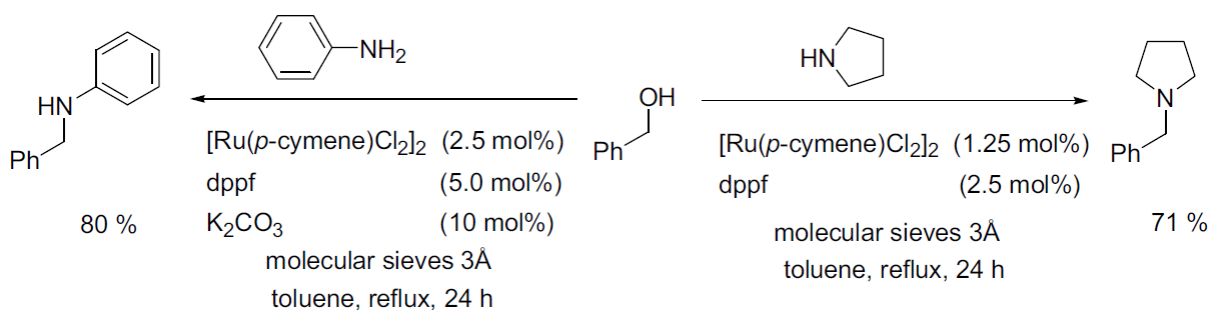
Scheme 1.6 – Borrowing Hydrogen Strategy in the alkylation of amines with alcohols.²⁷

The first homogeneous catalysts for *N*-alkylation of amines with alcohols were introduced by Grigg *et. al.*²⁸ and Watanabe *et. al.*²⁹ in the early 1980s. Grigg and co-workers described the *N*-alkylation of primary and secondary alkyl amines with primary alcohols such as methanol or ethanol with the rhodium catalyst [RhH(PPh₃)₄] being the most active. Watanabe and co-workers reported the ruthenium-catalyzed *N*-alkylation of aniline with primary alcohols with [RuCl₂(PPh₃)₃]. There have been several ruthenium³⁰⁻³³ and iridium³⁴⁻³⁶ catalysts reported subsequently. Many of these catalysts require forcing conditions which prevents their use with sensitive substrates. However, Yamaguchi and co-workers²⁶ have

already employed milder conditions with Cp*IrCl₂ as well as Beller's group using Ru₃(CO)₁₂ with bulky phosphines.³⁷

The most active catalysts for these reactions have been proved to be those of iridium, like [Ir(COD)Cl]₂ (COD = cyclooctadiene) or [Cp*Ir]₂, but ruthenium has also been used due to more accessible costs.⁶

Recently, J. Williams *et. al.*²⁴ have reported a high efficient *in situ* ruthenium catalyst consisting of [Ru(*p*-cymene)Cl₂]₂ and dppf for the *N*-alkylation of amines with primary alcohols. The reaction conditions are relatively mild and applicable to the alkylation of aryl amines as well as cyclic aliphatic amines such as pyrrolidine (scheme 1.7)^{1,24}.



Scheme 1.7 – Ruthenium-catalyzed *N*-alkylation of amines with primary alcohols by J. Williams *et. al.* showing the reaction yields.¹

As seen, *N*-alkylation is a very attractive method because (1) the overall reaction is atom efficient consuming all of the starting material; (2) it does not generate harmful by-products (only H₂O) and (3) alcohols are environmentally benign as well as more readily available than corresponding halides or carbonyl compounds in many cases.^{26,27} Although these reactions have been frequently applied, there is no catalytic method available for functionalized and sensitive substrates (alcohols and amines) under milder conditions (<100 °C). It was because of this fact that this project was carried out in order to look for more active catalysts which allow a broader substrate scope.

1.6 Mechanistic Features Common to the Reactions of Interest

Several studies have been carried out in order to understand the mechanistic pathway in hydrogen transfer reactions. The reactions mentioned before use transition

metal catalysts and Bäckvall and co-workers, despite not having entirely elucidate the mechanisms, have summarized some common features for these metals.² They found that routes involving the formation of a hydride intermediate are by far the most common. Such hydrides have indeed been isolated from transition metal-catalyzed hydrogen transfer reactions in some cases (figure 1.7).

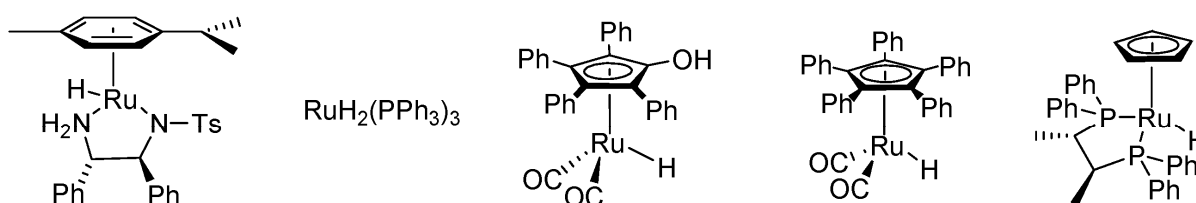


Figure 1.7 – Examples of metal hydrides that have been isolated or proven to take place in hydrogen transfer reactions.

Hydrogen transfers to ketones (aldehydes) are supposed to occur mainly by two pathways. Either by a hydridic route for transition metals as said before or by a direct hydrogen transfer that is thought to be the main pathway for main group metals. Indeed, the later pathway was one of the first approaches to reactions like transfer hydrogenations. It consists in the Meerwein-Ponndorf-Verley (MPV) reduction of ketones by alcohols or the reverse reaction, the Oppenauer oxidation. It is proposed to proceed through a six-membered transition state ring as shown in figure 1.8.

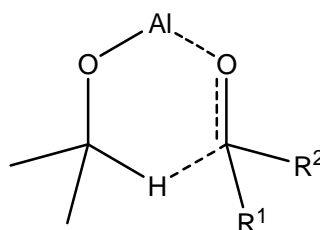
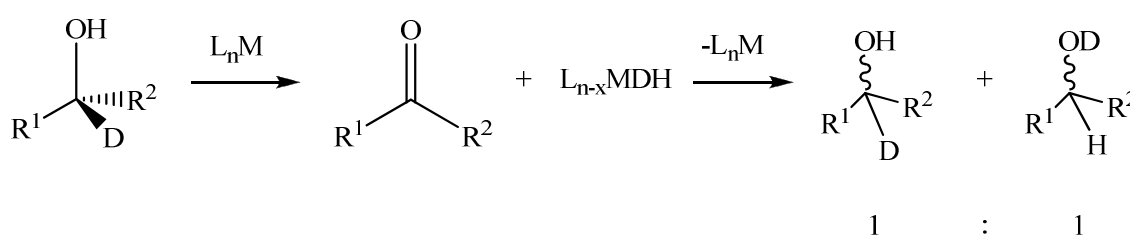


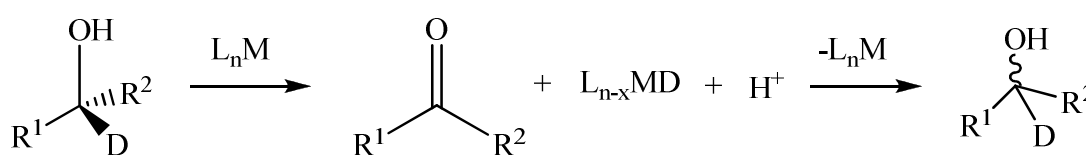
Figure 1.8 – Original version of the MPV reduction. Direct hydrogen transfer through an aluminium alkoxide using isopropanol reported in the early XX century.²

Due to the drawbacks of scaling up the MPV, namely the aluminium salt is often required in stoichiometric amount,¹⁷ there has been an increased interest in catalytic hydrogen transfer reactions. This led to the discovery of the catalytic activity of transition metals which were found to work via a hydridic route. Some research groups^{2, 38-40} have

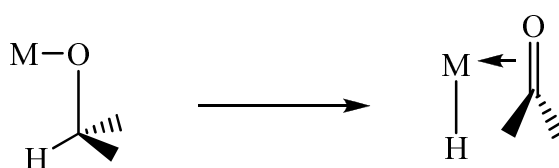
suggested that there are two possible main pathways for this route. It proceeds either by a dihydride or monohydride mechanism which will depend both on the metal employed and the ligands coordinated to that metal in the catalytic complex. Experimentally, it was found that while rhodium and iridium catalysts favor the monohydride route, the mechanism for ruthenium catalysts proceeds by either pathway depending on the ligands. Deuteration experiments are usually carried out to find out the route for each case. In the dihydride mechanism both hydrogens from C-H and O-H in the hydrogen donor are transferred to the metal as hydrides (scheme 1.8) whereas in the monohydride mechanism only the C-H hydrogen from the donor enters in the coordination sphere that way (scheme 1.9). The monohydride mechanism followed depends on both the catalyst and substrate and the classical is the one involving a metal alkoxide as intermediate.² This path is known as Inner-sphere pathway (scheme 1.10).



Scheme 1.8 – Racemisation of an α -deuterated chiral alcohol in the dihydride mechanism.²

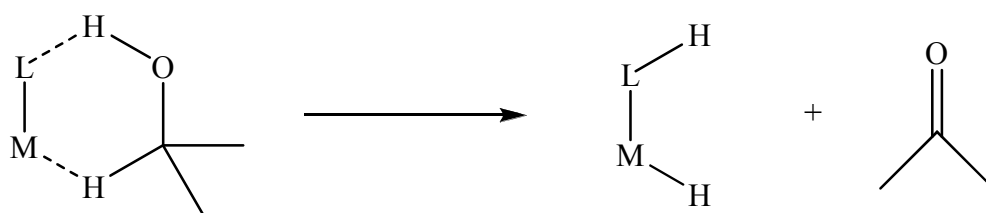


Scheme 1.9 – Racemisation of an α -deuterated chiral alcohol in the monohydride mechanism.²

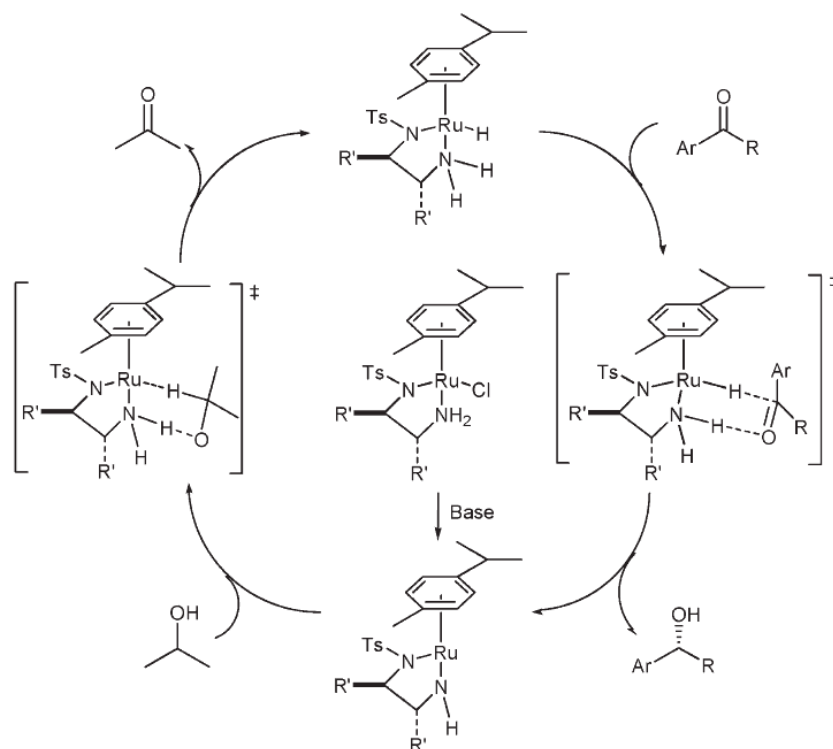


Scheme 1.10 – Inner-sphere pathway for monohydride mechanisms.²

After formation of the metal alkoxide by direct coordination of the alcohol to the metal, β -elimination takes place to give the metal hydride. However, this mechanism is thought of not being the most likely to occur in catalysts that contains a basic centre in one of their ligands. In these catalysts the basic center interacts by means of a hydrogen bond with the protic hydrogen from the donor, while the hydrogen in the carboxylic carbon bonds to the metal forming a six-membered transition state which promotes the hydride formation (scheme 1.11). So there is a simultaneous transfer of a proton to the metal and to the ligand without prior coordination of the substrate to the metal. This is a monohydride outer-sphere mechanism and an example of that is the so called Noyori's metal ligand bifunctional catalysis. The full catalytic cycle is outlined in Scheme 1.12.¹⁹ It proceeds in a concerted manner, but outer-sphere mechanisms can also occur in two discrete steps, where the protonation of the substrate precedes the hydride transfer.²



Scheme 1.11 – Outer-sphere concerted pathway for monohydride mechanisms.²

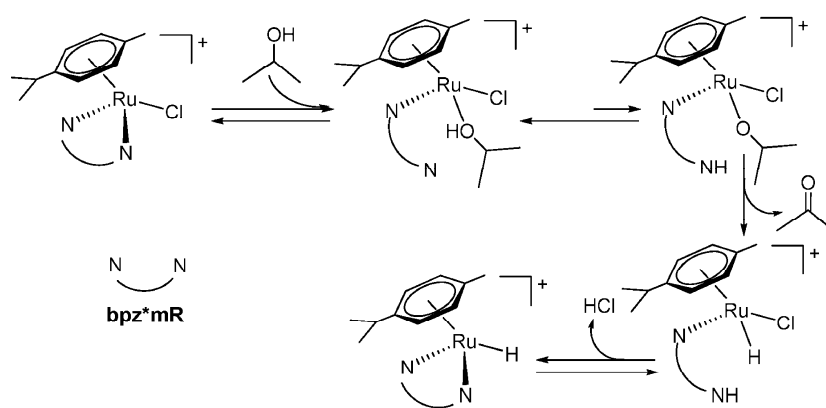


Scheme 1.12 – ATH of ketones by isopropanol via Noyori's metal–ligand bifunctional catalysis.¹⁹

In the Noyori's metal ligand bifunctional catalysis, Noyori employed chelating ligands with NH₂ groups like N-(*p*-toluenesulfonyl)-1,2-diphenylethylenediamine to form complexes like [RuCl(η^6 -arene)TsDPEN]. In this complex, the NH₂ group of the TsDPEN ligand needs to be treated with a base to achieve deprotonation and form the active species (scheme 1.12). These complexes proved to be highly efficient in asymmetric transfer hydrogenations.²⁰

The presence of a strong base like NaOH or KOH is usually a pre-requisite for bifunctional catalysis. This fact represents a drawback from an industrial point of view due to corrosion, possible negative effects in stereoselectivity and cannot be used for base-sensitive substrates. It has been demonstrated by Carrión and co-workers that hydrogen transfer hydrogenations can proceed without employing any base when ligands are of the type NN.⁴¹ They found possible the decoordination of the NN ligand and formation of an unsaturated species, which can first allow the coordination of alcohol forming an alkoxide to give a ruthenium hydride by β -elimination (inner-sphere pathway) and then the coordination of the substrate to be hydrogenated (scheme 1.13).

p-Cymene Based Ruthenium Complexes as Catalysts



Scheme 1.13 – Mechanism for the hydride formation in the catalytic transfer hydrogenation of ketones under base-free conditions proposed by Carrión *et al.*⁴¹

2. Results and Discussion

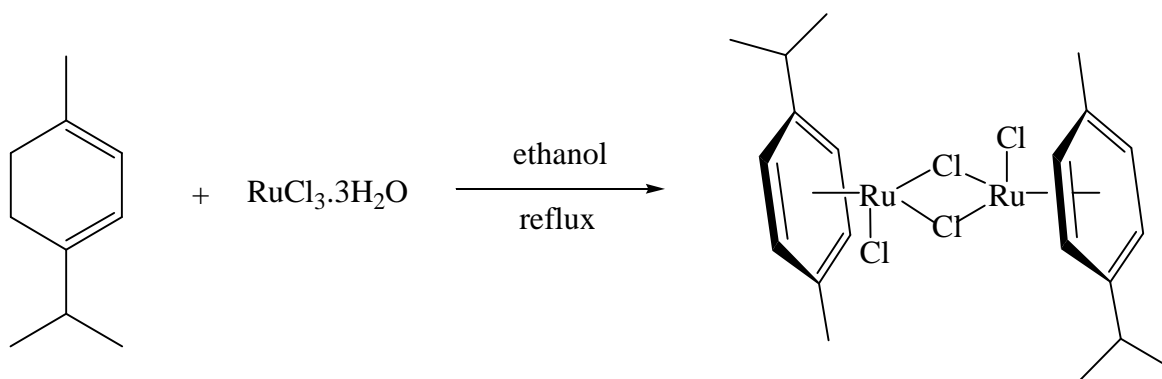
2.1 Target Molecules with Regard to Catalytic Studies

The initial target molecules of this project are complexes with the formula $[\text{RuX}_2(\eta^6\text{-cymene})]_2$, this is dihalide(*p*-cymene)ruthenium(II) dimers. These molecules are intended to be the precursors for possible ruthenium catalysts of the reactions under investigation. The reason to start with these *p*-cymene dimers is that the chlorine dimer $[\text{RuCl}_2(\textit{p}\text{-cymene})]_2$ (**1**) has been proved to be effective in the catalytic processes of interest for the project and has been widely used to synthesise *p*-cymene based ruthenium complexes which show promising catalytic potential. Different halides were incorporated in these complexes. Their different relative lability is expected to have different implications on the relative activity of these complexes. This is because the catalytic reactions of interest for this project are supposed to proceed via the formation of a ruthenium hydride complex, which would require the dissociation of a labile pre-existing ligand. Both the chlorine and iodine dimers, $[\text{RuCl}_2(\textit{p}\text{-cymene})]_2$ (**1**) and $[\text{RuI}_2(\textit{p}\text{-cymene})]_2$ (**2**) respectively, are commercially available but their syntheses are relatively simple. $[\text{RuCl}_2(\textit{p}\text{-cymene})]_2$ (**1**) was chosen as the starting material to try to obtain $[\text{RuBr}_2(\textit{p}\text{-cymene})]_2$ (**3**) and $[\text{RuI}_2(\textit{p}\text{-cymene})]_2$ (**2**) since it is the easily available one. Previous methods reporting the synthesis of the $[\text{RuCl}_2(\textit{p}\text{-cymene})]_2$ (**1**) include those of Bennett *et al.*⁴² and M. Spicer *et al.*⁴³ The synthesis of $[\text{RuI}_2(\textit{p}\text{-cymene})]_2$ (**2**) and $[\text{RuBr}_2(\textit{p}\text{-cymene})]_2$ (**3**) has been reported by C. Hartinger and co-workers⁴⁴.

The catalytic properties of these dimers in the presence of the phosphine ligands (dippf, DPEPhos and P^{*i*}Bu₃) selected by Astra Zeneca⁴⁵ (biopharmaceutical company) were evaluated mainly by ¹H NMR by the calculation of the percentage of conversion into the catalytic product. Some gas chromatography (GC) studies were attempted in order to monitor the reactions (% of conversion over time) but due to several complications not many results were obtained. The effect of different halides and different phosphine ligands in catalysis was evaluated. Some new ruthenium half-sandwich complexes were synthesised and the same studies were performed.

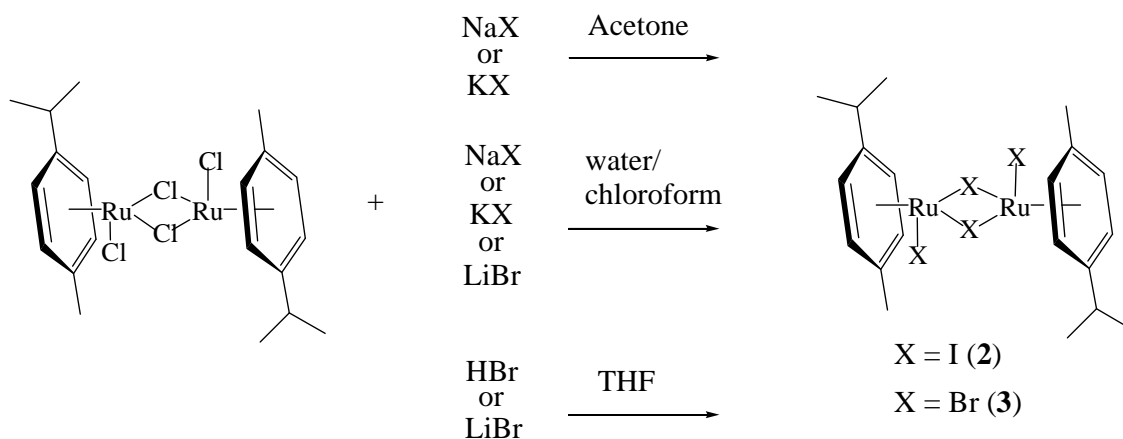
2.2 Synthesis of the Ruthenium Precursors [RuX₂(*p*-cymene)]₂ (X=Cl, Br, I)

[RuCl₂(*p*-cymene)]₂ (**1**) had already been synthesised within the McGowan's group with a procedure adapted from those cited before.⁴⁶ This procedure was optimized and used in this project. The dimer was obtained in 92% yield by a reaction between 4-methyl-1-(1-methylethyl)-1,3-cyclohexadiene (α -Terpinene) and RuCl₃·3H₂O in reflux of ethanol (scheme 2.1). Elemental analysis and mass spectrometry results matches to what is expected.



Scheme 2.1 – Synthesis of [RuCl₂(*p*-cymene)]₂ (**1**).

To synthesise [RuI₂(*p*-cymene)]₂ and [RuBr₂(*p*-cymene)]₂ it can be used RuI₃ and RuBr₃ as start materials but these ruthenium (III) complexes are expensive, so the following halide exchange reactions were carried out (scheme 2.2):



Scheme 2.2 – Synthesis carried out to obtain $[\text{RuI}_2(\textit{p}\text{-cymene})]_2$ (**2**) and $[\text{RuBr}_2(\textit{p}\text{-cymene})]_2$ (**3**).

The synthesis of $[\text{RuI}_2(\textit{p}\text{-cymene})]_2$ (**2**) and $[\text{RuBr}_2(\textit{p}\text{-cymene})]_2$ (**3**) was already attempted within the McGowan's group by A. Rodríguez.⁶ $[\text{RuI}_2(\textit{p}\text{-cymene})]_2$ (**2**) was obtained in a good yield (80%) by reacting $[\text{RuCl}_2(\textit{p}\text{-cymene})]_2$ (**1**) with NaI in acetone under a nitrogen atmosphere,¹⁴ according to a procedure that uses iridium instead of ruthenium.⁴⁷ The microcrystalline product was characterized by ¹H NMR and elemental analysis and was compared with the literature⁴⁴ which confirmed the product formation. In the literature⁴⁴ it is reported the synthesis of $[\text{RuI}_2(\textit{p}\text{-cymene})]_2$ (**2**) using the respective potassium salt (KI) and water/chloroform. They obtained a dark violet solid in 67% yield. These same two procedures were attempted before to obtain $[\text{RuBr}_2(\textit{p}\text{-cymene})]_2$ (**3**) but none of them were successful. In the first one (NaBr in acetone) a not clear ¹H NMR spectrum of the orange product was obtained and, if present, only 26% yield was achieved. In the second procedure (KBr in water/chloroform) again the ¹H NMR was not clear and no yield was calculated.

In this project, some other reactions were attempted by varying the solvent and the halide salt in order to obtain a better yield and a better product characterization. Reactions with the salts KI (dark violet color, 58% yield), NaBr (brown color, mixture of products) and KBr (red color, mixture of products) were attempted in acetone. In water/chloroform reactions was attempted the use of NaI (dark violet color, 91% yield), NaBr (orange color, 53%), KBr (orange color, 31%) and LiBr (orange color, 31%). LiBr and HBr in THF were also employed in the synthesis of $[\text{RuBr}_2(\textit{p}\text{-cymene})]_2$ (**3**) as suggested by a paper of Süss-Fink and co-workers⁴⁸ but the starting material was obtained after all.

Summarizing, the best results of the synthesis of $[\text{RuI}_2(\textit{p}\text{-cymene})]_2$ (**2**) and $[\text{RuBr}_2(\textit{p}\text{-cymene})]_2$ (**3**) were in water/chloroform employing NaI and NaBr respectively. $[\text{RuI}_2(\textit{p}\text{-cymene})]_2$ (**2**)

cymene)]₂ (**2**) was obtained in very good yield (91%) and ¹H NMR is very clear with all the signals being shifted (mainly downfield) compared to those of [RuCl₂(*p*-cymene)]₂ (**1**) (figure 2.1). The color is different as well; [RuI₂(*p*-cymene)]₂ (**2**) is a very dark violet, almost black solid, while [RuCl₂(*p*-cymene)]₂ (**1**) is red. [RuBr₂(*p*-cymene)]₂ (**3**) was obtained in 53% yield (orange), but the ¹H NMR peaks have the same chemical shift as [RuCl₂(*p*-cymene)]₂ (**1**) peaks. The only difference is that they are broadened. To conclude more about this fact, [RuCl₂(*p*-cymene)]₂ (**1**) was added to the NMR tube containing [RuBr₂(*p*-cymene)]₂ (**3**) and it was observed that the height of the peaks has increased, however the broadness has remained. It suggests that [RuBr₂(*p*-cymene)]₂ (**3**) is actually a mixture of [RuBr₂(*p*-cymene)]₂ (**3**) and [RuCl₂(*p*-cymene)]₂ (**1**) and the amount of [RuCl₂(*p*-cymene)]₂ (**1**) added just increased the amount of it in the mixture.

Full characterization data for compounds [RuCl₂(*p*-cymene)]₂ (**1**), [RuI₂(*p*-cymene)]₂ (**2**) and [RuBr₂(*p*-cymene)]₂ (**3**) can be found in the experimental section. ¹H NMR spectra of these three compounds are shown in figure 2.1 and a labelled diagram of complex **1** in figure 2.2. In table 2.1 is found the ¹H NMR chemical shift assignment for **1**.

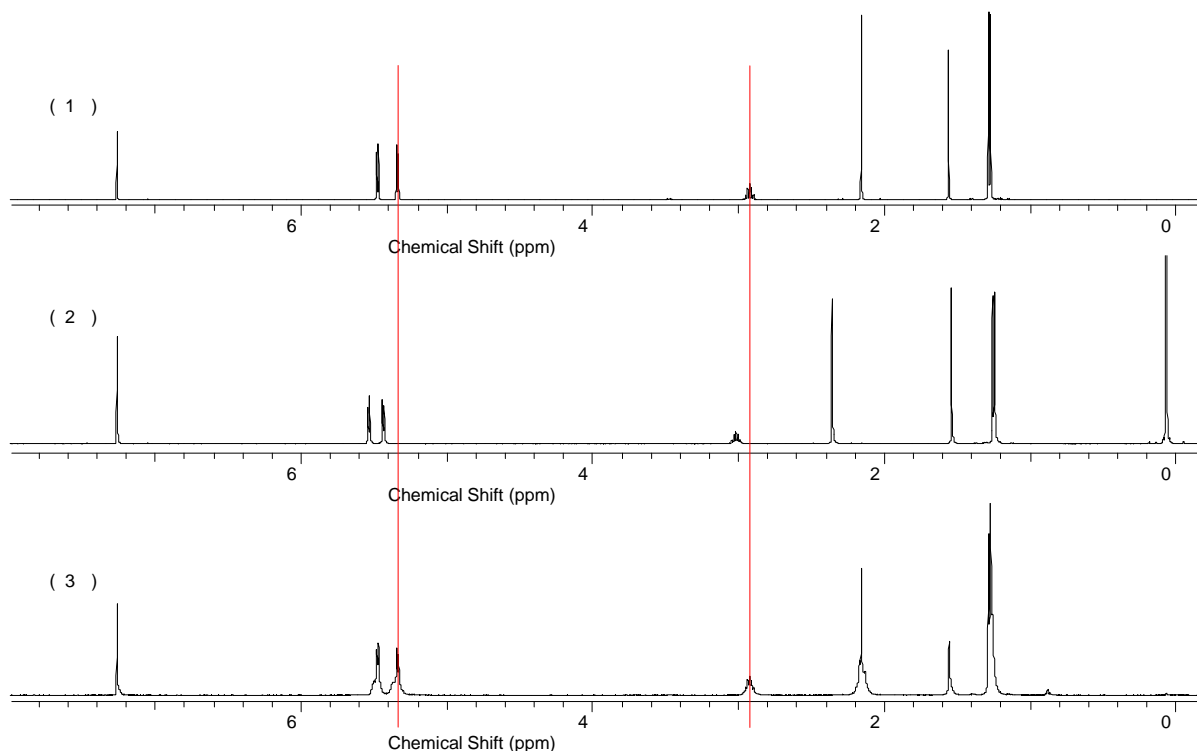


Figure 2.1 – ¹H NMR spectra of [RuCl₂(*p*-cymene)]₂ (**1**), [RuI₂(*p*-cymene)]₂ (**2**) and [RuBr₂(*p*-cymene)]₂ (**3**) in CDCl₃.

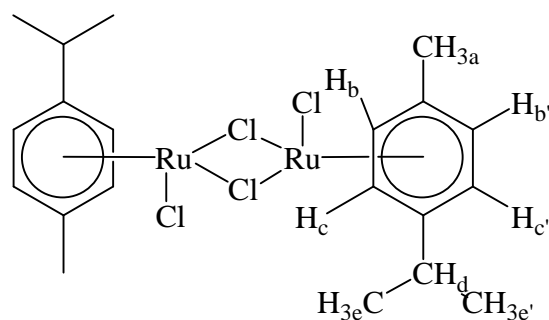


Figure 2.2 – Labelled diagram of $[\text{RuCl}_2(p\text{-cymene})]_2$ (**1**) for ^1H NMR purposes.

Table 2.1 – ^1H NMR chemical shift assignment of $[\text{RuCl}_2(p\text{-cymene})]_2$ (**1**).

Chemical Shift, δ (ppm) ^1H	Assignment
5.48 (d, 4H)	c, c'
5.35 (d, 4H)	b, b'
2.93 (sept, 2H)	d
2.17 (s, 6H)	a
1.29 (d, 12H)	e, e'

Protons b & b' and c & c' are not chemically equivalent and consequently the *p*-cymene ligand exhibits a quadruplet AB which integrates to 8H.

NMR spectroscopy allowed distinguishing $[\text{RuCl}_2(p\text{-cymene})]_2$ (**1**) from $[\text{Ru}_2(p\text{-cymene})]_2$ (**2**), but not from $[\text{RuBr}_2(p\text{-cymene})]_2$ (**3**). Also, elemental analysis and mass spectrometry agreed with what is expected for $[\text{RuCl}_2(p\text{-cymene})]_2$ (**1**) and $[\text{Ru}_2(p\text{-cymene})]_2$ (**2**) but not for $[\text{RuBr}_2(p\text{-cymene})]_2$ (**3**). These results associated with the fact that different exchange reactions led to different shades of orange when trying to get $[\text{RuBr}_2(p\text{-cymene})]_2$ (**3**) suggests that those reactions led to a mixture of both $[\text{RuCl}_2(p\text{-cymene})]_2$ (**1**) and $[\text{RuBr}_2(p\text{-cymene})]_2$ (**3**) which could not be separated. This difficulty in its preparation may be related with solubility issues, where the formation of NaCl from NaBr may not be favoured. $[\text{RuBr}_2(p\text{-cymene})]_2$ (**3**) was found to be successfully synthesised by G. Süss-Fink and co-workers⁴⁸ who reacted $[\text{Ru}_2(p\text{-cymene})_2\text{Cl}_2(\mu\text{-H})]$ with hydrobromic acid, but this method has not been tried in this project. Because of these issues with the synthesis of $[\text{RuBr}_2(p\text{-cymene})]_2$ (**3**) it was not used in further synthesis/catalytic reactions.

Complexes $[\text{RuCl}_2(\textit{p}\text{-cymene})]_2$ (**1**) and $[\text{Ru}_2(\textit{p}\text{-cymene})]_2$ (**2**) present similar solubilities and stability. Both of them are soluble in common solvents and are air stable. Water solubility is negligible.

2.3 Synthesis of *p*-cymene ruthenium monomers

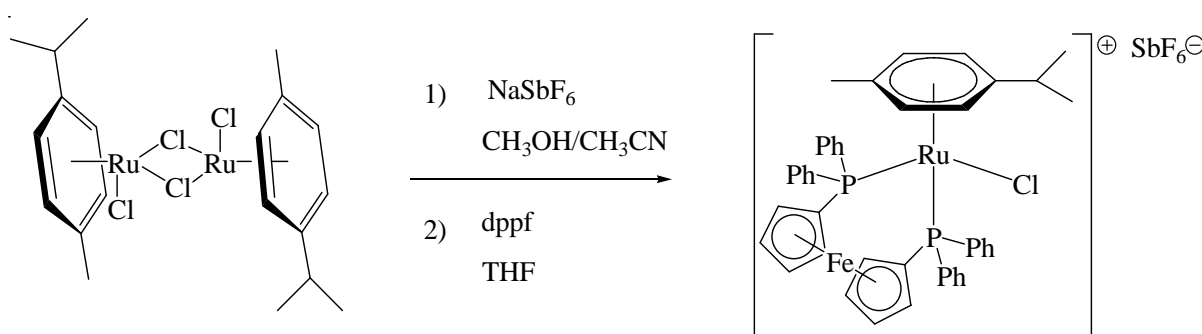
Some half-sandwich ruthenium complexes containing phosphine ligands were synthesised for the first time in order to test them as catalysts and conclude something about the mechanistic features. These complexes are important in the immobilization point of view for heterogeneous catalysis. A complex like that is often called a ruthenium monomer and is supposed to be formed and act as the actual pre-catalyst in reactions where dimers and for example a phosphine ligand like dppf are employed in one-pot reactions.²⁴ This idea comes from the metal ligand bifunctional catalysts developed by Noyori, specifically from the $[\text{RuClTsDPEN}(\textit{p}\text{-cymene})]$ complex, which was proven to be formed in the catalytic reaction between $[\text{RuCl}_2(\textit{p}\text{-cymene})]_2$ and TsDPEN ligand to act as the actual pre-catalysts in asymmetric transfer hydrogenations. The intermediates have been isolated and their structures determined by X-ray crystallography.^{19, 49, 50} The phosphine ligands that were employed in the catalytic reactions together with the dimers in this project were incorporated in some of these monomers so it is possible to compare the activity of the monomers to the one of the dimers. The focus was also to synthesise complexes with different counter-ions since it is expected that ruthenium complexes with larger, less coordinating anions should prove to be more effective as catalysts. This fact has already been proved by S. Lord⁵¹ from the McGowan's group in the hydrogenation of acetophenone employing ruthenium half-sandwich complexes with picolinamide and *p*-cymene ligands. This fact will be now verified in N-alkylations.

2.3.1 Synthesis of $[\text{RuCl}(\text{dppf})(\textit{p}\text{-cymene})]\text{SbF}_6$ (**4**)

The synthesis of $[\text{RuCl}(\text{dppf})(\textit{p}\text{-cymene})]\text{SbF}_6$ (**4**) was attempted by two different methods. The second one was attempted after the first one since it is simpler and gave good results when attempted before with other compounds.

2.3.1.1 Method 1

[RuCl(dppf)(*p*-cymene)]SbF₆ (**4**) was synthesised as shown in scheme 2.3. After stirring the chlorine dimer in a mixture of methanol-acetonitrile and NaSbF₆, dppf ligand in THF was added (1:2:2 molar ratio) and left stirring at room temperature. It was recrystallised from a mixture of ethanol and acetone to afford a brownish orange powder in 29% yield. This procedure was adapted from the protocol of synthesis of [RuCl(dppf)(*p*-cymene)]PF₆, this is complex **4** but with PF₆⁻ as counter-ion, reported by W. Kaim *et. al.*⁵² Syntheses of the same compound (with PF₆⁻) were after reported by M. Spicer and co-workers⁴³ and Y. Yamamoto *et. al.*⁵³ Compound **4** as far as it is known has not been synthesised before, is air and moisture stable, cationic 18-electron complex and was characterized by ¹H, ¹³C{¹H} and ³¹P{¹H} NMR, mass spectrometry and elemental analysis. The NMR studies that were done for compound **4** were sort of extensive since not that detailed NMR assignments were reported before in the literature for structure related compounds like [RuCl(dppf)(*p*-cymene)]PF₆^{43, 52, 53}, [RuCl(dppf)(η^5 -Cp)]⁵⁴ or [(*p*-Cymene)Ru(μ -Cl)₃RuCl(dppf)]⁵⁵.



Scheme 2.3 – Synthesis of [RuCl(dppf)(*p*-cymene)]SbF₆ (**4**).

2.3.1.1 Method 2

The method here attempted was based in the synthesis of *p*-cymene picolinamide ruthenium half-sandwich complexes reported by S. Lord⁵¹ from the McGowan's group.

[RuCl₂(*p*-cymene)]₂ (**1**) dissolved in methanol, was treated with dppf in the presence of NaSbF₆ in a 1:2:2 molar ratio at room temperature to precipitate an orange powder in

79% yield without the need of further purification. The product was only characterized by ^1H NMR.

2.3.1.2 ^1H , $^{13}\text{C}\{^1\text{H}\}$ and $^{31}\text{P}\{^1\text{H}\}$ NMR characterization for $[\text{RuCl}(\text{dppf})(p\text{-cymene})]\text{SbF}_6$ (**4**)

The following characterization was done with $[\text{RuCl}(\text{dppf})(p\text{-cymene})]\text{SbF}_6$ (**4**) synthesised by method 1. A labelled diagram of compound **4** is shown in figure 2.3. Spectral assignments for this compound are found in table 2.2. The ^1H NMR spectrum, $^{13}\text{C}\{^1\text{H}\}$ NMR spectrum and two partial HMQC spectra are shown in figures 2.5, 2.6 and 2.7, respectively.

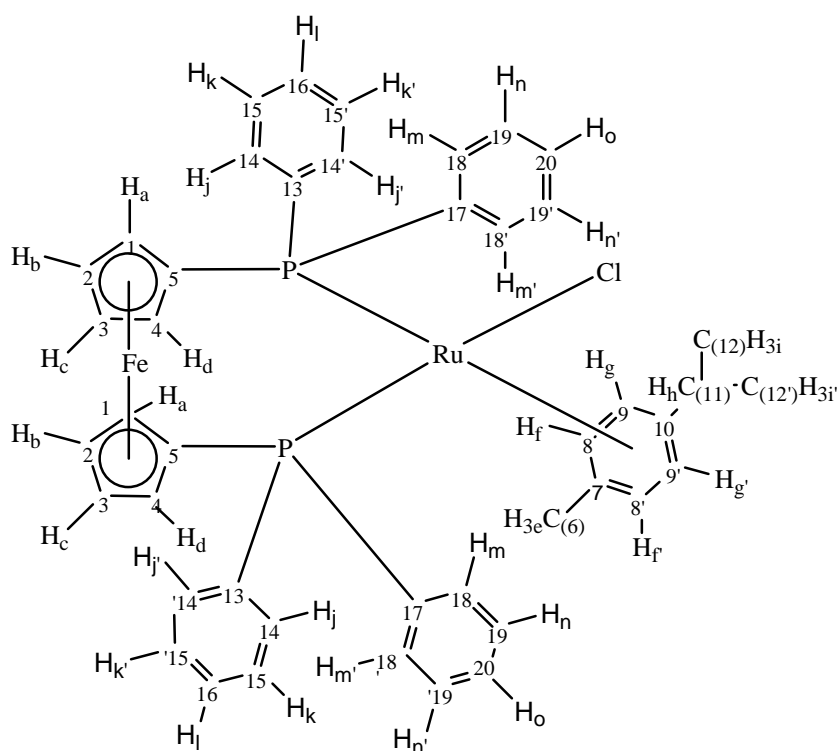


Figure 2.3 – Labelled diagram of $[\text{RuCl}(\text{dppf})(p\text{-cymene})]\text{SbF}_6$ (**4**) for NMR purposes.

Table 2.2 – ^1H and $^{13}\text{C}\{^1\text{H}\}$ NMR chemical shift assignment of $[\text{RuCl}(\text{dppf})(p\text{-cymene})]\text{SbF}_6$ (**4**) in $(\text{CD}_3)_2\text{CO}$.

Chemical Shift, δ (ppm) ^1H	Assignment	Chemical Shift, δ (ppm)	Assignment
7.87 (m, 4H)	j,j' or m,m'	139.55 ('t', 2C)	13 or 17
7.78 (m, 2H)	l or o	136.24 (t, 4C)	14,14' or 18,18'
7.72 (m, 4H)	k,k' or n,n'	134.92 ('t', 2H)	13 or 17
7.72 (m, 4H)	j,j' or m,m'	134.41 (t, 4C)	14,14' or 18,18'
7.52 (m, 2H)	l or o	132.97 (s, 2C)	16 or 20
7.50 (m, 4H)	k,k' or n,n'	131.61 (s, 2C)	16 or 20
6.12 (broad s, 2H)	g,g' or f,f'	129.40 (t, 4H)	15,15' or 19,19'
5.52 (d, 2H)	g,g' or f,f'	129.20 (t, 4H)	15,15' or 19,19'
5.06 (s, 2H)	a, b, c or d	100.08 (s, 1C)	7 or 10
4.49 (s, 2H)	a, b, c or d	97.29 ('t', 2C)	8,8' or 9,9'
4.40 (s, 2H)	a, b, c or d	91.77 (t, 2C)	8,8' or 9,9'
4.21 (s, 2H)	a, b, c or d	84.84 ('t', 1C)	5
2.75 (m, 1H)	h	79.36 (t, 1C)	1, 2, 3 or 4
1.05 (s, 3H)	e	75.81 (t, 1C)	1, 2, 3 or 4
0.88 (broad s, 6H)	i,i'	74.60 (t, 1C)	1, 2, 3 or 4
		70.24 (t, 1C)	1, 2, 3 or 4
		31.65 (s, 1C)	11
		21.00 (s, 2C)	12,12'
		14.95 (s, 1C)	6

The characteristic feature of the ^1H NMR spectrum (figure 2.5) is the presence of four kinds of protons in the range from δ 4.21 to 5.06 ppm, four sharp singlets corresponding to the Cp rings, which show the inequivalency of these protons. The Cp of the dppf group normally displays two signals in the ^1H NMR. This inequivalence comes from the rigid ferrocene moiety upon chelation of the dppf ligand,⁵³ as depicted in figure 2.4. The Cp rings are chemically equivalent. $^{13}\text{C}\{^1\text{H}\}$ NMR of these rings gave five signals, four of them are very well defined triplets corresponding to the CH groups and another one, an “irregular shape triplet” (figure 2.6, expansion at 84.84 ppm), corresponding to the quaternary carbon. These triplets arise from the coupling of the phosphorus and ruthenium atoms to the ^{13}C nuclei. Heteronuclear NMR spectroscopy (HMQC-correlation ^1H - $^{13}\text{C}\{^1\text{H}\}$) helped in the assignment of *p*-cymene and Cp peaks since they appear in the same region of the NMR spectrum (figure 2.7b). COSY experiments were also important in the assignment of the *p*-cymene peaks. DEPT ^{13}C NMR experiments were useful in the assignment of the quaternary carbons.

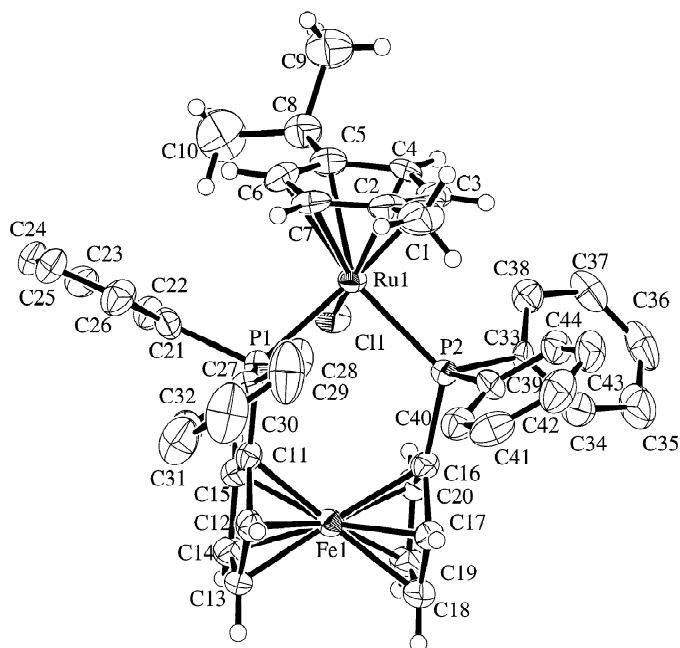


Figure 2.4 – Crystal structure of $[\text{RuCl}(\text{dppf})(p\text{-cymene})]\text{PF}_6$ reported by M. Spicer *et. al.*⁴³ The ligand phenyl protons and PF_6 are omitted for clarity.

The phenyl protons appeared in the ^1H NMR spectrum as a group of four multiplets where it is possible to assign six different signals with the help of HMQC (figure 2.7a). Three of those signals correspond to the *ortho*, *meta* and *para* protons of 2 equivalent phenyl rings and the other three to the other two phenyl rings. In the $^{13}\text{C}\{^1\text{H}\}$ NMR it is possible to observe four peaks to each pair of equivalent phenyl rings (2). Two of these peaks are triplets and corresponds to the *ortho* and *meta* carbons. The *para* carbons come as a singlet and the quaternary ones as an “irregular shape triplet”. The different multiplicity of these aromatic peaks is due to the distance to the phosphorus atom, not occurring any coupling in the case of the furthest carbons (*para*).

The $^{31}\text{P}\{^1\text{H}\}$ NMR spectrum showed a single singlet at δ 37.78 ppm which represents the chemical equivalence of the phosphorus atoms. This fact corroborates with the chemical equivalence of the Cp rings and the existence of two pairs of equivalent phenyl groups as said before in the ^1H and $^{13}\text{C}\{^1\text{H}\}$ NMR analysis. Mass spectrum and elemental analysis are in agreement to what is expected for the proposed structure.

p-Cymene Based Ruthenium Complexes as Catalysts

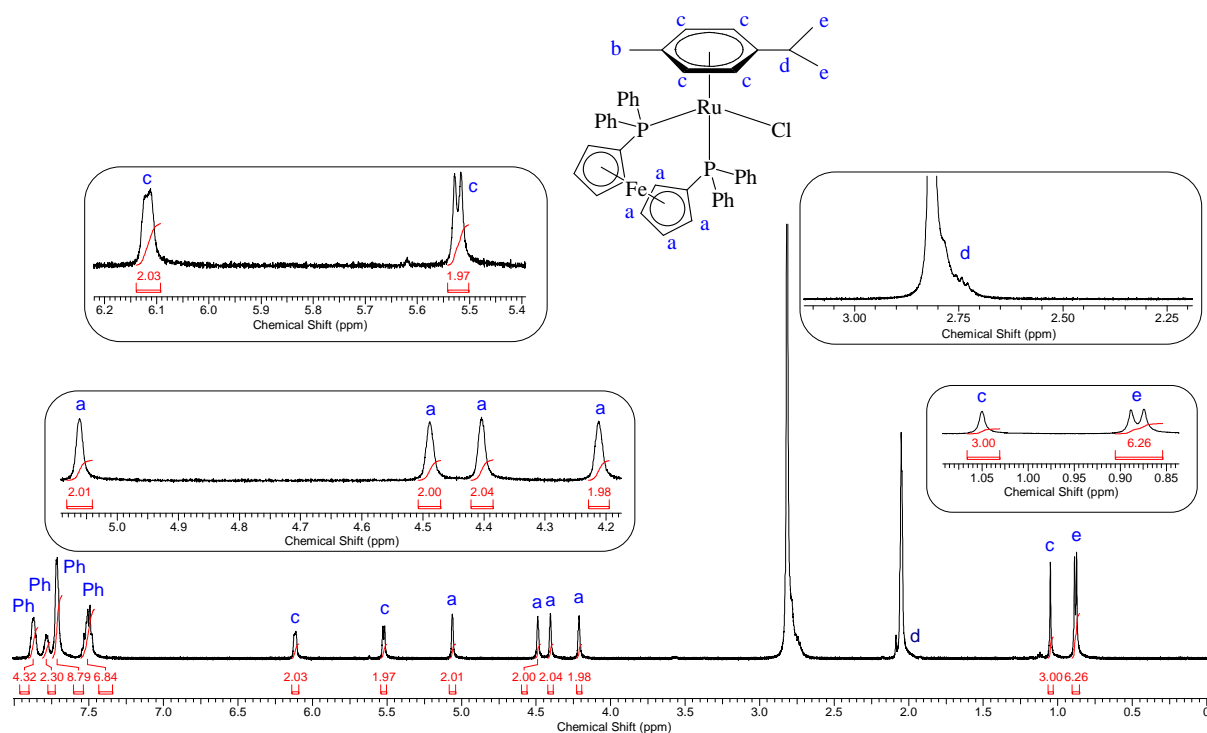


Figure 2.5 – ^1H NMR spectrum of $[\text{RuCl}(\text{dppf})(p\text{-cymene})]\text{SbF}_6$ (4) in $(\text{CD}_3)_2\text{CO}$ with expansions of the Cp and *p*-cymene peaks.

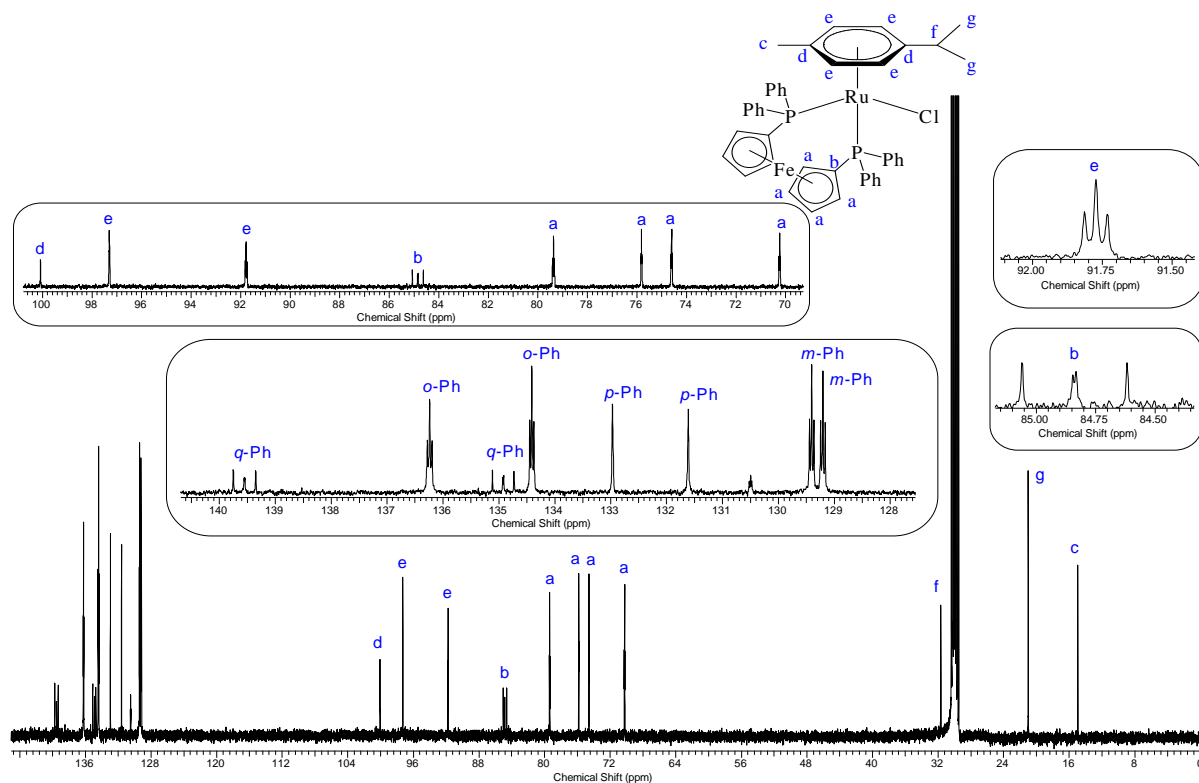


Figure 2.6 – $^{13}\text{C}\{^1\text{H}\}$ NMR spectrum of $[\text{RuCl}(\text{dppf})(p\text{-cymene})]\text{SbF}_6$ (4) in $(\text{CD}_3)_2\text{CO}$ with expansions of the phenyl, Cp and *p*-cymene peaks. *o* = ortho, *p* = para, *m* = meta, *q* = quaternary carbon.

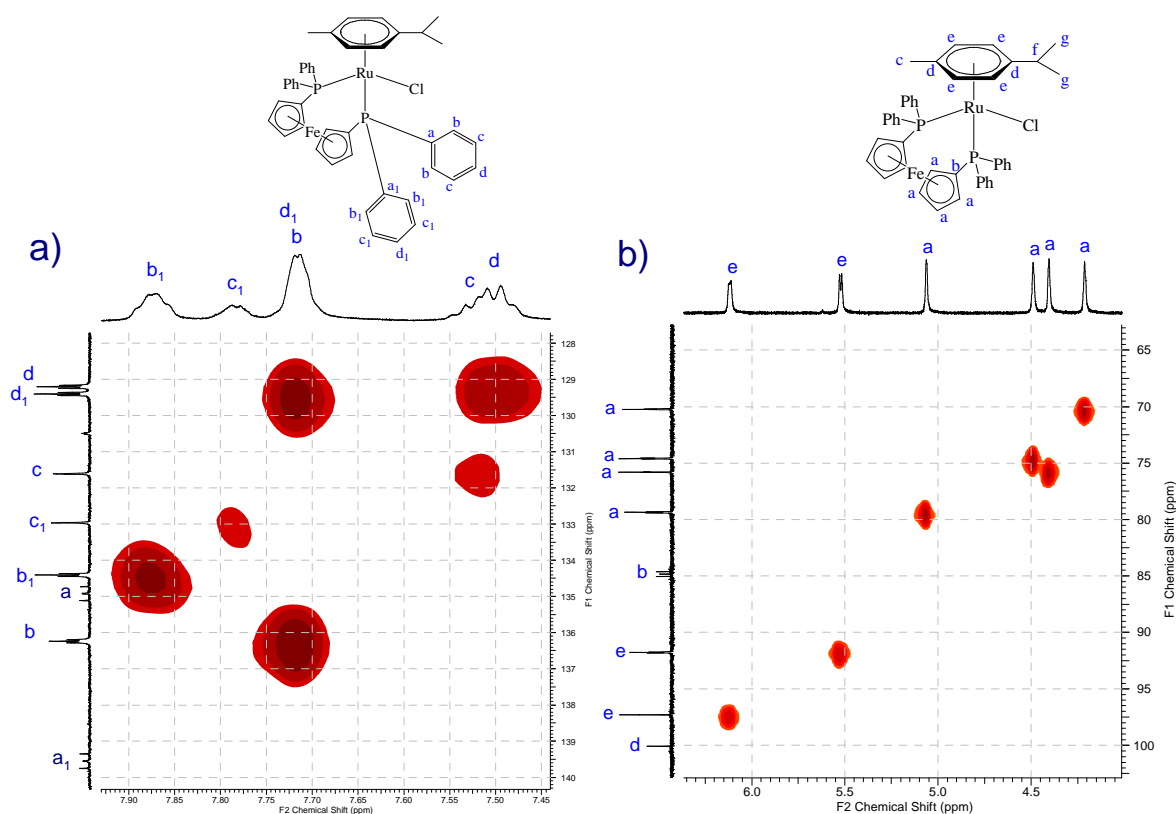


Figure 2.7 – Expansions of HMQC NMR spectrum of $[\text{RuCl}(\text{dppf})(p\text{-cymene})]\text{SbF}_6$ (**4**) in $(\text{CD}_3)_2\text{CO}$. a) phenyl protons region. b) Cp and aromatic *p*-cymene protons region.

2.3.2 Synthesis of $[\text{Ru}(\text{dppf})(p\text{-cymene})]\text{SbF}_6$ (**5**)

$[\text{Ru}(\text{dppf})(p\text{-cymene})]\text{SbF}_6$ (**5**) was synthesised according to the synthesis of $[\text{RuCl}(\text{dppf})(p\text{-cymene})]\text{SbF}_6$ (**4**) but using $[\text{Ru}_2(p\text{-cymene})]_2$ (**2**) as the starting material instead of $[\text{RuCl}_2(p\text{-cymene})]_2$ (**1**). As in compound **4**, it was also recrystallised from a mixture of ethanol and acetone and a brownish red solid was obtained in 12% yield. $\text{Ru}(\text{dppf})(p\text{-cymene})]\text{SbF}_6$ (**5**) is air and moisture stable, cationic 18-electron compound. It was characterized by ^1H , $^{13}\text{C}\{^1\text{H}\}$ and $^{31}\text{P}\{^1\text{H}\}$ NMR, mass spectrometry and elemental analysis. The later analysis differs from the expected. For example, for the iodine it was found 22.45% whereas the calculated percentage is 11.01. Despite of this, mass spectrum shows the correct molecular peak at m/z 917.0 which corresponds to $[\text{M}] - \text{SbF}_6$. The ^1H NMR pattern for this compound, although quite similar to the analogous $[\text{RuCl}(\text{dppf})(p\text{-cymene})]\text{SbF}_6$ (**4**), has a feature that allows distinguishing both. As shown for $[\text{Ru}_2(p\text{-cymene})]_2$ (**2**), with this iodine complex there was again a significantly downfield shift of the aromatic *p*-cymene peaks and also the CH peak from the $\text{CH}(\text{CH}_3)_2$ group when compared to those of the

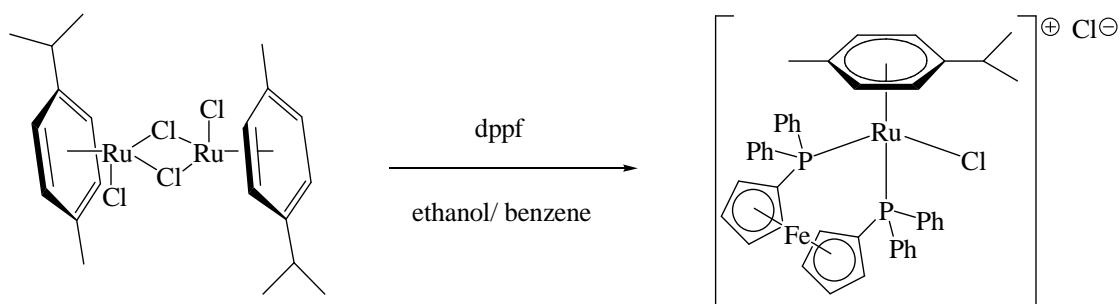
corresponding chlorine version [RuCl(dppf)(*p*-cymene)]SbF₆ (**4**). The latter peak was also the one that suffered the biggest shift which suggests that this proton should be the one closer to the iodine atom.

2.3.3 Synthesis of [RuCl(dppf)(*p*-cymene)]BF₄ (**6**)

Method 2 of synthesis of [RuCl(dppf)(*p*-cymene)]SbF₆ (**4**) was followed but this time AgBF₄ was used instead of NaSbF₆. [RuCl₂(*p*-cymene)]₂ (**1**), dissolved in methanol, was treated with dppf in the presence of the salt. The precipitation of a white powder (NaCl) occurred instead of the product. The product was precipitated from chloroform by diethyl ether. [RuCl(dppf)(*p*-cymene)]BF₄ (**6**) is a yellow, air and moisture stable, cationic 18-electron compound which was obtained in 33% yield. It was characterized by ¹H, ¹³C{¹H} and ³¹P{¹H} NMR, mass spectrometry and elemental analysis. Elemental analysis results are not the best for the chlorine content (5.40 % found against 3.89 % calculated) which is thought to be related with possible NaCl still present in the solid obtained. Further washings with water might have helped.

2.3.4 Synthesis of [RuCl(dppf)(*p*-cymene)]Cl (**7**)

The synthesis of [RuCl(dppf)(*p*-cymene)]Cl (**7**) was based in the synthesis of the analogous [RuCl(*p*-cymene)(Me-Duphos)]Cl reported by P. Pregosin *et. al.*⁵⁶ Two molar equivalents of dppf ligand and one molar equivalent of [RuCl₂(*p*-cymene)]₂ (**1**) were reacted in a mixture of ethanol and benzene (scheme 2.4). Solvents were removed under reduced pressure. The resulting residue was dissolved in dichloromethane and diethyl ether precipitated a light orange product. It was recrystallized from methanol-diethyl ether and characterized by ¹H and ³¹P{¹H} NMR, mass spectrometry and elemental analysis. All these techniques match to what is expected for the proposed structure.



Scheme 2.4 – Synthesis $[\text{RuCl}(\text{dppf})(p\text{-cymene})]\text{Cl}$ (**7**).

If a comparison is made between the structures of $[\text{RuCl}(\text{dppf})(p\text{-cymene})]\text{SbF}_6$ (**4**), $[\text{RuCl}(\text{dppf})(p\text{-cymene})]\text{BF}_4$ (**6**) and $[\text{RuCl}(\text{dppf})(p\text{-cymene})]\text{Cl}$ (**7**) it comes immediately that the only difference lies in the counter-ion. So, it is expected that the NMR spectra are quite similar. In fact, the ^1H NMR shifts (in CDCl_3) are almost exactly the same for the same peaks in the different compounds. But, there is a peak that can tell the difference between these structures. It is the aromatic *p*-cymene proton peak most downfield shifted (assigned with an “X” in figure 2.8). From compound **4** (SbF_6 counter-ion) to **6** (BF_4) there is a downfield shift of 0.11 ppm and from **4** to **7** (Cl counter-ion) of 0.21 ppm. This fact allows differentiating these compounds without the need of elemental analysis.

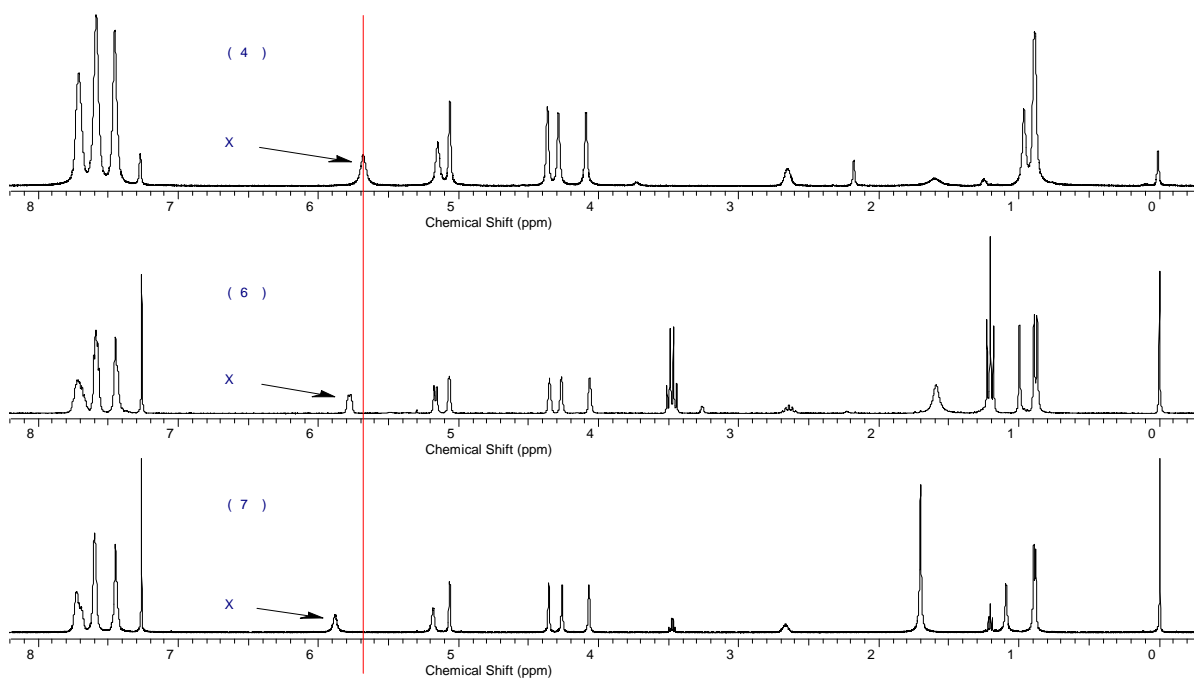


Figure 2.8 – ^1H NMR spectra of compounds $[\text{RuCl}(\text{dppf})(p\text{-cymene})]\text{SbF}_6$ (**4**), $[\text{RuCl}(\text{dppf})(p\text{-cymene})]\text{BF}_4$ (**6**) and $[\text{RuCl}(\text{dppf})(p\text{-cymene})]\text{Cl}$ (**7**) in CDCl_3 . X = *p*-cymene peak that undergoes shifting according to the different counter-ion of the complex.

2.3.5 Synthesis of $[\text{Ru}_2(\text{CH}_3\text{CN})_2(\text{DPEPhos})_2]\text{SbF}_6$ (**8**)

$[\text{Ru}_2(\text{CH}_3\text{CN})_2(\text{DPEPhos})_2]\text{SbF}_6$ (**8**) was synthesised in an attempt to obtain $[\text{RuCl}(\text{DPEPhos})(p\text{-cymene})]\text{SbF}_6$. The same methodology as $[\text{RuCl}(\text{dppf})(p\text{-cymene})]\text{SbF}_6$ (**4**) (acetonitrile/methanol solvent system) was followed but instead of using dppf, DPEPhos was used as the phosphine ligand. Instead of obtaining the monomer, a trichloro-bridged dimer containing two DPEPhos and two acetonitrile molecules was the product. *p*-Cymene displacement has occurred. The product was recrystallised twice, the first time from ethanol and the second time from methanol to afford a pale yellow solid in 10% yield. It was characterized by ^1H , $^{13}\text{C}\{^1\text{H}\}$ and $^{31}\text{P}\{^1\text{H}\}$ NMR, mass spectrometry and elemental analysis. The results from these techniques are in agreement with the proposed structure. Structure related compounds have been previously reported in the literature employing different methods of synthesis. For example, the more similar ones $[\text{Ru}_2\text{Cl}_3(\text{PP})_2(\text{MeCN})_2]\text{PF}_6$ (PP= dppb or diop, X=Cl or PF_6) were prepared from $\text{RuCl}_4(\text{PP})_2$ or $\text{RuCl}_2(\text{PP})(\text{PPh}_3)^{57}$.

2.3.5.1 X-ray crystal structure analysis of complex **8**

The molecular structure of $[\text{Ru}_2(\text{NCCH}_3)_2(\text{DPEPhos})_2]\text{SbF}_6$ (**8**) can be seen in figure 2.9. Yellow needles suitable for X-ray crystallography were obtained by vapour diffusion of pentane into a saturated solution of the complex in chloroform. Complex **8** crystallised in a monoclinic cell and structural solution was performed in the space group $\text{P}2_1/\text{c}$. The coordination about each Ru center is distorted octahedral. Complex **8** is face-sharing bioctahedra, containing two metal centres bridged by three chloride ligands. The average Ru-Cl bond length is 2.478 Å, which is comparable with the corresponding average Ru-Cl bond length (2.483 Å) in the related structure compound $[\text{Ru}(\text{dcypb})(\text{CO})]_2(\mu\text{-Cl})_3\text{Cl}$,⁵⁸ where dcypb=1,4-bis(dicyclohexylphosphino)butane. Also bond angles fall within the same values as those of $[\text{Ru}(\text{dcypb})(\text{CO})]_2(\mu\text{-Cl})_3\text{Cl}$ (crystal data, labelled molecular structure and selected bond lengths and angles of $[\text{Ru}_2(\text{NCCH}_3)_2(\text{DPEPhos})_2]\text{SbF}_6$ (**8**) are in appendixes 16, 17 and 18, respectively).

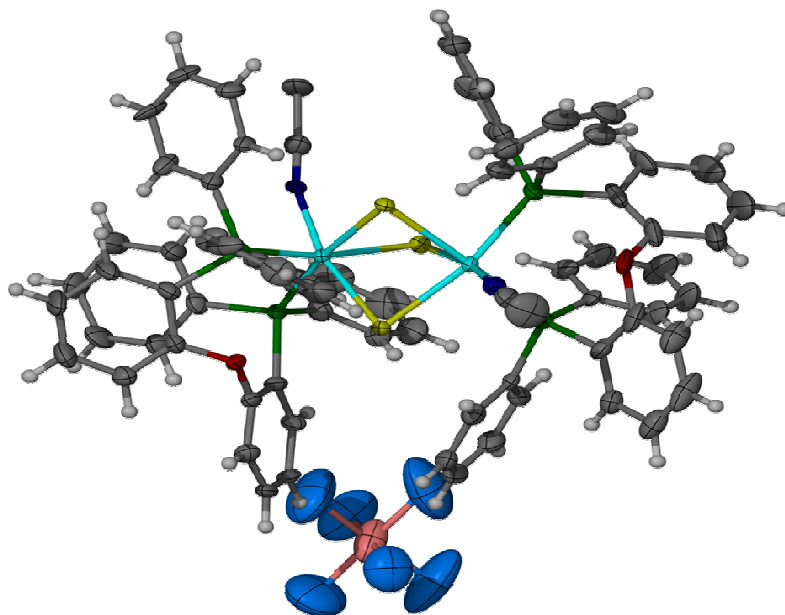
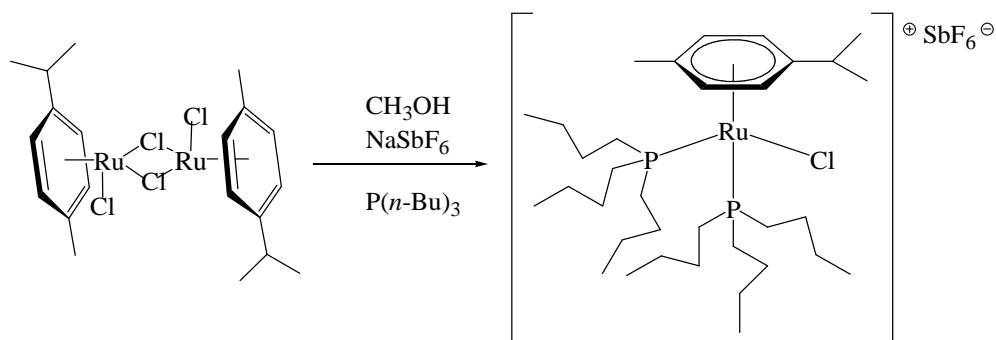


Figure 2.9 – Molecular structure of $[\text{Ru}_2(\text{NCCH}_3)_2(\text{DPEPhos})_2]\text{SbF}_6$ (**8**) obtained by X-ray crystallography in this project.

2.3.6 Synthesis of $[\text{RuCl}(\text{P}(n\text{-Bu}_3))_2(p\text{-cymene})]\text{SbF}_6$ (**9**)

In the literature it is possible to find the synthesis of the structure related compound $[\text{RuCl}(\eta^6\text{-C}_6\text{H}_6)\text{P}(n\text{-Bu}_3)_2]\text{Cl}$ reported by P. Pregosin *et. al.*⁵⁶ However, it has a different η^6 -arene ligand and different counter-ion so the method 2 of synthesis of $[\text{RuCl}(\text{dppf})(p\text{-cymene})]\text{SbF}_6$ (**4**) was followed.

Starting with $[\text{RuCl}_2(p\text{-cymene})]_2$ (**1**), SbF_6^- was used in methanol as counter-ion. The phosphine ligand, tri-*n*-butylphosphine, was employed in excess. The general synthetic route can be seen in scheme 2.5. After filtering the NaCl formed, the product was obtained from chloroform and pentane to afford crystalline orange clusters. $[\text{RuCl}(\text{P}(n\text{-Bu}_3))_2(p\text{-cymene})]\text{SbF}_6$ (**9**) is an air stable, cationic 18-electron compound which was obtained in 13% yield. Although air stable it is not stable in CDCl_3 solutions since a change in color was observed (gets darker/ brown) after one or two days. Also the ^1H NMR spectrum suffers an increase in the number of peaks. It was characterized by ^1H , $^{13}\text{C}\{^1\text{H}\}$ and $^{31}\text{P}\{^1\text{H}\}$ NMR, mass spectrometry and elemental analysis which are in agreement with the proposed structure.



Scheme 2.5 – Synthesis of $[\text{RuCl}(\text{P}(n\text{-Bu}_3)_2(\textit{p}\text{-cymene})_2)]\text{SbF}_6$ (**9**).

2.3.7 Synthesis of $[\text{Ru}(\text{P}(n\text{-Bu}_3)_2(\textit{p}\text{-cymene})_2)]\text{SbF}_6$ (**10**)

$[\text{Ru}(\text{P}(n\text{-Bu}_3)_2(\textit{p}\text{-cymene})_2)]\text{SbF}_6$ (**10**) was obtained according to the synthesis of $[\text{RuCl}(\text{P}(n\text{-Bu}_3)_2(\textit{p}\text{-cymene})_2)]\text{SbF}_6$ (**9**) but $[\text{RuCl}_2(\textit{p}\text{-cymene})_2]$ (**1**) was used as the starting material instead of $[\text{Ru}_2(\textit{p}\text{-cymene})_2]$ (**2**). After filtering the NaCl formed, a red wine color powder was precipitated from chloroform by diethyl ether. $[\text{Ru}(\text{P}(n\text{-Bu}_3)_2(\textit{p}\text{-cymene})_2)]\text{SbF}_6$ (**10**) is an air stable, cationic 18-electron compound which was obtained in 48% yield. As $[\text{RuCl}(\text{P}(n\text{-Bu}_3)_2(\textit{p}\text{-cymene})_2)]\text{SbF}_6$ (**9**), it is not very stable in CDCl_3 solutions. It was characterized by ^1H , $^{13}\text{C}\{^1\text{H}\}$ and $^{31}\text{P}\{^1\text{H}\}$ NMR, mass spectrometry and elemental analysis. The later analysis differs slightly from the expected but, as in $[\text{Ru}(\text{dppf})(\textit{p}\text{-cymene})_2]\text{SbF}_6$ (**5**), mass spectrum shows the correct molecular peak at m/z 767.3 which corresponds to $[\text{M}] - \text{SbF}_6$.

2.3.8 Synthesis of $[\text{RuCl}(\text{P}(i\text{-Bu}_3)_2(\textit{p}\text{-cymene})_2)]\text{SbF}_6$ (**11**)

$[\text{RuCl}(\text{P}(i\text{-Bu}_3)_2(\textit{p}\text{-cymene})_2)]\text{SbF}_6$ (**11**) was synthesised according to the same method (reagents and quantities) as $[\text{RuCl}(\text{P}(n\text{-Bu}_3)_2(\textit{p}\text{-cymene})_2)]\text{SbF}_6$ (**9**), which means phosphine ligand in excess as well. But in this synthesis the white precipitate was not readily formed. After obtaining the yellow product by precipitation from chloroform with diethyl ether, it was washed with diethyl ether and water to remove NaCl and afford fine yellow needles. $[\text{RuCl}(\text{P}(i\text{-Bu}_3)_2(\textit{p}\text{-cymene})_2)]\text{SbF}_6$ (**11**) (figure 2.10) is an air stable cationic 18-electron compound and as $[\text{RuCl}(\text{P}(n\text{-Bu}_3)_2(\textit{p}\text{-cymene})_2)]\text{SbF}_6$ (**9**), it is not very stable in CDCl_3 solutions.

It was characterized by ^1H , $^{13}\text{C}\{^1\text{H}\}$ and $^{31}\text{P}\{^1\text{H}\}$ NMR, mass spectrometry and elemental analysis which are in agreement with the proposed structure.

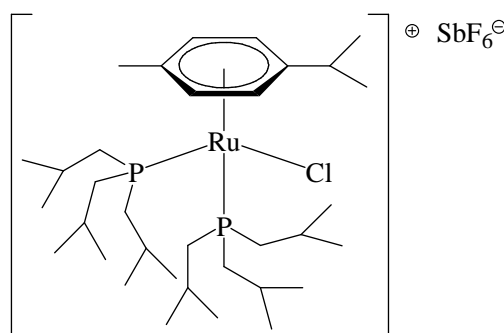
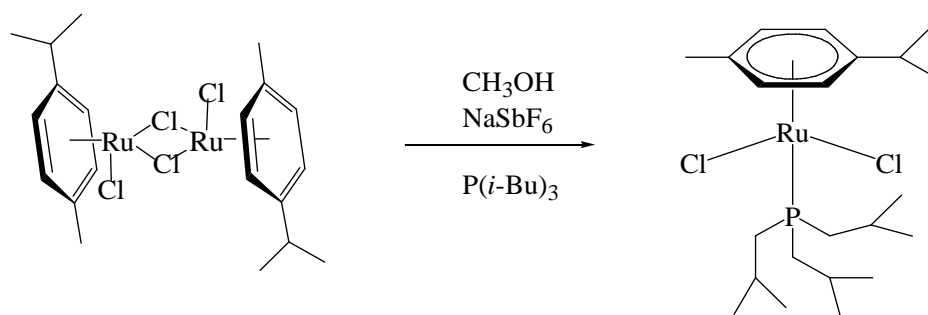


Figure 2.10 – Molecular structure of $[\text{RuCl}(\text{P}(i\text{-Bu}_3))_2(\textit{p}\text{-cymene})]\text{SbF}_6$ (**11**).

2.3.9 Synthesis of $[\text{RuCl}_2\text{P}(i\text{-Bu}_3)(\textit{p}\text{-cymene})]$ (**12**)

This monosubstituted monomer was actually obtained in an attempt to synthesise the disubstituted one $[\text{RuCl}(\text{P}(i\text{-Bu}_3))_2(\textit{p}\text{-cymene})]\text{SbF}_6$ (**11**). Scheme 2.5 was followed but no excess of phosphine was employed (scheme 2.6). Two molar equivalents of phosphine to one molar equivalent of ruthenium were used. A brown solution was obtained and the solvent was evaporated under reduced pressure. The resulting residue was dissolved in chloroform and a layer of pentane added and left in the freezer overnight. Both a brownish red powder and a yellow powder were obtained. After NMR and mass spectrometry analysis it was possible to conclude that the brownish red powder was the monosubstituted monomer $[\text{RuCl}_2\text{P}(i\text{-Bu}_3)(\textit{p}\text{-cymene})]$ (**12**) and the yellow one the disubstituted $[\text{RuCl}(\text{P}(i\text{-Bu}_3))_2(\textit{p}\text{-cymene})]\text{SbF}_6$ (**11**). The brownish red powder was recrystallized from acetone and was characterized by ^1H NMR, mass spectrometry and elemental analysis which are in agreement with the proposed structure. $[\text{RuCl}_2\text{P}(i\text{-Bu}_3)(\textit{p}\text{-cymene})]$ (**12**) is an air stable, neutral 18-electron compound and as $[\text{RuCl}(\text{P}(n\text{-Bu}_3))_2(\textit{p}\text{-cymene})]\text{SbF}_6$ (**9**), it is not very stable in CDCl_3 solutions. No yield was calculated but by looking at the amount obtained, it was low. This compound has been previously synthesised by S. Nolan and co-workers.⁵⁹



Scheme 2.6 – Synthesis of $[\text{RuCl}_2\text{P}(i\text{-Bu}_3)(p\text{-cymene})]$ (**12**).

2.3.10 Synthesis of $[\text{RuCl}_2\text{P}(n\text{-Bu}_3)(p\text{-cymene})]$ (**13**)

This monosubstituted complex was obtained according to scheme 2.5 but without employing any NaSbF_6 and any excess of phosphine ligand $\text{P}(n\text{-Bu}_3)$. One molar equivalent of phosphine per one molar equivalent of ruthenium was used. After removing the solvent under reduced pressure, the solid was dissolved in chloroform and precipitated with diethyl ether. $[\text{RuCl}_2\text{P}(n\text{-Bu}_3)(p\text{-cymene})]$ (**13**) is a red air stable, neutral 18-electron compound which was obtained in 60% yield. It was characterized by ^1H NMR and mass spectrometry which are in agreement with the proposed structure. This compound has been previously synthesised by Bennett and co-workers.⁶⁰

2.3.11 Synthesis of $[\text{RuCl}(\text{P}(\text{CH}_3)_3)_2(p\text{-cymene})]\text{SbF}_6$ (**14**)

This complex disubstituted with $\text{P}(\text{CH}_3)_3$ ligand was synthesised according to scheme 2.5. The phosphine ligand was employed in excess. A white precipitate was formed and filtered. The product was obtained from chloroform by precipitation with diethyl ether. $[\text{RuCl}(\text{P}(\text{CH}_3)_3)_2(p\text{-cymene})]\text{SbF}_6$ (**14**) is a yellow air stable, cationic 18-electron compound which was obtained in 26% yield. It was characterized by ^1H and $^{31}\text{P}\{^1\text{H}\}$ NMR and mass spectrometry which are in agreement with the proposed structure. Elemental analysis was also performed but the percentages are slightly deviated from the calculated values. $[\text{RuCl}(\text{P}(\text{CH}_3)_3)_2(p\text{-cymene})]\text{SbF}_6$ (**14**) with PF_6^- as counter-ion instead of SbF_6^- has been previously reported in the literature by H. Werner and co-workers.⁶¹

2.3.12 Synthesis of $[\text{RuCl}_2\text{PPh}(\text{OCH}_3)_2(p\text{-cymene})]$ (**15**)

As $[\text{RuCl}(\text{P}(i\text{-Bu}_3))_2(p\text{-cymene})]\text{SbF}_6$ (**11**), a monosubstituted monomer (figure 2.11) was obtained in an attempt to synthesise the disubstituted one. In this case, even an excess of phosphine (PhPCl_2) was not enough to obtain the disubstituted version. This is probably due to the reaction that the phosphine undergoes before coordinating to the metal centre which may form side species. The phosphine loses its chlorines when contacting with the reaction solvent (methanol). Scheme 2.5 was followed with the respective phosphine ligand (PhPCl_2). After reflux and evaporation of solvent under reduced pressure the red wine color oil obtained was dissolved in chloroform and a layer of pentane added and left in the freezer overnight. Pentane was filtered and diethyl ether added to precipitate a red wine color powder. It was washed with diethyl ether and water. $[\text{RuCl}_2\text{PPh}(\text{OCH}_3)_2(p\text{-cymene})]$ (**15**) is an air stable, neutral 18-electron compound obtained in 82% yield. It was characterized by ^1H NMR and mass spectrometry which are in agreement with the proposed structure.

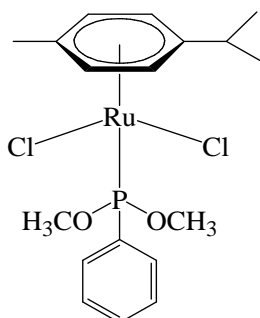
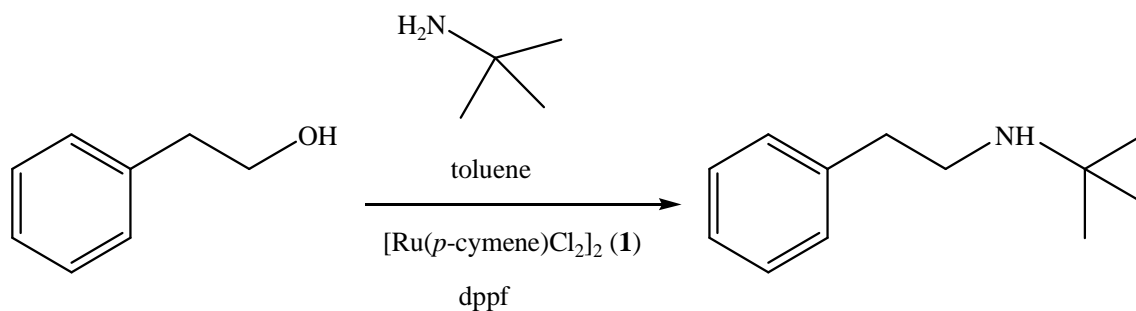


Figure 2.11 – Molecular structure of $[\text{RuCl}_2\text{PPh}(\text{OCH}_3)_2(p\text{-cymene})]$ (**15**).

2.4 Catalytic Studies

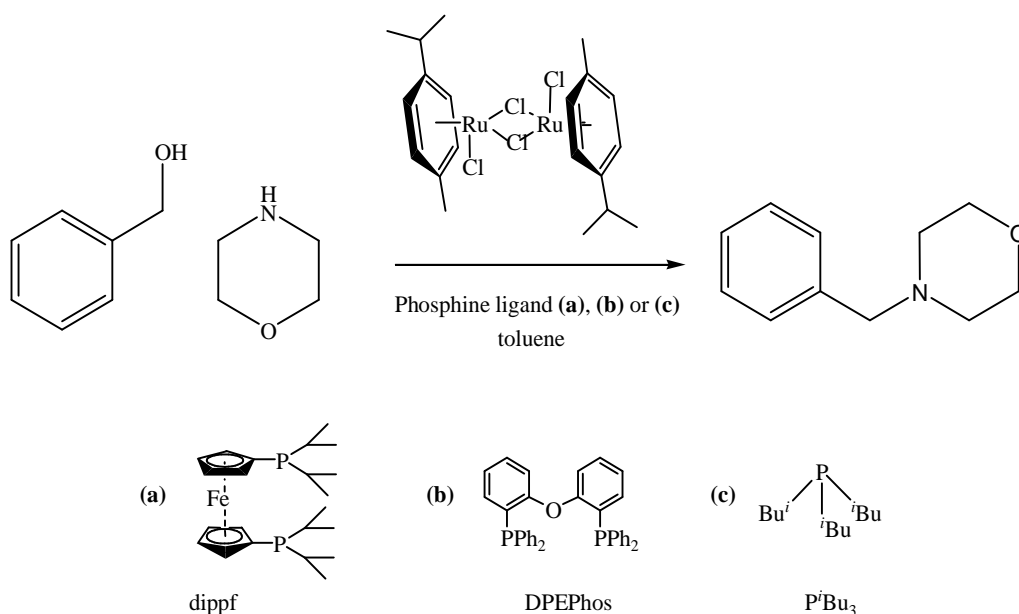
2.4.1 Redox Neutral Alkylations (N-alkylations)

In this project the N-alkylation of tert-butylamine with phenethyl alcohol was chosen as the model for establishing a competent catalyst for the alkylation of amines with alcohols (scheme 2.7). It was chosen because it was already attempted in the laboratory and its conditions already optimised.



Scheme 2.7 – N-alkylation of phenethyl alcohol with tert-butylamine.

The N-alkylations were carried out following the procedure described by J. Williams *et. al.*²⁴ The substrate:catalyst ratio (phenethyl alcohol:ruthenium) was 20:1 on a molar basis for all the reactions with dimers (2.5 mol % dimer, 5 mol % in ruthenium). With monomers, some reactions were 20:1 (5 mol % monomer, 5 mol % in ruthenium) and some others were 40:1 which allowed concluding something about catalyst loading. When dimers were used the dimer:phosphine ratio was 1:2 but when monomers were employed no phosphine ligand was added to this one-pot reaction. To the pot were also added phenethyl alcohol and tert-butyl amine (1:1) in toluene and stirred under reflux for 24 hours. The reactions were set one by one in round-bottom flasks out in the open air without degassing or inert gas protection throughout. *Astra Zeneca*⁴⁵ (biopharmaceutical company) selected the phosphine ligands to be used because they showed together with [RuCl₂(*p*-cymene)]₂ (1) a big catalytic potential of the active catalyst in the N-alkylation depicted in scheme 2.8. Conversion rates greater than 97% were obtained. *Astra Zeneca* also did some solvent screening and found out that the best ones appear to be Tetralin or Toluene.



Scheme 2.8 – Catalytic synthesis of 4-(phenylmethyl)morpholine by N-alkylation.

In the published conditions of the model N-alkylation of this project²⁴ it is reported the use of K₂CO₃ as a base, inert atmosphere, and anhydrous conditions (dry toluene and molecular sieves). But a former colleague from the McGowan's group (Alan Myden) found out that there is no need of such precautions. Following that he managed to obtain the product in 79% conversion.

The optimised conditions in the McGowan's group were followed. The reaction was attempted again to check if same results are obtained and to try to isolate the product since it is not commercially available. After several attempts of trying to isolate the product when using [RuCl₂(*p*-cymene)]₂ (**1**) as pre-catalyst and dppf as the phosphine ligand, none of them were successful. Column chromatography was performed but it did not work using either diethyl ether or a mixture of ethyl acetate-hexane as the eluent. A mixture of the starting material, the product and several other impurities was always the result. The product, (2-phenylethyl)tert-butylamine, was isolated together with phenethyl alcohol by reduced pressure distillation which allowed the assignment of the retention time of the product in gas chromatography since the product is not commercially available.

After the preliminary studies mentioned above, the project moved into testing all the dimer-ligand pairs as well as the monomers as N-alkylation catalysts. Reaction conversions were calculated by ¹H NMR.

2.4.1.1 ¹H NMR Results

Since it was not possible to isolate the product, conversions were calculated instead of yields. The spectrum of one of the catalytic reactions can be seen in figure 2.12 in which are shown the peaks which integrals were used to calculate the product conversion. As reported by J. Williams and co-workers¹ the N-alkylation of tert-butylamine with phenethyl alcohol using ruthenium dimer-phosphine pairs is often accompanied by the formation of appreciable quantities of PhCH₂CH₂O₂CCH₂Ph so, where present, the conversions accounted this fact. If both the alcohol and ester peaks are present, the product conversion is calculated by manually integrating the alcohol peak against the product and ester peaks. If only the ester peak is present, the product conversion is calculated integrating the ester peak against the product peak. This ester is formed presumably from addition of alcohol to the intermediate aldehyde and oxidation of the so-formed hemi-acetal. This fact was seen with the dimer-ligand catalytic systems but also with the ruthenium monomers.

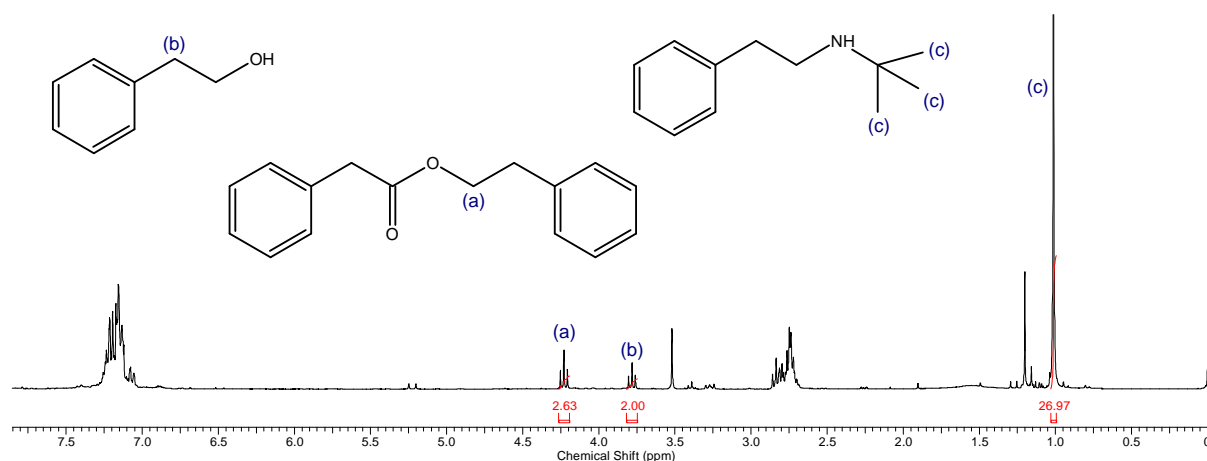


Figure 2.12 – ¹H NMR spectrum of the oily residue obtained after filtration of the reaction mixture through celite of the N-alkylation of tert-butylamine with phenethyl alcohol by [RuCl(dppf)(*p*-cymene)]Cl (**7**). Substrate:catalyst ratio of 40:1. (a), (b) and (c) are the peaks which integrals were used to calculate the product conversion.

The results from the N-alkylation reactions of tert-butylamine with phenethyl alcohol are shown in table 2.3.

Table 2.3 – Results for the N-alkylation of tert-butylamine with phenethyl alcohol. Catalyst/ligand evaluation.

Entry	Complex	Ligand	S/C [a]	Amine (%) [b]	Ester (%)	Unreacted alcohol (%)
1	[RuCl ₂ (<i>p</i> -cymene)] ₂ (1)	–	20	2 ^[c] (0)	(8)	92 ^[c] (92)
2	1	dppf	20	75 (100)	7 (0)	18 (0)
3	1	DPEPhos	20	60	37	4
4	1	dippf	20	79 (80)	21 (20)	0 (0)
5	1	P(<i>i</i> -Bu) ₃	20	28	0	72
6	[RuI ₂ (<i>p</i> -cymene)] ₂ (2)	–		3 ^[c]	-	84 ^[c]
7	2	dppf	20	75	25	0
8	2	DPEPhos	20	96	3	1
9	2	dippf	20	72	27	1
10	[RuCl(dppf)(<i>p</i> -cymene)]SbF ₆ (4)	–	40	36	0	64
11	[RuCl(dppf)(<i>p</i> -cymene)]BF ₄ (6)	–	40	61	19	20
12	[RuCl(dppf)(<i>p</i> -cymene)]BF ₄ (6)	–	20	36	50	14
13	[RuCl(dppf)(<i>p</i> -cymene)]Cl (7)	–	40	45	40	15
14	[RuCl(dppf)(<i>p</i> -cymene)]Cl (7)	–	20	82	12	6
15	[RuI(dppf)(<i>p</i> -cymene)]SbF ₆ (5)	–	40	85	15	0
16	[Ru ₂ Cl ₃ (DPEPhos) ₂ (CH ₃ CN) ₂]SbF ₆ (8)	–	40	28	60	12
17	[RuI(P(<i>n</i> -Bu) ₃) ₂ (<i>p</i> -cymene)]SbF ₆ (10)	–	40	0	1	99
18	[RuCl(P(<i>i</i> -Bu) ₃) ₂ (<i>p</i> -cymene)]SbF ₆ (11)	–	40	9	0	91
19	[RuCl ₂ (P(<i>n</i> -Bu) ₃) ₂ (<i>p</i> -cymene)] (13)	–	40	0	0	100
20	[RuCl(P(CH ₃) ₃) ₂ (<i>p</i> -cymene)]SbF ₆ (14)	–	40	0	0	100

[a] S/C = substrate/catalyst ratio

[b] Values given are conversions with respect to unreacted alcohol or unreacted ester when no unreacted alcohol is present, as determined by analysis of the ¹H NMR spectra. Figures in parentheses are conversions obtained for the same reaction reported in the literature employing additional 10 mol% K₂CO₃, 3 Å molecular sieves and inert atmosphere.

[c] This conversion was calculated by GC by the area normalization procedure (comparing peak areas)

As it is possible to be seen, just employing the dimers in the absence of any additional ligand (DPE) afforded negligible consumption of the starting material, which means that the dimers themselves do not form any active species towards the N-alkylation under study. On the other hand, all the dimer-ligand pairs (**1**-dppf, **2**-dppf, **1**-DPEPhos...) and all the monomers containing bidentate ligands form catalytically active species. This fact supports the idea of having a monomer that will be the actual pre-catalyst. Another idea that is supported by the results obtained is that by starting the reaction with [RuCl(dppf)(*p*-cymene)]Cl (**7**) (entry 14) instead of the corresponding dimer-ligand pair (entry 2), the results are better (increase of product conversion and reduction in the percentage of unreacted alcohol) since a mechanistic step is thought to have been eliminated. By looking at the results it is also possible to see that the presence of iodine in the complexes instead of chlorine led in the majority of the reactions to an improvement of the catalytic performance in terms of product conversion and/or reduction in the percentage of unreacted alcohol. For

example, from entry 3 ($[\text{RuCl}_2(\textit{p}\text{-cymene})]_2$ (**1**)-DPEPhos) to the corresponding iodine entry (8) it is possible to see an increase of 36% in terms of amine conversion. Entry 3 is indeed the best result obtained for the N-alkylation under investigation with 96% conversion. Also, $[\text{Ru}(\text{dppf})(\textit{p}\text{-cymene})]\text{SbF}_6$ (**5**) showed a very high conversion (85%) when compared to the respective chlorine analogue $[\text{RuCl}(\text{dppf})(\textit{p}\text{-cymene})]\text{SbF}_6$ (**4**) (entry 10, 36%) in spite of having produced the ester derivative (15%) which was not formed in entry 10. This improvement of performance when iodine is present in the pre-catalysts instead of the chlorine atom is thought to be related to the higher lability of the iodine because by being more labile, iodine is easier displaced from the complex to give the actual active intermediate which needs to have a vacant site in order to carry on the N-alkylation.

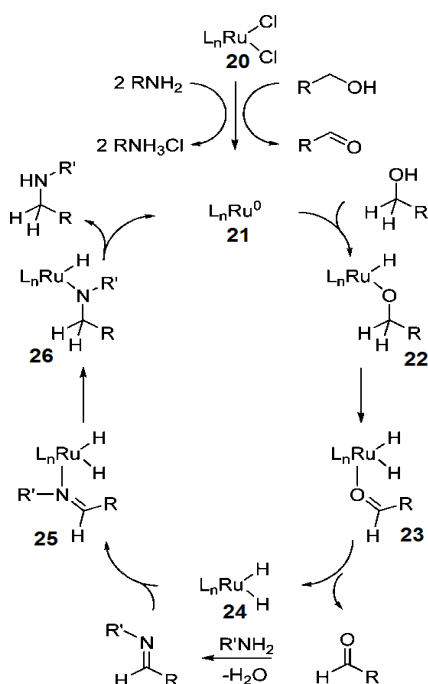
When comparing the different phosphine ligands it is possible to see that the results obtained for dppf and dippf are quite similar. The similarities in their structures seem to be the more plausible explanation. A comparison can also be made with the monomers containing different counter-ions, $[\text{Ru}(\text{dppf})(\textit{p}\text{-cymene})]\text{SbF}_6$ (**4**), $[\text{RuCl}(\text{dppf})(\textit{p}\text{-cymene})]\text{BF}_4$ (**6**) and $[\text{RuCl}(\text{dppf})(\textit{p}\text{-cymene})]\text{Cl}$ (**7**). It can be seen that the amount of unreacted alcohol decreases from **4** to **7** (entry 10, 11 and 13). But the yield does not increase in the same pattern. This fact goes against the idea that ruthenium complexes with larger, less coordinating anions should be more effective in catalysis.

Another curious fact found herein is that $[\text{RuCl}_2(\textit{p}\text{-cymene})]_2$ (**1**) showed a very poor catalytic performance in the presence of the monodentate ligand $\text{P}(\textit{i}\text{-Bu}_3)$ (entry 5) with 72% of unreacted alcohol and 28% of product. This result is against the one expected since $\text{P}(\textit{i}\text{-Bu}_3)$ was recommended by *Astra Zeneca*⁴⁵ as a very good phosphine ligand for this type of reactions. The first thought was that since the reactions have been ran out in the open air without degassing or inert gas protection throughout, the phosphines might have been oxidised into phosphine oxides. So the same reaction was ran under an inert dry nitrogen atmosphere, with all the glassware being properly dried, dry toluene and degassed reagents. Molecular sieves were employed in the reaction. Even with these conditions, the reaction output was even worse than before, with 96% of unreacted alcohol and 0% of product. This result found with $[\text{RuCl}_2(\textit{p}\text{-cymene})]_2$ (**1**) and $\text{P}(\textit{i}\text{-Bu}_3)$ was corroborated with the poor catalytic results shown by the respective disubstituted monomer $[\text{RuCl}(\text{P}(\textit{i}\text{-Bu})_3)_2(\textit{p}\text{-cymene})]\text{SbF}_6$ (**11**) (entry 18, 9% product conversion). The other disubstituted monomers ($[\text{Ru}(\text{P}(\textit{n}\text{-Bu})_3)_2(\textit{p}\text{-cymene})]\text{SbF}_6$ (**10**) and $[\text{RuCl}(\text{P}(\text{CH}_3)_3)_2(\textit{p}\text{-cymene})]\text{SbF}_6$ (**14**)) do not form

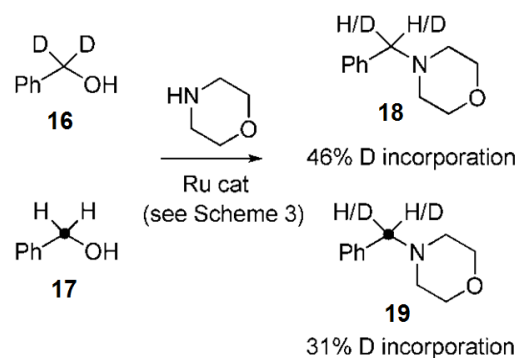
any active catalytic species (0% product, ≈100% alcohol). With these results some speculation could arise whether it is necessary the monomer to be mono or disubstituted with phosphine but results obtained with the mono substituted monomer [RuCl₂P(*n*-Bu₃)(*p*-cymene)] (**13**) shows that no catalytic species is formed as well (0% product, 100% alcohol).

In terms of substrate/catalyst (S/C) ratios the results are somewhat contradictory. When S/C ratio was 40 with [RuCl(dppf)(*p*-cymene)]Cl (**7**) the product conversion was 45%; when the amount of ruthenium was doubled (20 of S/C ratio) the product conversion has doubled as well (82%). But for [RuCl(dppf)(*p*-cymene)]BF₄ (**6**) the opposite situation occurred (entries 11 and 12). The only factor common to both compounds is that when S/C ratio is increased the amount of unreacted alcohol diminishes. About [Ru₂(NCCH₃)₂(DPEPhos)₂]SbF₆ (**8**), it shows low amount of unreacted alcohol (12%) but the biggest amount of ester within all the entries (68%), and consequently one of the lowest product conversions (28%). Is though, an interesting result, since it forms catalytically active species.

As it was possible to see throughout the results mentioned before, almost every reaction produced the ester PhCH₂CH₂O₂CCH₂Ph as a side product. However, there was not a pattern that could be assigned. For example, [RuI(dppf)(*p*-cymene)]SbF₆ (**4**) (entry 10) gave no ester but [RuCl(dppf)(*p*-cymene)]BF₄ (**6**) that just differs in the counter-ion gave 19% (entry 11). This randomness formation of ester may be related with mechanistic issues or reaction kinetics. The mechanism of N-alkylation of secondary amines with primary alcohols proposed by J. Williams and co-workers¹ is shown in scheme 2.9.



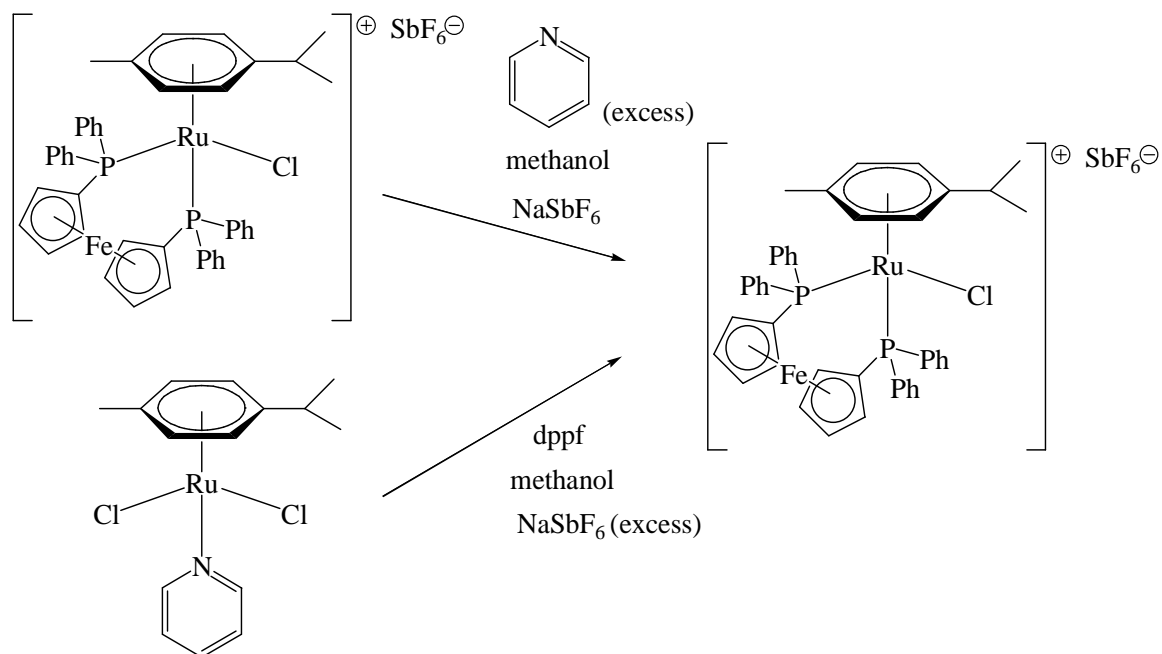
Scheme 2.9 – Proposed mechanism by J. Williams and co-workers¹ of *N*-Alkylation Reactions Involving Enantiomerically Pure Substrates.



Scheme 2.10 – Hydrogen/Deuterium crossover study in Morpholine Alkylation by J. Williams and co-workers.¹

In the borrowing hydrogen mechanism proposed it is believed that *p*-cymene is dissociated in the active complex since J. Williams and co-workers¹ showed that the reaction of $[\text{RuCl}_2(\textit{p}\text{-cymene})]_2$ (**1**) with BINAP and the diamine DPEN leads to the formation of the Noyori complex $\text{Ru}(\text{BINAP})(\text{DPEN})\text{Cl}_2$. In other words, they showed the displacement of *p*-cymene. They also observed *p*-cymene in the crude ¹H NMR spectra at the end of *N*-alkylation reactions they performed. Because of this, they believe that complex **20** is generated where L_n represents the bidentate phosphine and probably amine ligands. To have some more insight about incorporation of both amines and phosphines into the same monomer, the reaction between $[\text{RuCl}(\text{dppf})(\textit{p}\text{-cymene})]\text{SbF}_6$ (**4**) and a big excess of pyridine (16 molar equivalents) in the presence of an equivalent of NaSbF_6 was attempted, at room temperature (see scheme 2.11). The starting monomer was obtained in the end. Also, the pyridine monomer $[\text{RuCl}_2(\textit{p}\text{-cymene})(\text{NC}_5\text{H}_5)]$ was reacted by a person in the group (A. Rodríguez) with one molar equivalent of dppf in the presence of 10 molar equivalents of NaSbF_6 which afforded $[\text{RuCl}(\text{dppf})(\textit{p}\text{-cymene})]\text{SbF}_6$ (**4**). These two reactions show the bigger lability of chlorine atoms and pyridine compared to dppf and *p*-cymene since the last ones

remained complexed in the first reaction and pyridine and chlorine did not in the second one. These facts do not support the first mechanistic step proposed by J. Williams and co-workers.



Scheme 2.9 – Reaction between $[\text{RuCl}(\text{dppf})(p\text{-cymene})]\text{SbF}_6$ (**4**) and pyridine (top left) and between $[\text{RuCl}_2(p\text{-cymene})(\text{NC}_5\text{H}_5)]$ and dppf (bottom left).

The second mechanistic step in their sequence consists in the activation of complex **20** by exchange of a chloride with alcohol, and loss of HCl. The alkoxy complex then formed undergoes a β -hydride transfer giving $\text{LnRuHCl}(\text{O}=\text{CHR})$ which leads to complex **21** by loss of aldehyde and HCl. Oxidative addition of the alcohol provides the alkoxy hydride complex **22**, which can then undergo β -hydride transfer to form the aldehyde complex **23**. It was proven by the authors that this complex can dissociate from the ruthenium and that imine formation does not necessarily take place while coordinated. They performed a crossover experiment (scheme 2.10) where the deuterated alcohol **16** and the ^{13}C labeled alcohol **17** were reacted in the same pot with morpholine to provide the *N*-benzylated morpholine adducts **18** and **19**. They observed deuterium incorporation in both the unlabeled product **18** and the labeled product **19**. Was therefore a crossover of the deuterium to the ^{13}C labelled benzyl group. By other words, there was the displacement of aldehyde from a non-deuterated complex (**23**) and later, the imine that resulted from this aldehyde, complexed to a deuterated ruthenium dihydride (**24**) which transferred its protons to it. Also, the higher

deuterium incorporation found in compound **53** is consistent with the fact that only one of the C-D bonds needs to be broken in order for the reaction to take place. The dissociation of the aldehyde, imine formation and recomplexation leads to the imine complex **25**, presumably by the dihydride complex **24**. Complex **25** then undergoes β -hydride transfer to give the amido complex **26** which suffers reductive elimination to afford the amine product and the regeneration of the ruthenium(0) complex **21**.

The dissociation process found for the intermediate aldehyde may explain some of the results obtained in the N-alkylations of this project, namely the ester conversions. For example, the N-alkylations where no ester formation was seen may be explained in terms of not occurring the dissociation of the intermediate aldehyde. This should prevent the aldehyde from reacting with unreacted alcohol and forming the ester. The different values of ester conversions from compound to compound may also be explained in part in terms of preferred routes of the catalytic intermediates. Some catalytic intermediates may undergo N-alkylation mainly by dissociation of the aldehyde intermediate giving a considerable amount of ester while others may prefer the non-dissociation mechanistic step. Reaction kinetics is also thought to be responsible for the differences found for ester conversions.

2.4.1.2 Gas Chromatography Analysis

The model N-alkylation of this project was monitored by gas chromatography. Just the pre-catalyst pair $[\text{RuCl}_2(p\text{-cymene})]_2(\mathbf{1})\text{-dppf}$ was followed by this technique. The procedure is based on previous work done in a similar field by the Process Lab of the School of Chemistry of the University of Leeds under the supervision of Dr. John Blacker. It consisted of taking 20 μL samples from the reaction mixture from time to time during 24 hours, diluting them with acetonitrile and adding decane as a standard. Conversions were calculated using the internal standard method.

The results from the N-alkylation catalysed by $[\text{RuCl}_2(p\text{-cymene})]_2(\mathbf{1})$ and dppf during 24 hours are shown in table 2.4 and during the first 5 hours plotted in figure 2.13.

Table 2.4 – Alcohol and product concentrations over time in the N-alkylation catalysed by $[\text{RuCl}_2(p\text{-cymene})]_2$ (**1**) in the presence of dppf.

Time/ hours	Concentration Alcohol/ M	Concentration Product/ M	Conversion / %
0	1.82E-01	0.00E+00	0.0
0.25	1.92E-01	1.92E-03	1.1
0.5	1.58E-01	2.29E-03	1.3
0.75	1.70E-01	2.10E-03	1.2
1	1.68E-01	4.74E-03	2.6
1.25	1.60E-01	6.04E-03	3.3
1.5	1.65E-01	8.36E-03	4.6
1.75	1.61E-01	1.00E-02	5.5
2	1.64E-01	1.25E-02	6.9
2.5	1.48E-01	1.45E-02	8.0
3	1.51E-01	1.83E-02	10.1
4	1.44E-01	2.31E-02	12.7
5	1.27E-01	2.51E-02	13.8
23	7.49E-02	4.02E-02	22.1
24	6.57E-02	3.65E-02	20.1

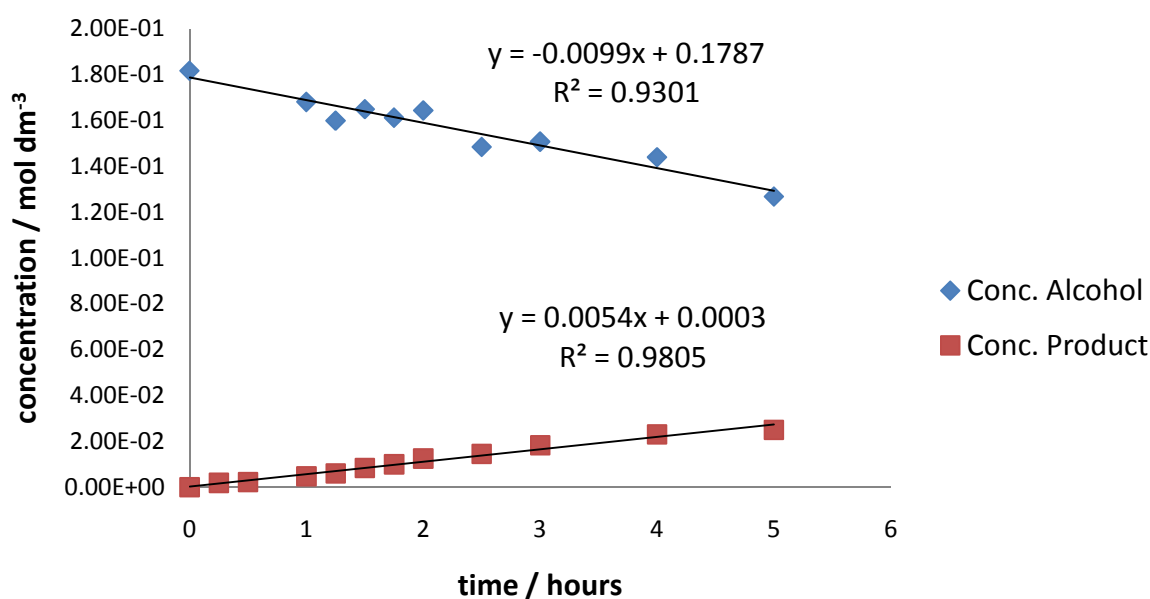


Figure 2.13 – Variation of the product and alcohol concentration in an N-alkylation catalysed by $[\text{RuCl}_2(p\text{-cymene})]_2$ (**1**) in the presence of dppf ligand.

As it is possible to see from table 2.4, conversions were all very low in comparison to what was expected. From the ¹H NMR for the same reaction (not for the same experiment), the final conversion (after 24h) was 75% for the amine product. Although the results obtained by ¹H NMR come from a different experiment, both reactions were run under the

same conditions and the high conversion found by ^1H NMR agrees with the literature¹. The same reaction was ran again and followed by GC but more or less the same conversions were obtained. Conversions were recalculated using the area normalization procedure (comparing peak areas) instead of the internal standard method but low conversions were also obtained. This reaction was found to be very sensitive to changes in solvent volume, fact that was taken into account while running the reactions.

Another curious observation from table 2.4 is that the initial alcohol concentration (1.82E-01 M) does not match to the expected value (3E-01 M). Though, it is possible to see from figure 2.13 that the rate of decrease of the alcohol concentration ($0.0099 \text{ mol dm}^{-3} \text{ h}^{-1}$) is higher than the rate of formation of the product ($0.0054 \text{ mol dm}^{-3} \text{ h}^{-1}$) which is consistent with the observation made before in the ^1H NMR analysis that the reaction is forming a side product, namely $\text{PhCH}_2\text{CH}_2\text{O}_2\text{CCH}_2\text{Ph}$.

After 23 hours of reflux, the product concentration was $4.02 \times 10^{-2} \text{ M}$ and after 24 hours it was $3.65 \times 10^{-2} \text{ M}$. This fact means that the reaction had already proceeded to completion.

Due to the incoherence of the conversions, due to the inoperability of the gas chromatographer for a long period of time and some issues concerning the method of analysis, the reactions followed by gas chromatography were abandoned.

2.4.2 Transfer hydrogenations

In this project two transfer hydrogenations were studied, namely the reduction of acetophenone and the reduction of benzaldehyde. Both were carried out using the same general procedure. The substrate:catalyst ratio (acetophenone or benzaldehyde:ruthenium) was 100:1 on a molar basis (0.5 % mol dimer or 1 % mol monomer). As in N-alkylations, when dimers were used the dimer:phosphine ratio was 1:2 but when monomers were employed no phosphine ligand was added to the reaction. The reactions were set in a Radley's carousel (figure 2.14), which was set upon a stirrer hot plate. This type of apparatus ensures that several reactions are run under the same conditions which give faster and more comparable results. The reactions were set under normal atmosphere.

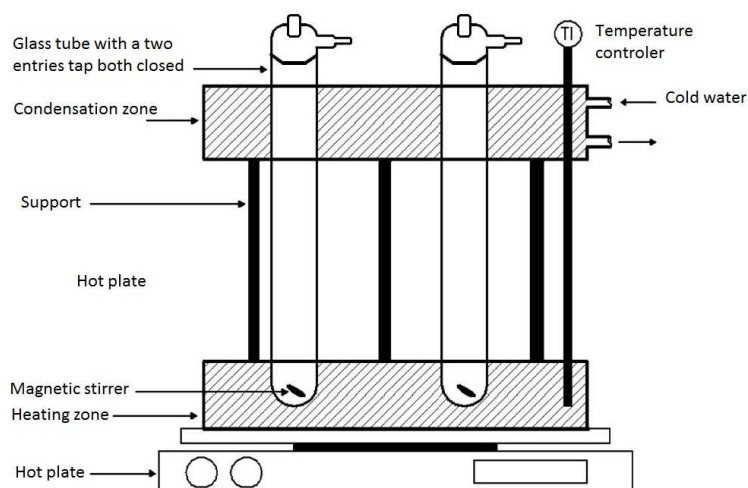


Figure 2.14 – Schematic for the Radley’s carousel used for batch reactions. Adapted from J. Williams and co-workers.²⁷

2.4.2.1 Reduction of Acetophenone

The usual transfer hydrogenation that is tried within McGowan’s group is the one involving acetophenone reduction with isopropanol and potassium tert-butoxide (figure 2.15). This reaction yields a racemic mixture since the ligands employed are not chiral. But the project is not concerned about obtaining enantiopure compounds, but more interested about catalytic activity. So the reaction output, this is the conversion (which includes both isomers), was calculated by ^1H NMR like in the N-alkylations. In figure 2.15 can be seen the product and starting material peaks used to figure out the conversions. The reactions were catalysed by the dimer-ligand catalytic systems and by the monomers that have been synthesised.

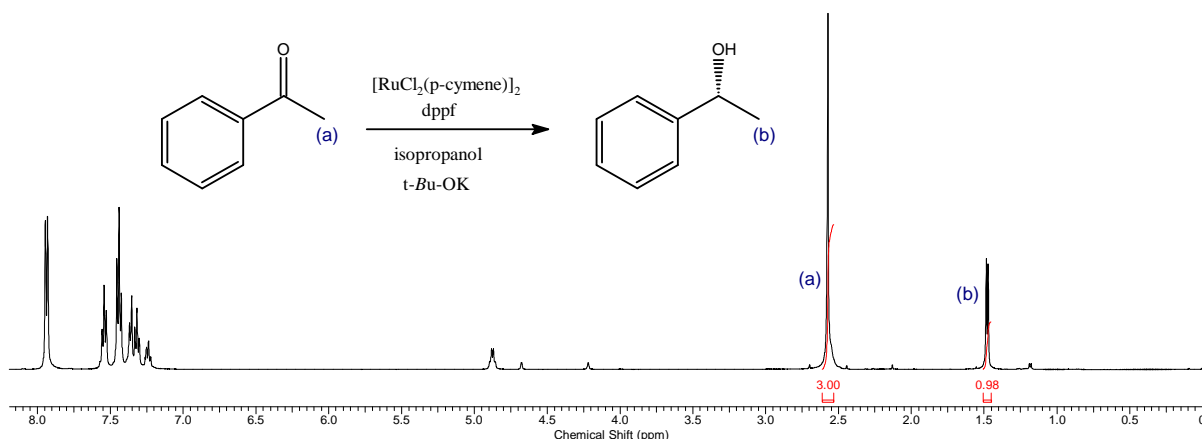


Figure 2.15 – ¹H NMR spectrum of the oily residue obtained after evaporation of the reaction mixture of the conversion of acetophenone to 1-phenylethanol by transfer hydrogenation using [RuCl₂(*p*-cymene)]₂(**1**)-dppf as pre-catalyst. The reaction scheme is also depicted. (a) and (b) are the peaks which integrals were used to calculate the product conversion.

The results from the reduction of acetophenone by transfer hydrogenation are shown in table 2.5. This table also contains results of the same transfer hydrogenations using different catalysts that can be found in the literature and may be useful to make some comparisons.

Table 2.5 – Results for the reduction of acetophenone to 1-phenylethanol by transfer hydrogenation. The base employed is *t*-BuOK and the hydrogen source is isopropanol unless otherwise stated.

Complex	Ligand	Temp. (°C)	h	S/C	Conv. (%)
[RuCl ₂ (<i>p</i> -cymene)] ₂ (1)	–				67
1	dppf				25
1	DPEPhos				21
1	dippf				43
[RuI ₂ (<i>p</i> -cymene)] ₂ (2)	–				19
2	dppf	60	20	100	22
2	DPEPhos				7
2	dippf				54
[RuCl(dppf)(<i>p</i> -cymene)]Cl (7)	–				8
[Ru ₂ Cl ₃ (DPEPhos) ₂ (CH ₃ CN) ₂]SbF ₆ (8)	–				40
[RuI(P(<i>n</i> -Bu) ₃) ₂ (<i>p</i> -cymene)]SbF ₆ (10)	–				3
1	A	40	20	200	10 ^[a]
1	B	40	20	200	5 ^[a]
[RuCl ₂ (η ⁶ -mesitylene)] ₂	(<i>S,S</i>)- TsDPEN	r.t.	15	200	95 ^[b]
[RuCl(<i>S,S</i>)-TsDPEN(η ⁶ -mesitylene)]	–	28	20	200	99 ^[c]

[a] Ligand A and B are depicted in figure 2.16. Ketone:base:[RuCl₂(*p*-cymene)]₂:ligand = 200:20:1:2.⁶²

[b] The value in percentage is actually the yield of the reaction. Ketone:Ru:(*S,S*)-TsDPEN:KOH = 200:1:2:5.⁵⁰

[c] The value in percentage is actually the yield of the reaction. It was carried out in a formic acid-triethylamine mixture (5:2, 2.5 mL).²⁰

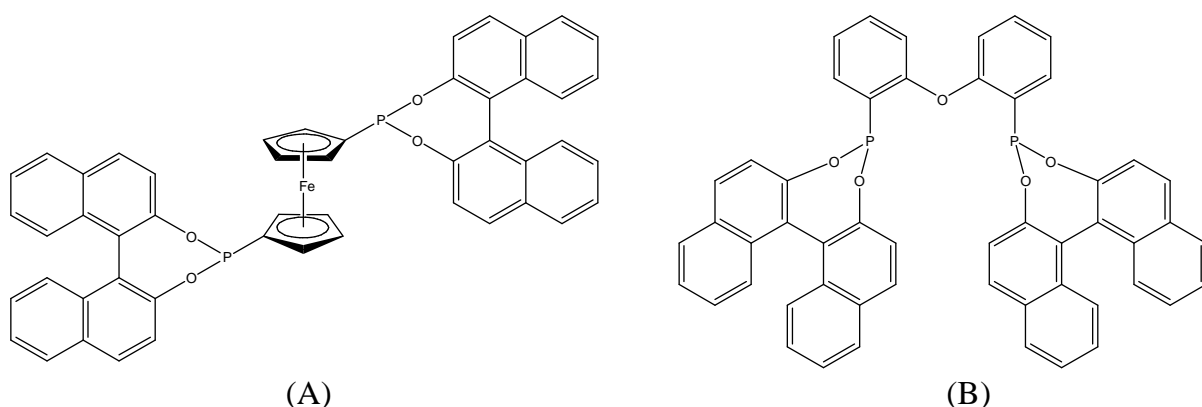
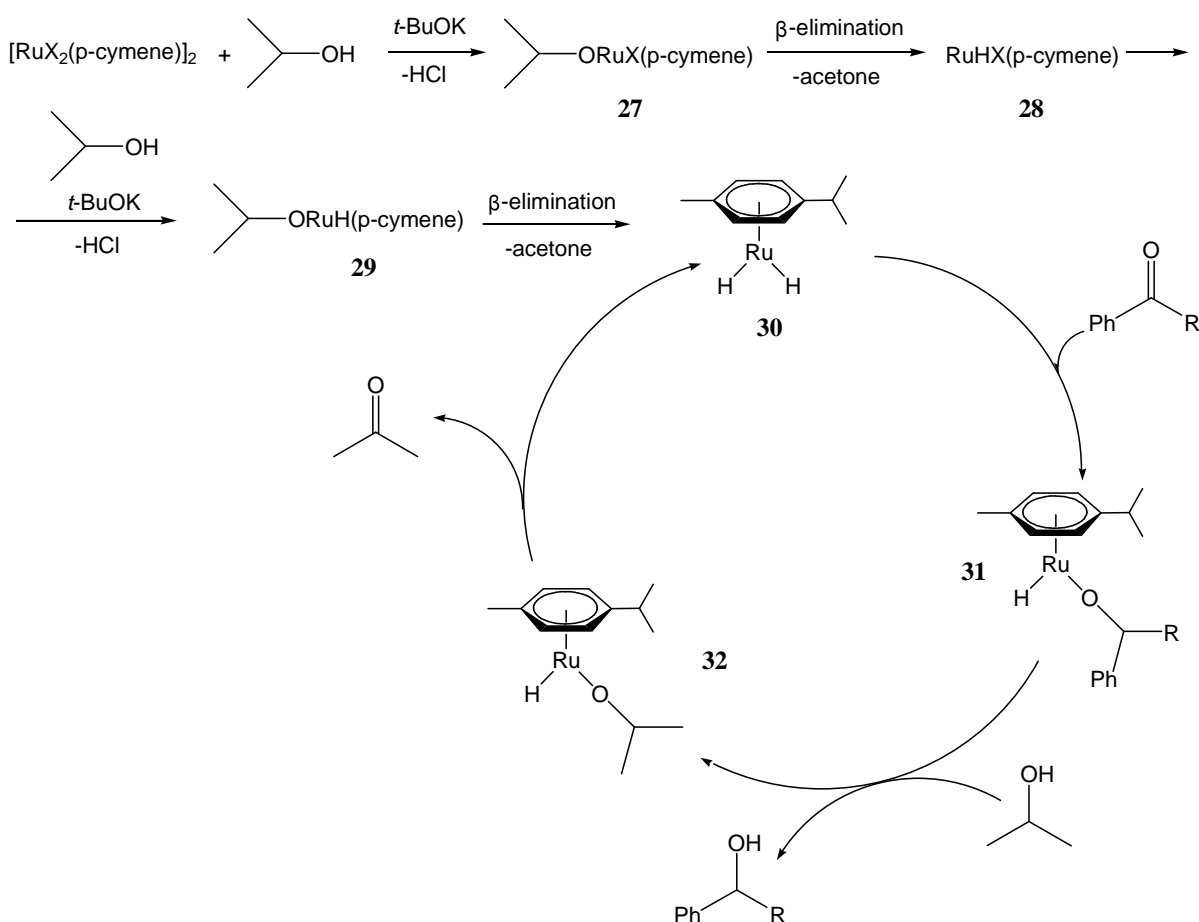


Figure 2.16 – BINOL-derived diphosphonites which have proven to be excellent ligands for asymmetric olefin hydrogenation and other reactions.⁶² A = 1,1'-Bis[(11bR)-dinaphtho[2,1-d:1', 2'-f][1,3,2]dioxaphosphepin-4-yl]ferrocene; B = (11bR, 11'bR)-4,4'-(Oxydi-2,1-phenylene)bis-dinaphtho[2,1-d:, 1', 2'-f][1,3,2]dioxaphosphepin.

It can be seen that the conversion pattern in the reduction of acetophenone is basically opposite to the one shown by the same pre-catalysts in N-alkylations and that none of the pre-catalysts showed the high efficiency of the $[\text{RuCl}_2(\eta^6\text{-mesitylene})]_2$ –(S,S)-TsDPEN dimer-ligand pair or the renowned complex $[\text{RuCl}(\text{S,S})\text{-TsDPEN}(\eta^6\text{-mesitylene})]$, both disclosed by Noyori and co-workers^{20, 50}. In here, $[\text{RuCl}_2(p\text{-cymene})]_2$ (**1**) in the absence of any additional ligand afforded the best product conversion while in the corresponding N-alkylation it afforded minimal consumption of starting material. Also, the presence of phosphine ligands together with $[\text{RuCl}_2(p\text{-cymene})]_2$ (**1**) did not improve or did not improve much the percentage of starting material converted, whereas in N-alkylation it was crucial. This may be explained in terms of mechanistic features as it is going to be discussed later. A result found in the literature⁶² with $[\text{RuCl}_2(p\text{-cymene})]_2$ (**1**) in the presence of a dppf related ligand (A) gave a poor conversion into the product as well, proving the inefficacy of these ligands. Another fact is that $[\text{RuI}_2(p\text{-cymene})]_2$ (**2**) did not improve the conversion when compared to $[\text{RuCl}_2(p\text{-cymene})]_2$ (**1**) (except in the case of the $[\text{RuI}_2(p\text{-cymene})]_2$ (**2**)-dppf pair). Something can also be said about the pair $[\text{RuI}_2(p\text{-cymene})]_2$ (**2**)-DPEPhos which in the N-alkylation was the best pre-catalyst. This time, it was one of the worst (7% conversion). The same can be said about $[\text{RuCl}(\text{dppf})(p\text{-cymene})]\text{Cl}$ (**7**). Poor results were also found in the literature⁶² with a DPEPhos related ligand (B) proving the inefficacy of these ligands. $[\text{RuI}(\text{P}(n\text{-Bu})_3)_2(p\text{-cymene})]\text{SbF}_6$ (**10**) showed again that is not suitable for the catalytic reactions under study (only 3% conversion). $[\text{Ru}_2(\text{NCCH}_3)_2(\text{DPEPhos})_2]\text{SbF}_6$ (**8**) although not

being the best pre-catalyst, it showed it forms catalytically active species in both transfer hydrogenations and N-alkylations. Just to have more insight about trichloro-bridged complexes, in the literature it is possible to find that the structure related compound $[\text{Ru}_2\text{Cl}_3(\text{dppb})_2(\text{MeCN})_2]\text{PF}_6$ (dppb = diphenylphosphino butane) forms catalytically active species in the reduction of $\text{CH}_2\text{N}=\text{C}(\text{R})\text{Ph}$ ($\text{R}=\text{H}$ or Me) with H_2 .⁶³

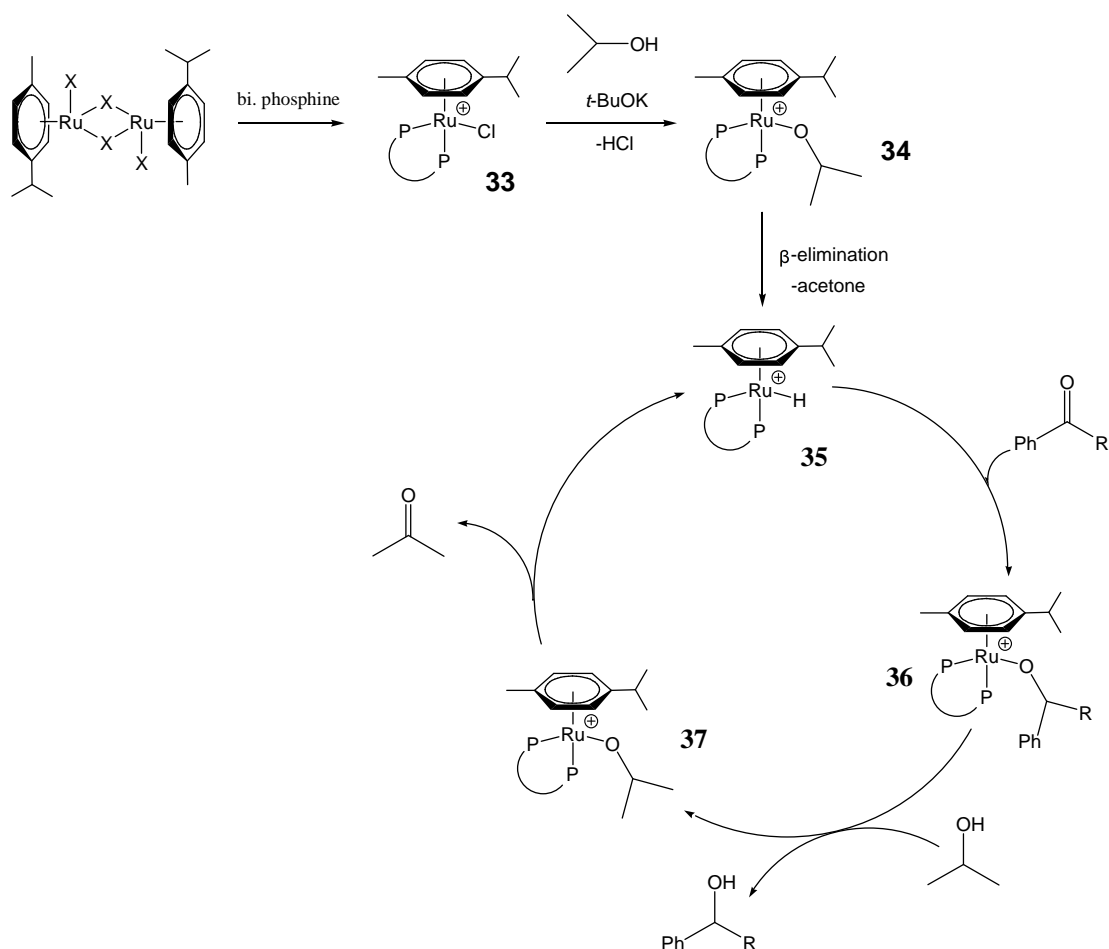
In a typical hydrogenation reaction, the basic requirements are the formation of metal hydride species and a free coordination site for maintaining the catalytic cycle.² In the present case, there is the generation of different hydrides according to the pre-catalyst employed. For the dimers it selves it is supposed to occur the generation of a metal dihydride according to what was proven for the complex $\text{RuCl}_2(\text{PPh}_3)_3$ ($\text{RuH}_2(\text{PPh}_3)_3$ being the active catalyst)¹⁷ which is similar to each half of the ruthenium dimer, $\text{RuX}_2(\textit{p}\text{-cymene})$ ($\text{X}=\text{Cl}$ or I). A proposed mechanism for the reduction of acetophenone and benzaldehyde catalysed by ruthenium dimers is shown in scheme 2.12.



Scheme 2.10 – Proposed catalytic cycle in the present study for the reduction of acetophenone ($\text{R}=\text{CH}_3$) and benzaldehyde ($\text{R}=\text{H}$) employing ruthenium dimers in the absence of any additional ligands. $\text{X} = \text{halide}$.

The reaction of the ruthenium dimer with isopropanol in the presence of a base facilitates the formation of a ruthenium alkoxide (**27**) by abstracting the proton of the alcohol. The alkoxide then undergoes a β -elimination to give the chloride/iodide-monohydride complex **28**. In order to turn the complex catalytically active it needs to go through the base-promoted sequence of alkoxyde formation- β -elimination a second time to replace also the second halide by hydride. This gives the dihydride complex **30** which is thought to be the active catalyst. Then occurs the addition of the acetophenone/benzaldehyde into the coordination sphere of the metal followed by a migratory insertion into the Ru-H bond to give the alkoxy complex **31**. This complex then undergoes a reductive elimination followed by an oxidative addition of isopropanol releasing the corresponding product. The complex then formed, **32**, suffers a reductive elimination releasing acetone.

As seen, the dimers in the absence of any additional ligands are supposed to follow the dihydride mechanism. The same route was not found by Backväll and co-workers for the complex $[\text{RuCl}(\text{dppp})(p\text{-cymene})]\text{Cl}^2$ (dppp = 1,3-Bis(diphenylphosphino)propane). By deuteration experiments they found out that this complex undergoes transfer hydrogenation mainly by a monohydride mechanism. This result suggests that the monomers synthesised in this project, few of them quite similar in structure to $[\text{RuCl}(\text{dppp})(p\text{-cymene})]\text{Cl}$, should follow the same route. By association, the dimer-ligand pairs herein studied should follow the monohydride path as well. A proposed mechanism for this path is shown in scheme 2.13.



Scheme 2.11 – Proposed catalytic cycle in the present study for the reduction of acetophenone (R=CH₃) and benzaldehyde (R=H) employing ruthenium dimers in the presence of biphosphine ligands or just employing diphosphine ruthenium monomers (**33**). X = halide.

The complexation of a bidentate phosphine to the ruthenium dimer should lead to the formation of the cationic 18 electron complex [Ru(P-P)(*p*-cymene)Cl]⁺ (**33**). In order to turn it catalytically active it needs to go through the base-promoted sequence of alkoxide formation-β-elimination to give the hydride complex **35**. Then occurs the addition of the acetophenone/benzaldehyde into the coordination sphere of the metal followed by a migratory insertion into the Ru-H bond to give the alkoxide complex **36**. In order to maintain the catalytic cycle this complex needs to generate a free coordination site. The idea is that the phosphine ligand behaves as hemilabile, alternating between bidentate to monodentate coordination thereby allowing coordination of isopropanol to take place and then the releasing of the product. This path should not be in principle very favourable due to the strong binding of chelate complexes. This fact might explain the poor results obtained for the dimers in the presence of the diphosphine ligands and for the monomers.

2.4.2.2 Reduction of Benzaldehyde

The other transfer hydrogenation that was studied in this project was the reduction of benzaldehyde with isopropanol and potassium tert-butoxide in the presence of the same pre-catalysts mentioned before. For this reaction the product does not consist in a racemic mixture. Conversions were calculated as before. In figure 2.17 it can be seen the product and starting material peaks used to figure out the conversions.

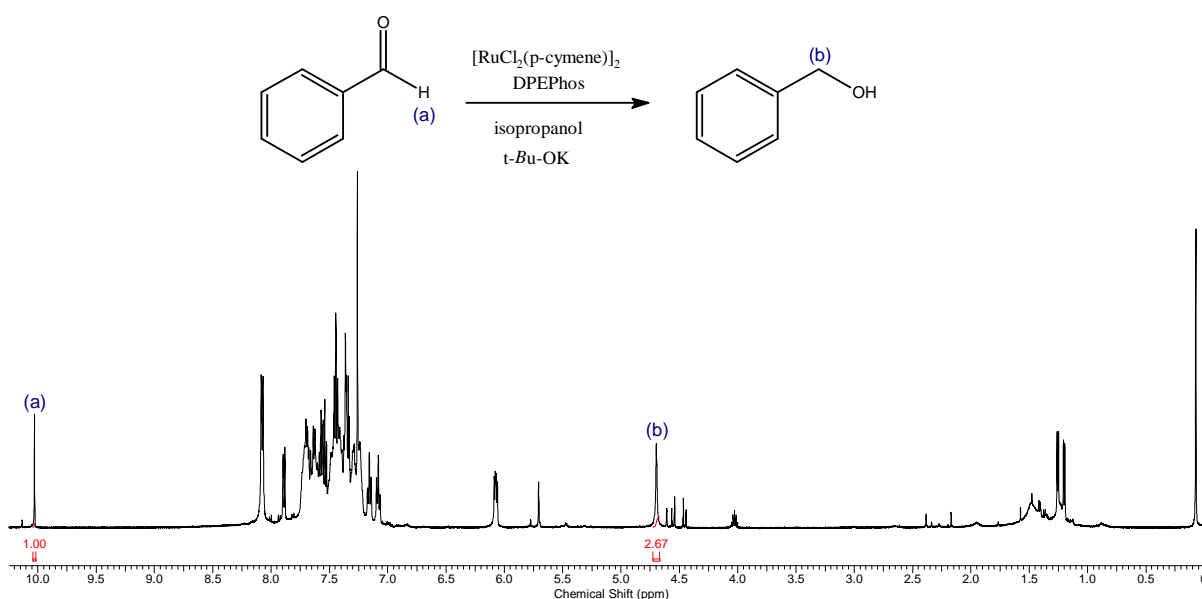


Figure 2.17 – ¹H NMR spectrum of the oily residue obtained after evaporation of the reaction mixture of the conversion of benzaldehyde to benzyl alcohol by transfer hydrogenation using [RuCl₂(*p*-cymene)]₂ (1)-DPEPhos as pre-catalyst. The reaction scheme is also depicted. (a) and (b) are the peaks which integrals were used to calculate the product conversion.

The results from the reduction of benzaldehyde by transfer hydrogenation are shown in table 2.6 and a comparison of the catalytic activities according to the substrate (acetophenone or benzaldehyde) is depicted in figure 2.18.

Table 2.6 – Results for the reduction of benzaldehyde to benzyl alcohol by transfer hydrogenation. The base employed is *t*-BuOK and the hydrogen source is isopropanol.

Complex	Ligand	Substrate	Temp. (°C)	h	S/C	Conv. (%)
[RuCl ₂ (<i>p</i> -cymene)] ₂ (1)	–	Benzaldehyde	60	20	100	73
1	dppf					55
1	DPEPhos					57
1	dippf					0
[RuCl ₂ (<i>p</i> -cymene)] ₂ (1)	–					68
2	dppf					55
2	DPEPhos					34
[RuCl(dppf)(<i>p</i> -cymene)]Cl (7)	–					47
[RuI(P(<i>n</i> -Bu) ₃) ₂ (<i>p</i> -cymene)]SbF ₆ (10)	–					12

From table 2.6 it can be seen that the conversion pattern is basically the same shown by the same pre-catalysts in the reduction of acetophenone. Again, [RuCl₂(*p*-cymene)]₂ (**1**) in the absence of any additional ligand afforded the best product conversion and the presence of phosphine ligands did not improve the percentage of starting material converted. Another similar fact is that [RuI₂(*p*-cymene)]₂ (**2**) did not improve the conversion when comparing to [RuCl₂(*p*-cymene)]₂ (**1**). For this reaction, although showing again the poorest performances, the [RuI₂(*p*-cymene)]₂ (**2**)-DPEPhos pair and [RuCl(dppf)(*p*-cymene)]Cl (**7**) gave substantially better conversions compared to those in the reduction of acetophenone (34 and 47% dimer-ligand pair and monomer respectively, against 7 and 8%). In fact, all the pre-catalysts tested in the reduction of benzaldehyde showed a better performance (substantial increase in conversion) in comparison with their performance in the reduction of acetophenone (figure 2.18). This is thought to be related to the CH₃ group in the acetophenone that provides steric hindrance for the insertion of this ketone into the coordination sphere of the metal.

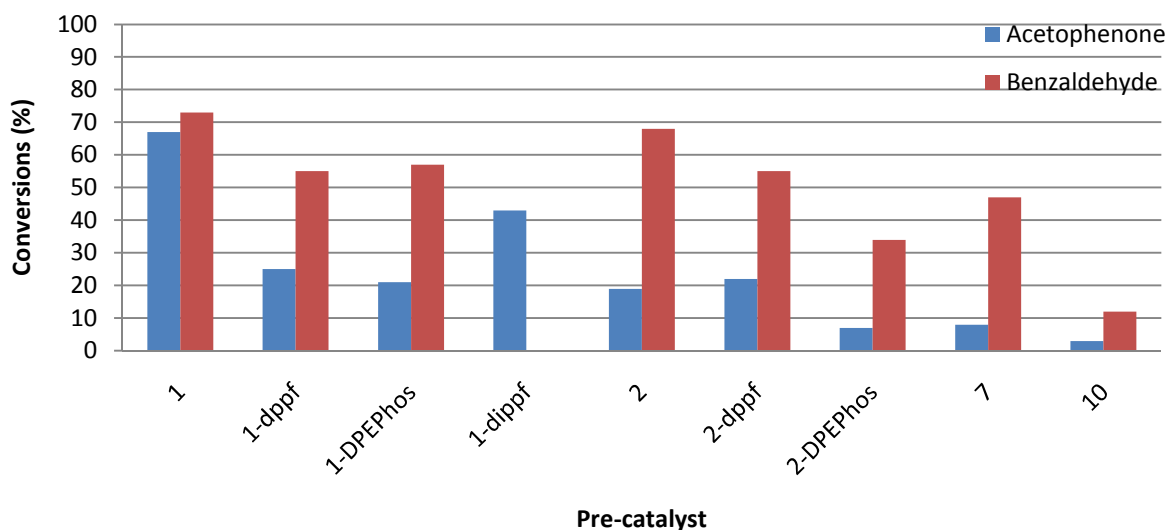


Figure 2.18 – Comparison of the catalytic activities according to the substrate in the reduction of acetophenone and benzaldehyde by transfer hydrogenation.

3. Conclusions

A range of *in situ* generated catalysts (*p*-cymene ruthenium dimers in the presence of phosphines) and *p*-cymene based ruthenium monomers have been employed in the N-alkylation of *t*-butylamine with phenethyl alcohol and reduction of acetophenone and benzaldehyde by transfer hydrogenation.

Some *p*-cymene based ruthenium half-sandwich complexes (monomers) have been successfully prepared with various phosphine ligands (dppf, $P(n\text{-Bu})_3$, $P(i\text{-Bu})_3$, $P(\text{CH}_3)_3$, PhPCl_2), some of them forming catalytically active species towards the reactions of interest.

It has been demonstrated that *p*-cymene based ruthenium complexes can provide highly active and selective catalysts in the alkylation of *t*-butylamine with phenethyl alcohol either by the use of dimers in the presence of phosphines or by the use of phosphine containing monomers. Namely $[\text{Ru}_2(\textit{p}\text{-cymene})]$ with DPEPhos (substrate/catalyst ratio of 20) gave 96% conversion into the amine product and $[\text{Ru}(\text{dppf})(\textit{p}\text{-cymene})]\text{SbF}_6$ (**5**) gave 85% with a substrate/catalyst ratio of 40 being the only precursor with this S/C ratio giving 0% of unreacted alcohol, which is a very promising result. Also, these reactions have been run out in the open air without degassing or inert gas protection throughout which is not the typical approach found in the literature and which can be very appealing in the industrial point of view.

More conclusions about N-alkylations are drawn as follows:

- Results suggest that $[\text{RuX}(\text{LL})(p\text{-cymene})]^+$ complexes where X=halide and LL=bidentate ligand are the catalytic precursors in reactions employing $[\text{RuX}_2(p\text{-cymene})]_2$ and bidentate phosphines;
- The presence of iodine in the ruthenium complexes instead of chlorine usually led to an increase in the catalytic activity of the active catalyst species formed;
- When comparing the effect of the counter-ion, namely between $[\text{RuCl}(\text{dppf})(p\text{-cymene})]\text{SbF}_6$ (**4**), $[\text{RuCl}(\text{dppf})(p\text{-cymene})]\text{BF}_4$ (**6**) and $[\text{RuCl}(\text{dppf})(p\text{-cymene})]\text{Cl}$ (**7**), **7** seems to be the best catalyst precursor (82% conversion into amine), which is expected to be the species formed in the reaction;
- Monodentate phosphines seem to be not suitable for these reactions since their incorporation in the catalyst precursors led to inactive or very poor catalytic species;
- The formation of ester as side product seen in these reactions may be explained in terms of the dissociation process found in the mechanism for the intermediate aldehyde complex.

In the transfer hydrogenation reactions concerning the reduction of acetophenone and benzaldehyde, it has been demonstrated that the catalyst precursors employed are not the most suitable for these reactions. Overall, conversions up to 73% were obtained which lag far behind the 100% reported in the literature for several other catalysts, the most representative ones disclosed by Noyori.

Although the conversions obtained for the reduction reactions are not very appealing for further use of the catalyst precursors, the results allowed to draw some interesting conclusions:

- The dimers in absence of any additional ligand afforded the best product conversion and the presence of phosphine ligands and iodine in the catalyst precursors did not improve or did not improve much the percentage of starting material converted. These facts are somewhat opposite to the trends in N-alkylations;
- Again, monodentate phosphines seem not to be suitable for hydrogen transfer reactions, with complex $[\text{RuI}(\text{P}(n\text{-Bu})_3)_2(p\text{-cymene})]\text{SbF}_6$ (**10**) forming a very poor catalytic

species (3% and 12% conversion for the reduction of acetophenone and benzaldehyde, respectively);

– The results suggest that the dimers in the absence of any additional ligands follow a catalytic mechanism other than the one followed by dimers in the presence of phosphines or by ruthenium monomers and a catalytic cycle for both cases has been proposed.

– All the pre-catalysts tested in the reduction of benzaldehyde showed a better performance (substantial increase in conversion) in comparison with their performance in the reduction of acetophenone.

Unexpected complex $[\text{Ru}_2\text{Cl}_3(\text{DPEPhos})_2(\text{CH}_3\text{CN})_2]\text{SbF}_6$ (**8**) has been synthesised and has shown it forms catalytically active species in both the alkylation of *t*-butylamine (28% of amine and only 12% of unreacted alcohol) and reduction of acetophenone (40% conversion) giving moderate conversions. The use of trichloro-bridged complexes in such reactions has not been demonstrated before as far as it is known which opens new fields of application for these complexes.

4. Future Work

As it was possible to be seen, the most promising results were achieved in N-alkylations. Because of this and since these reactions have been much less documented than transfer hydrogenations of unsaturated compounds and are increasing their importance to the pharmaceutical industry, future work would focus on this type of reaction.

An important work for those who later want to carry on this investigation is the monitoring of the best pre-catalysts ($[\text{Ru}_2(p\text{-cymene})]_2\text{-DPEPhos}$, $[\text{Ru}(\text{dppf})(p\text{-cymene})]\text{SbF}_6$ (**5**) and $[\text{RuCl}(\text{dppf})(p\text{-cymene})]\text{Cl}$ (**7**)) in N-alkylations by GC. This will allow gaining more insight about reaction kinetics and a comparison of pre-catalysts in terms of fastness/velocity constants can be made. This will also allow the determination of when the N-alkylations are finished leading to an improvement of the method.

Studies that can be of a great importance are those investigating the effects of changing the reaction conditions in the N-alkylations using the best pre-catalysts found.

Namely, studies employing lower boiling point solvents which would permit the application of N-alkylations to sensitive substrates.

The next step in this project would have been the immobilization of the pre-catalysts for heterogeneous catalysis. Homogeneous catalysts usually offer the best results in activity and selectivity, however they have a major drawback in recyclability processes, because they are not easily separated and recovered from a reaction mixture. This clearly limits their industrial applications. To overcome this, immobilization of the best pre-catalysts found in this project would have been attempted.

The synthesis and application of more *p*-cymene based ruthenium monomers incorporating bidentate phosphines and iodine seems to be the path to follow in N-alkylations.

5. Experimental Procedures

5.1 General Experimental Considerations

Unless otherwise stated, all manipulations involving the synthesis of the compounds mentioned were under normal atmosphere, with no need of using standard Schlenk line techniques.

Chemicals were obtained from Sigma-Aldrich Chemicals Co. (this includes deuterated NMR solvents), Alfa Aesar, Fisher Scientific, SAFC Supply Solutions, Fluka Analytical, Acros Organics, VWR International Ltd. and the Department of Chemistry breached bottle store, and they were used without further purification.

The NMR spectra were acquired by the author using a Bruker DPX 300 MHz spectrometer, a Bruker DRX 500 MHz spectrometer or by Mr. Simon Barrett using a Bruker DRX 500 MHz spectrometer. Microanalyses were obtained by Mr. Ian Blakely at the University of Leeds Microanalytical Service. Mass Spectra were obtained by Ms. Tanya Marinko-Covell at the University of Leeds Mass Spectrometry Service. X-ray diffraction data were collected and solved by Mr. Colin Kilner and Mr. David Crabtree, on a Nonius KappaCCD area detector diffractometer using graphite monochromated Mo-K α radiation ($\lambda = 0.71073 \text{ \AA}$).

All the complexes herein synthesised were properly dried under vacuum and anhydrous conditions before submitting them to elemental analysis although some NMR spectra show several solvent peaks.

5.2 Synthesis of the complexes

5.2.1 Synthesis of $[\text{RuCl}_2(\textit{p}\text{-cymene})]_2 - \text{C}_{20}\text{H}_{28}\text{Cl}_4\text{Ru}_2$ (1)

α -Terpinene (23 mL, 0.13 mol, 90%) was added to a solution of $\text{RuCl}_3 \cdot 3\text{H}_2\text{O}$ (5.02 g, 19.2 mmol) in ethanol (200 mL) and heated under reflux for 24 hours. After reducing the volume *in vacuo* (1:3), the solution was stored in the freezer (-20 °C) overnight. A red precipitate was filtered off, washed with ice cold diethyl ether and dried *in vacuo* to yield a red crystalline powder.

Yield: 5.39 g, 8.81 mmol (92%)

Analysis for $\text{C}_{20}\text{H}_{28}\text{Cl}_4\text{Ru}_2$

Found: C 39.35; H 4.60; Cl 23.05 %

Calculated: C 39.22; H 4.61; Cl 23.16 %

^1H NMR (CDCl_3 , 500.23 MHz, 300 K): δ = 1.28 [d, 12H, $^3\text{J}(\text{}^1\text{H}, \text{}^1\text{H})$ = 6.84 Hz, 6H, $\text{CH}(\text{CH}_3)_2$], 2.16 [s, 6H, $\text{C}_6\text{H}_4\text{CH}_3$], 2.92 [sept, 2H, $\text{CH}(\text{CH}_3)_2$], 5.34 [d, $^3\text{J}(\text{}^1\text{H}, \text{}^1\text{H})$ = 5.56 Hz, 4H, $\eta^6\text{-C}_6\text{H}_4$], 5.47 [d, $^3\text{J}(\text{}^1\text{H}, \text{}^1\text{H})$ = 5.56 Hz, 4H, $\eta^6\text{-C}_6\text{H}_4$] ppm;

ES MS (+): m/z 575.9 [MH^+] – Cl.

5.2.2 Synthesis of $[\text{RuI}_2(\textit{p}\text{-cymene})]_2 - \text{C}_{20}\text{H}_{28}\text{I}_4\text{Ru}_2$ (2)

A solution of NaI (3.6572 g, 24.4 mmols) in water (32 cm^3) was added to a solution of $[\text{RuCl}_2(\textit{p}\text{-cymene})]_2$ (1) (489.6 mg, 0.8 mmols) in CHCl_3 (40 cm^3). It was stirred at room temperature for three days. The two phases were separated and the organic phase was washed with water (1 \times 40 cm^3) and brine (1 \times 40 cm^3). It was dried over anhydrous Na_2SO_4 and CHCl_3 was evaporated. The solid was dissolved in dichloromethane and precipitated with hexane to yield a very dark violet crystalline powder.

Yield: 709.6 mg, 0.725 mmol (91%)

Analysis for $\text{C}_{20}\text{H}_{28}\text{I}_4\text{Ru}_2$

Found: C 24.90; H 3.50 %

Calculated: C 24.56; H 2.88 %

$^1\text{H NMR}$ (CDCl_3 , 500.23 MHz, 300 K): $\delta = 1.25$ [d, 12H, $^3\text{J}(^1\text{H}, ^1\text{H}) = 6.84$ Hz, 6H, $\text{CH}(\text{CH}_3)_2$], 2.36 [s, 6H, $\text{C}_6\text{H}_4\text{CH}_3$], 3.02 [sept, 2H, $\text{CH}(\text{CH}_3)_2$], 5.43 [d, $^3\text{J}(^1\text{H}, ^1\text{H}) = 5.98$ Hz, 4H, $\eta^6\text{-C}_6\text{H}_4$], 5.53 [d, $^3\text{J}(^1\text{H}, ^1\text{H}) = 5.98$ Hz, 4H, $\eta^6\text{-C}_6\text{H}_4$] ppm.

ES MS (+): m/z 852.7 [MH^+] – I.

5.2.3 Synthesis of $[\text{RuBr}_2(\textit{p}\text{-cymene})]_2 - \text{C}_{20}\text{H}_{28}\text{Br}_4\text{Ru}_2$ (3)

This experimental procedure did not obtain the product pure neither useful to use in further reactions. It just shows the attempt that has worked better to try to obtain this dimer.

A solution of NaBr (1.2552 g, 12.2 mmols) in water (16 cm^3) was added to a solution of $[\text{RuCl}_2(\textit{p}\text{-cymene})]_2$ (**1**) (0.1224 g, 0.2 mmols) in CHCl_3 (10 cm^3) and heated under reflux for 1 day. It was left just stirring for more 2 days. The two phases were separated and the organic layer was washed with water (2 \times 20 cm^3) and brine (1 \times 20 cm^3). It was dried over anhydrous Na_2SO_4 and CHCl_3 evaporated. The solid was dissolved in dichloromethane and precipitated with hexane to yield an orange powder.

Yield: 83.4 mg, 0.106 mmol (53%)

Analysis for $\text{C}_{20}\text{H}_{28}\text{Br}_4\text{Ru}_2$

Found: C 36.80; H 4.25 %

Calculated: C 30.40; H 3.57 %

$^1\text{H NMR}$ (CDCl_3 , 500.23 MHz, 300 K): same as compound **1** but broadened.

5.2.4 Synthesis of $[\text{RuCl}(\text{dppf})(\textit{p}\text{-cymene})]\text{SbF}_6 - \text{C}_{44}\text{H}_{42}\text{P}_2\text{ClFeRu}(\text{SbF}_6)$ (4)

5.2.4.1 Method 1

To a suspension of $[\text{RuCl}_2(\textit{p}\text{-cymene})]_2$ (**1**) (200 mg, 0.328 mmol) in a mixture of $\text{CH}_3\text{OH}/\text{CH}_3\text{CN}$ (1:1, 20 cm^3) was added NaSbF_6 (169.7 mg, 0.656 mmol). The mixture was stirred for 30 minutes to yield an orange solution. After this time, dppf (379.8 mg, 0.685 mmol) dissolved in THF (30 cm^3) was added and left stirring for 1h. The solvent was removed

in vacuo to give a dark orange solid. It was washed with an ethanol/water (4:1) mixture and filtered. The solid was recrystallised from a mixture of ethanol/acetone (4:1) and washed with ethanol and water to afford a brownish orange powder.

Yield: 201.8 mg, 0.190 mmol (29%)

Analysis for C₄₄H₄₂P₂ClFeRu(SbF₆)

Found: C 49.75; H 3.95; Cl 3.30 %

Calculated: C 49.81; H 3.99; Cl 3.34 %

¹H NMR ((CD₃)₂CO, 500.23 MHz, 300 K): δ = 0.88 [d, ³J(¹H, ¹H) = 6.95 Hz, 6H, CH(CH₃)₂], 1.05 [s, 3H, C₆H₄CH₃], 2.75 [m, 1H, CH(CH₃)₂], 4.21 [s, 2H, Cp], 4.40 [s, 2H, Cp], 4.49 [s, 2H, Cp], 5.06 [s, 2H, Cp], 5.52 [d, ³J(¹H, ¹H) = 5.96 Hz, 2H, η⁶-C₆H₄], 6.12 [‘d’, ³J(¹H, ¹H) = 5.96 Hz, 2H, η⁶-C₆H₄], 7.50 [m, 4H, m-CH of Ph], 7.52 [m, 2H, p-CH of Ph], 7.72 [m, 4H, o-CH of Ph], 7.72 [m, 4H, m-CH of Ph], 7.78 [m, 2H, p-CH of Ph], 7.87 [m, 4H, o-CH of Ph] ppm.

¹H NMR (CDCl₃, 500.23 MHz, 300 K): δ = 0.88 [s (br.), 6H, CH(CH₃)₂], 0.96 [s, 3H, C₆H₄CH₃], 2.64 [s (br.), 1H, CH(CH₃)₂], 4.08 [s, 2H, Cp], 4.28 [s, 2H, Cp], 4.36 [s, 2H, Cp], 5.05 [s, 2H, Cp], 5.14 [s (br.), 2H, η⁶-C₆H₄], 5.67 [s (br.), 2H, η⁶-C₆H₄], 7.39-7.49, 7.52-7.63, 7.65-7.75 [3m, 20H, CH of Ph] ppm.

¹³C{¹H} NMR ((CD₃)₂CO), 125.76 MHz, 300 K): δ = 14.95 [s, 1C, CH₃ of CH₃C(CH)₂(CH)₂CCH(CH₃)₂], 21.00 [s, 2C, CH₃ of CH₃C(CH)₂(CH)₂CCH(CH₃)₂], 31.65 [s, 1C, CH of CH₃C(CH)₂(CH)₂CCH(CH₃)₂], 74.60 [t, 1C, CH of Cp], 70.24 [t, 1C, CH of Cp], 79.36 [t, 1C, CH of Cp], 75.81 [t, 1C, CH of Cp], 84.84 [virtual triplet, 1C, Quaternary C of Cp], 91.77 [t, 2C, CH of CH₃C(CH)₂(CH)₂CCH(CH₃)₂], 97.29 [‘t’, 2C, CH of CH₃C(CH)₂(CH)₂CCH(CH₃)₂], 100.08 [s, 1C, Quaternary C of CH₃C(CH)₂(CH)₂CCH(CH₃)₂], 129.40, 129.20 [2t, 8C, m-CH of Ph], 132.97, 131.61 [2s, 4C, p-CH Ph], 134.41 [t, 4C, o-CH of Ph], 134.92 [virtual triplet, 2C, Quaternary C of Ph], 136.24 [t, 4C, o-CH of Ph], 139.55 [virtual triplet, 2C, Quaternary C of Ph] ppm.

³¹P{¹H} NMR ((CD₃)₂CO, 121.49 MHz, 300 K): δ = 37.78 (s) ppm.

ES MS (+): m/z 852.1 [M] – SbF₆.

5.2.4.2 Method 2

To a suspension of [RuCl₂(*p*-cymene)]₂ (**1**) (159.2 mg, 0.260 mmol) in methanol (20 cm³) were added NaSbF₆ (134.5 mg, 0.520 mmol) and dppf (288.2 mg, 0.520 mmol). The

mixture was heated under reflux for 3 hours to yield an orange precipitate. It was filtered and washed with diethyl ether and water to yield the product as an orange powder.

Yield: 435.8 mg, 0.411 mmol (79%)

¹H NMR (CDCl₃, 500.23 MHz, 300 K): δ = 0.88 [d, ³J(¹H,¹H) = 6.95 Hz, 6H, CH(CH₃)₂], 0.95 [s, 3H, C₆H₄CH₃], 2.63 [sept, 1H, CH(CH₃)₂], 4.07 [s, 2H, Cp], 4.27 [s, 2H, Cp], 4.35 [s, 2H, Cp], 5.06 [s, 2H, Cp], 5.13 [d, ³J(¹H,¹H) = 6.16 Hz, 2H, η⁶-C₆H₄], 5.66 [‘d’, ³J(¹H,¹H) = 6.16 Hz, 2H, η⁶-C₆H₄], 7.39-7.49, 7.52-7.63, 7.65-7.75 [3m, 20H, CH of Ph] ppm.

5.2.5 Synthesis of [RuI(dppf)(*p*-cymene)]SbF₆ – C₄₄H₄₂P₂FeRuI(SbF₆) (5)

To a suspension of [RuI₂(*p*-cymene)]₂ (**2**) (320.8 mg, 0.328 mmol) in a mixture of CH₃OH/CH₃CN (1:1, 20 cm³) was added NaSbF₆ (169.7 mg, 0.656 mmol). The mixture was stirred for 30 minutes to yield red wine color solution. After this time, dppf (379.8 mg, 0.685 mmol) dissolved in THF (30 cm³) was added and left stirring for 1h. The solvent was removed *in vacuo* to give a dark red wine solid. It was washed with an ethanol/water (4:1) mixture and filtered. The solid was recrystallised from a mixture of acetone/ethanol (4:1) and washed with ethanol and water to afford a red wine color powder.

Yield: 92.2 mg, 0.080 mmol (12%)

Analysis for C₄₄H₄₂P₂FeRuI(SbF₆)

Found: C 49.95; H 4.00; I 22.45 %

Calculated: C 45.86; H 3.67; I 11.01%

¹H NMR (CDCl₃, 500.23 MHz, 300 K): δ = 0.75 [d, ³J(¹H,¹H) = 6.95 Hz, 6H, CH(CH₃)₂], 1.05 [s, 3H, C₆H₄CH₃], 3.72 [m, 1H, CH(CH₃)₂], 4.12 [s, 2H, Cp], 4.21 [s, 2H, Cp], 4.39 [s, 2H, Cp], 5.38 [d, ³J(¹H,¹H) = 6.36 Hz, 2H, η⁶-C₆H₄], 5.44 [s, 2H, Cp], 5.95 [d, ³J(¹H,¹H) = 6.36 Hz, 2H, η⁶-C₆H₄], 7.39-7.45, 7.47-7.53, 7.54-7.60, 7.61-7.68 [4m, 20H, CH of Ph] ppm.

¹³C{¹H} NMR (CDCl₃, 75.48 MHz, 300 K): δ = 15.16 [s, 1C, CH₃ of CH₃C(CH)₂(CH)₂CCH(CH₃)₂], 21.34 [s, 2C, CH₃ of CH₃C(CH)₂(CH)₂CCH(CH₃)₂], 32.49 [s, 1C, CH of CH₃C(CH)₂(CH)₂CCH(CH₃)₂], 69.53 [t, 1C, CH of Cp], 73.29 [t, 1C, CH of Cp], 75.26 [t, 1C, CH of Cp], 79.31 [t, 1C, CH of Cp], 91.67 [t, 2C, CH of CH₃C(CH)₂(CH)₂CCH(CH₃)₂], 96.11 [s (br.), 2C, CH of CH₃C(CH)₂(CH)₂CCH(CH₃)₂], 104.97 [s, 1C, Quaternary C of CH₃C(CH)₂(CH)₂CCH(CH₃)₂], 128.28, 128.42 [2t, 8C, *m*-CH of Ph], 130.90, 132.12 [2s, 4C, *p*-CH Ph], 133.92 [t, 4C, *o*-CH of Ph],

135.24 [t, 4C, *o*-CH of Ph], 135.81 [virtual triplet, 2C, Quaternary C of Ph], 140.15 [virtual triplet, 2C, Quaternary C of Ph] ppm.

$^{31}\text{P}\{^1\text{H}\}$ NMR (CDCl₃, 121.49 MHz, 300 K): δ = 36.95 (s) ppm.

ES MS (+): *m/z* 917.0 [M] – SbF₆.

5.2.6 Synthesis of [RuCl(dppf)(*p*-cymene)]BF₄ – C₄₄H₄₂P₂ClFeRu(BF₄) (6)

To a suspension [RuCl₂(*p*-cymene)]₂(**1**) (79.6 mg, 0.130 mmol) in methanol (10 cm³) were added AgBF₄ (50.6 mg, 0.260 mmol) and dppf (144.1 mg, 0.260 mmol). The mixture was heated under reflux for 2.5h to yield a yellow solution containing a white precipitate. It was filtered off and the solvent removed *in vacuo* to give an orange solid. It was dissolved in chloroform and a layer of pentane was added and left in the freezer overnight. Pentane was removed and the orange residue was washed with diethyl ether and water to afford a yellow powder.

Yield: 79.3 mg, 0.087 mmol (33%)

Analysis C₄₄H₄₂P₂ClFeRu(BF₄)

Found: C 55.45; H 4.50; Cl 5.40*%

Calculated: C 57.95; H 4.64; Cl 3.89 %

* means that the sample used in the chlorine analysis is different from the sample used in the carbon and proton analysis but both samples belong to the same reaction.

^1H NMR (CDCl₃, 300.13 MHz, 300 K): δ = 0.88 [d, $^3J(^1\text{H}, ^1\text{H})$ = 6.99 Hz, 6H, CH(CH₃)₂], 1.00 [s, 3H, C₆H₄CH₃], 2.64 [sept, 1H, CH(CH₃)₂], 4.06 [s, 2H, Cp], 4.26 [s, 2H, Cp], 4.35 [s, 2H, Cp], 5.07 [s, 2H, Cp], 5.16 [d, $^3J(^1\text{H}, ^1\text{H})$ = 6.04 Hz, 2H, η^6 -C₆H₄], 5.78 [‘d’, $^3J(^1\text{H}, ^1\text{H})$ = 6.04 Hz, 2H, η^6 -C₆H₄], 7.39-7.49, 7.53-7.63, 7.64-7.77 [3m, 20H, CH of Ph] ppm.

$^{13}\text{C}\{^1\text{H}\}$ NMR (CDCl₃, 125.76 MHz, 300 K): δ = 14.73 [s, 1C, CH₃ of CH₃C(CH)₂(CH)₂CCH(CH₃)₂], 20.72 [s, 2C, CH₃ of CH₃C(CH)₂(CH)₂CCH(CH₃)₂], 31.13 [s, 1C, CH of CH₃C(CH)₂(CH)₂CCH(CH₃)₂], 69.13 [t, 1C, CH of Cp], 73.74 [t, 1C, CH of Cp], 74.82 [t, 1C, CH of Cp], 78.67 [t, 1C, CH of Cp], 83.86 [virtual triplet, 1C, Quaternary C of Cp], 90.83 [t, 2C, CH of CH₃C(CH)₂(CH)₂CCH(CH₃)₂], 96.34 [s, 2C, CH of CH₃C(CH)₂(CH)₂CCH(CH₃)₂], 99.44 [s, 1C, Quaternary C of CH₃C(CH)₂(CH)₂CCH(CH₃)₂], 128.55, 128.57 [2m, 8C, *m*-CH of Ph], 130.93, 132.32 [2s, 4C, *p*-CH Ph], 133.16 [t, 4C, *o*-CH of Ph], 133.67 [virtual triplet, 2C, Quaternary C of Ph], 135.29 [t, 4C, *o*-CH of Ph], 138.40 [virtual triplet, 2C, Quaternary C of Ph] ppm.

$^{31}\text{P}\{^1\text{H}\}$ NMR (CDCl_3 , 121.49 MHz, 300 K): $\delta = 36.28$ (s) ppm.

ES MS (+): m/z 825.1 [M] – BF_4 .

5.2.7 Synthesis of $[\text{RuCl}(\text{dppf})(p\text{-cymene})]\text{Cl} - \text{C}_{44}\text{H}_{42}\text{P}_2\text{ClFeRu}(\text{Cl})$ (7)

A mixture of $[\text{RuCl}_2(p\text{-cymene})]_2$ (**1**) (153.1 mg, 0.250 mmol) and dppf (277.2 mg, 0.500 mmol) in 8 mL of ethanol and 1 mL of benzene was heated at 55°C for 50 min. It was left stirring overnight. The solvents were evaporated under reduced pressure. The resulting residue was dissolved in dichloromethane and diethyl ether was added to precipitate a light orange powder. The product was recrystallized from methanol-diethyl ether to afford a light orange powder.

Yield: 221.9 mg, 0.258 mmol (>100%)

Analysis $\text{C}_{44}\text{H}_{42}\text{P}_2\text{ClFeRu}(\text{Cl})$

Found: C 58.80; H 5.00; 8.20 %

Calculated: C 61.41; H 4.92; Cl 8.24 %

^1H NMR (CDCl_3 , 500.23 MHz, 300 K): $\delta = 0.89$ [d, $^3J(^1\text{H}, ^1\text{H}) = 6.76$ Hz, 6H, $\text{CH}(\text{CH}_3)_2$], 1.09 [s, 3H, $\text{C}_6\text{H}_4\text{CH}_3$], 2.67 [m, 1H, $\text{CH}(\text{CH}_3)_2$], 4.07 [s, 2H, Cp], 4.26 [s, 2H, Cp], 4.35 [s, 2H, Cp], 5.06 [s, 2H, Cp], 5.18 [s (br.), 2H, $\eta^6\text{-C}_6\text{H}_4$], 5.88 [s (br.), 2H, $\eta^6\text{-C}_6\text{H}_4$], 7.40-7.49, 7.55-7.64, 7.65-7.77 [3m, 20H, CH of Ph] ppm.

$^{31}\text{P}\{^1\text{H}\}$ NMR (CDCl_3 , 121.49 MHz, 300 K): $\delta = 36.44$ (s) ppm.

ES MS (+): m/z 825.1 [M] – Cl.

5.2.8 Synthesis of $[\text{Ru}_2\text{Cl}_3(\text{DPEPhos})_2(\text{CH}_3\text{CN})_2]\text{SbF}_6 - \text{C}_{76}\text{H}_{62}\text{O}_2\text{N}_2\text{P}_4\text{Cl}_3\text{Ru}_2(\text{SbF}_6)$ (8)

To a suspension of $[\text{RuCl}_2(p\text{-cymene})]_2$ (**1**) (200 mg, 0.328 mmol) in a mixture of $\text{CH}_3\text{OH}/\text{CH}_3\text{CN}$ (1:1, 20 cm^3) was added NaSbF_6 (169.7 mg, 0.656 mmol). The mixture was stirred for 30 minutes to yield an orange solution. After this time, DPEPhos (368.9 mg, 0.685 mmol) dissolved in THF (30 cm^3) was added and left stirring for 1h. The solvent was removed *in vacuo* to give a bright orange solid. It was washed with an ethanol/water (4:1) mixture and filtered. The solid was first recrystallised from ethanol to yield a yellow powder which was after recrystallised from methanol to afford a powder in the same color.

Yield: 67.7 mg, 0.040 mmol (6%)

Analysis for C₇₆H₆₂O₂N₂P₄Cl₃Ru₂(SbF₆)

Found: C 53.30; H 3.65; N 1.50; Cl 6.65* %

Calculated: C 53.59; H 3.67; N 1.64; Cl 6.24 %

* means that the sample used in the chlorine analysis is different from the sample used in the carbon and proton analysis but both samples belong to the same reaction.

¹H NMR (CDCl₃, 500.23 MHz, 300 K): δ = 1.64 [s (br.), 6H, NCCH₃], 6.38-7.81 (m, 62H, DPEPhos).

¹³C{¹H} NMR (CDCl₃, 75.47 MHz, 300 K): more NMR experiments needed to correctly assign all the peaks (spectrum shown in the appendix 8.1).

ES MS (+): m/z 1469.1 [MH⁺] – SbF₆.

5.2.9 Synthesis of [RuCl(P(*n*-Bu)₃)₂(*p*-cymene)]SbF₆ – C₃₄H₆₈P₂ClRu(SbF₆) (9)

To a suspension of [RuCl₂(*p*-cymene)]₂ (**1**) (79.6 mg, 0.130 mmol) in methanol (10cm³) were added NaSbF₆ (67.3 mg, 0.260 mmol) and P(*n*-Bu)₃ (0.24 cm³, 0.970 mmol). The mixture was heated under reflux for 2 hours to yield a yellow/orange solution containing a white precipitate. It was filtered off and the solvent removed under reduced pressure. The resulting residue was dissolved in chloroform and a layer of pentane was added and left in the freezer overnight. Pentane was removed and the orange powder obtained was washed with diethyl ether and water to afford crystalline orange clusters.

Yield: 30.2 mg, 0.0331 mmol (13%)

Analysis for C₃₄H₆₈P₂ClRu(SbF₆)

Found: C 44.55; H 7.55; Cl 3.75 %

Calculated: C 44.82; H 7.52; Cl 3.89 %

¹H NMR (CDCl₃, 500.23 MHz, 297 K): δ = 0.96 [t, 18H, CH₃CH₂CH₂CH₂-], 1.28 [d, ³J(¹H, ¹H) = 6.95 Hz, 6H, CH(CH₃)₂], 1.38-1.47 [m, 18H, CH₂ of *n*-Bu], 1.47-1.55 [m, 6H, CH₂ of *n*-Bu], 1.74-1.85 [m, 6H, CH₂ of *n*-Bu], 2.04 [s, 3H, C₆H₄CH₃], 2.05-2.14 [m, 6H, CH₂ of *n*-Bu], 2.64 [sept, 1H, CH(CH₃)₂], 5.60 [d, ³J(¹H, ¹H) = 6.16 Hz, 2H, η⁶-C₆H₄], 6.03 [‘d’, ³J(¹H, ¹H) = 6.16 Hz, 2H, η⁶-C₆H₄] ppm.

¹³C{¹H} NMR (CDCl₃, 125.76 MHz, 300 K): δ = 13.85 [s, 6C, CH₃CH₂CH₂CH₂-], 18.36 [s, 1C, CH₃ of CH₃C(CH)₂(CH)₂CCH(CH₃)₂], 21.77 [s, 2C, CH₃ of CH₃C(CH)₂(CH)₂CCH(CH₃)₂], 24.52 [t, 6C, CH₃CH₂CH₂CH₂-], 26.40 [t, 6C, CH₃CH₂CH₂CH₂-], 28.42 [t, 6C, CH₃CH₂CH₂CH₂-], 31.33 [s, 1C,

CH of CH₃C(CH)₂(CH)₂CCH(CH₃)₂], 86.45 [t, 2C, CH of CH₃C(CH)₂(CH)₂CCH(CH₃)₂], 95.81 [s, 2C, CH of CH₃C(CH)₂(CH)₂CCH(CH₃)₂] ppm.

³¹P{¹H} NMR (CDCl₃, 121.49 MHz, 300 K): δ = 14.09 [s, major peak], 31.44 [s, small peak] ppm.

ES MS (+): m/z 675.4 [M] – SbF₆.

5.2.10 Synthesis of [Ru(P(*n*-Bu)₃)₂(*p*-cymene)]SbF₆ – C₃₄H₆₈P₂Ru(SbF₆) (10)

To a suspension of [Ru₂(*p*-cymene)]₂ (**2**) (127.2 mg, 0.130 mmol) in methanol (10 cm³) were added NaSbF₆ (67.3 mg, 0.260 mmol) and P(*n*-Bu)₃ (0.24 cm³, 0.970 mmol). The mixture was heated under reflux for 3.5h to yield a light red solution containing a white precipitate. It was filtered off and the solvent removed under reduced pressure. The resulting residue was dissolved in chloroform and a layer of pentane was added and left in the freezer overnight. Pentane was removed and the dark red residue obtained was washed with diethyl ether and water to afford a red wine color powder.

Yield: 125.6 mg, 0.125 mmol (48%)

Analysis for C₃₄H₆₈P₂Ru(SbF₆)

Found: C 42.80; H 7.40 %

Calculated: C 40.73; H 6.84 %

¹H NMR (CDCl₃, 500.23 MHz, 299 K): δ = 0.93-1.01 [m, 18H, CH₃CH₂CH₂CH₂], 1.29 [d, ³J(¹H,¹H) = 6.95 Hz, 6H, CH(CH₃)₂], 1.40-1.50 [m, 18H, CH₂ of *n*-Bu], 1.50-1.57 [m, 6H, CH₂ of *n*-Bu], 1.88-1.99 [m, 6H, CH₂ of *n*-Bu], 2.18-2.29 [m, 6H, CH₂ of *n*-Bu], 2.29 [s, 3H, C₆H₄CH₃], 3.21 [sept, 1H, CH(CH₃)₂], 5.63 [d, ³J(¹H,¹H) = 6.16 Hz, 2H, η⁶-C₆H₄], 6.37 [‘d’, ³J(¹H,¹H) = 6.16 Hz, 2H, η⁶-C₆H₄] ppm.

¹³C{¹H} NMR more NMR experiments needed to correctly assign all the peaks (spectrum shown in the appendix 10.1)

¹P{¹H} NMR (CDCl₃, 121.49 MHz, 300 K): δ = 11.53 [s, major peak], 31.57 [s, medium size peak], 36.23 [s, small peak] ppm.

ES MS (+): m/z 767.3 [M] – SbF₆.

5.2.11 Synthesis of $[\text{RuCl}(\text{P}(i\text{-Bu})_3)_2(\textit{p}\text{-cymene})]\text{SbF}_6 - \text{C}_{34}\text{H}_{68}\text{P}_2\text{ClRu}(\text{SbF}_6)$ (11)

To a suspension of $[\text{RuCl}_2(\textit{p}\text{-cymene})]_2$ (**1**) (79.6 mg, 0.130 mmol) in methanol (10cm³) were added NaSbF_6 (67.3 mg, 0.260 mmol) and $\text{P}(i\text{-Bu})_3$ (0.24 cm³, 0.970 mmol). The mixture was heated under reflux for 3h to yield a red/brown solution. The solvent was removed under reduced pressure. The resulting residue was dissolved in chloroform and diethyl ether was added. A yellow precipitate was formed straight away and filtered. It was washed with diethyl ether and water to afford fine yellow needles in 26% yield (62.6 mg, 0.069 mmol).

Yield: 62.6 mg, 0.069 mmol (26%)

Analysis for $\text{C}_{34}\text{H}_{68}\text{P}_2\text{ClRu}(\text{SbF}_6)$

Found: C 44.30; H 7.50; Cl 3.55* %

Calculated: C 44.82; H 7.52; Cl 3.89 %

* means that the sample used in the chlorine analysis is different from the sample used in the carbon and proton analysis but both samples belong to the same reaction.

¹H NMR (CDCl_3 , 500.23 MHz, 298 K): $\delta = 1.08$ [d, $^3J(^1\text{H}, ^1\text{H}) = 6.36$ Hz, 18H, $(\text{CH}_3)_2\text{CHCH}_2\text{CH}_2$], 1.14 [d, $^3J(^1\text{H}, ^1\text{H}) = 6.56$ Hz, 18H, $(\text{CH}_3)_2\text{CHCH}_2\text{CH}_2$], 1.29 [d, $^3J(^1\text{H}, ^1\text{H}) = 6.95$ Hz, 6H, $\text{CH}(\text{CH}_3)_2$], 1.80-1.89 [m, 6H, $(\text{CH}_3)_2\text{CHCH}_2$ -], 2.06-2.20 [m, 12H, $(\text{CH}_3)_2\text{CHCH}_2$ -], 2.62 [sept, 1H, $\text{CH}(\text{CH}_3)_2$], 5.65 [d, $^3J(^1\text{H}, ^1\text{H}) = 6.16$ Hz, 2H, $\eta^6\text{-C}_6\text{H}_4$], 5.92 [‘d’, $^3J(^1\text{H}, ^1\text{H}) = 6.16$ Hz, 2H, $\eta^6\text{-C}_6\text{H}_4$] ppm.

¹³C{¹H} NMR more NMR experiments needed to correctly assign all the peaks (spectrum shown in the appendix 11.1)

¹P{¹H} NMR (CDCl_3 , 202.46 MHz, 299 K): $\delta = 0.06$ [s, small peak], 18.19 [s, major peak], 28.87 [s, small peak] ppm.

ES MS (+): m/z 675.4 [M] – SbF_6 .

5.2.12 Synthesis of $[\text{RuCl}_2\text{P}(i\text{-Bu})_3(\textit{p}\text{-cymene})] - \text{C}_{22}\text{H}_{41}\text{PCl}_2\text{Ru}$ (12)

To a suspension of $[\text{RuCl}_2(\textit{p}\text{-cymene})]_2$ (**1**) (79.6 mg, 0.130 mmol) in methanol (10cm³) were added NaSbF_6 (67.3 mg, 0.260 mmol) and $\text{P}(i\text{-Bu})_3$ (0.13 cm³, 0.520 mmol). The mixture was heated under reflux for 3.50h to yield a red/brown solution. The solvent was removed under reduced pressure. The resulting residue was dissolved in chloroform and a layer of pentane was added and left in the freezer overnight. Both a brownish red powder and a

yellow powder were obtained. The brownish red powder was recrystallized from acetone to afford a powder in the same color. No yield was calculated, but it was low.

Analysis for C₂₂H₄₁PCl₂Ru

Found: C 51.60; H 8.10; 14.20* %

Calculated: C 51.96; H 8.13; Cl 13.94 %

* means that the sample used in the chlorine analysis is different from the sample used in the carbon and proton analysis but both samples belong to the same reaction.

¹H NMR (CDCl₃, 300.13 MHz, 300 K): δ = 1.05 [d, ³J(¹H, ¹H) = 6.42 Hz, 18H, (CH₃)₂CHCH₂-], 1.28 [d, ³J(¹H, ¹H) = 6.99 Hz, 6H, CH(CH₃)₂], 1.99-2.07 [m, 6H, (CH₃)₂CHCH₂-], 2.07-2.21 [m, 3H, (CH₃)₂CHCH₂-], 2.10 [s, 3H, C₆H₄CH₃], 2.86 [sept, 1H, CH(CH₃)₂], 5.30 [d, ³J(¹H, ¹H) = 5.67 Hz, 2H, η⁶-C₆H₄], 5.43 [d, ³J(¹H, ¹H) = 5.67 Hz, 2H, η⁶-C₆H₄] ppm.

ES MS (+): m/z 473.2 [M] – Cl.

5.2.13 Synthesis of [RuCl₂P(*n*-Bu)₃(*p*-cymene)] – C₂₂H₄₁PCl₂Ru (13)

To a suspension of [RuCl₂(*p*-cymene)]₂ (**1**) (159.2 mg, 0.260 mmol) in methanol (20cm³) was added P(*n*-Bu)₃ (0.13 cm³, 0.520 mmol). The mixture was stirred for 30 min. The solvent was removed under reduced pressure. The resulting residue was dissolved in chloroform and diethyl ether was added to precipitate a red powder. It was filtered and washed with diethyl ether to afford a red product.

Yield: 158.5 mg, 0.312 mmol (60%)

¹H NMR (CDCl₃, 300.13 MHz, 300 K): δ = 0.92 [t, 9H, CH₃CH₂CH₂CH₂], 1.24 [d, ³J(¹H, ¹H) = 6.89 Hz, 6H, CH(CH₃)₂], 1.31-1.54 [m, 12H, CH₂ of *n*-Bu], 1.92-2.04 [m, 6H, CH₂ of *n*-Bu], 2.07 [s, 3H, C₆H₄CH₃], 2.83 [sept, 1H, CH(CH₃)₂], 5.38 [d, ³J(¹H, ¹H) = 6.23 Hz, 2H, η⁶-C₆H₄], 5.42 [d, ³J(¹H, ¹H) = 6.23 Hz, 2H, η⁶-C₆H₄] ppm.

ES MS (+): m/z 473.2 [M] – Cl.

5.2.14 Synthesis of [RuCl(P(CH₃)₃)₂(*p*-cymene)]SbF₆ – RuC₁₆H₃₂P₂Cl(SbF₆) (14)

To a suspension of [RuCl₂(*p*-cymene)]₂ (**1**) (79.6 mg, 0.130 mmol) in methanol (10cm³) were added NaSbF₆ (67.3 mg, 0.260 mmol) and P(CH₃)₃ (0.10 cm³, 0.970 mmol). The mixture was heated under reflux for 3h to yield yellow solution containing a white precipitate. It was

filtered off and the solvent removed under reduced pressure. The resulting residue was dissolved in chloroform and diethyl ether was added to precipitate a yellow powder. It was washed with diethyl ether and water to afford a powder in the same color.

Yield: 44.4 mg, 0.067 mmol (26%)

Analysis for RuC₁₆H₃₂P₂Cl(SbF₆)

Found: C 32.45; H 5.60 %

Calculated: C 29.18; H 4.90 %

¹H NMR (CDCl₃, 500.23, 299 K MHz): δ = 1.24 [d, 6H, ³J(¹H, ¹H) = 6.95 Hz, 6H, CH(CH₃)₂], 1.70 [t, 18H, (CH₃)₃], 2.16 [s, 3H, C₆H₄CH₃], 2.67 [sept, 1H, CH(CH₃)₂], 5.76 [d, ³J(¹H, ¹H) = 5.96 Hz, 2H, η⁶-C₆H₄], 6.44 [‘d’, ³J(¹H, ¹H) = 5.96 Hz, 2H, η⁶-C₆H₄] ppm.

¹P{¹H} NMR (CDCl₃, 121.49 MHz, 300 K): δ = 2.93 (s) ppm.

ES MS (+): m/z 423.1 [M] – SbF₆.

5.2.15 Synthesis of [RuCl₂PPh(OCH₃)₂(*p*-cymene)] – [RuC₁₈H₂₅PO₂Cl₂] (15)

To a suspension of [RuCl₂(*p*-cymene)]₂ (**1**) (79.6 mg, 0.130 mmol) in methanol (10cm³) were added NaSbF₆ (67.3 mg, 0.260 mmol) and PhPCl₂ (0.13 cm³, 0.960 mmol). The mixture was heated under reflux for 3.5h to yield a red wine color solution. The solvent was removed under reduced pressure and the resulting residue was dissolved in chloroform and a layer of pentane added and left in the freezer overnight. Pentane was removed and diethyl ether was added to precipitate a red wine color powder. It was washed with diethyl ether and water to yield a powder in the same color.

Yield: 100.9 mg, 0.212 mmol (82% yield)

¹H NMR (CDCl₃, 500.23 MHz, 299 K): δ = 1.07 [d, 6H, ³J(¹H, ¹H) = 6.95 Hz, 6H, CH(CH₃)₂], 1.92 [s, 3H, C₆H₄CH₃], 2.69 [sept, 1H, CH(CH₃)₂], 3.79, 3.82 [2s, 6H, OCH₃], 5.24 [d, ³J(¹H, ¹H) = 5.96 Hz, 2H, η⁶-C₆H₄], 5.29 [‘d’, ³J(¹H, ¹H) = 5.96 Hz, 2H, η⁶-C₆H₄] ppm.

ES MS (+): m/z 441.0 [M] – Cl.

5.3 Catalytic Reactions

5.3.1 Redox Neutral Alkylations

For *in situ* generated catalysts: $[\text{RuX}_2(\textit{p}\text{-cymene})]_2$ (0.0459 g X=Cl or 0.733 g X=I, 0.075 mmol) and the phosphine ligand (0.15 mmol for bidentate phosphines or 0.30 mmol for monodentate) were placed in a round bottom flask. *tert*-Butylamine (0.32 mL, 3 mmol), phenethyl alcohol (0.36 mL, 3 mmol) and toluene (10 mL) were added dropwise. The reaction mixture was allowed to stir and heated at reflux for 24 hours. It was filtered through celite and washed with dichloromethane, the filtrate collected and solvents evaporated *in vacuo*. An NMR of the oily residue obtained is acquired to figure out the conversions. The product (*t*-butyl(2-phenylethyl)amine) obtained employing the $[\text{RuCl}_2(\textit{p}\text{-cymene})]_2$ (1)-dppf pair was isolated together with phenethyl alcohol by distillation under reduced pressure to yield a pale yellow liquid. $^1\text{H NMR}$ (CDCl_3 , 500.23 MHz, 300 K): $\delta = 1.01$ [s, 9H, $\text{NH}(\text{CH}_3)_3$], 2.69-2.74 (m, 2H, CH_2), 2.74-2.79 [m, 2H, CH_2], 7.10-7.25 [m, 5H, C_6H_5] ppm. This is consistent with literature data.^{24, 64}

When ruthenium monomers were used, no phosphine ligand was added to the reaction pot. 0.0375 mmol of the monomer were used for S/C ratios of 40 and 0.075 mmol for S/C ratios of 20.

5.3.1.1 $^1\text{H NMR}$ Analysis

As said before, in the model N-alkylation of this project there is often the formation of appreciable quantities of $\text{PhCH}_2\text{CH}_2\text{O}_2\text{CCH}_2\text{Ph}$ so, where present, the conversions accounted this fact. If both the alcohol and ester peaks are present, the product conversion is calculated by manually integrating the alcohol peak against the product and ester peaks. If only the ester peak is present, the product conversion is calculated integrating the ester peak against the product peak. An example of how these conversions were calculated is shown below for the monomer **7** (integrals are found in figure 2.12).

After the integrations are done, there is the normalization of each peak where each integral is divided by the number of protons corresponding to that peak. But since the ester is formed by two molecules of alcohol, the ester integral still needs to be multiplied by two.

Then to calculate a specific conversion it is necessary to divide its value obtained after normalization by the sum of all normalized results and multiply by 100. The equations for the alcohol, amine and ester are:

$$\text{alcohol \%} = \frac{\frac{\text{alcohol peak int.}}{2}}{\frac{\text{alcohol peak int.}}{2} + \frac{\text{amine peak int.}}{2} + \left(\frac{\text{ester peak int.} \times 2}{2}\right)} \times 100$$

$$= \frac{\frac{2}{2}}{\frac{2}{2} + \frac{26.97}{9} + \left(\frac{2.63 \times 2}{2}\right)} \times 100 = 15$$

$$\text{amine \%} = \frac{\frac{26.97}{9}}{\frac{2}{2} + \frac{26.97}{9} + \left(\frac{2.63 \times 2}{2}\right)} \times 100 = 45$$

$$\text{ester \%} = \frac{\left(\frac{2.63 \times 2}{2}\right)}{\frac{2}{2} + \frac{26.97}{9} + \left(\frac{2.63 \times 2}{2}\right)} \times 100 = 40$$

5.3.1.2 Gas Chromatography Analysis

Every sample submitted to GC analysis was made up of 20 μL of the substance being analysed (starting material or reaction mixture) and 4 μL of decane as internal standard. All of them were also diluted with 2 mL of acetonitrile. The 20 and the 4 μL were measured with a 25 ± 0.25 μL micropipette. In the catalytic reactions, the same procedure of 5.3.1 was followed but now taking from time to time 20 μL of the reaction mixture. The GC samples were prepared as described above and since they were only analysed hours later, they were immediately stored in the freezer for a couple of hours in order to extinguish the reaction. The concentration of the starting alcohol and of the product was obtained using the internal standard method described in the literature⁶⁵ and a summary of it is shown bellow. The actual procedure was adapted from the one used in the Process Lab of the School of Chemistry.

The internal standard method uses an internal standard which is a known amount of a compound, in the present case decane, different from the analyte (*t*-butyl(2-

phenylethyl)amine), which is added to the unknown. Then the signal from the analyte is compared with the signal from the internal standard to find out how much analyte is present. Internal standards are specially useful for analyses in which the quantity of sample analysed or the instrument response varies slightly from run to run for reasons that are difficult to control.

Initially it is necessary to measure the relative response of the detector to the standard and analyte. Usually a known mixture of standard and analyte is prepared with known concentrations of both, but since the analyte in this project is not commercially available and the one obtained in here is mixed with some alcohol, another strategy was followed. Two solutions were prepared. One made up of 20 μ L of alcohol, 4 μ L of decane and 2 mL of acetonitrile and another one made up of 20 μ L of the mixture product-alcohol, 4 μ L of decane and 2 mL of acetonitrile. From the first one the internal response factor of the alcohol (IRF) was calculated as follows:

$$\frac{\text{alcohol area}}{[\text{alcohol}]} = IRF_{\text{alcohol}} \left(\frac{\text{decane area}}{[\text{decane}]} \right) \Leftrightarrow IRF_{\text{alcohol}} = \frac{\text{alcohol area} \times [\text{decane}]}{[\text{alcohol}] \times \text{decane area}}$$

Using the IRF found for the alcohol, the alcohol concentration in second solution was calculated from respective the GC data using the equation above. By the product:alcohol ratio found in the product-alcohol mixture by ^1H NMR, the product concentration in the second solution was extrapolated from the alcohol concentration found. After finding the product concentration in the second solution, the product IRF was calculated as follows:

$$IRF_{\text{product}} = \frac{\text{product area} \times [\text{decane}]}{[\text{product}] \times \text{decane area}}$$

Using the product and decane area found from every GC sample of the N-alkylation reaction, the product concentration was calculated using the following equation:

$$[\text{product}] = \frac{\text{product area} \times [\text{decane}]}{IRF_{\text{product}} \times \text{decane area}}$$

Since the product was diluted from 20 μ L (reaction) to 2 mL (GC vial), the concentration of product in the reaction pot was obtained by multiplying the concentration of product found, by the inverse of the dilution factor, this is ($2 \times 10^{-3} / 20 \times 10^{-6}$). To obtain the conversions the following equation was employed:

$$conversion_{product}(\%) = \frac{[product]}{[alcohol]_{time=0}} \times 100$$

5.3.2 Transfer Hydrogenations

Both reductions (acetophenone and benzaldehyde) were carried out using the same general procedure.⁶⁶ The pre-catalyst dimer-ligand pair (0.005 mmol of dimer, 0.010 mmol of bidentate phosphine) or the monomer (0.010 mmol) was placed in a carousel tube. 9 mL of isopropanol were added and the mixture left stirring. After 15 minutes, 1.01 mg (0.009 mmol) of *t*-BuOK dissolved in 1 mL of isopropanol were added dropwise. The reaction mixture was stirred at 60 °C for 1h. Then, acetophenone (0.12 mL, 1 mmol) or benzaldehyde (0.10 mL, 1 mmol) was added and the mixture left to stir at 60 °C for more 20h (S/C ratio of 100:1). The reactions were set under normal atmosphere with the refrigeration system turned on. To get the conversions, the resulting solutions were evaporated *in vacuo* and the oily residue obtained submitted to ¹H NMR analysis. Conversions were calculated as shown for the N-alkylations, by manually integrating a characteristic substrate (acetophenone/benzaldehyde) peak against the product peak. No side product was considered (substrate:product ratio equal to 1). Peaks chosen are shown in figure 2.15 and 2.17).

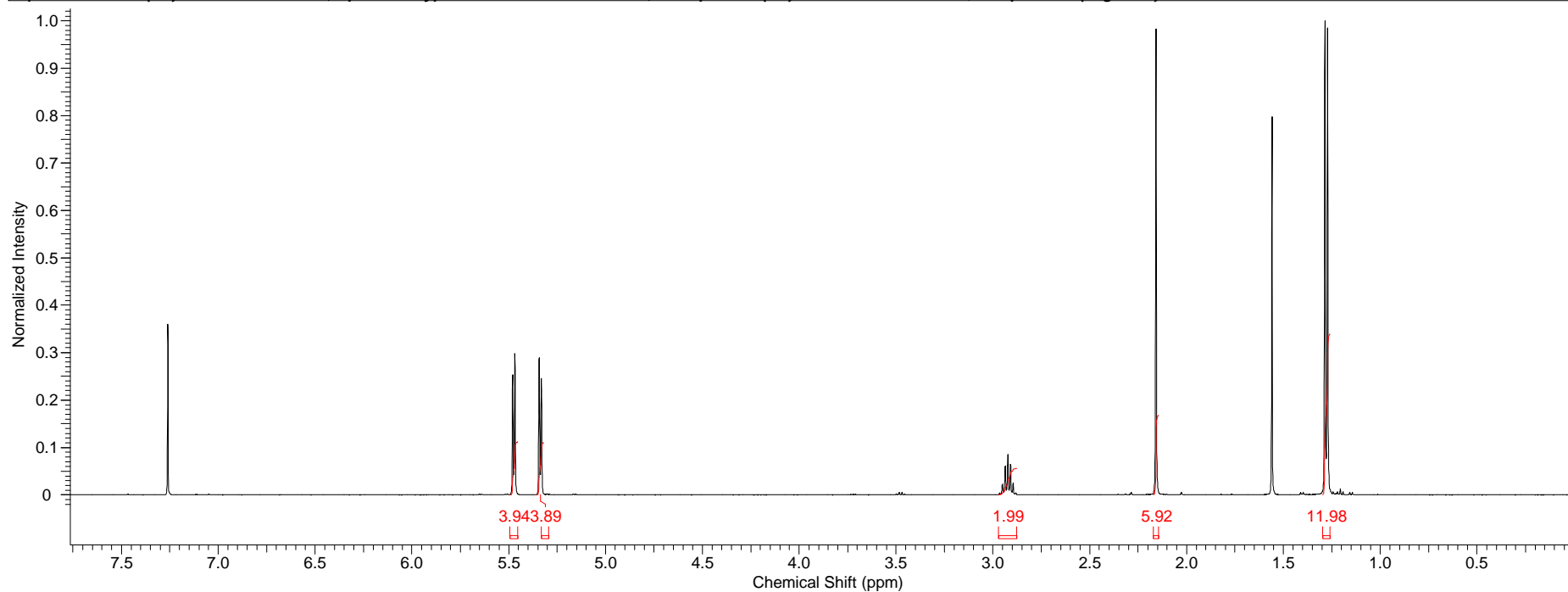
6. References

1. M. H. S. A. Hamid, C. L. Allen, G. W. Lamb, A. C. Maxwell, H. C. Maytum, A. J. A. Watson and J. M. J. Williams, *Journal of the American Chemical Society*, 2009, **131**, 1766-1774.
2. J. S. M. Samec, J.-E. Backvall, P. G. Andersson and P. Brandt, *Chemical Society Reviews*, 2006, **35**, 237-248.
3. D. Hollmann, Universität Rostock, 2008.
4. R. Noyori, M. Yamakawa and S. Hashiguchi, *The Journal of Organic Chemistry*, 2001, **66**, 7931-7944.
5. B. Therrien, *Coordination Chemistry Reviews*, 2009, **253**, 493-519.
6. A. Rodríguez, Leeds, 2010.
7. R. Toreki, *Phosphine Complexes*, <http://www.ilpi.com/organomet/phosphine.html>, Accessed 19/10/2010, 2010.
8. L. Adrio and K. Hii, *Organometallic Chemistry*, 2009, **35**, 62-92.
9. K. Fagnou and M. Lautens, *Angewandte Chemie International Edition*, 2002, **41**, 26-47.
10. M. A. Fernandez-Zumel, B. Lastra-Barreira, M. Scheele, J. Diez, P. Crochet and J. Gimeno, *Dalton Transactions*, 2010, **39**, 7780-7785.
11. D. G. Gillingham, O. Kataoka, S. B. Garber and A. H. Hoveyda, *Journal of the American Chemical Society*, 2004, **126**, 12288-12290.
12. L. Adrio and K. Hii, *Organometallic Chemistry*, 2009, **35**, 62-92.
13. T. Naota, H. Takaya and S.-I. Murahashi, *Chemical Reviews*, 1998, **98**, 2599-2660.
14. R. Andrea, Leeds, 2010.
15. *Handbook of Homogeneous Hydrogenation*, WILEY-VCH Verlag GmbH & Co. KGaA, Weinheim, 2007.
16. W. Baratta and P. Rigo, *European Journal of Inorganic Chemistry*, 2008, **2008**, 4041-4053.
17. J.-E. Bäckvall, *Journal of Organometallic Chemistry*, 2002, **652**, 105-111.
18. C. Wang, X. Wu and J. Xiao, *Chemistry – An Asian Journal*, 2008, **3**, 1750-1770.
19. X. Wu and J. Xiao, *Chemical Communications*, 2007, 2449-2466.
20. A. Fujii, S. Hashiguchi, N. Uematsu, T. Ikariya and R. Noyori, *Journal of the American Chemical Society*, 1996, **118**, 2521-2522.
21. N. Debono, M. Besson, C. Pinel and L. Djakovitch, *Tetrahedron Letters*, 2004, **45**, 2235-2238.
22. J. Li, Y. Zhang, D. Han, Q. Gao and C. Li, *Journal of Molecular Catalysis A: Chemical*, 2009, **298**, 31-35.
23. X. Li, J. Blacker, I. Houson, X. Wu and J. Xiao, *Synlett*, 2006, **2006**, 1155-1160.
24. M. H. S. A. Hamid and J. M. J. Williams, *Chemical Communications*, 2007, 725-727.
25. S. A. Lawrence, University of Cambridge, 2004.
26. K.-i. Fujita, Z. Li, N. Ozeki and R. Yamaguchi, *Tetrahedron Letters*, 2003, **44**, 2687-2690.
27. G. W. Lamb, F. A. Al Badran, J. M. J. Williams and S. T. Kolczkowski, *Chemical Engineering Research and Design*, 2010, **88**, 1533-1540.
28. R. Grigg, T. R. B. Mitchell, S. Sutthivaiyakit and N. Tongpenyai, *Journal of the Chemical Society, Chemical Communications*, 1981, 611-612.
29. Y. Watanabe, Y. Tsuji, H. Ige, Y. Ohsugi and T. Ohta, *The Journal of Organic Chemistry*, 1984, **49**, 3359-3363.
30. Y. Watanabe, Y. Morisaki, T. Kondo and T.-a. Mitsudo, *The Journal of Organic Chemistry*, 1996, **61**, 4214-4218.
31. S. Ganguly and D. M. Roundhill, *Polyhedron*, 1990, **9**, 2517-2526.
32. K.-T. Huh, Y. Tsuji, M. Kobayashi, F. Okuda and Y. Watanabe, *Chem. Lett.*, 1988, 449.
33. S. Naskar and M. Bhattacharjee, *Tetrahedron Letters*, 2007, **48**, 3367-3370.
34. G. Cami-Kobeci, P. A. Slatford, M. K. Whittlesey and J. M. J. Williams, *Bioorganic & Medicinal Chemistry Letters*, 2005, **15**, 535-537.

35. G. Cami-Kobeci and J. M. J. Williams, *Chemical Communications*, 2004, 1072-1073.
36. B. Blank, M. Madalska and R. Kempe, *Advanced Synthesis & Catalysis*, 2008, **350**, 749-758.
37. D. Hollmann, A. Tillack, D. Michalik, R. Jackstell and M. Beller, *Chemistry – An Asian Journal*, 2007, **2**, 403-410.
38. D. S. Matharu, J. E. D. Martins and M. Wills, *Chemistry – An Asian Journal*, 2008, **3**, 1374-1383.
39. K.-i. Fujita, N. Tanino and R. Yamaguchi, *Organic Letters*, 2006, **9**, 109-111.
40. J.-W. Handgraaf, J. N. H. Reek and E. J. Meijer, *Organometallics*, 2003, **22**, 3150-3157.
41. M. C. Carrión, F. Sepúlveda, F. A. Jalón, B. R. Manzano and A. M. Rodríguez, *Organometallics*, 2009, **28**, 3822-3833.
42. M. A. Bennett, T. N. Huang, T. W. Matheson, A. K. Smith, S. Ittel and W. Nickerson, *Inorganic Syntheses*, 1982, **21**, 74-78.
43. S. B. Jensen, S. J. Rodger and M. D. Spicer, *Journal of Organometallic Chemistry*, 1998, **556**, 151-158.
44. M. G. Mendoza-Ferri, C. G. Hartinger, A. A. Nazarov, R. E. Eichinger, M. A. Jakupec, K. Severin and B. K. Keppler, *Organometallics*, 2009, **28**, 6260-6265.
45. P. Murray and R. Cox, Astra Zeneca, 2010.
46. Z. Almodares, Leeds, 2010.
47. T. Screen, *Personal Communication*, 2010.
48. G. Süss-Fink, E. Garcia Fidalgo, A. Neels and H. Stoeckli-Evans, *Journal of Organometallic Chemistry*, 2000, **602**, 188-192.
49. K.-J. Haack, S. Hashiguchi, A. Fujii, T. Ikariya and R. Noyori, *Angewandte Chemie International Edition in English*, 1997, **36**, 285-288.
50. S. Hashiguchi, A. Fujii, J. Takehara, T. Ikariya and R. Noyori, *J. Am. Chem. Soc.*, 1995, **117**, 7562-7563.
51. S. Lord, University of Leeds, 2007.
52. T. Sixt, M. Sieger, M. J. Krafft, D. Bubrin, J. Fiedler and W. Kaim, *Organometallics*, 2010, **29**, 5511-5516.
53. J.-F. Mai and Y. Yamamoto, *Journal of Organometallic Chemistry*, 1998, **560**, 223-232.
54. L. Paim, A. Batista, F. Dias, C. Golfeto, J. Ellena, H. Siebald and J. Ardisson, *Transition Metal Chemistry*, 2009, **34**, 949-954.
55. C. Albrecht, S. Gauthier, J. Wolf, R. Scopelliti and K. Severin, *European Journal of Inorganic Chemistry*, 2009, **2009**, 967-967.
56. Y. Chen, M. Valentini, P. S. Pregosin and A. Albinati, *Inorganica Chimica Acta*, 2002, **327**, 4-14.
57. D. E. Fogg and B. R. James, *Inorganic Chemistry*, 1997, **36**, 1961-1966.
58. S. D. Drouin, S. Monfette, D. Amoroso, G. P. A. Yap and D. E. Fogg, *Organometallics*, 2005, **24**, 4721-4728.
59. S. A. Serron and S. P. Nolan, *Organometallics*, 1995, **14**, 4611-4616.
60. M. A. Bennett and A. K. Smith, *Journal of the Chemical Society, Dalton Transactions*, 1974, 233-241.
61. H. Werner and R. Werner, *Chemische Berichte*, 1982, **115**, 3766-3780.
62. M. T. Reetz and X. Li, *Journal of the American Chemical Society*, 2006, **128**, 1044-1045.
63. D. E. Fogg, B. R. James and M. Kilner, *Inorganica Chimica Acta*, 1994, **222**, 85-90.
64. A. Padwa, D. J. Austin, A. T. Price, M. A. Semones, M. P. Doyle, M. N. Protopopova, W. R. Winchester and A. Tran, *Journal of the American Chemical Society*, 1993, **115**, 8669-8680.
65. D. o. Chemistry, *Internal Standards*, <http://www.chemistry.adelaide.edu.au/external/soc-rel/content/int-std.htm>, Accessed 31/03/2011, 2011.
66. Pfizer, *Personal Communication*, 2011.

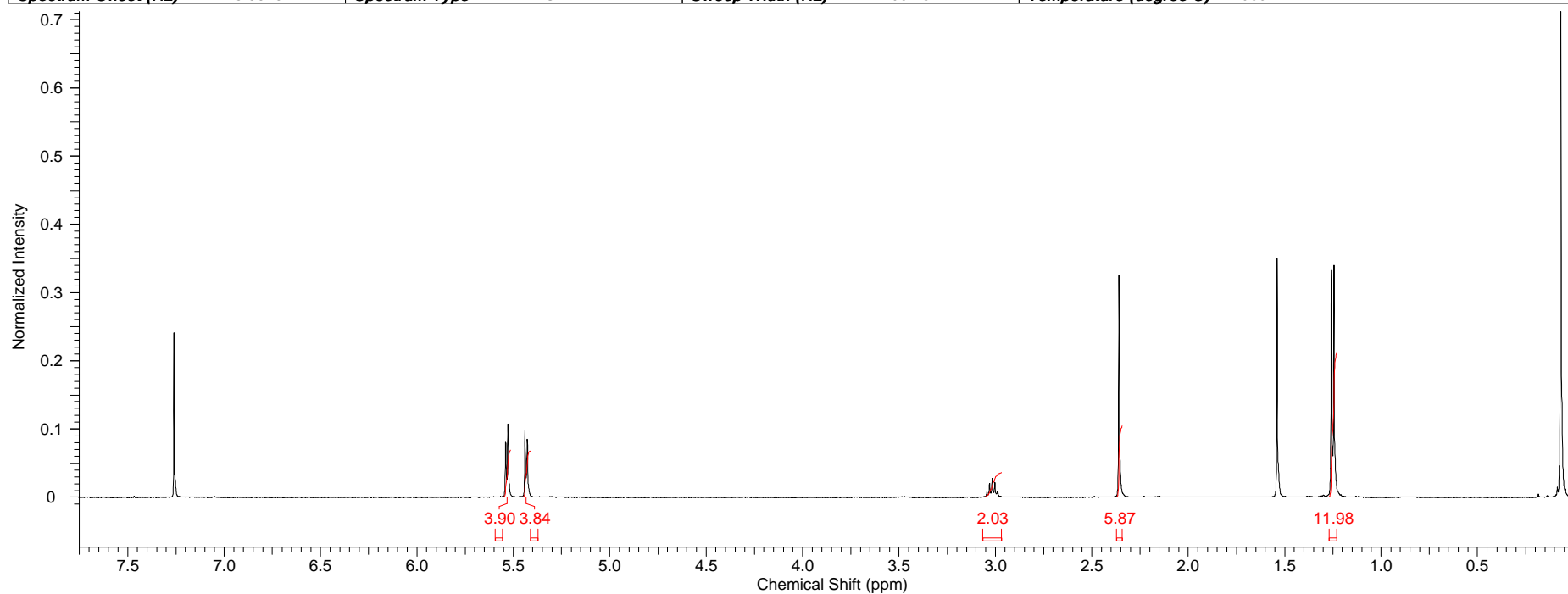
APPENDIX 1 – ¹H NMR spectrum of [RuCl₂(*p*-cymene)]₂ (1) in CDCl₃

Acquisition Time (sec)	1.1698	Comment	Full Name Joel Fonseca Room No. 1.29 Sample jdaf1.1		Date	12 Nov 2010 15:21:36	
Date Stamp	12 Nov 2010 15:21:36	File Name	F:\Leeds Spectra\JDAF1.1\10\PDATA\1\1r				
Frequency (MHz)	500.23	Nucleus	1H	Number of Transients	32	Origin	avance500
Original Points Count	8192	Owner	gen	Points Count	16384	Pulse Sequence	zg30
Receiver Gain	362.00	SW(cyclical) (Hz)	7002.80	Solvent	CHLOROFORM-d		
Spectrum Offset (Hz)	2725.3328	Spectrum Type	STANDARD	Sweep Width (Hz)	7002.37	Temperature (degree C)	27.000



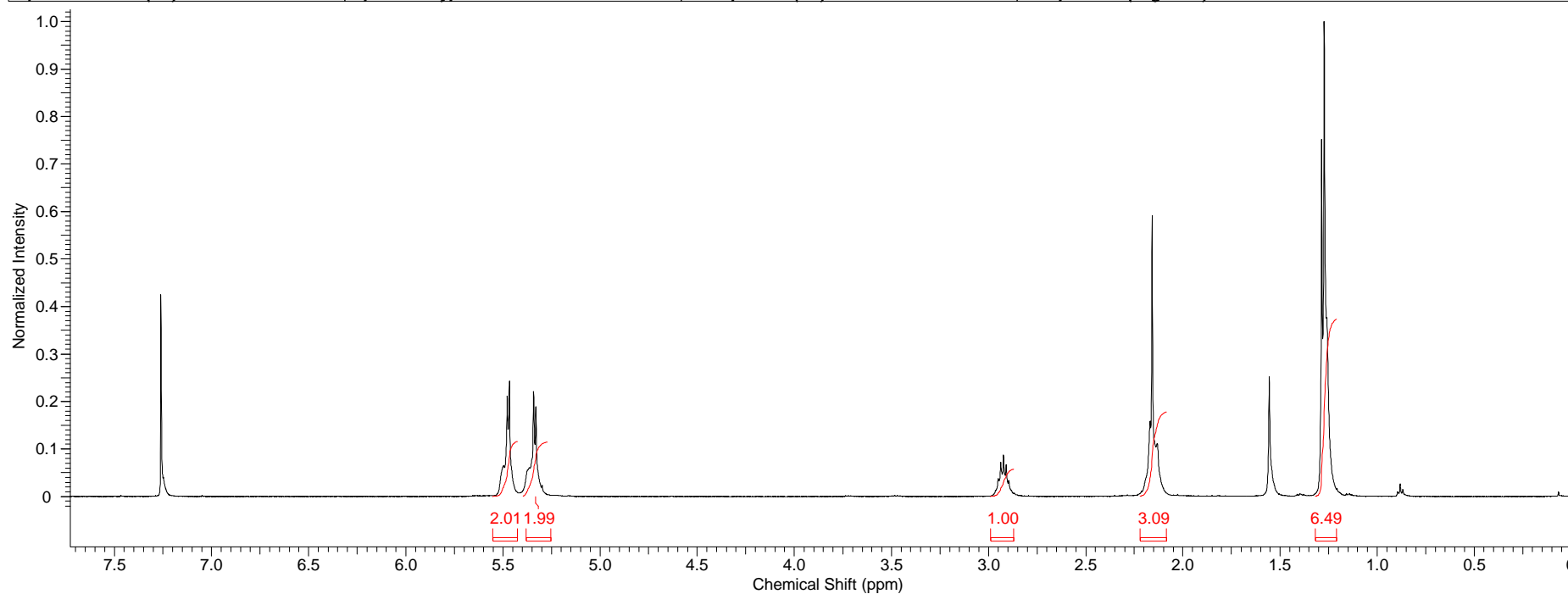
APPENDIX 2 – ¹H NMR spectrum of [RuI₂(*p*-cymene)]₂ (2) in CDCl₃

Acquisition Time (sec)	1.1698	Comment	Full Name Joel Fonseca Room No. 1.29 Sample jdaf2	Date	09 Nov 2010 11:37:36		
Date Stamp	09 Nov 2010 11:37:36	File Name	C:\Users\Joel Fonseca\Desktop\LAB WORK\Leeds Spectra\JDAF2\10\PDATA\1\1r				
Frequency (MHz)	500.23	Nucleus	1H	Number of Transients	32	Origin	avance500
Original Points Count	8192	Owner	gen	Points Count	16384	Pulse Sequence	zq30
Receiver Gain	362.00	SW(cyclical) (Hz)	7002.80	Solvent	CHLOROFORM-d		
Spectrum Offset (Hz)	2725.3325	Spectrum Type	STANDARD	Sweep Width (Hz)	7002.37	Temperature (degree C)	27.000



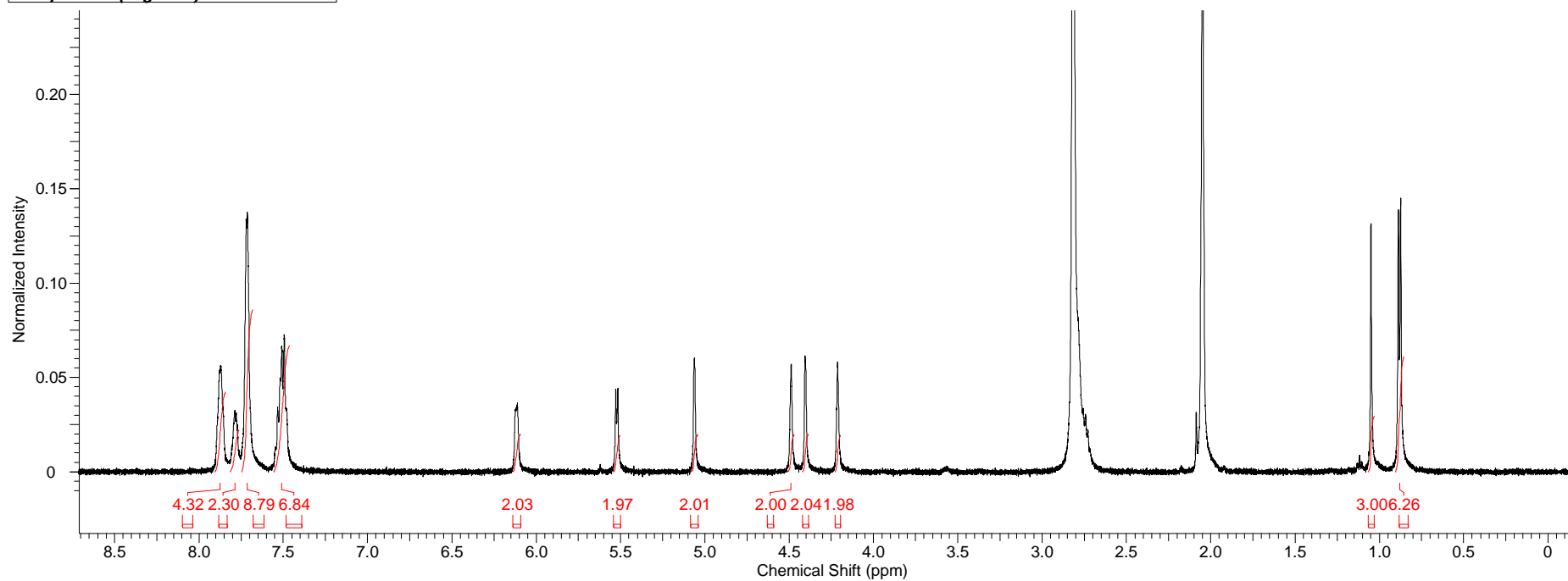
APPENDIX 3 – ¹H NMR spectrum of [RuBr₂(*p*-cymene)]₂ (3) in CDCl₃

Acquisition Time (sec)	1.1698	Comment	Full Name Joel Fonseca Room No. 1.29 Sample jdaf3	Date	10 Nov 2010 10:18:40		
Date Stamp	10 Nov 2010 10:18:40	File Name	C:\Users\Joel Fonseca\Desktop\LAB WORK\Leeds Spectra\JDAF3\1\PDATA\1\1r				
Frequency (MHz)	500.23	Nucleus	1H	Number of Transients	32	Origin	avance500
Original Points Count	8192	Owner	gen	Points Count	16384	Pulse Sequence	zg30
Receiver Gain	362.00	SW(cyclical) (Hz)	7002.80	Solvent	CHLOROFORM-d		
Spectrum Offset (Hz)	2724.9050	Spectrum Type	STANDARD	Sweep Width (Hz)	7002.37	Temperature (degree C)	27.000



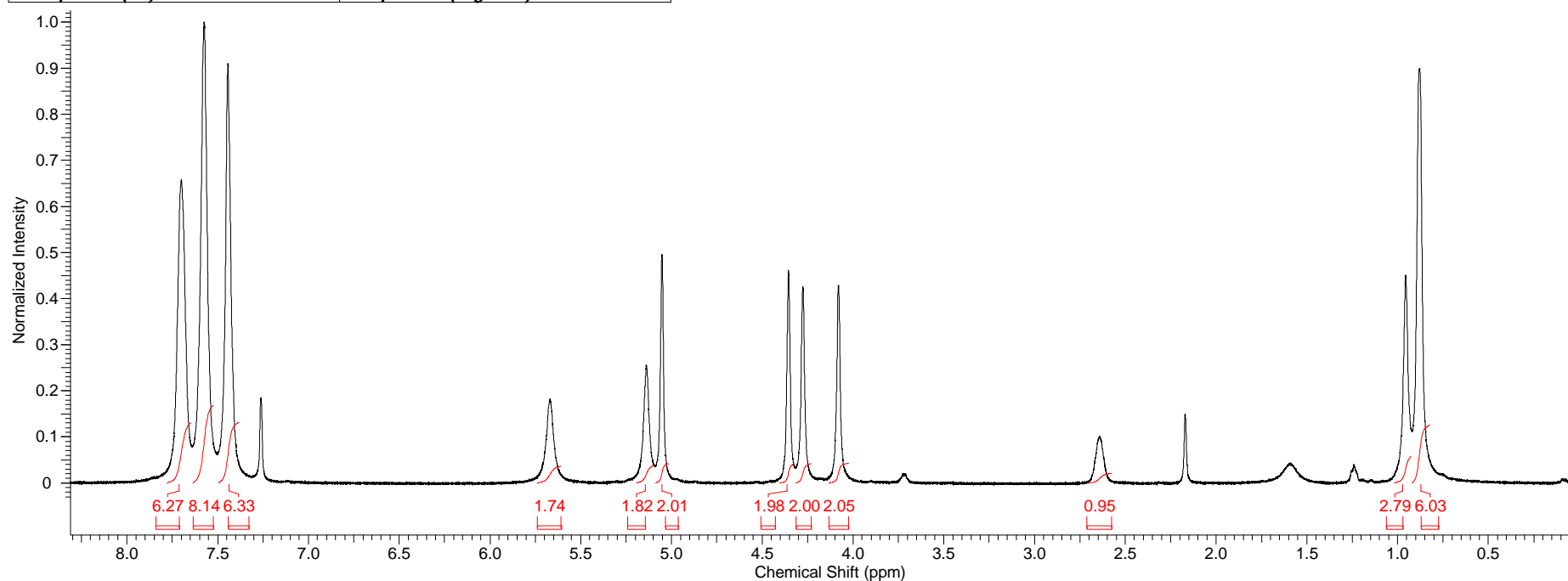
APPENDIX 4 – ¹H NMR spectrum of [RuCl(dppf)(*p*-cymene)]SbF₆ (4) (method 1) in (CD₃)₂CO

Acquisition Time (sec)	2.5166	Comment	Full Name Joel Fonseca Room No. 1.29 Sample jdaf15_2nd_pp_recris				
Date	24 Feb 2011 10:42:08	Date Stamp	24 Feb 2011 10:42:08				
File Name	F:\Leeds Spectra\jdaf15_2nd_pp_recris\10\pdata\1\1r	Frequency (MHz)	500.23	Nucleus	1H		
Number of Transients	32	Origin	avance500	Original Points Count	16384	Owner	nmr
Points Count	32768	Pulse Sequence	zg30	Receiver Gain	812.70	SW(cyclical) (Hz)	6510.42
Solvent	Acetone	Spectrum Offset (Hz)	2739.4031	Spectrum Type	STANDARD	Sweep Width (Hz)	6510.22
Temperature (degree C)	27.000						



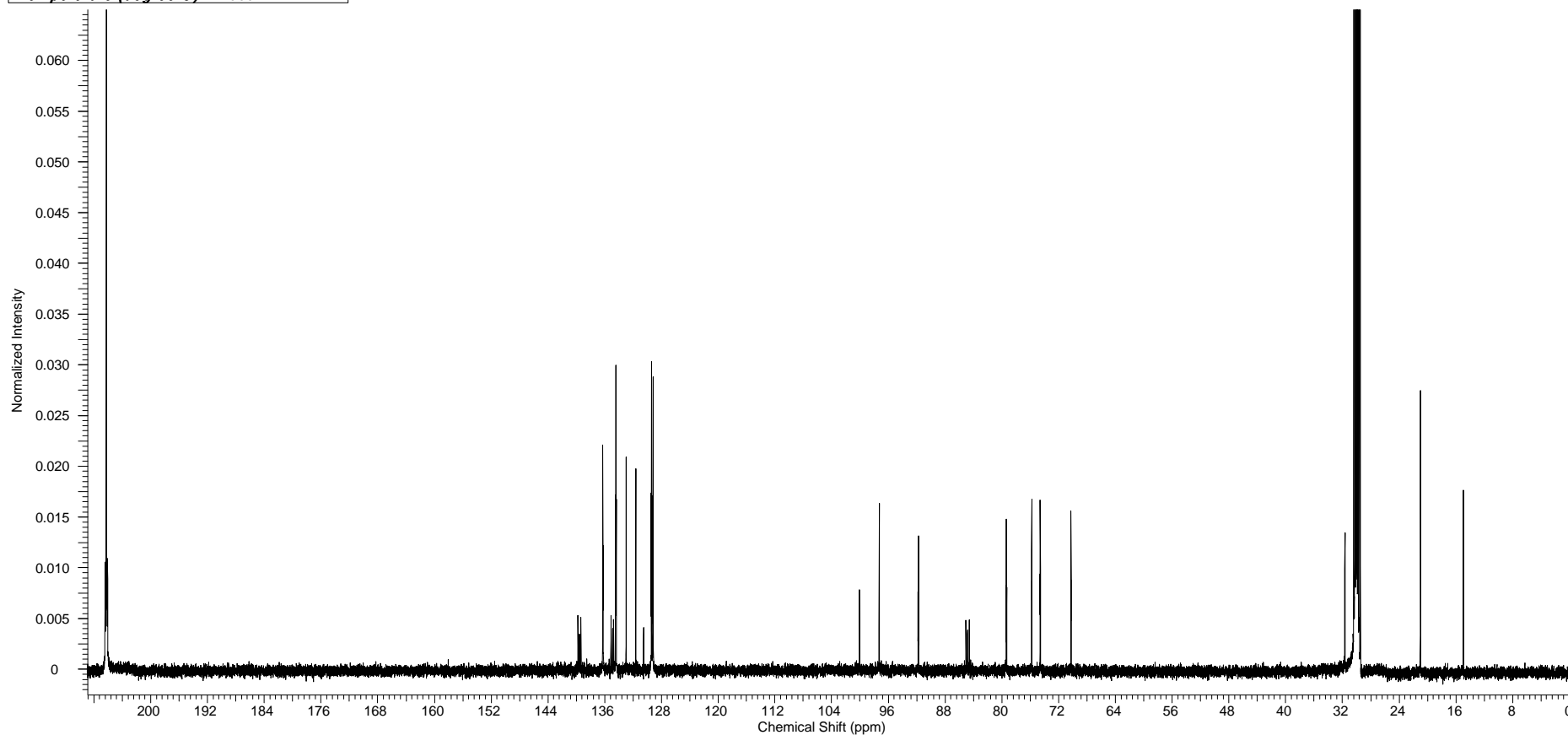
APPENDIX 4.1 – ¹H NMR spectrum of [RuCl(dppf)(*p*-cymene)]SbF₆ (4) (method 1) in CDCl₃

Acquisition Time (sec)	2.5166	Comment	Full Name Joel Fonseca Room No. 1.29 Sample jdaf15_2nd_CDCl3				
Date	07 Mar 2011 18:12:16	Date Stamp	07 Mar 2011 18:12:16				
File Name	F:\Leeds Spectra\jdaf15_2nd_CDCl3\10\PDATA\1\1r	Frequency (MHz)	500.23	Nucleus	1H		
Number of Transients	32	Origin	avance500	Original Points Count	16384	Owner	nmr
Points Count	32768	Pulse Sequence	zq30	Receiver Gain	256.00	SW(cyclical) (Hz)	6510.42
Solvent	CHLOROFORM-d	Spectrum Offset (Hz)	2739.6184	Spectrum Type	STANDARD		
Sweep Width (Hz)	6510.22	Temperature (degree C)	27.000				



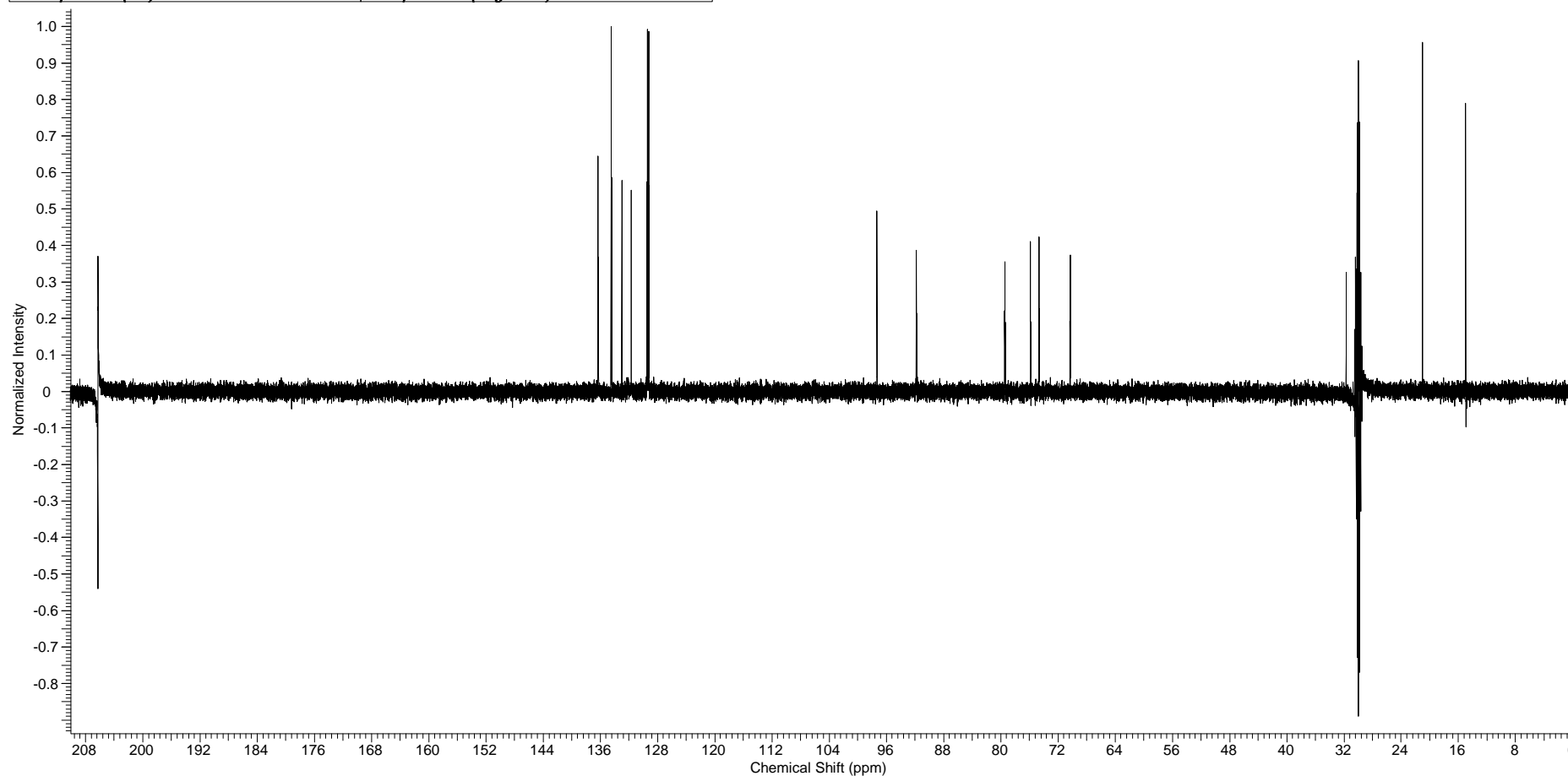
APPENDIX 4.2 – $^{13}\text{C}\{^1\text{H}\}$ NMR spectrum of $[\text{RuCl}(\text{dppf})(p\text{-cymene})]\text{SbF}_6$ (4) (method 1) in $(\text{CD}_3)_2\text{CO}$

Acquisition Time (sec)	0.9306	Comment	Name : Joel Fonseca Roo/Lab : 1.29 Sample : jda15-2nd_C44_H42_P2_Fe_Cl_Ru_Sb_F6_NMR_service		
Date	11 Mar 2011 19:07:44	Date Stamp	11 Mar 2011 19:07:44		
File Name	F:\Leeds Spectra\jda15-2nd.INO\10\PDATA\1\1r	Frequency (MHz)	125.76	Nucleus	^{13}C
Number of Transients	4096	Origin	drx500	Original Points Count	32768
Points Count	131072	Pulse Sequence	zgpg30	Receiver Gain	9195.20
Solvent	Acetone	Spectrum Offset (Hz)	15162.1211	Spectrum Type	STANDARD
Temperature (degree C)	27.000			SW(cyclical) (Hz)	35211.27
				Sweep Width (Hz)	35211.00



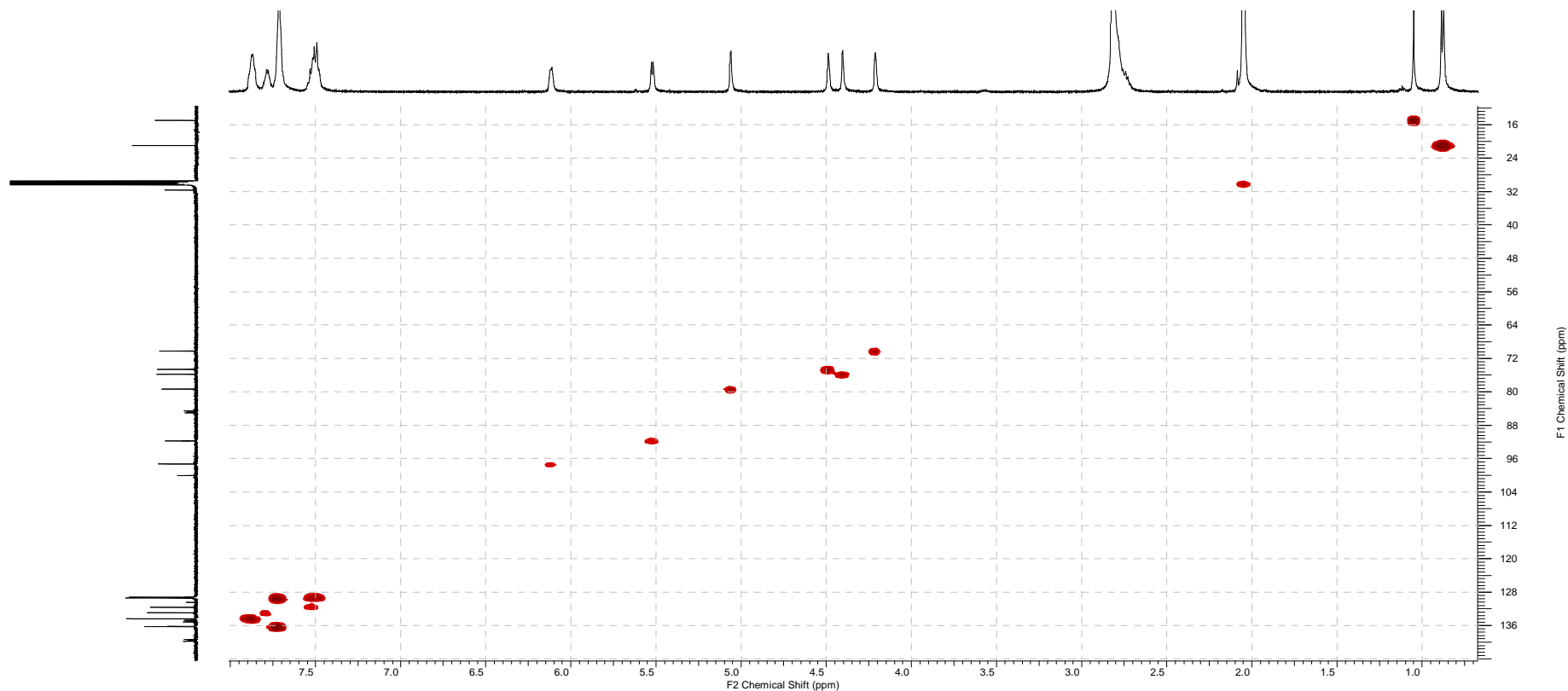
APPENDIX 4.3 – DEPT $^{13}\text{C}\{^1\text{H}\}$ NMR spectrum of $[\text{RuCl}(\text{dppf})(\textit{p}\text{-cymene})]\text{SbF}_6$ (4) (method 1) in $(\text{CD}_3)_2\text{CO}$

Acquisition Time (sec)	1.0813	Comment	Name.- Joel D. Fonseca Room/Lab No.- 1.29 Sample.- R15 2nd C44 H42 Fe RuCl Sb F6 NMR service		
Date	25 Feb 2011 18:29:20	Date Stamp	25 Feb 2011 18:29:20		
File Name	F:\Leeds Spectral\daf15_dept and cosy_cm_R15_2nd.INO\10\PDATA\1\1r		Frequency (MHz)	125.76	
Nucleus	^{13}C	Number of Transients	28672	Origin	drx500
Owner	gen	Points Count	262144	Pulse Sequence	dept135
SW(cyclical) (Hz)	30303.03	Solvent	Acetone	Receiver Gain	6502.00
Sweep Width (Hz)	30302.92	Temperature (degree C)	27.000	Spectrum Offset (Hz)	13283.0537
				Spectrum Type	DEPT135



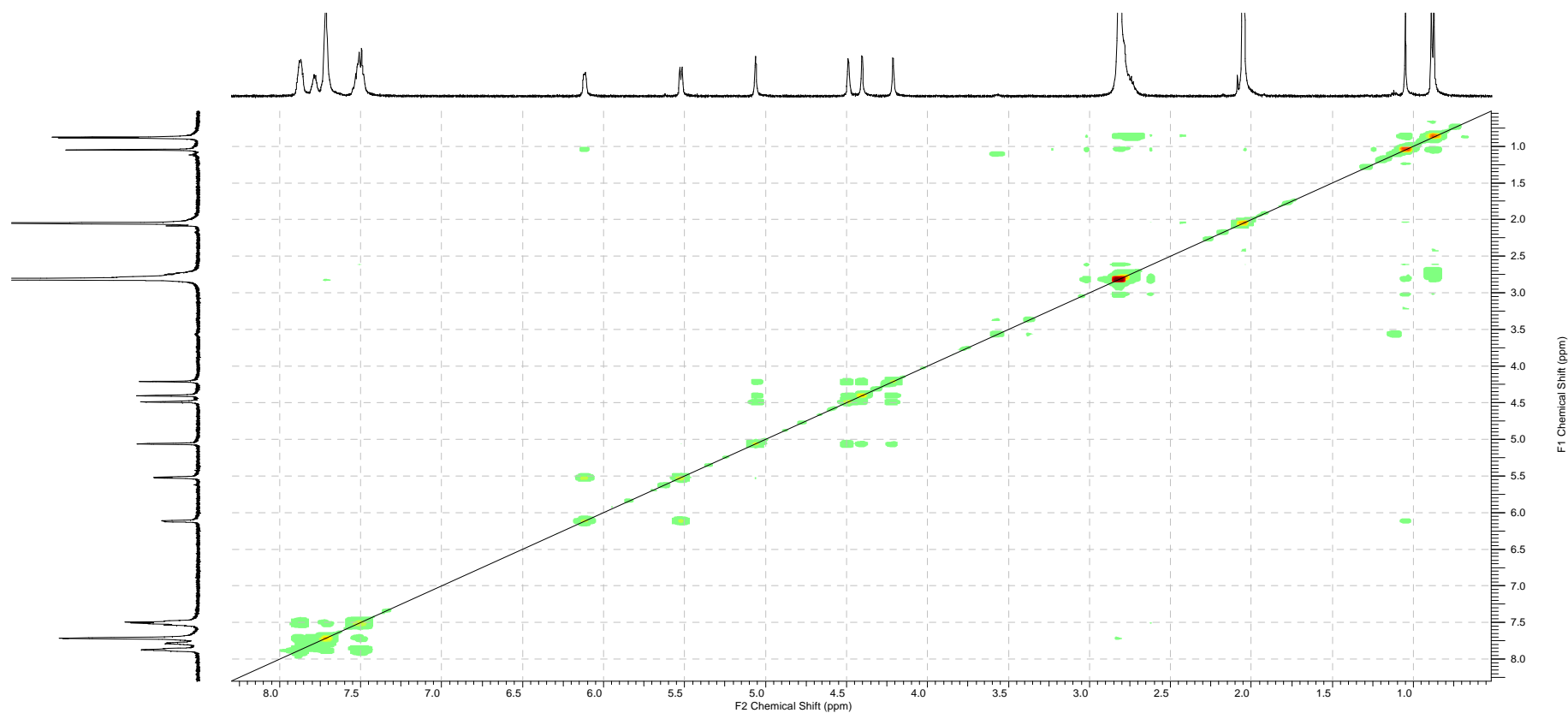
APPENDIX 4.4 – HMQC NMR spectrum of [RuCl(dppf)(*p*-cymene)]SbF₆ (4) (method 1) in (CD₃)₂CO

Acquisition Time (sec)	(0.1620, 0.0050)	Comment	5 mm BBI 1H-BB Z-GRD Z8107/0199
Date	11 Mar 2011 17:46:00	File Name	F:\Leeds Spectra\jdaf15_2nd_C&H\12\PDATA\1\2rr
Frequency (MHz)	(500.23, 125.79)	Nucleus	(1H, 13C)
Number of Transients	16	Origin	avance500
Original Points Count	(896, 120)	Owner	nmr
Points Count	(2048, 512)	Pulse Sequence	hmqcgpqf
Solvent	Acetone	Spectrum Type	HMQC
Sweep Width (Hz)	(5528.27, 23853.87)	Temperature (degree C)	27.000
Title	Full Name Joel Fonseca Room No. 1.29 Sample jdaf15_2nd_C&H		

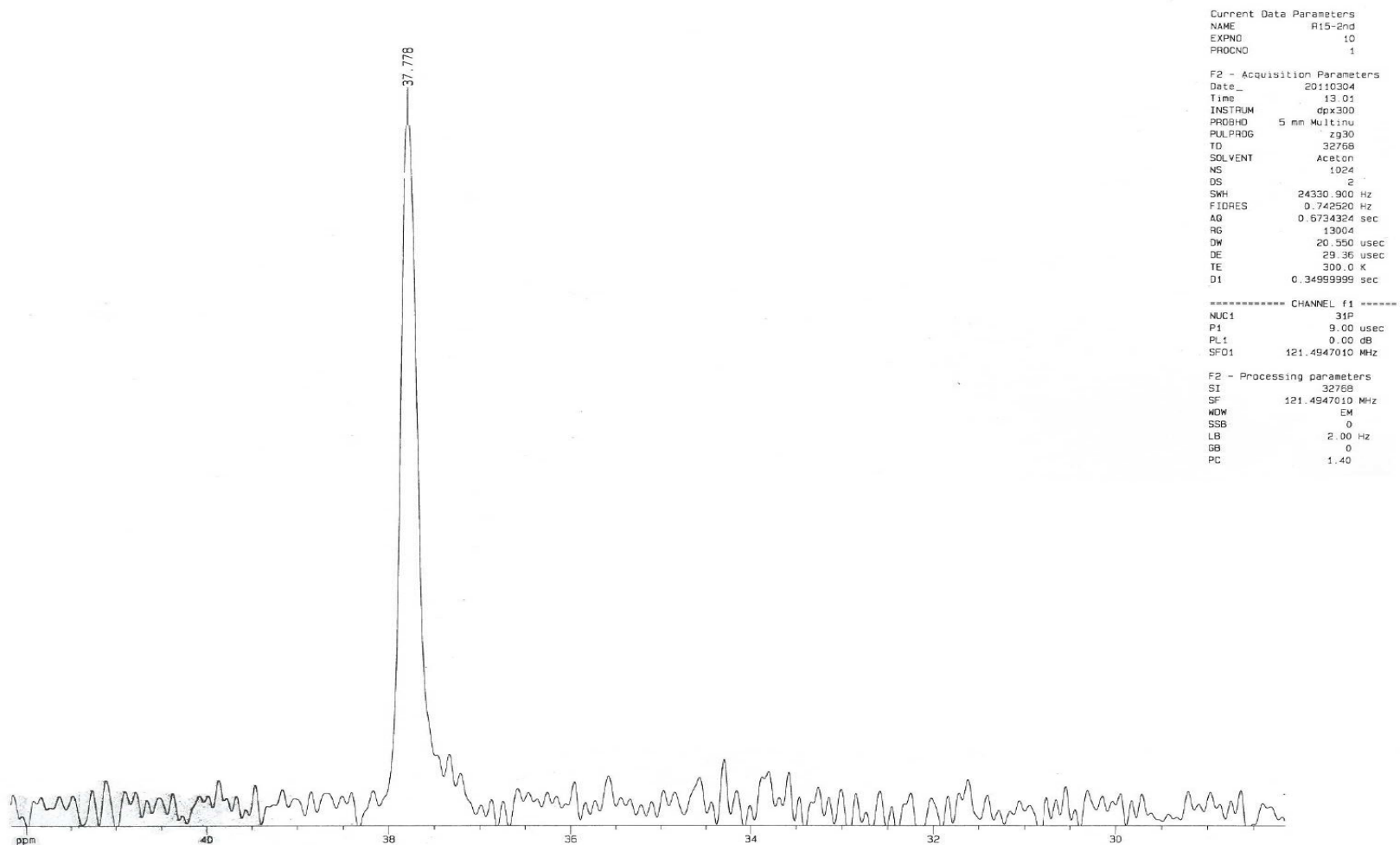


APPENDIX 4.5 – COSY NMR spectrum of [RuCl(dppf)(*p*-cymene)]SbF₆ (4) (method 1) in (CD₃)₂CO

Acquisition Time (sec)	(0.2630, 0.0411)	Comment	5 mm QNP 1H/13C/11B/31P Z-grad Z5626/0001
Date	01 Mar 2011 16:47:00		
File Name	F:\Leeds Spectra\daf15_dept and cosy_cm_R15_2nd.INO\15\PDATA\1\2rr		
Frequency (MHz)	(500.13, 500.13)	Nucleus	(1H, 1H)
Number of Transients	48	Origin	drx500
Original Points Count	(1024, 160)	Owner	gen
Points Count	(2048, 1024)	Pulse Sequence	cosy_gpqf
Solvent	Acetone	Spectrum Type	COSY
Sweep Width (Hz)	(3892.18, 3890.28)	Temperature (degree C)	27.000
Title	Name.- Joel D. Fonseca Room/Lab No.- 1.29 Sample.- R15 2nd C44 H42 Fe RuCl Sb F6 NMR service		



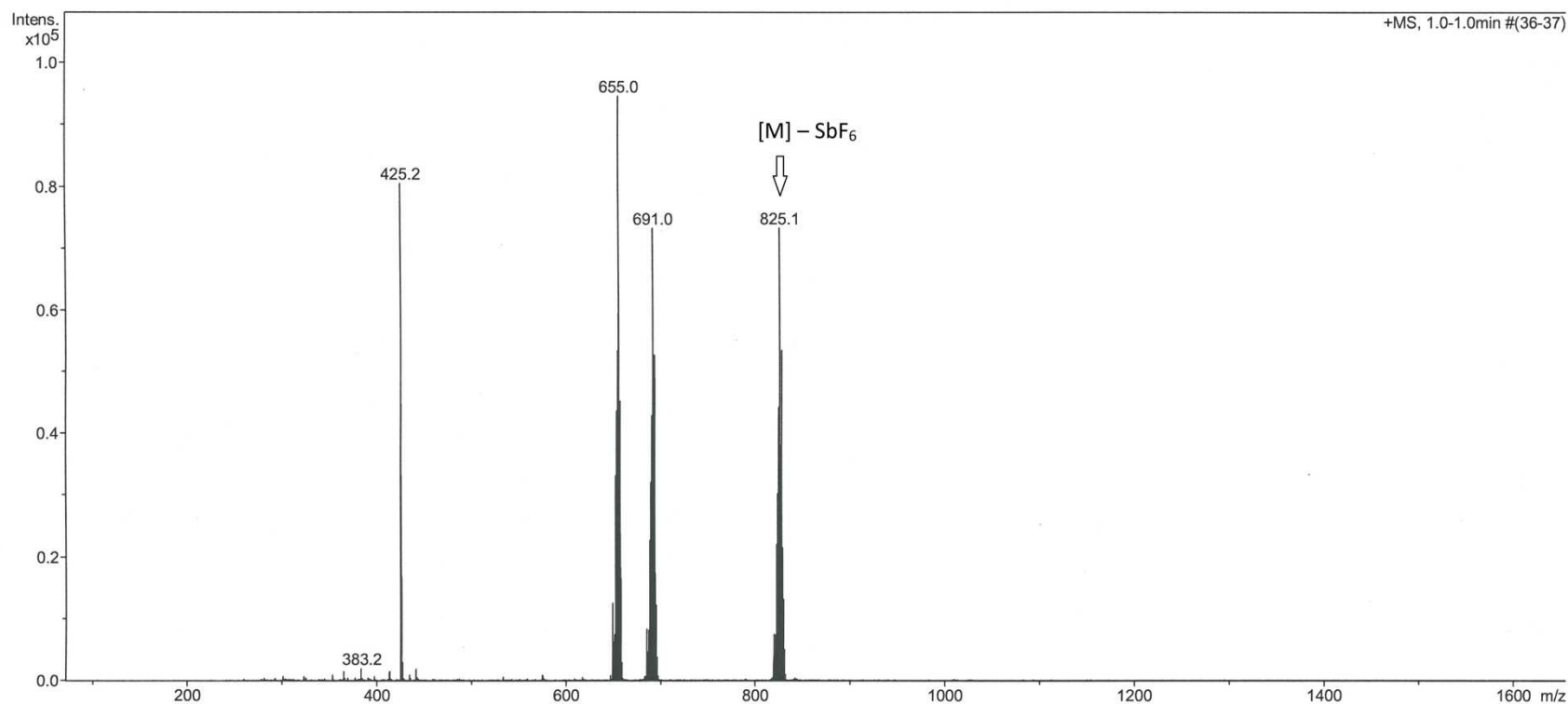
APPENDIX 4.6 – $^{31}\text{P}\{^1\text{H}\}$ NMR spectrum of $[\text{RuCl}(\text{dppf})(p\text{-cymene})]\text{SbF}_6$ (4) (method 1) in $(\text{CD}_3)_2\text{CO}$



APPENDIX 4.7 – Mass spectrum of [RuCl(dppf)(*p*-cymene)]SbF₆ (4) (method 1)

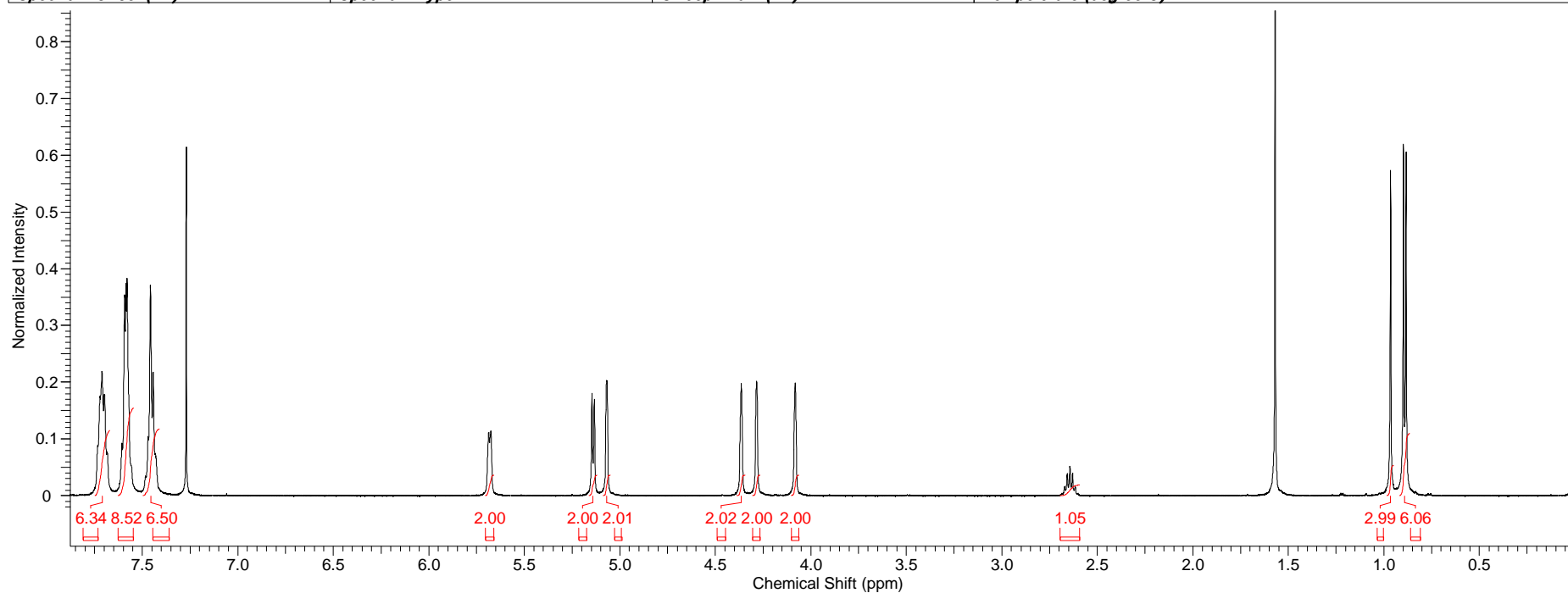
School of Chemistry Mass Spectrometry Service

Comment	jdaf-15	Operator	Tanya
Sample Name	113794	Acquisition Date	13/05/2011 12:16:04
Analysis Name	D:\Data\May 2011\113794_1-A,8_01_13345.d		
Method	steve 200-2500 lc.m		
Instrument	micrOTOF	Source Type	ESI
		Ion Polarity	Positive
		Scan Begin	50 m/z
		Scan End	2500 m/z



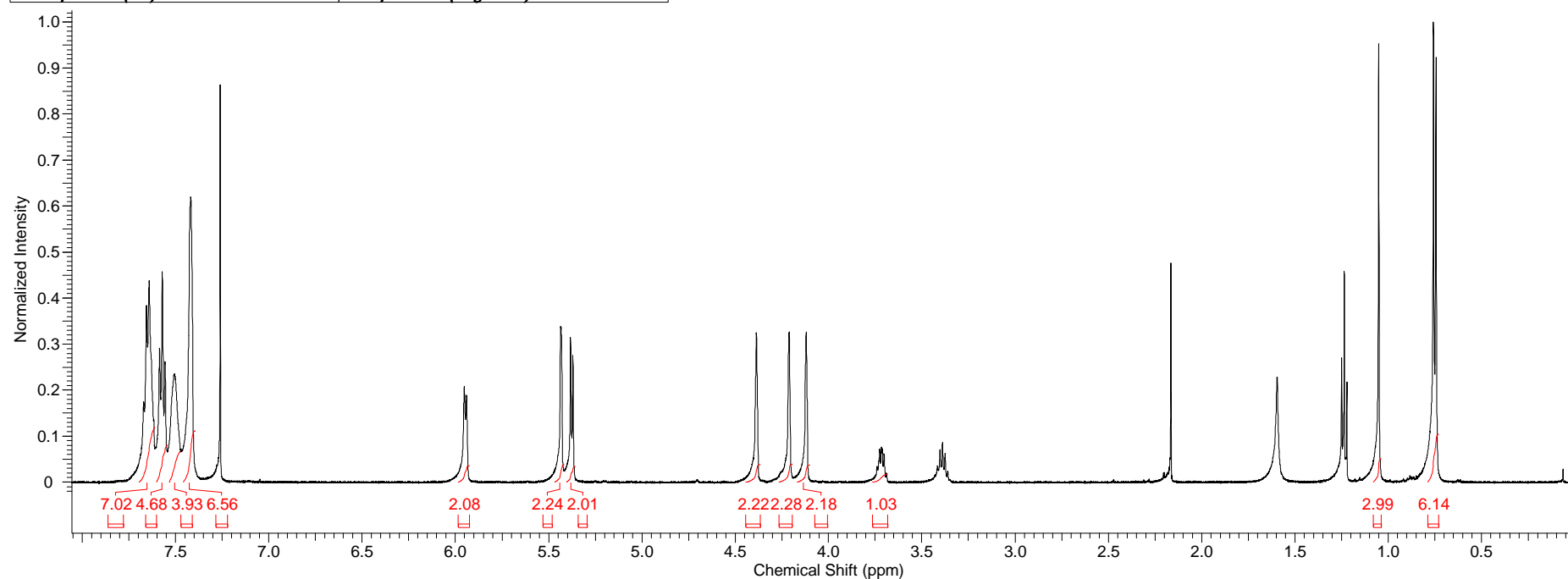
APPENDIX 4.8 – ¹H NMR spectrum of [RuCl(dppf)(*p*-cymene)]SbF₆ (4) (method 2) in CDCl₃

Acquisition Time (sec)	2.5166	Comment	Full Name - Joel Fonseca Room No. - 1.29 Sample - jdaf76	Date	01 Aug 2011 11:54:56		
Date Stamp	01 Aug 2011 11:54:56		File Name	F:\Leeds Spectra\jdaf76\10\PDATA\1\1r			
Frequency (MHz)	500.23	Nucleus	1H	Number of Transients	32	Origin	avance500
Original Points Count	16384	Owner	nmr	Points Count	32768	Pulse Sequence	zg30
Receiver Gain	256.00	SW(cyclical) (Hz)	6510.42	Solvent	CHLOROFORM-d		
Spectrum Offset (Hz)	2740.7151	Spectrum Type	STANDARD	Sweep Width (Hz)	6510.22	Temperature (degree C)	27.000



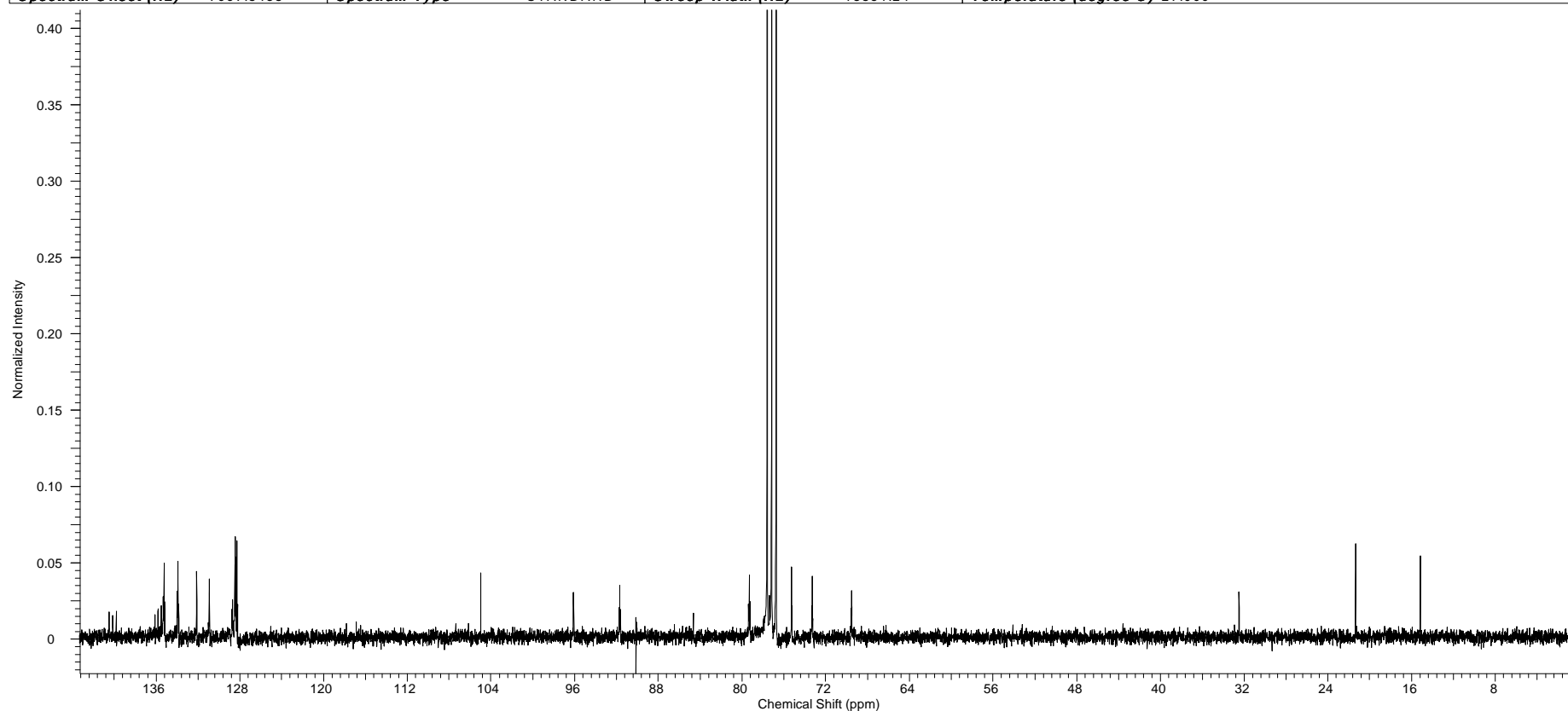
APPENDIX 5 – ¹H NMR spectrum of [Ru(dppf)(*p*-cymene)]SbF₆ (5) in CDCl₃

Acquisition Time (sec)	2.5166	Comment	Full Name - Joel Fonseca Room No. - 1.29 Sample - jdaf17_protons				
Date	21 Mar 2011 11:09:52	Date Stamp	21 Mar 2011 11:09:52				
File Name	F:\Leeds Spectra\jdaf17_protons\10\PDATA\1\1r	Frequency (MHz)	500.23	Nucleus	1H		
Number of Transients	32	Origin	avance500	Original Points Count	16384	Owner	nmr
Points Count	32768	Pulse Sequence	zg30	Receiver Gain	181.00	SW(cyclical) (Hz)	6510.42
Solvent	CHLOROFORM-d	Spectrum Offset (Hz)	2734.7197	Spectrum Type	STANDARD		
Sweep Width (Hz)	6510.22	Temperature (degree C)	27.000				



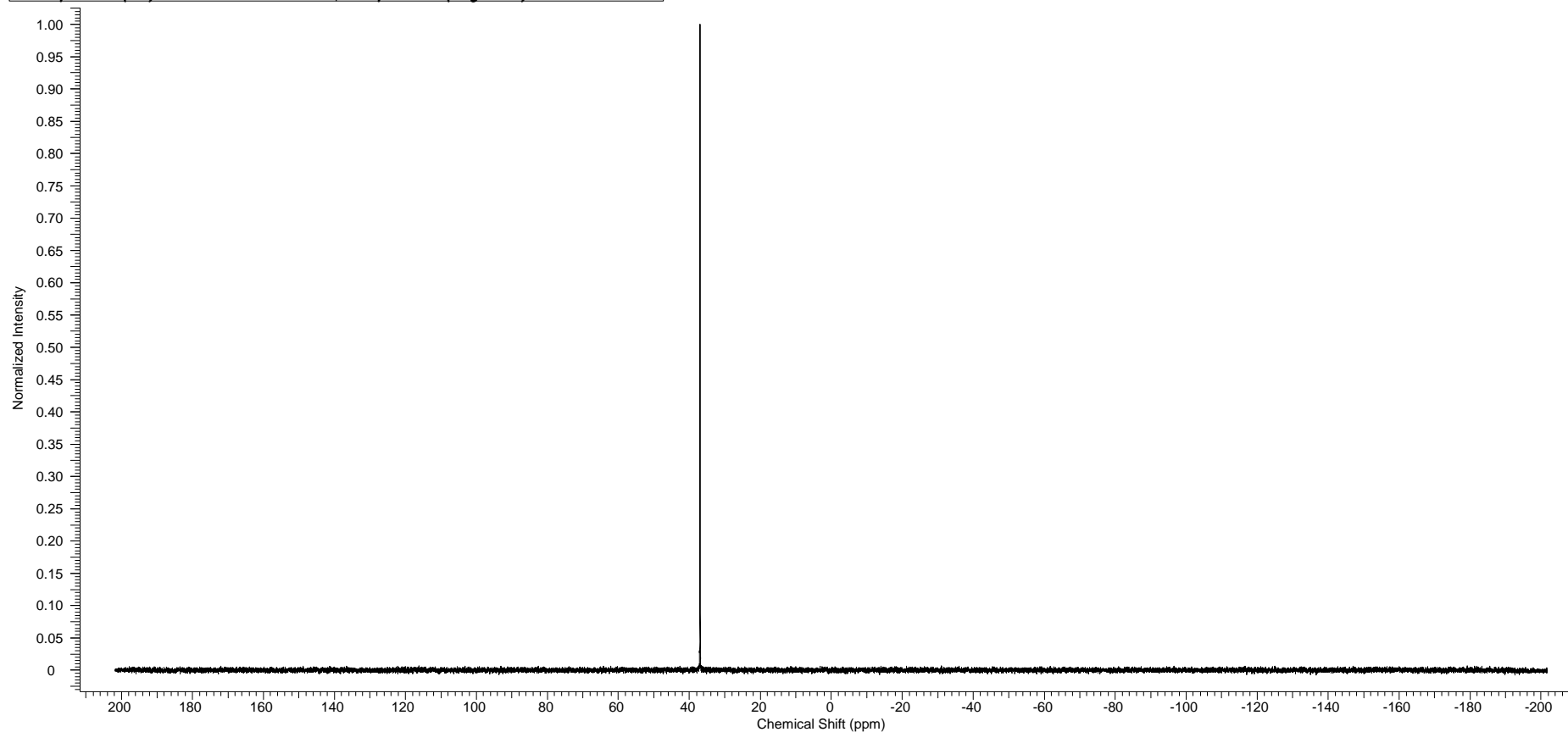
APPENDIX 5.1 – $^{13}\text{C}\{^1\text{H}\}$ NMR spectrum of $[\text{Ru}(\text{dppf})(p\text{-cymene})]\text{SbF}_6$ (5) in CDCl_3

Acquisition Time (sec)	0.8700	Comment	Name Joel Fonseca Room 1.29 Sample jdaf17_c13	Date	26 Mar 2011 03:12:00		
Date Stamp	26 Mar 2011 03:12:00		File Name	F:\Leeds Spectra\jdaf17_c13\10\fid			
Frequency (MHz)	75.48	Nucleus	^{13}C	Number of Transients	8192	Origin	dpx300
Original Points Count	16384	Owner	gen	Points Count	16384	Pulse Sequence	zg30pg
Receiver Gain	8192.00	SW(cyclical) (Hz)	18832.39	Solvent	CHLOROFORM-d		
Spectrum Offset (Hz)	7697.8438	Spectrum Type	STANDARD	Sweep Width (Hz)	18831.24	Temperature (degree C)	27.000



APPENDIX 5.2 – $^{31}\text{P}\{^1\text{H}\}$ NMR spectrum of $[\text{Ru}(\text{dppf})(\textit{p}\text{-cymene})]\text{SbF}_6$ (5) in CDCl_3

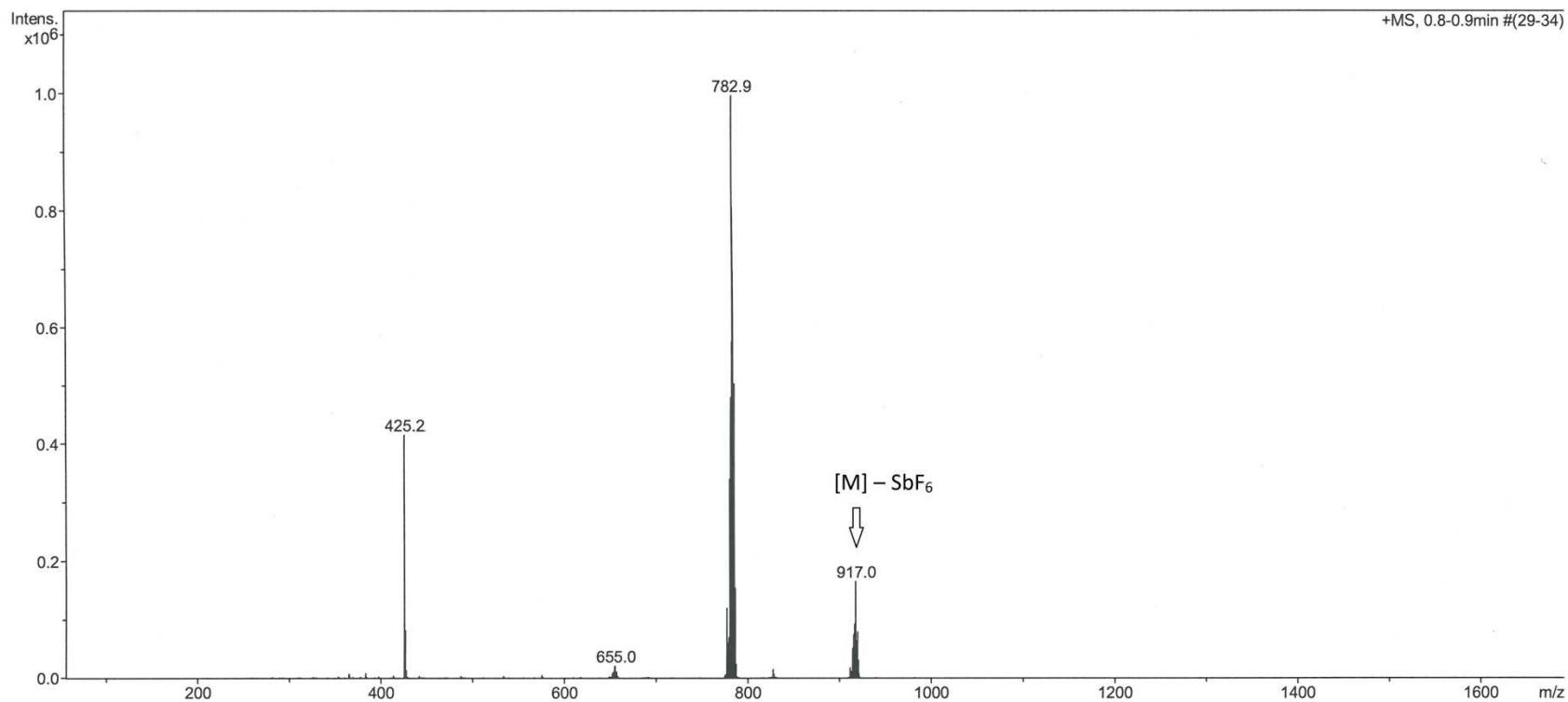
Acquisition Time (sec)	0.6685	Comment	Name- Joel Fonseca Room No- 1.29 Sample- jdaf17_new_31P		
Date	05 Aug 2011 11:50:40	Date Stamp	05 Aug 2011 11:50:40		
File Name	F:\Leeds Spectra\jdaf17_new_31P\10\PDATA\1\1r	Frequency (MHz)	121.49	Nucleus	31P
Number of Transients	160	Origin	spect	Original Points Count	32768
Points Count	65536	Pulse Sequence	zpgpg30	Receiver Gain	2050.00
Solvent	CHLOROFORM-d	Spectrum Offset (Hz)	-0.0039	SW(cyclical) (Hz)	49019.61
Sweep Width (Hz)	49018.86	Temperature (degree C)	27.020	Spectrum Type	STANDARD



APPENDIX 5.3 – Mass spectrum of [Ru(dppf)(*p*-cymene)]SbF₆ (5)

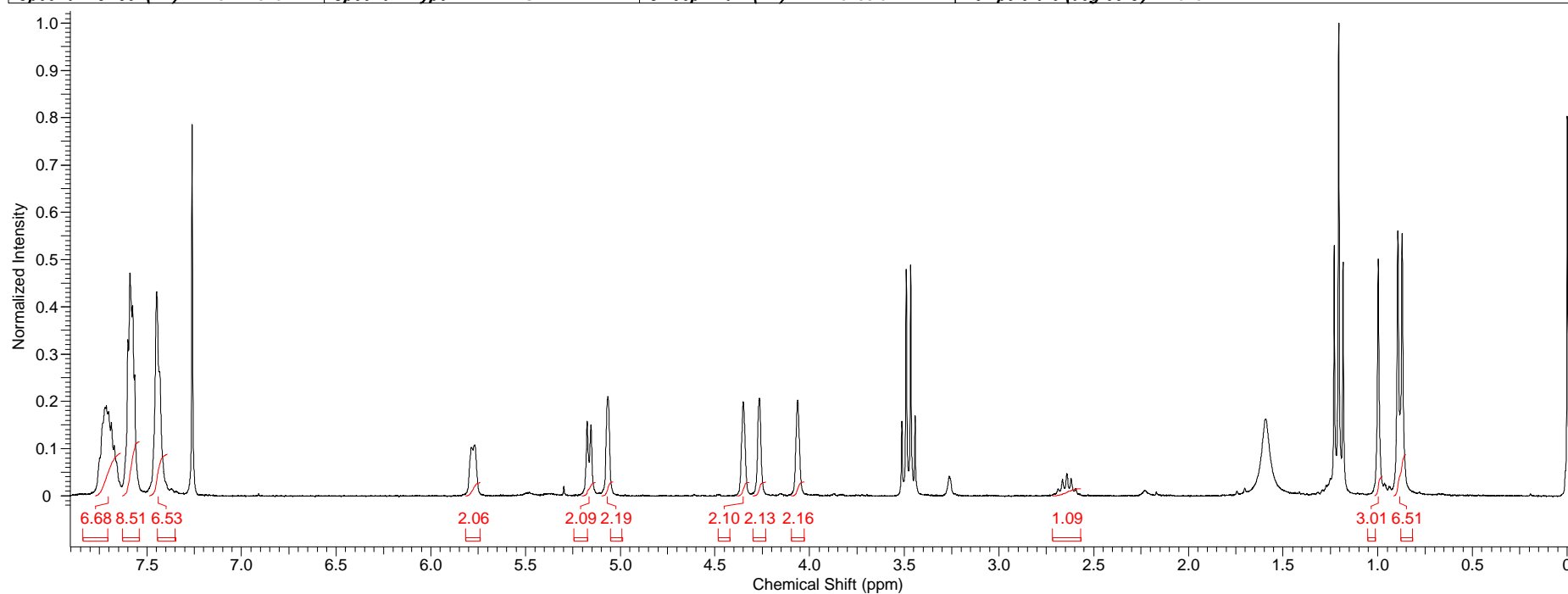
School of Chemistry Mass Spectrometry Service

Comment	jdaf 17	Operator	Tanya						
Sample Name	113795	Acquisition Date	13/05/2011 14:50:14						
Analysis Name	D:\Data\May 2011\113795_1-B,2_01_13348.d								
Method	steve 200-2500 lc.m								
Instrument	micrOTOF	Source Type	ESI	Ion Polarity	Positive	Scan Begin	50 m/z	Scan End	2500 m/z



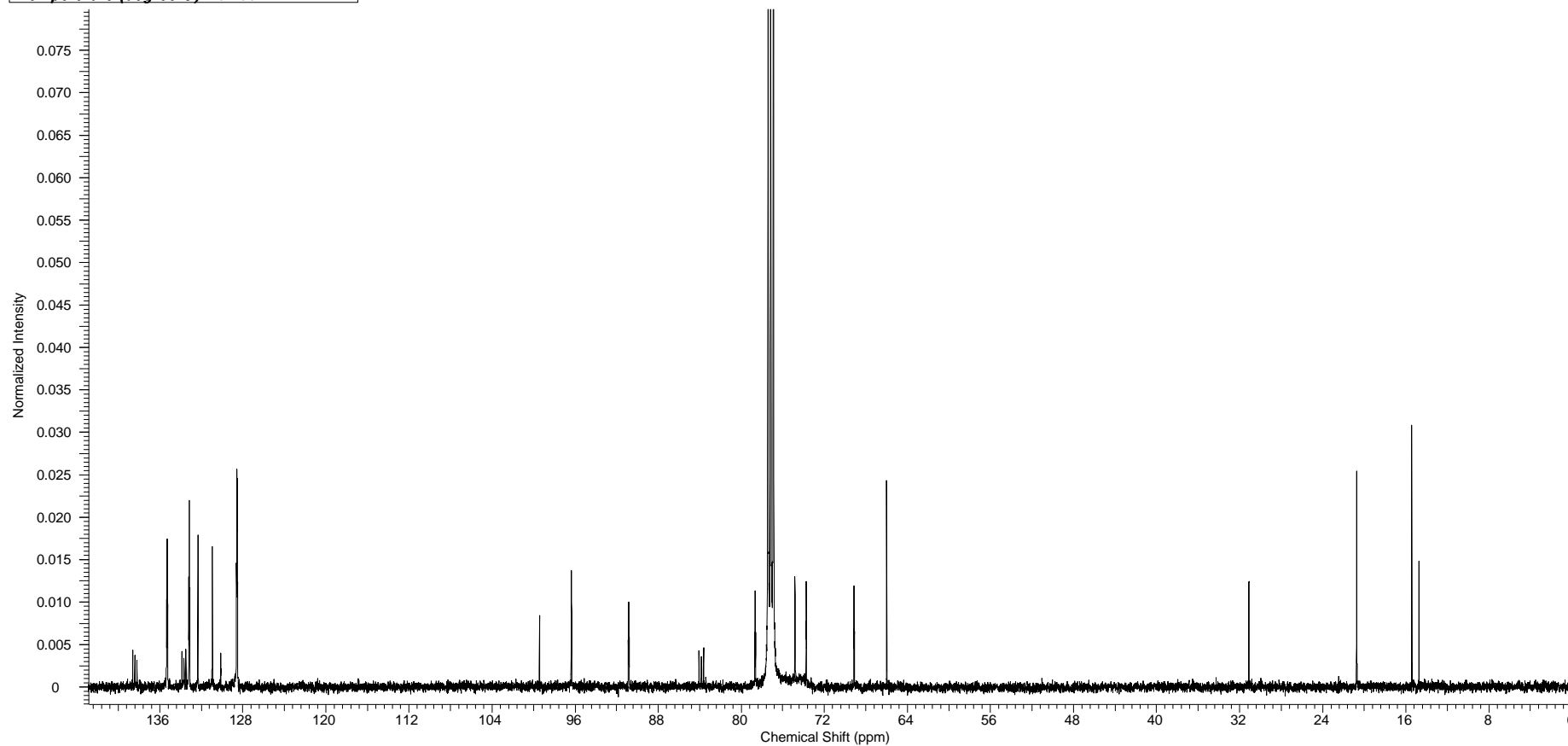
APPENDIX 6 – ¹H NMR spectrum of [RuCl(dppf)(*p*-cymene)]BF₄ (6) in CDCl₃

Acquisition Time (sec)	5.2953	Comment	Name- Joel Fonseca Room No- 1.29 Sample- jdaf25	Date	07 Jun 2011 12:29:04		
Date Stamp	07 Jun 2011 12:29:04	File Name	F:\Leeds Spectra\jdaf25\10\PDATA\1\1r				
Frequency (MHz)	300.13	Nucleus	1H	Number of Transients	32	Origin	spect
Original Points Count	32768	Owner	nmr	Points Count	65536	Pulse Sequence	zg30
Receiver Gain	322.00	SW(cyclical) (Hz)	6188.12	Solvent	CHLOROFORM-d		
Spectrum Offset (Hz)	1847.2825	Spectrum Type	STANDARD	Sweep Width (Hz)	6188.02	Temperature (degree C)	27.043



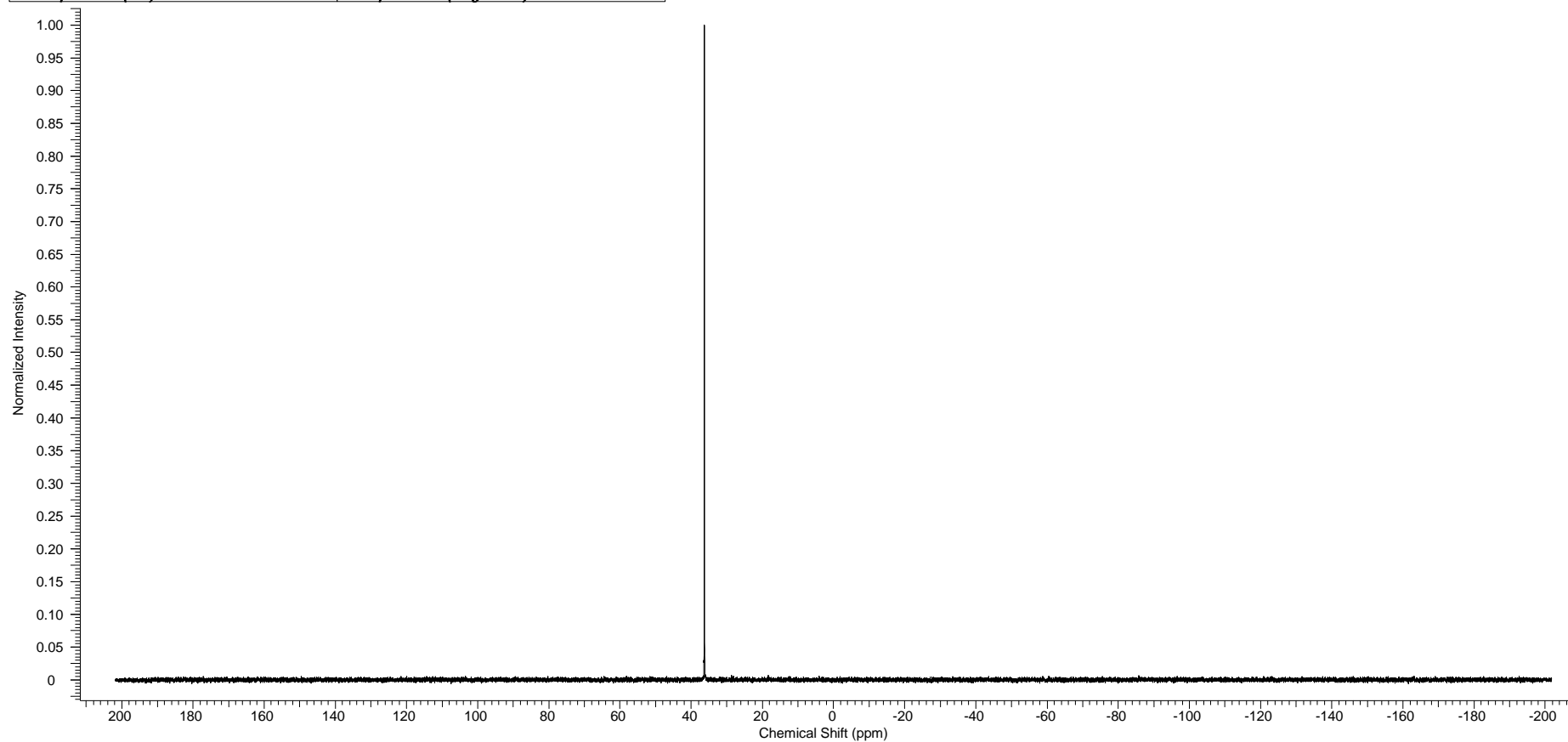
APPENDIX 6.1 – $^{13}\text{C}\{^1\text{H}\}$ NMR spectrum of $[\text{RuCl}(\text{dppf})(\textit{p}\text{-cymene})]\text{BF}_4$ (6) in CDCl_3

Acquisition Time (sec)	0.6980	Comment	Name.- Joel Fonseca Room/Lab No.- 1.29 Sample.- JDAF 25 RuCl(C34 H28 Fe P2) C10 H14 BF4 NMR service		
Date	10 Jun 2011 16:30:08	Date Stamp	10 Jun 2011 16:30:08		
File Name	F:\Leeds Spectra\jdaf25.INO\10\PDATA\1\1r	Frequency (MHz)	125.76	Nucleus	^{13}C
Number of Transients	24576	Origin	drx500	Original Points Count	24576
Points Count	131072	Pulse Sequence	zpgpg30	Receiver Gain	9195.20
Solvent	CHLOROFORM-d	Spectrum Offset (Hz)	15058.1514	Spectrum Type	STANDARD
Temperature (degree C)	26.160			SW(cyclical) (Hz)	35211.27
				Sweep Width (Hz)	35211.00



APPENDIX 6.2 – $^{31}\text{P}\{^1\text{H}\}$ NMR spectrum of $[\text{RuCl}(\text{dppf})(p\text{-cymene})]\text{BF}_4$ (6) in CDCl_3

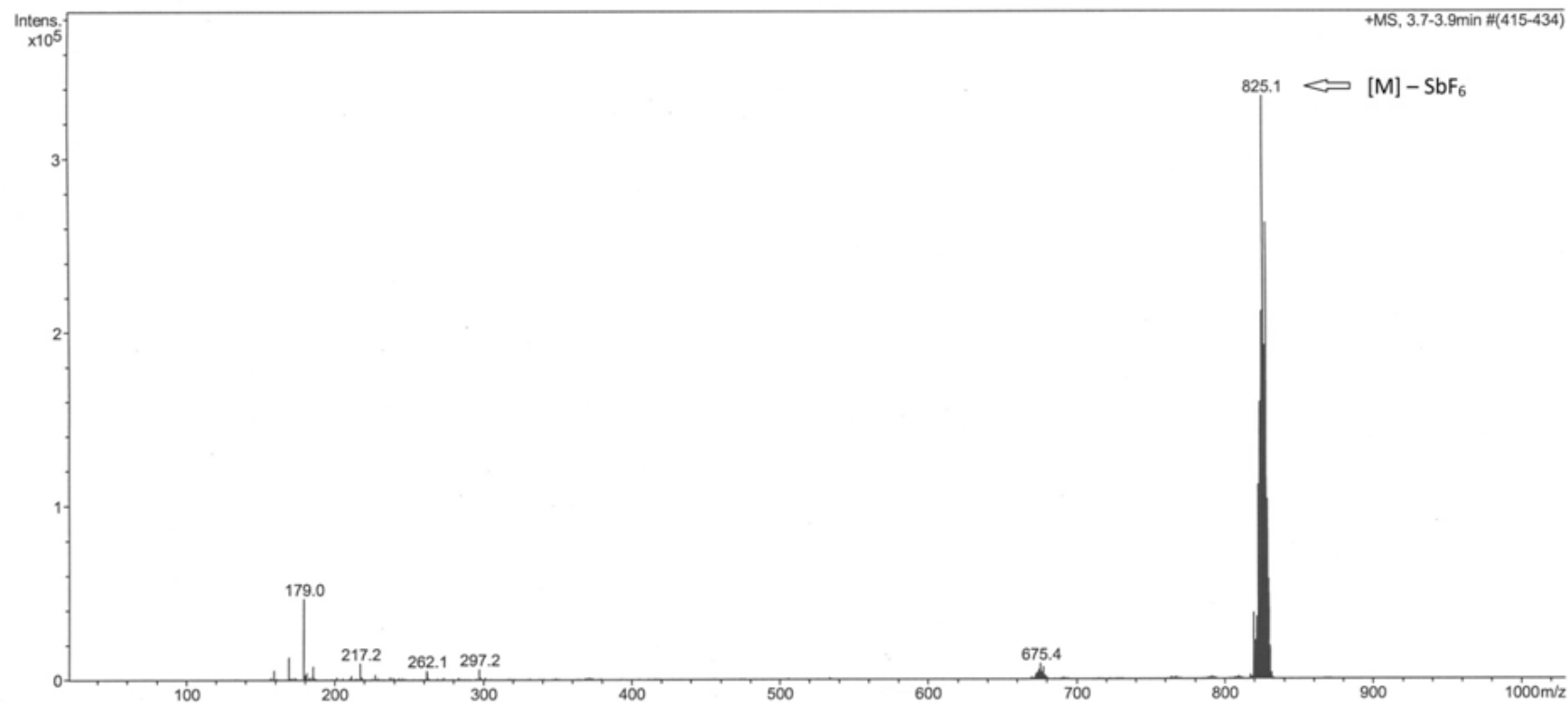
Acquisition Time (sec)	0.6685	Comment	Name- Joel Fonseca Room No- 1.29 Sample- jdaf25_new_31P				
Date	05 Aug 2011 12:18:24	Date Stamp	05 Aug 2011 12:18:24				
File Name	F:\Leeds Spectra\jdaf25_new_31P\10\PDATA\1\1r	Frequency (MHz)	121.49	Nucleus	31P		
Number of Transients	160	Origin	spect	Original Points Count	32768	Owner	nmr
Points Count	65536	Pulse Sequence	zpgg30	Receiver Gain	2050.00	SW(cyclical) (Hz)	49019.61
Solvent	CHLOROFORM-d	Spectrum Offset (Hz)	-0.0039	Spectrum Type	STANDARD		
Sweep Width (Hz)	49018.86	Temperature (degree C)	26.983				



APPENDIX 6.3 – Mass spectrum of [RuCl(dppf)(*p*-cymene)]BF₄ (6)

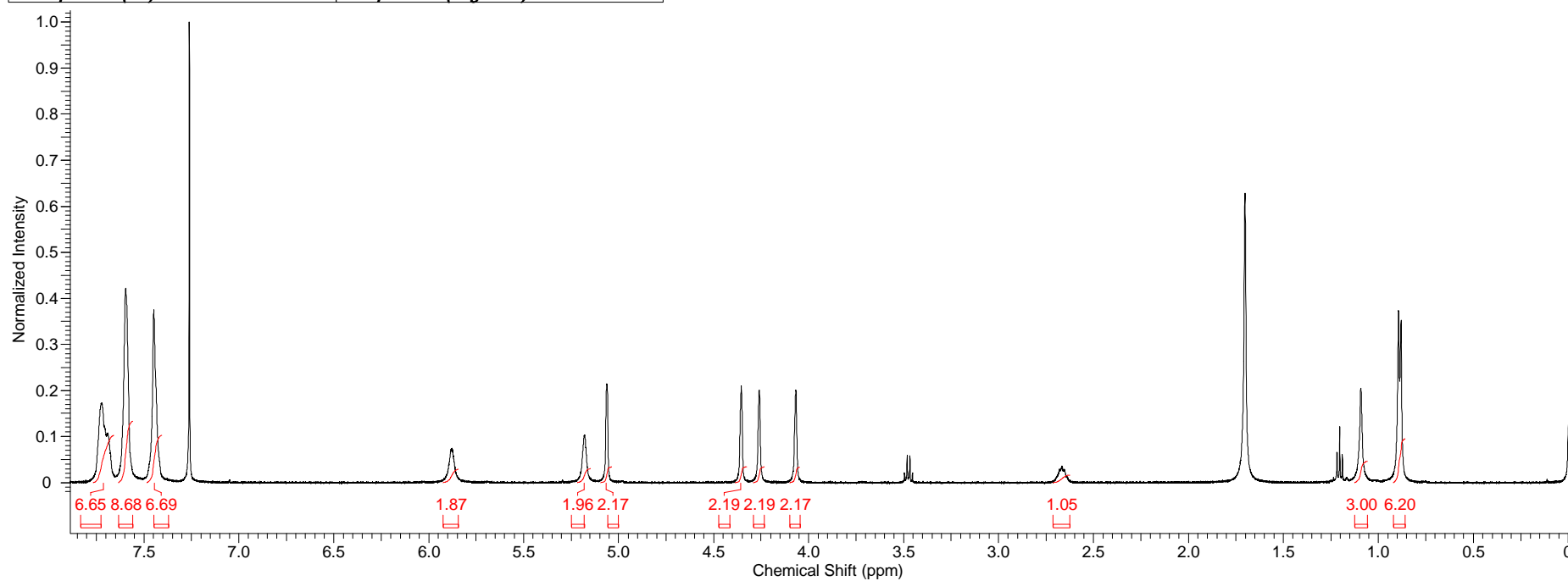
School of Chemistry Mass Spectrometry Service

Comment	jdaf-25	Operator	Tanya
Sample Name	114144	Acquisition Date	17/06/2011 15:09:06
Analysis Name	D:\Data\June2011\114144.d		
Method	Anneke 50-1000 syringe.m		
Instrument	micrOTOF	Source Type	ESI
		Ion Polarity	Positive
		Scan Begin	50 m/z
		Scan End	1000 m/z



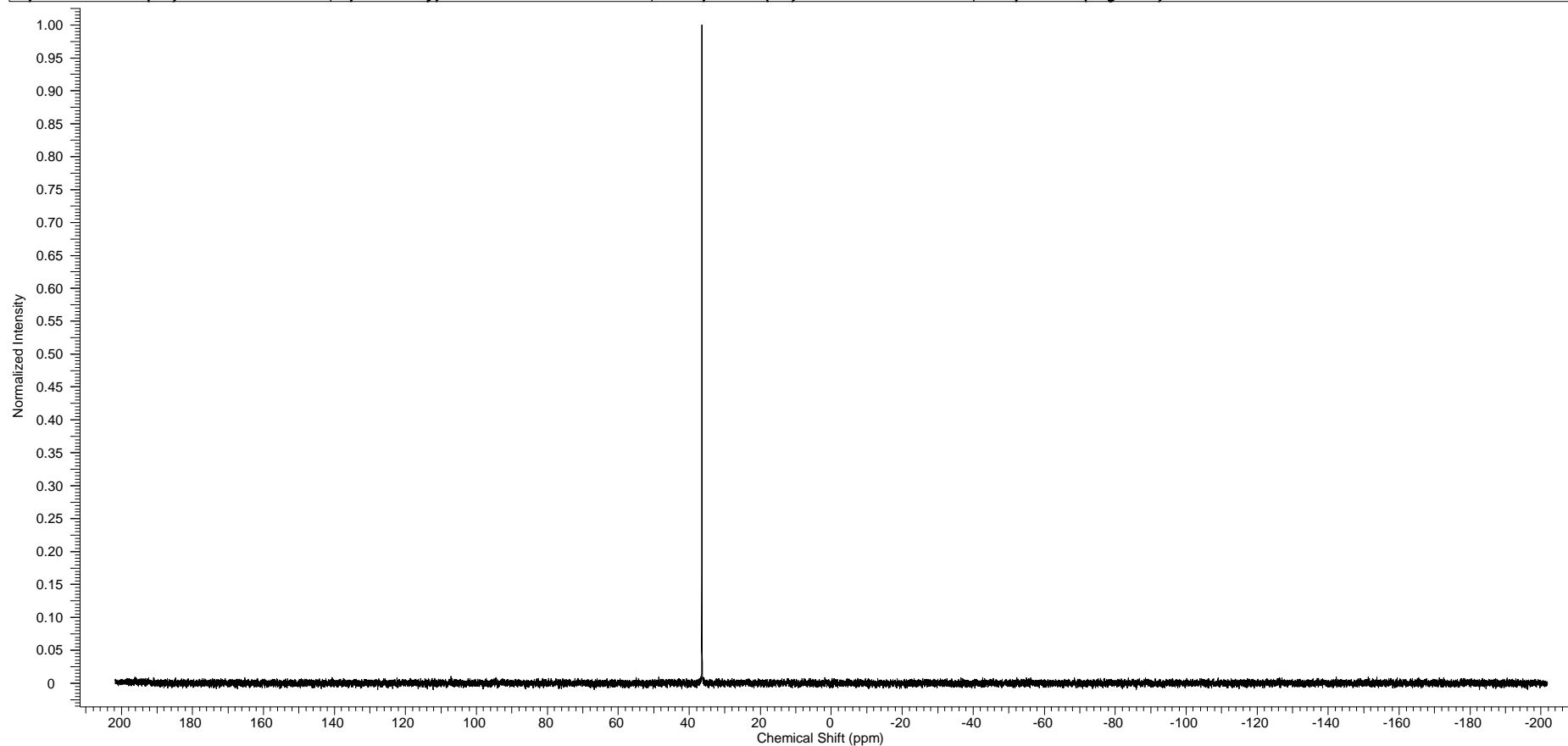
APPENDIX 7 – ¹H NMR spectrum of [RuCl(dppf)(*p*-cymene)]Cl (7) in CDCl₃

Acquisition Time (sec)	2.5166	Comment	Full Name - Joel Fonseca Room No. - 1.29 Sample - jdaf45_recrys		
Date	06 Jul 2011 15:56:00	Date Stamp	06 Jul 2011 15:56:00		
File Name	F:\Leeds Spectra\jdaf45_recrys\10\PDATA\1\1r	Frequency (MHz)	500.23	Nucleus	1H
Number of Transients	32	Origin	avance500	Original Points Count	16384
Points Count	32768	Pulse Sequence	zq30	Receiver Gain	256.00
Solvent	CHLOROFORM-d	Spectrum Offset (Hz)	2734.5208	SW(cyclical) (Hz)	6510.42
Sweep Width (Hz)	6510.22	Temperature (degree C)	27.000	Spectrum Type	STANDARD



APPENDIX 7.1 – $^{31}\text{P}\{^1\text{H}\}$ NMR spectrum of $[\text{RuCl}(\text{dppf})(p\text{-cymene})]\text{Cl}$ (7) in CDCl_3

Acquisition Time (sec)	0.6685	Comment	Name- Joel Fonseca Room No- 1.29 Sample- jdaf45_31P	Date	29 Jul 2011 15:53:52		
Date Stamp	29 Jul 2011 15:53:52		File Name	F:\Leeds Spectra\jdaf45_31P\10\PDATA\1\1r			
Frequency (MHz)	121.49	Nucleus	31P	Number of Transients	160	Origin	spect
Original Points Count	32768	Owner	nmr	Points Count	65536	Pulse Sequence	zpgpg30
Receiver Gain	2050.00	SW(cyclical) (Hz)	49019.61	Solvent	CHLOROFORM-d		
Spectrum Offset (Hz)	-0.0039	Spectrum Type	STANDARD	Sweep Width (Hz)	49018.86	Temperature (degree C)	27.043



APPENDIX 7.2 – Mass spectrum of [RuCl(dppf)(*p*-cymene)]Cl (7)

School of Chemistry Mass Spectrometry Service

Comment

Sample Name

jdaf45_37911

Analysis Name

D:\Data\stuartwarriner\chmslw\jdaf45_37911_1-D,5_01_13953.d

Method

xxx-omc.m

Instrument

micrOTOF

Source Type

ESI

Ion Polarity

Positive

Scan Begin

50 m/z

Scan End

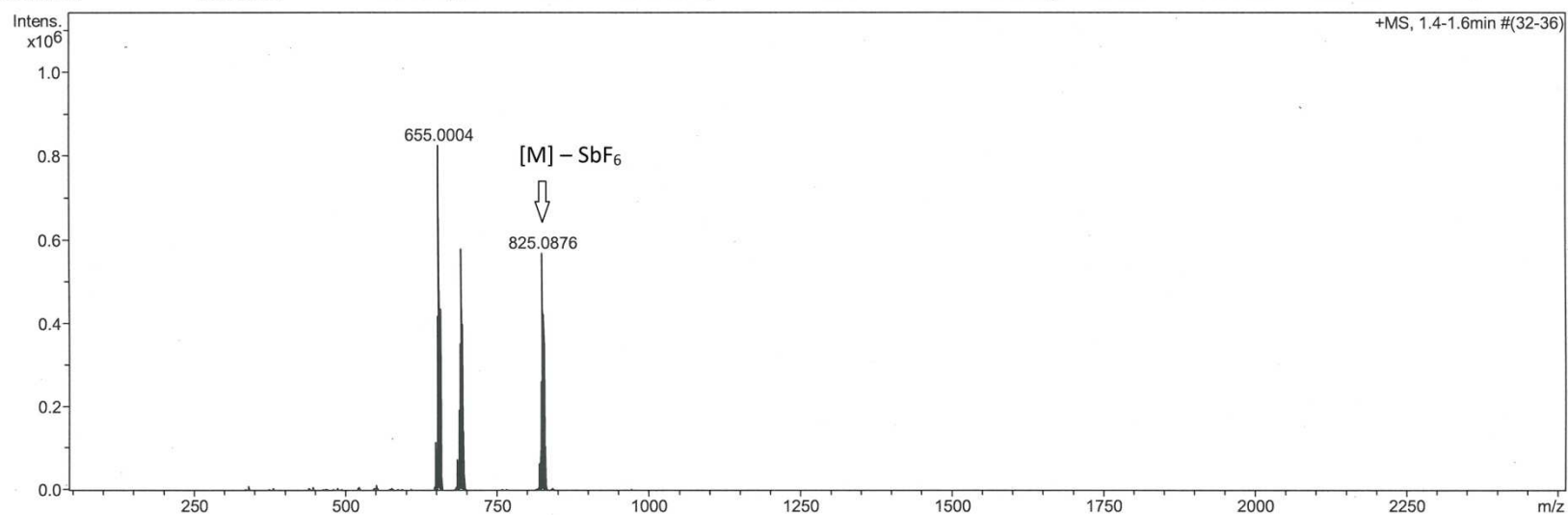
2500 m/z

Operator

Tanya

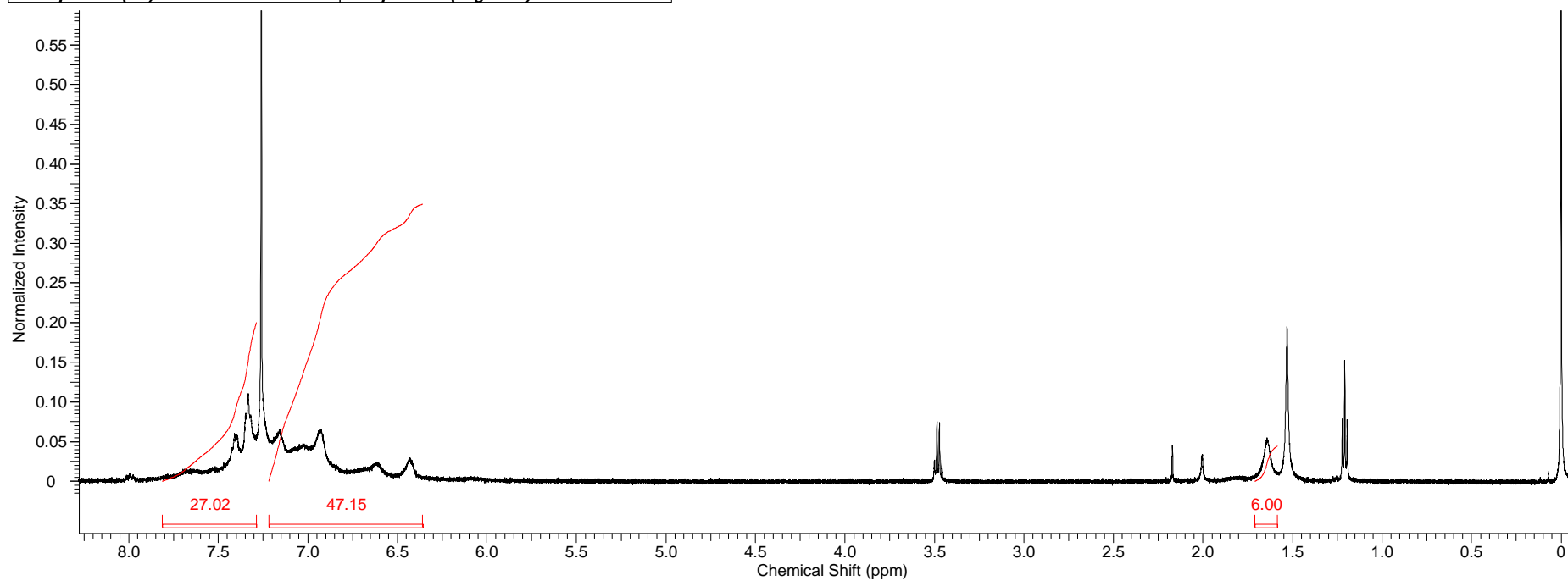
Acquisition Date

10/07/2011 15:24:16



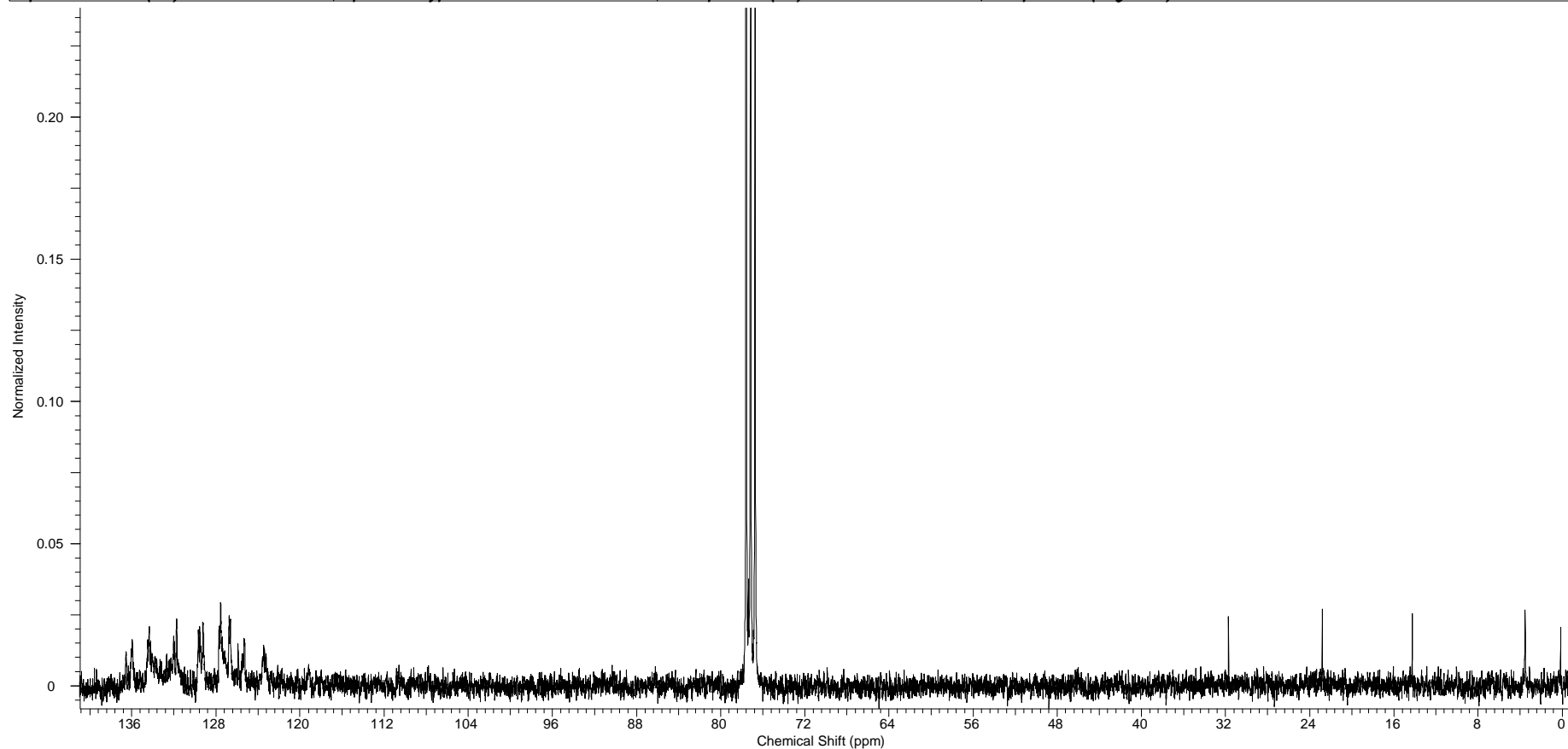
APPENDIX 8 – ¹H NMR spectrum of [Ru₂Cl₃(DPEPhos)₂(CH₃CN)₂]SbF₆ (8) in CDCl₃

Acquisition Time (sec)	2.5166	Comment	Full Name - Joel Fonseca Room No. - 1.29 Sample - jdaf18_recrys		
Date	13 Apr 2011 15:21:52	Date Stamp	13 Apr 2011 15:21:52		
File Name	F:\Leeds Spectra\jdaf18_2nd_recrys (5)\20\pdata\1\1r	Frequency (MHz)	500.23	Nucleus	1H
Number of Transients	32	Origin	avance500	Original Points Count	16384
Points Count	32768	Pulse Sequence	zg30	Receiver Gain	512.00
Solvent	CHLOROFORM-d	Spectrum Offset (Hz)	2734.3459	SW(cyclical) (Hz)	6510.42
Sweep Width (Hz)	6510.22	Temperature (degree C)	27.000	Spectrum Type	STANDARD



APPENDIX 8.1 – $^{13}\text{C}\{^1\text{H}\}$ NMR spectrum of $[\text{Ru}_2\text{Cl}_3(\text{DPEPhos})_2(\text{CH}_3\text{CN})_2]\text{SbF}_6$ (8) in CDCl_3

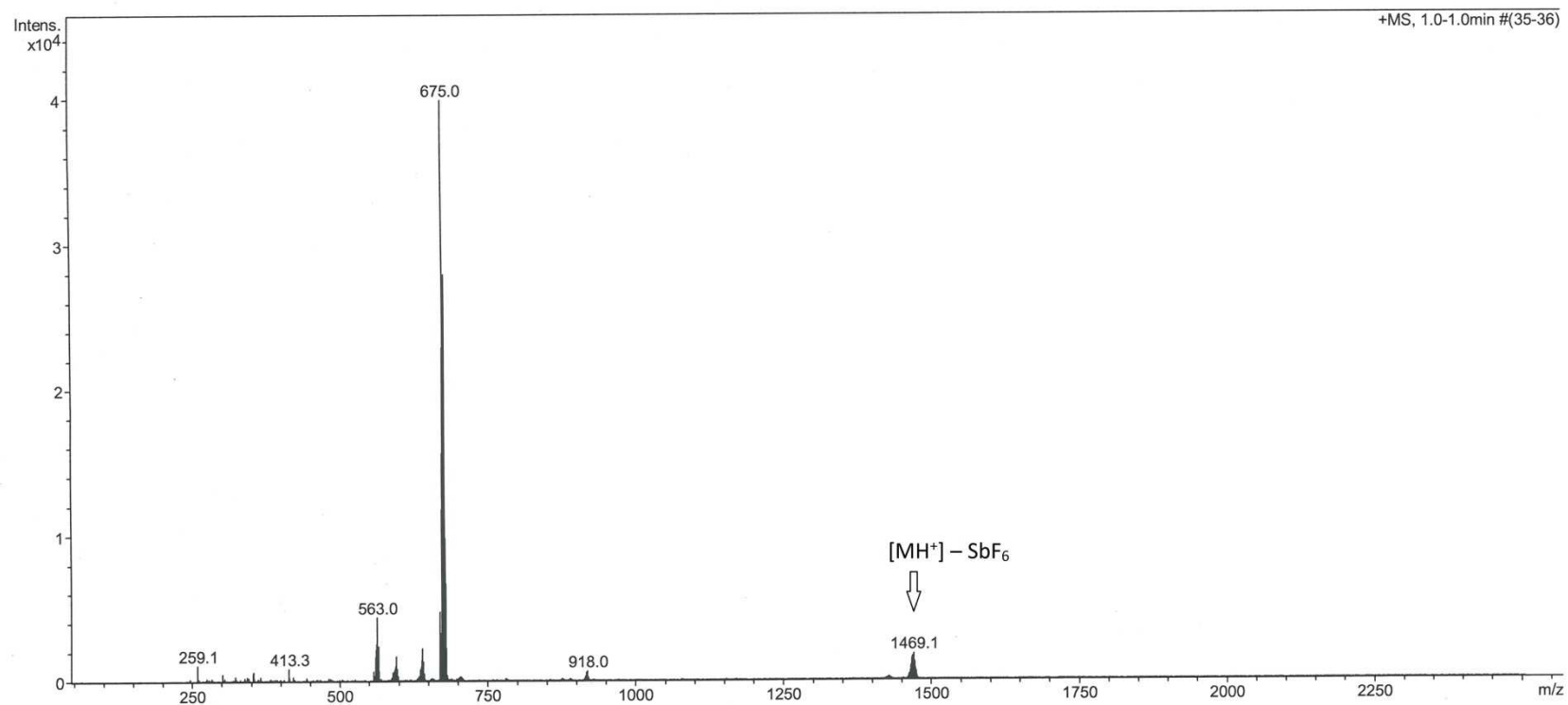
Acquisition Time (sec)	0.8039	Comment	Name- Joel Fonseca Room No- 1.29 Sample- jdaf18_13C	Date	12 May 2011 00:55:44		
Date Stamp	12 May 2011 00:55:44	File Name	F:\Leeds Spectra\jdaf18_13C\10\PDATA\1\1r				
Frequency (MHz)	75.47	Nucleus	13C	Number of Transients	5760	Origin	spect
Original Points Count	16384	Owner	nmr	Points Count	32768	Pulse Sequence	zpgg30
Receiver Gain	2050.00	SW(cyclical) (Hz)	20380.44	Solvent	CHLOROFORM-d		
Spectrum Offset (Hz)	8312.4932	Spectrum Type	STANDARD	Sweep Width (Hz)	20379.81	Temperature (degree C)	27.030



APPENDIX 8.2 – Mass spectrum of $[\text{Ru}_2\text{Cl}_3(\text{DPEPhos})_2(\text{CH}_3\text{CN})_2]\text{SbF}_6$ (8)

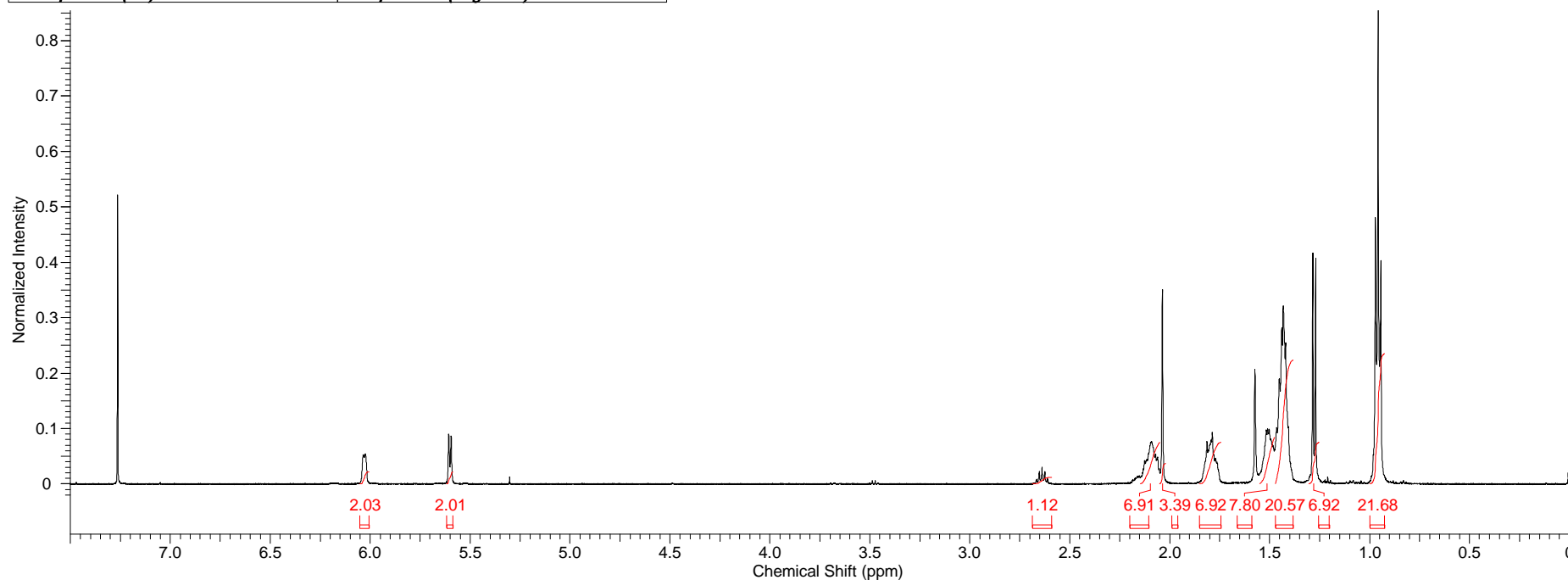
School of Chemistry Mass Spectrometry Service

Comment	jdaf-18	Operator	Tanya						
Sample Name	114045	Acquisition Date	07/06/2011 16:33:23						
Analysis Name	D:\Data\June2011\114045_1-B,9_01_13624.d								
Method	steve 200-2500 lc.m								
Instrument	micrOTOF	Source Type	ESI	Ion Polarity	Positive	Scan Begin	50 m/z	Scan End	2500 m/z



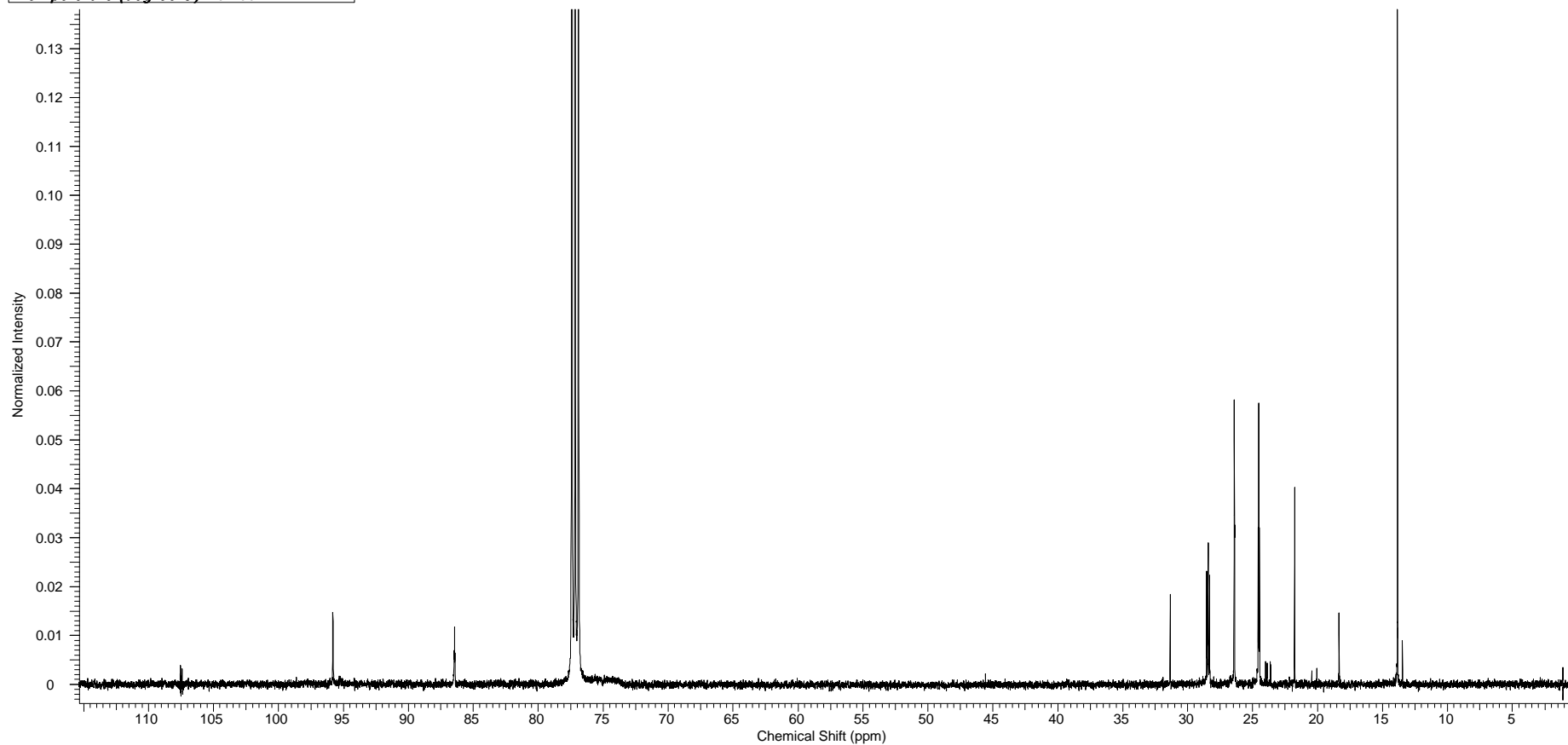
APPENDIX 9 – ¹H NMR spectrum of [RuCl(P(*n*-Bu)₃)₂(*p*-cymene)]SbF₆ (9) in CDCl₃

Acquisition Time (sec)	2.5166	Comment	Full Name - Joel Fonseca Room No. - 1.29 Sample - jdaf21_protons		
Date	01 Jun 2011 20:01:20	Date Stamp	01 Jun 2011 20:01:20		
File Name	F:\Leeds Spectra\jdaf21_protons\10\PDATA\1\1r	Frequency (MHz)	500.23	Nucleus	1H
Number of Transients	32	Origin	avance500	Original Points Count	16384
Points Count	32768	Pulse Sequence	zq30	Receiver Gain	456.10
Solvent	CHLOROFORM-d	Spectrum Offset (Hz)	2736.1270	SW(cyclical) (Hz)	6510.42
Sweep Width (Hz)	6510.22	Temperature (degree C)	24.200	Spectrum Type	STANDARD



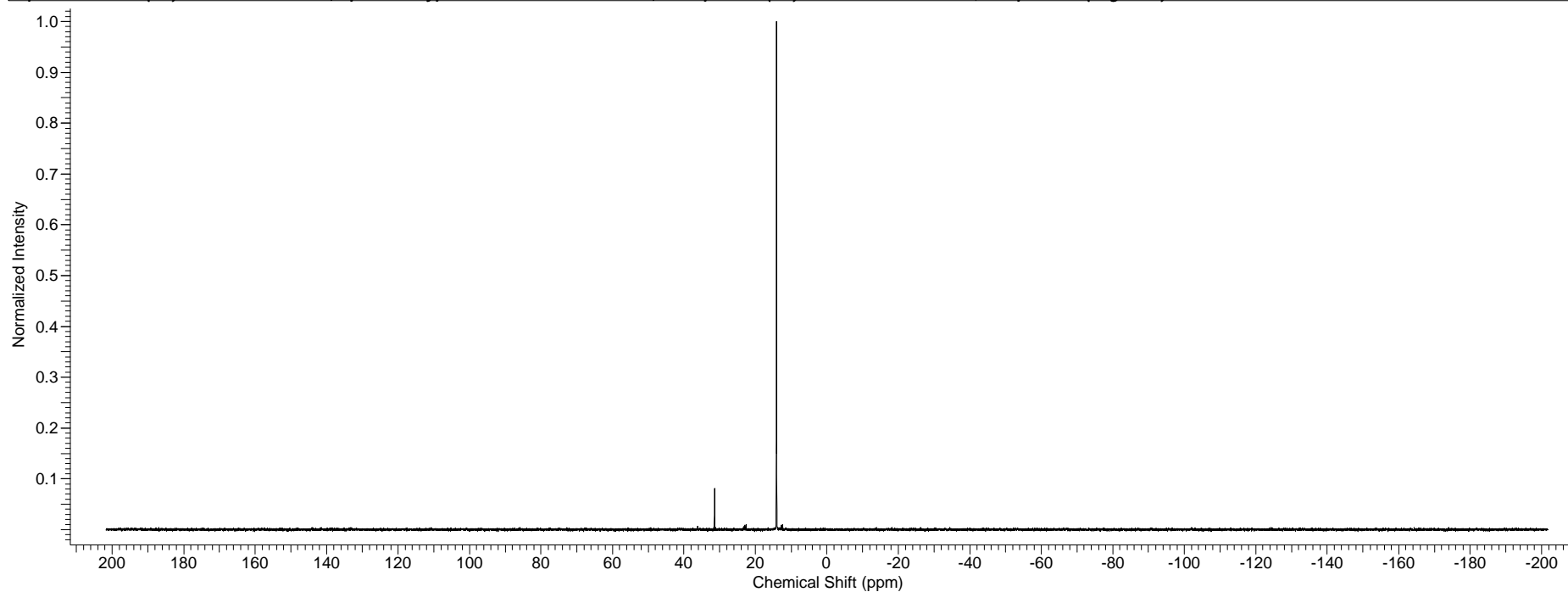
APPENDIX 9.1 – $^{13}\text{C}\{^1\text{H}\}$ NMR spectrum of $[\text{RuCl}(\text{P}(n\text{-Bu})_3)_2(p\text{-cymene})]\text{SbF}_6$ (9) in CDCl_3

Acquisition Time (sec)	0.6980	Comment	Name.- Joel Fonseca Room/Lab No.- 1.29 Sample.- JDAF 21 RuCl(C12 H27 P)2 C10 H14 NMR service		
Date	09 Jun 2011 19:16:32	Date Stamp	09 Jun 2011 19:16:32		
File Name	F:\Leeds Spectra\jdaf21.INO\10\PDATA\1\1r	Frequency (MHz)	125.76	Nucleus	^{13}C
Number of Transients	18432	Origin	drx500	Owner	gen
Points Count	131072	Pulse Sequence	zgpg30	Receiver Gain	9195.20
Solvent	CHLOROFORM-d	Spectrum Offset (Hz)	15058.1514	Spectrum Type	STANDARD
Temperature (degree C)	26.160	Sweep Width (Hz)	35211.00		



APPENDIX 9.2 – $^{31}\text{P}\{^1\text{H}\}$ NMR spectrum of $[\text{RuCl}(\text{P}(n\text{-Bu})_3)_2(p\text{-cymene})]\text{SbF}_6$ (9) in CDCl_3

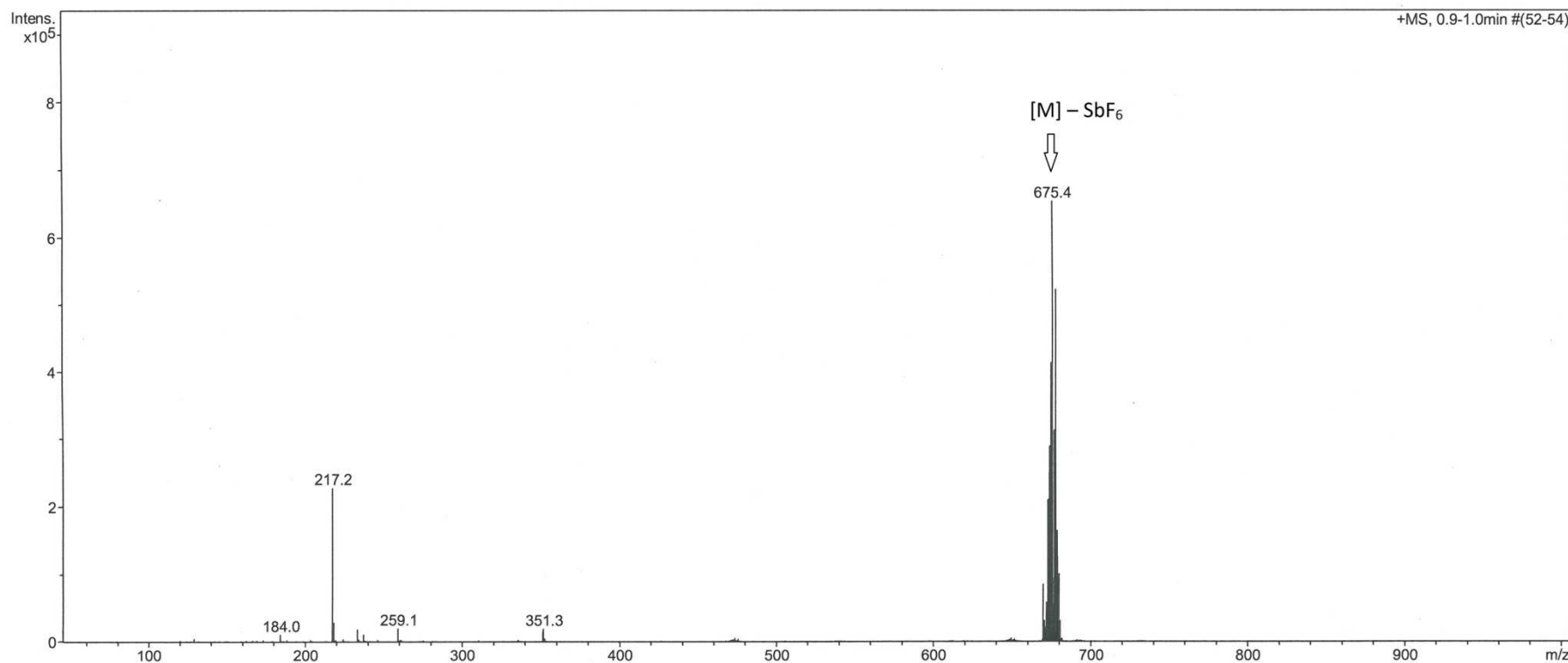
Acquisition Time (sec)	0.6685	Comment	Name- Joel Fonseca Room No- 1.29 Sample- jdaf21_31P	Date	03 Jun 2011 12:01:20		
Date Stamp	03 Jun 2011 12:01:20		File Name	F:\Leeds Spectra\jdaf21_31P\10\PDATA\1\1r			
Frequency (MHz)	121.49	Nucleus	31P	Number of Transients	160	Origin	spect
Original Points Count	32768	Owner	nmr	Points Count	65536	Pulse Sequence	zgpg30
Receiver Gain	2050.00	SW(cyclical) (Hz)	49019.61	Solvent	CHLOROFORM-d		
Spectrum Offset (Hz)	-0.0039	Spectrum Type	STANDARD	Sweep Width (Hz)	49018.86	Temperature (degree C)	26.933



APPENDIX 9.3 – Mass spectrum of $[\text{RuCl}(\text{P}(n\text{-Bu})_3)_2(p\text{-cymene})]\text{SbF}_6$ (9)

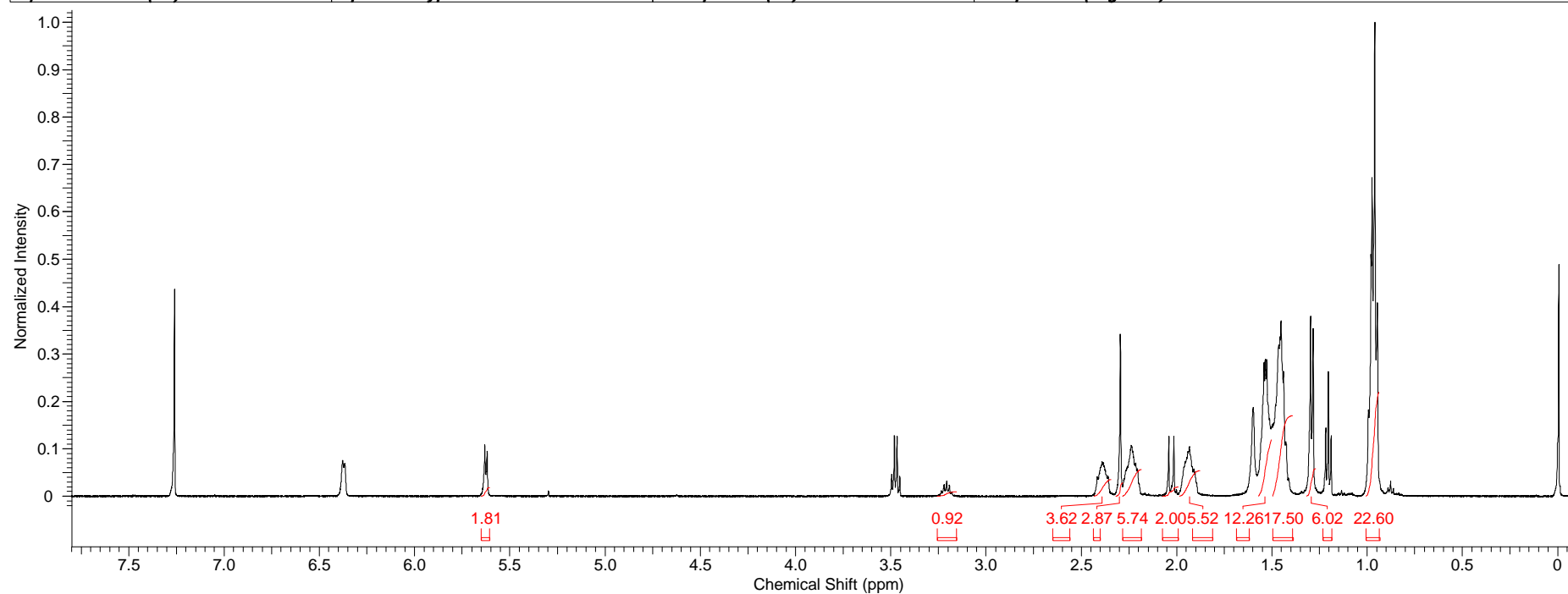
School of Chemistry Mass Spectrometry Service

Comment	jdaf-21	Operator	Tanya
Sample Name	114026	Acquisition Date	06/06/2011 14:43:42
Analysis Name	D:\Data\June2011\114026_1-C,3_01_13594.d		
Method	anneke 50-1000 lc.m		
Instrument	micrOTOF	Source Type	ESI
		Ion Polarity	Positive
		Scan Begin	50 m/z
		Scan End	1000 m/z



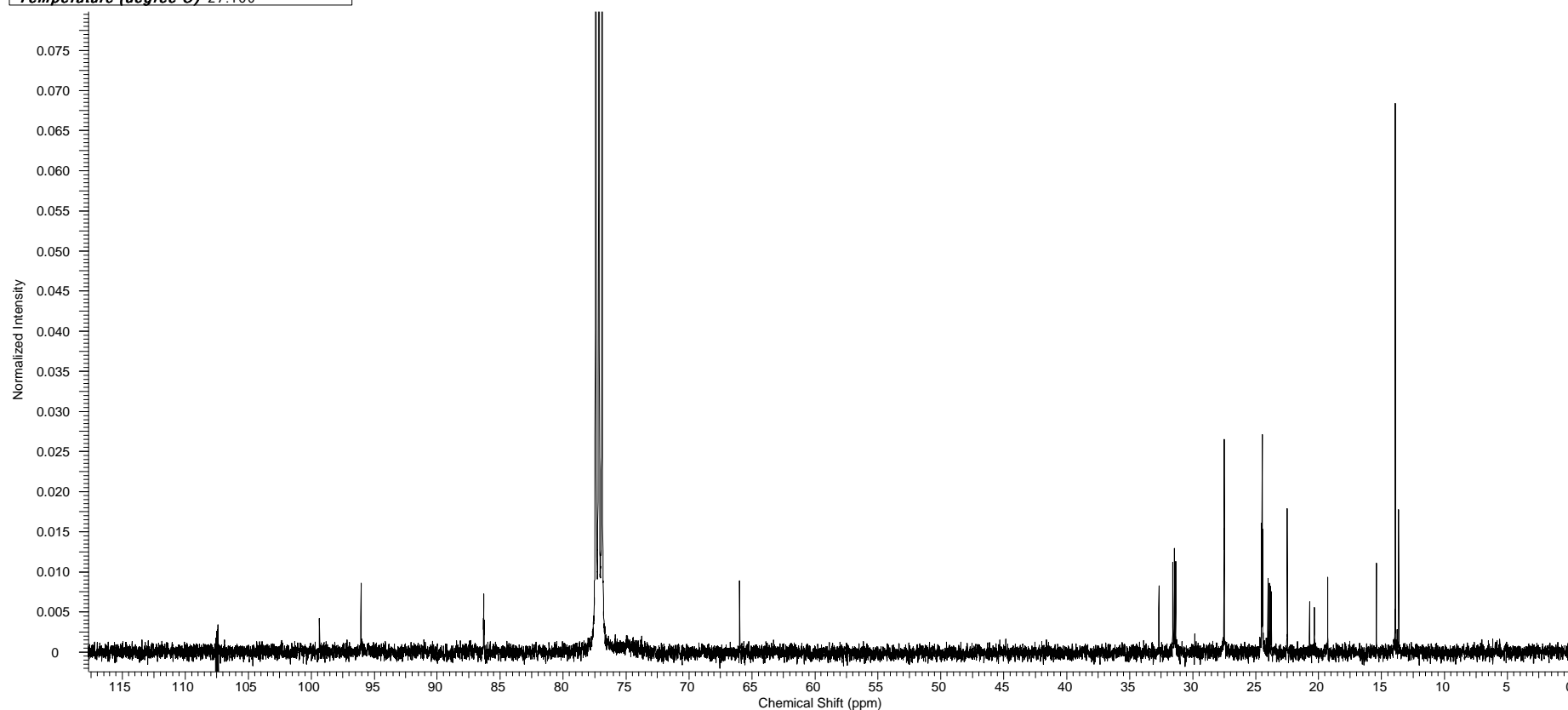
APPENDIX 10 – ¹H NMR spectrum of [Ru(P(*n*-Bu)₃)₂(*p*-cymene)]SbF₆ (10) in CDCl₃

Acquisition Time (sec)	2.5166	Comment	Full Name - Joel Fonseca Room No. - 1.29 Sample - jdaf24	Date	03 Jun 2011 14:07:12		
Date Stamp	03 Jun 2011 14:07:12	File Name	F:\Leeds Spectra\jdaf24\10\PDATA\1\1r				
Frequency (MHz)	500.23	Nucleus	1H	Number of Transients	32	Origin	avance500
Original Points Count	16384	Owner	nmr	Points Count	32768	Pulse Sequence	zg30
Receiver Gain	322.50	SW(cyclical) (Hz)	6510.42	Solvent	CHLOROFORM-d		
Spectrum Offset (Hz)	2734.7197	Spectrum Type	STANDARD	Sweep Width (Hz)	6510.22	Temperature (degree C)	25.400



APPENDIX 10.1 – $^{13}\text{C}\{^1\text{H}\}$ NMR spectrum of $[\text{Ru}(\text{P}(n\text{-Bu})_3)_2(p\text{-cymene})]\text{SbF}_6$ (10) in CDCl_3

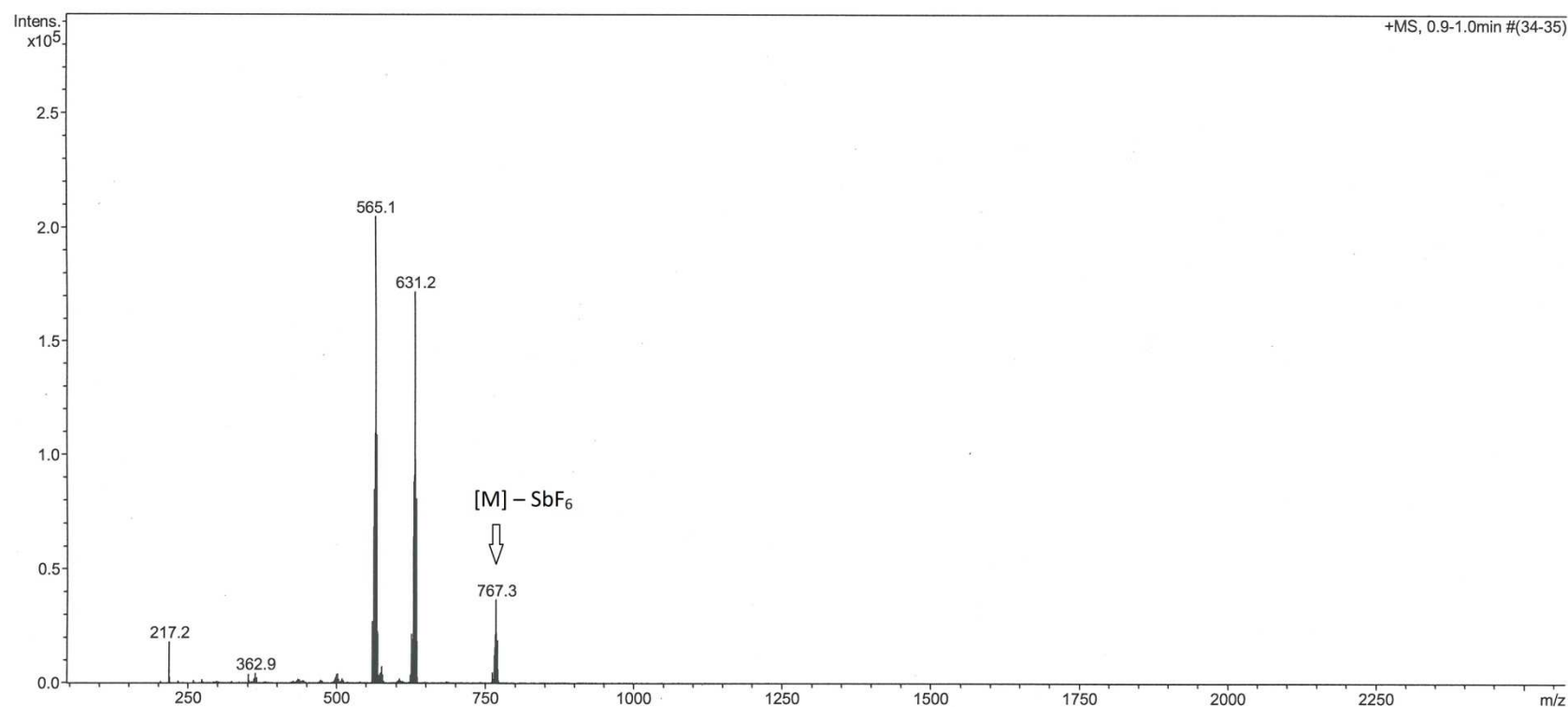
Acquisition Time (sec)	0.5603	Comment	Name.- Joel Fonseca Room/Lab No.- 1.29 Sample.- jdaf 24 Ru(C42 H27 P)2 C10H14 NMR service		
Date	08 Jun 2011 16:38:40	Date Stamp	08 Jun 2011 16:38:40		
File Name	F:\Leeds Spectra\jdaf24.INO\12\pdata\1\1r	Frequency (MHz)	125.76	Nucleus	^{13}C
Number of Transients	12288	Origin	drx500	Original Points Count	24576
Points Count	262144	Pulse Sequence	zgpg30	Receiver Gain	9195.20
Solvent	CHLOROFORM-d	Spectrum Offset (Hz)	15058.3525	Spectrum Type	STANDARD
Temperature (degree C)	27.160	Sweep Width (Hz)	43859.48		



APPENDIX 10.2 – Mass spectrum of [Ru(P(*n*-Bu)₃)₂(*p*-cymene)]SbF₆ (10)

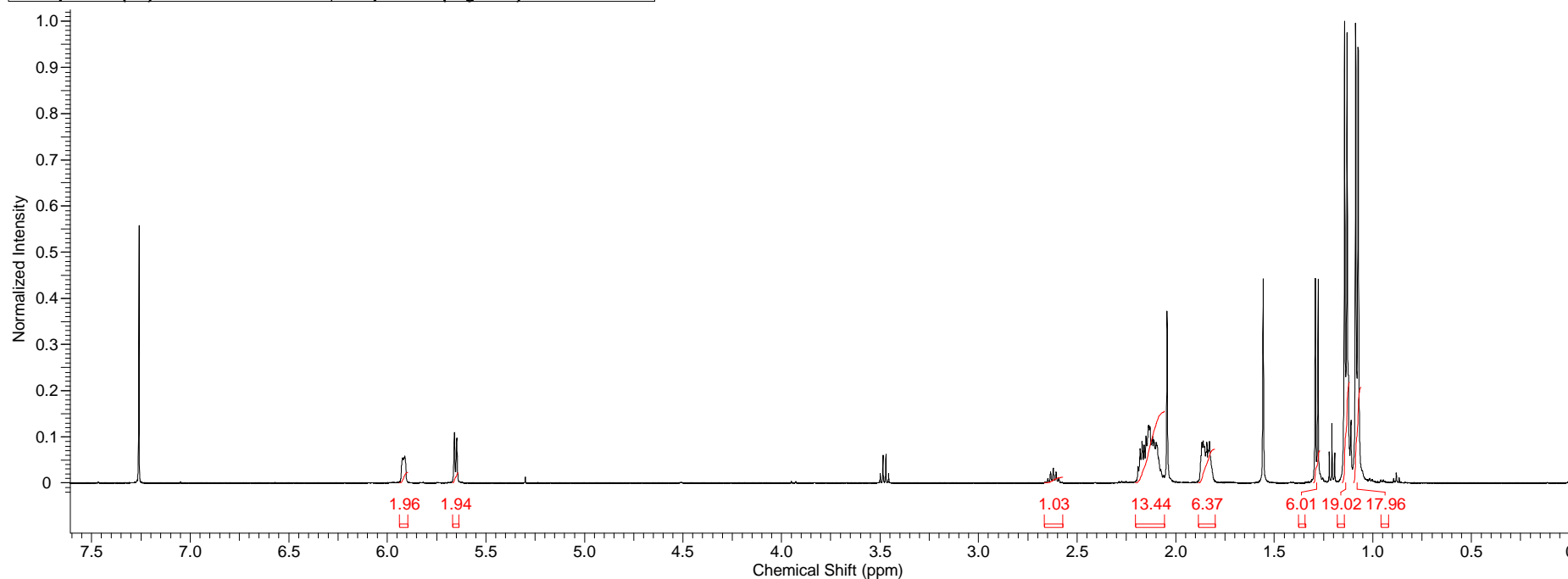
School of Chemistry Mass Spectrometry Service

Comment	jdaf-24	Operator	Tanya						
Sample Name	114044	Acquisition Date	07/06/2011 16:04:18						
Analysis Name	D:\Data\June2011\114044_1-B,8_01_13623.d								
Method	steve 200-2500 lc.m								
Instrument	micrOTOF	Source Type	ESI	Ion Polarity	Positive	Scan Begin	50 m/z	Scan End	2500 m/z



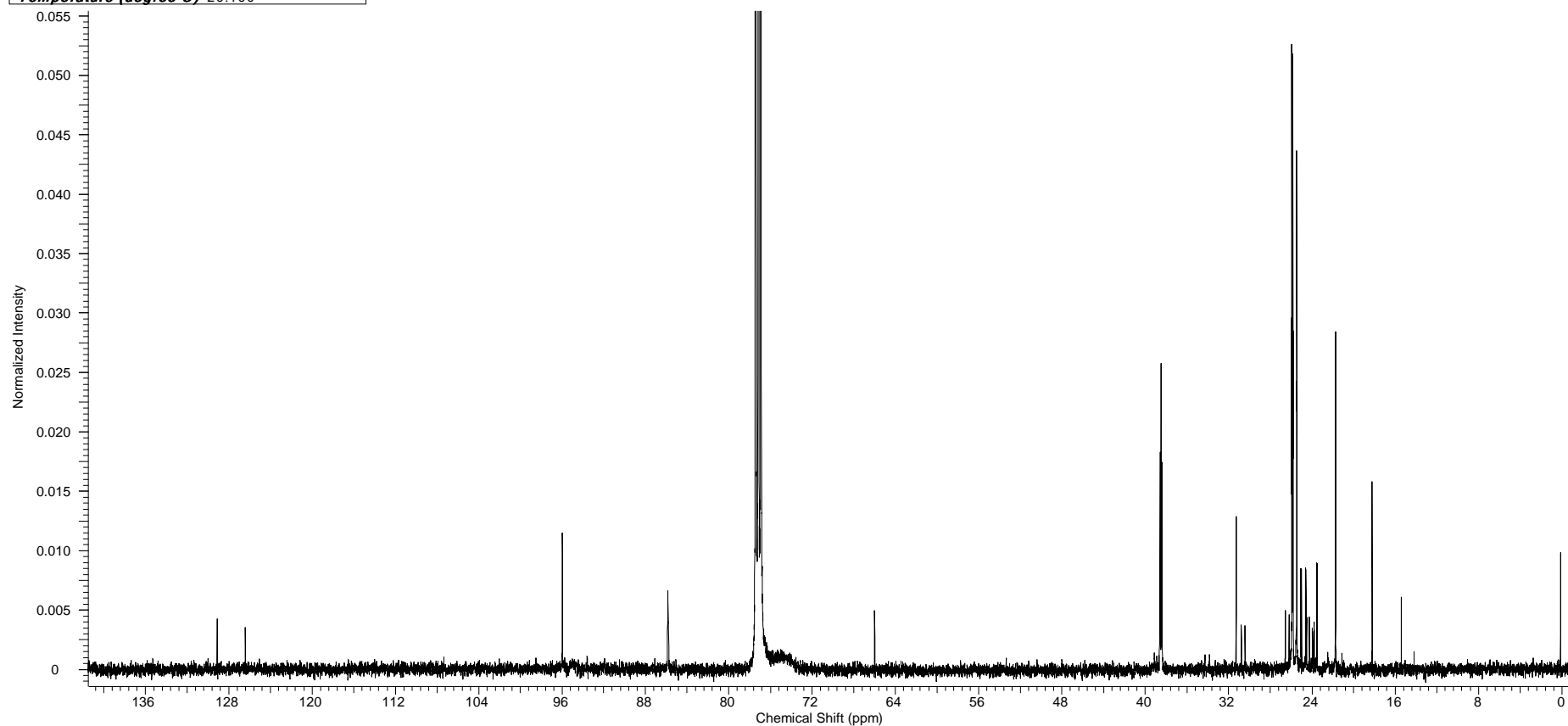
APPENDIX 11 – ¹H NMR spectrum of [RuCl(P(*i*-Bu)₃)₂(*p*-cymene)]SbF₆ (11) in CDCl₃

Acquisition Time (sec)	2.5166	Comment	Full Name - Joel Fonseca Room No. - 1.29 Sample - jdaf26.1		
Date	09 Jun 2011 11:20:48	Date Stamp	09 Jun 2011 11:20:48		
File Name	F:\Leeds Spectra\jdaf26.1\10\PDATA\1\1r	Frequency (MHz)	500.23	Nucleus	1H
Number of Transients	32	Origin	avance500	Original Points Count	16384
Points Count	32768	Pulse Sequence	zg30	Receiver Gain	322.50
Solvent	CHLOROFORM-d	Spectrum Offset (Hz)	2734.5210	SW(cyclical) (Hz)	6510.42
Sweep Width (Hz)	6510.22	Temperature (degree C)	25.200	Spectrum Type	STANDARD



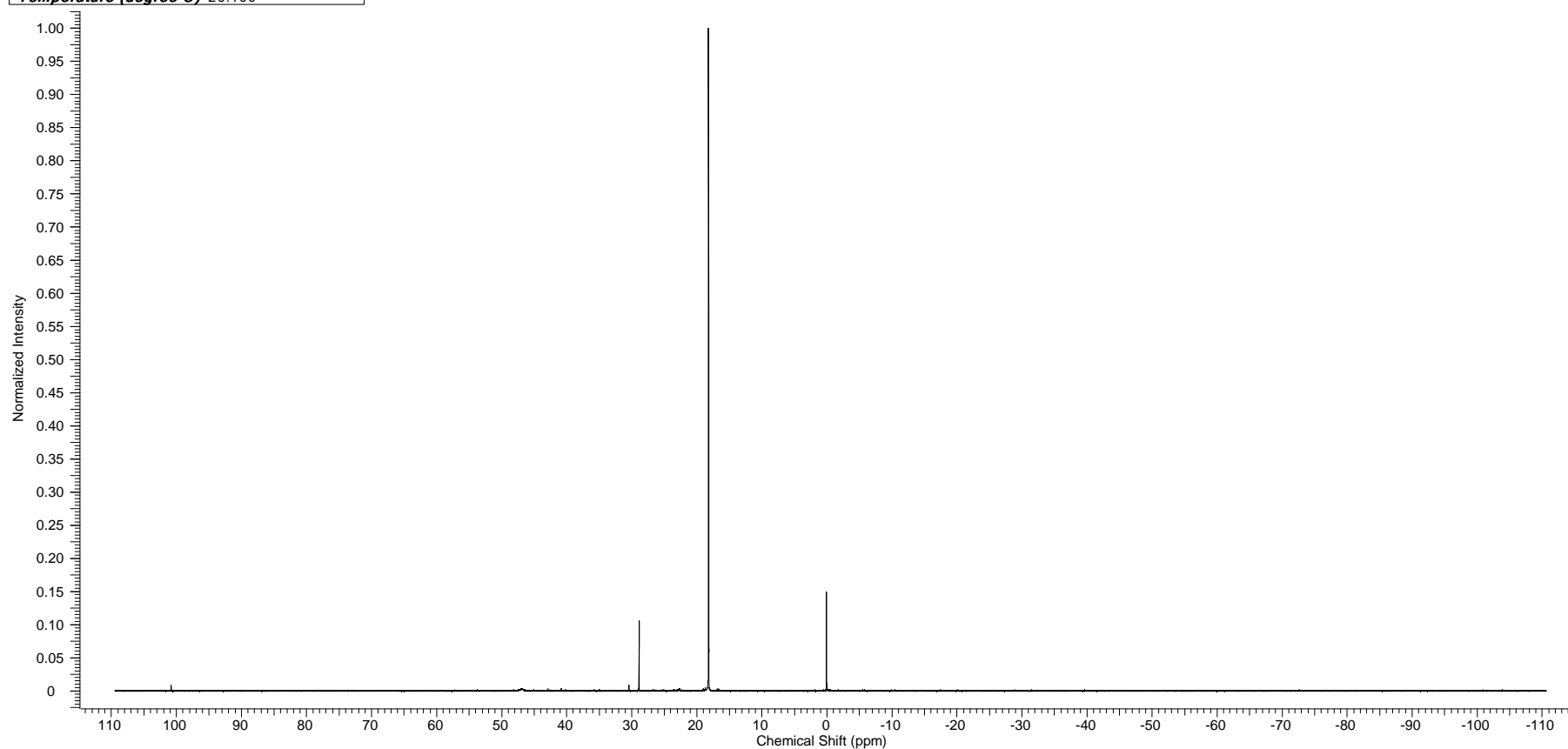
APPENDIX 11.1 – $^{13}\text{C}\{^1\text{H}\}$ NMR spectrum of $[\text{RuCl}(\text{P}(i\text{-Bu})_3)_2(p\text{-cymene})]\text{SbF}_6$ (11) in CDCl_3

Acquisition Time (sec)	0.6980	Comment	Name.- Joel Fonseca Room/Lab No.- 1.29 Sample.- JDAF 26.1 RuCl(C12 H27 P)2 C10 H14 SbF6 NMR service		
Date	12 Jun 2011 02:44:32	Date Stamp	12 Jun 2011 02:44:32		
File Name	F:\Leeds Spectra\jdaf26_1.INO\10 (jdaf26.1_13C NMR)\pdata\1\1r	Frequency (MHz)	125.76	Nucleus	13C
Number of Transients	24576	Origin	drx500	Original Points Count	24576
Points Count	131072	Pulse Sequence	zgpg30	Receiver Gain	9195.20
Solvent	CHLOROFORM-d	Spectrum Offset (Hz)	15058.4199	Spectrum Type	STANDARD
Temperature (degree C)	26.160			SW(cyclical) (Hz)	35211.27
				Sweep Width (Hz)	35211.00



APPENDIX 11.2 – $^{31}\text{P}\{^1\text{H}\}$ NMR spectrum of $[\text{RuCl}(\text{P}(i\text{-Bu})_3)_2(p\text{-cymene})]\text{SbF}_6$ (11) in CDCl_3

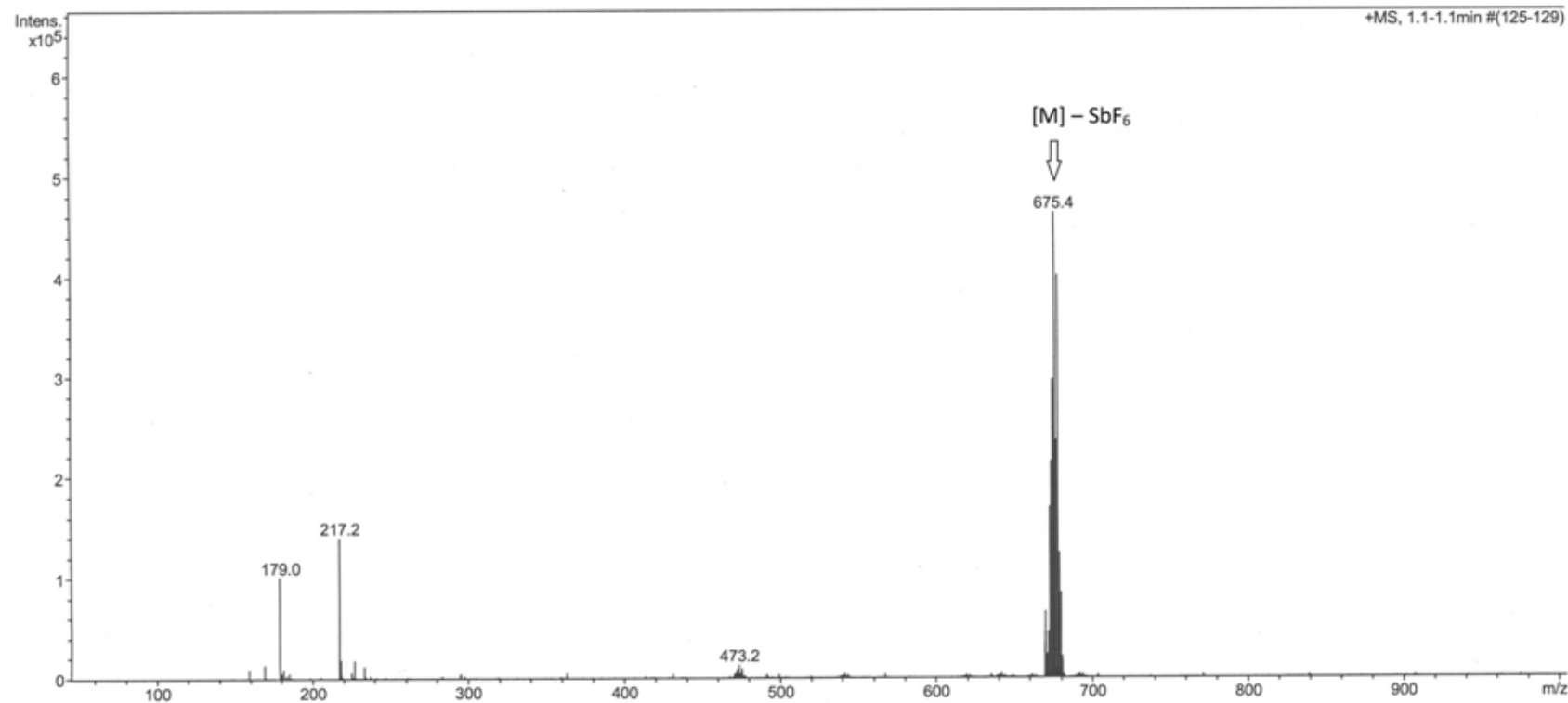
Acquisition Time (sec)	0.7356	Comment	Name.- Joel Fonseca Room/Lab No.- 1.29 Sample.- JDAF 26.1 RuCl(C12 H27 P)2 C10 H14 SbF6 NMR service		
Date	13 Jun 2011 06:15:44	Date Stamp	13 Jun 2011 06:15:44		
File Name	F:\Leeds Spectra\jdaf26_1.INO\12 (jdaf26.1_31P)\pdata\111r	Frequency (MHz)	202.46	Nucleus	31P
Number of Transients	8192	Origin	drx500	Original Points Count	32768
Points Count	65536	Pulse Sequence	zgpg30	Receiver Gain	11585.20
Solvent	CHLOROFORM-d	Spectrum Offset (Hz)	-116.1026	Spectrum Type	STANDARD
Temperature (degree C)	26.160	Sweep Width (Hz)	44542.75		



APPENDIX 11.3 – Mass spectrum of $[\text{RuCl}(\text{P}(i\text{-Bu})_3)_2(p\text{-cymene})]\text{SbF}_6$ (11)

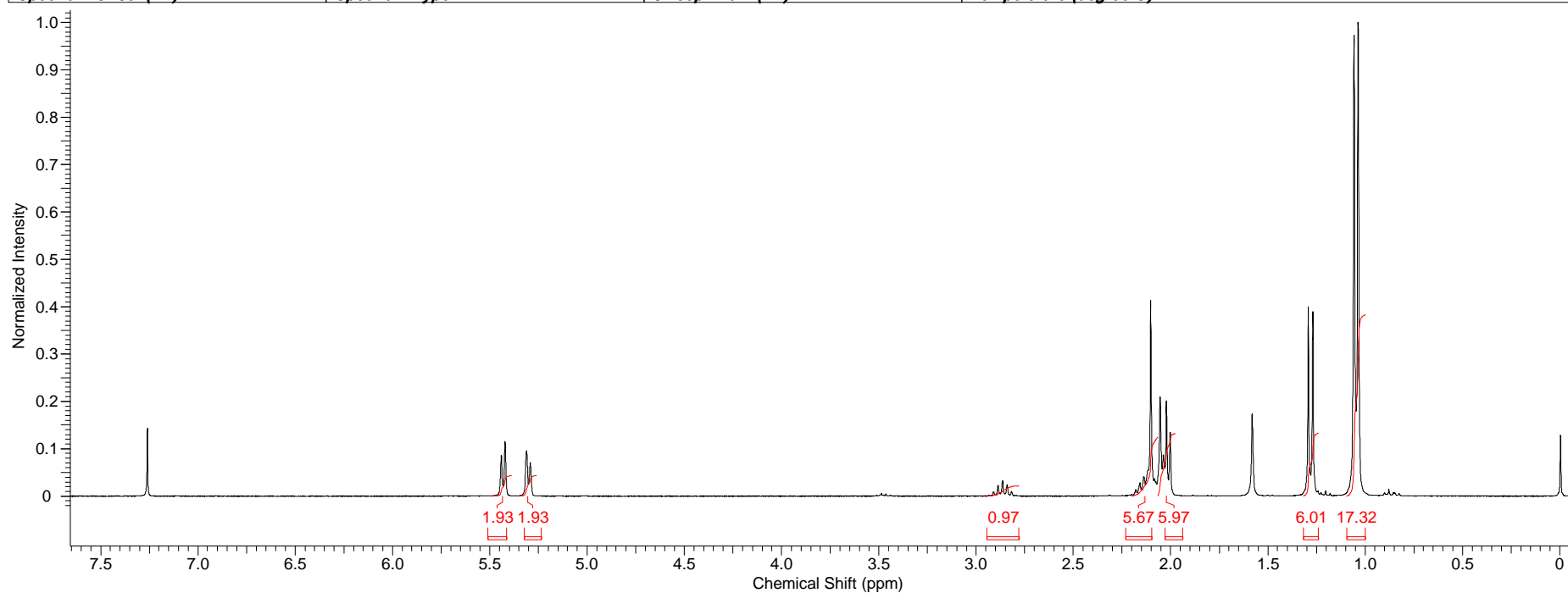
School of Chemistry Mass Spectrometry Service

Comment	jdaf-26.1	Operator	Tanya
Sample Name	114143	Acquisition Date	17/06/2011 14:57:06
Analysis Name	D:\Data\June2011\114143.d		
Method	Anneke 50-1000 syringe.m		
Instrument	micrOTOF	Source Type	ESI
		Ion Polarity	Positive
		Scan Begin	50 m/z
		Scan End	1000 m/z



APPENDIX 12 – ¹H NMR spectrum of [RuCl₂P(*i*-Bu)₃(*p*-cymene)] (12) in CDCl₃

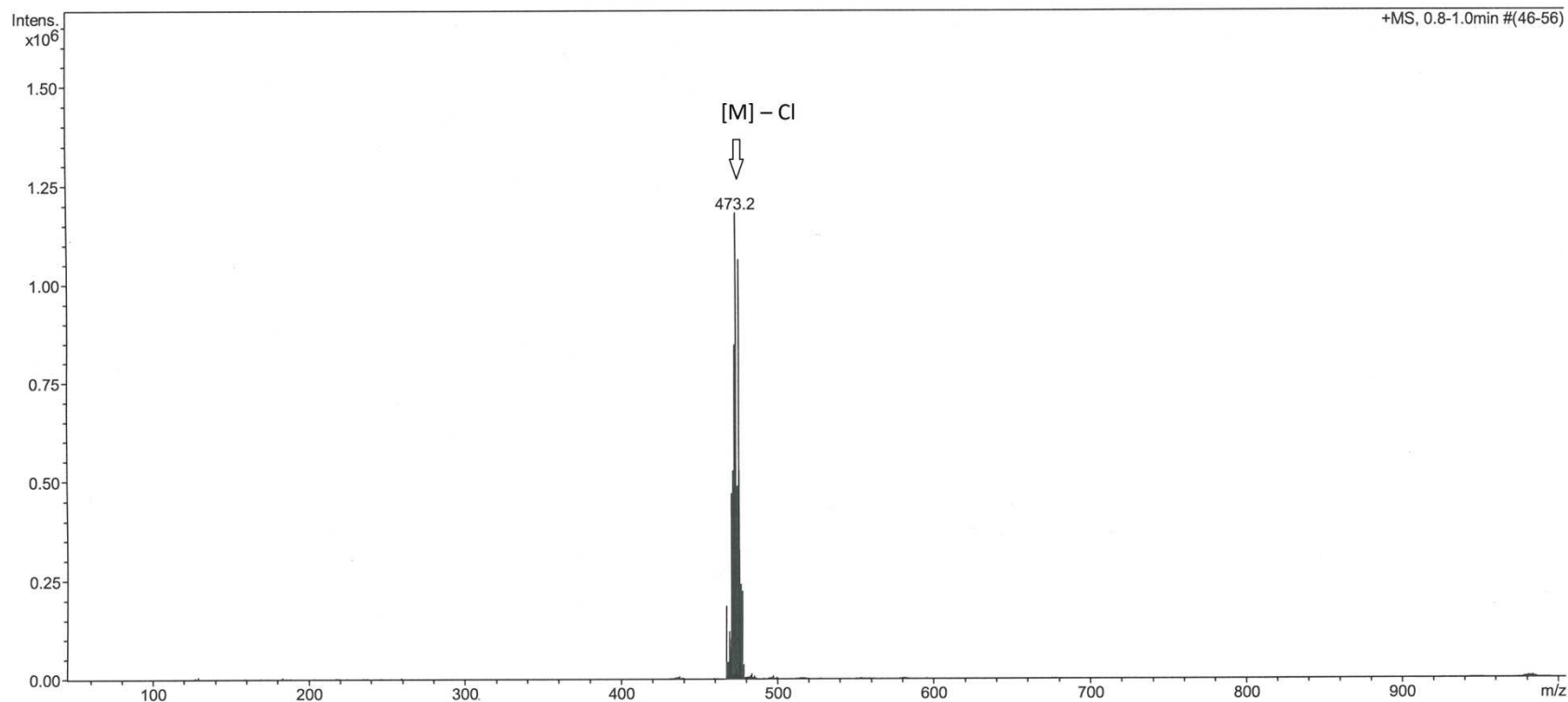
Acquisition Time (sec)	5.2953	Comment	Name- Joel Fonseca Room No- 1.29 Sample- jdaf27pp	Date	15 Jun 2011 17:14:56		
Date Stamp	15 Jun 2011 17:14:56	File Name	F:\Leeds Spectra\jdaf27pp\10\PDATA\1\1r				
Frequency (MHz)	300.13	Nucleus	1H	Number of Transients	32	Origin	spect
Original Points Count	32768	Owner	nmr	Points Count	65536	Pulse Sequence	zg30
Receiver Gain	228.00	SW(cyclical) (Hz)	6188.12	Solvent	CHLOROFORM-d		
Spectrum Offset (Hz)	1847.1880	Spectrum Type	STANDARD	Sweep Width (Hz)	6188.02	Temperature (degree C)	26.875



APPENDIX 12.1 – Mass spectrum of [RuCl₂P(*i*-Bu)₃(*p*-cymene)] (12)

School of Chemistry Mass Spectrometry Service

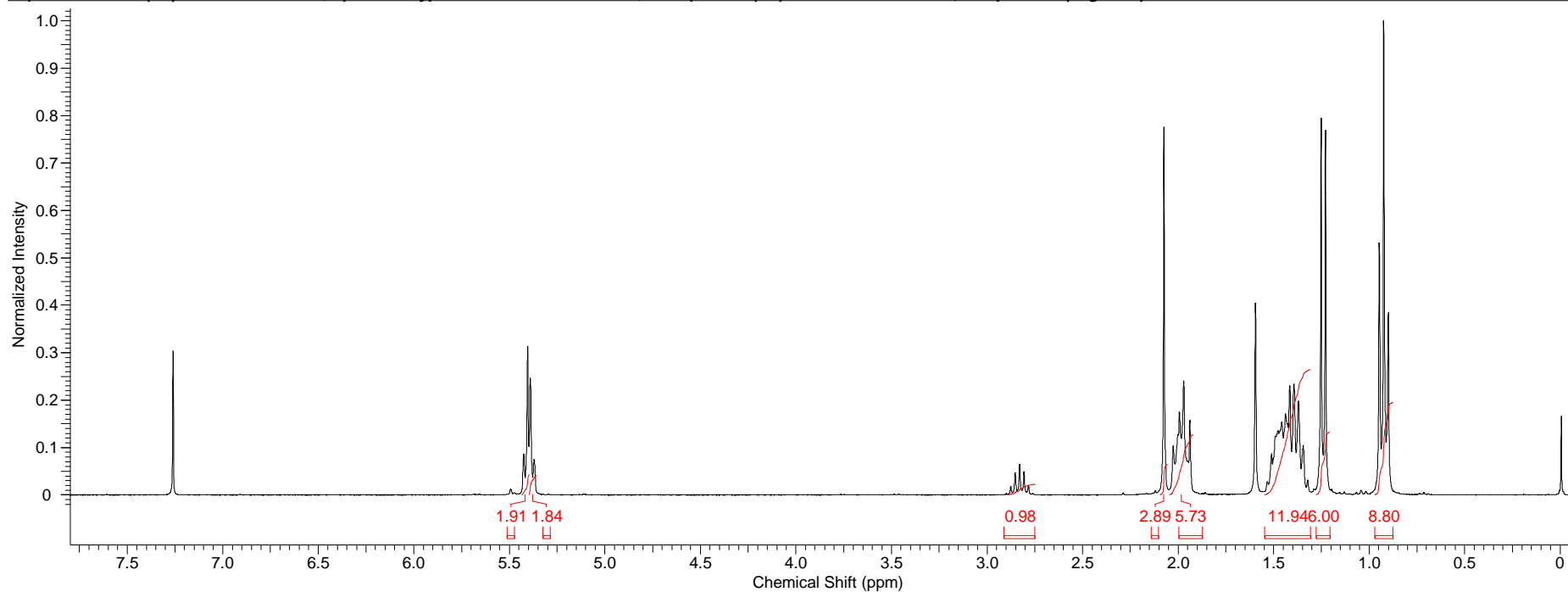
Comment	jda-27 /1 step	Operator	Tanya
Sample Name	114169	Acquisition Date	20/06/2011 17:31:07
Analysis Name	D:\Data\June2011\114169_1-B,8_01_13779.d		
Method	anneke 50-1000 lc.m		
Instrument	micrOTOF	Source Type	ESI
		Ion Polarity	Positive
		Scan Begin	50 m/z
		Scan End	1000 m/z



mm

APPENDIX 13 – ¹H NMR spectrum of [RuCl₂P(*n*-Bu)₃(*p*-cymene)] (13) in CDCl₃

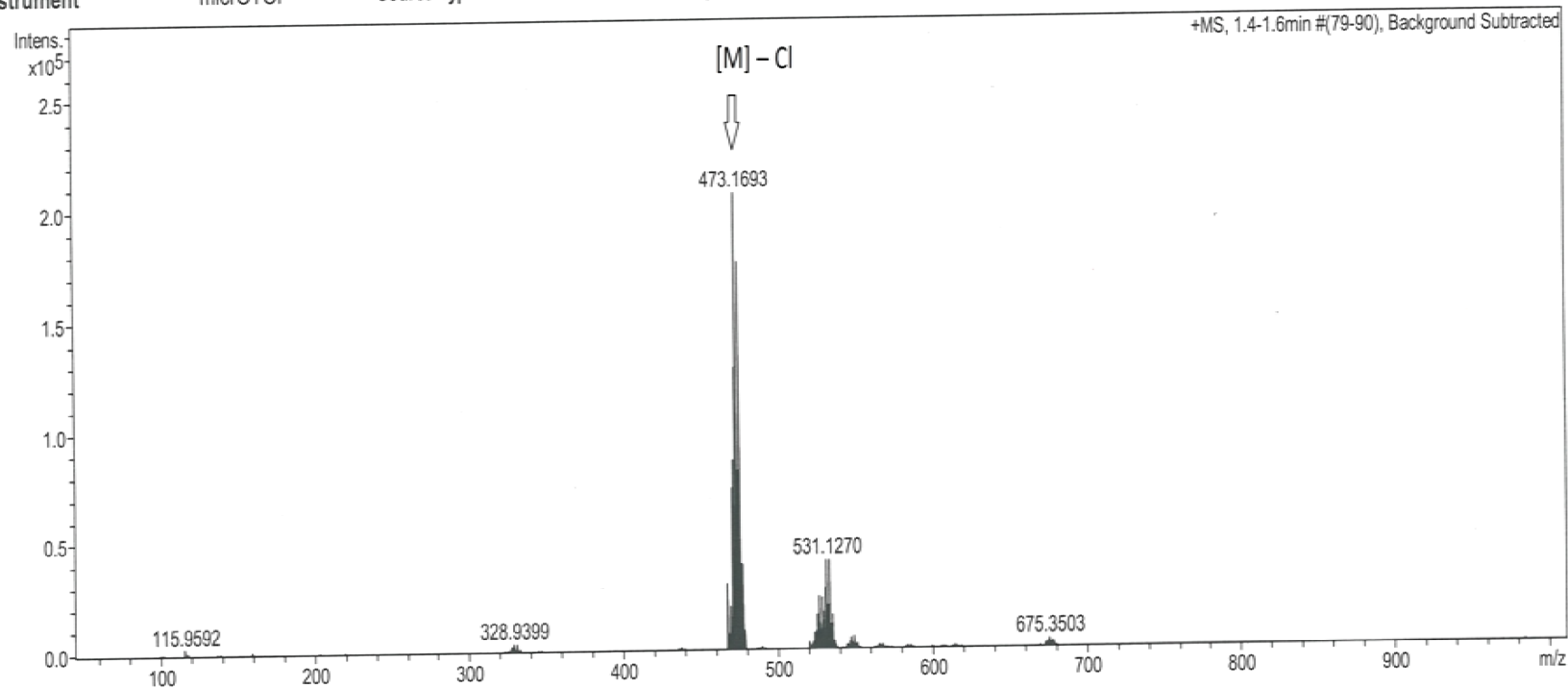
Acquisition Time (sec)	5.2953	Comment	Name- Joel Fonseca Room No- 1.29 Sample- jdaf33	Date	24 Jun 2011 17:25:36		
Date Stamp	24 Jun 2011 17:25:36		File Name	F:\Leeds Spectra\jdaf33\10\PDATA\1\1r			
Frequency (MHz)	300.13	Nucleus	1H	Number of Transients	32	Origin	spect
Original Points Count	32768	Owner	nmr	Points Count	65536	Pulse Sequence	zg30
Receiver Gain	228.00	SW(cyclical) (Hz)	6188.12	Solvent	CHLOROFORM-d		
Spectrum Offset (Hz)	1847.2825	Spectrum Type	STANDARD	Sweep Width (Hz)	6188.02	Temperature (degree C)	27.109



APPENDIX 13.1 – Mass spectrum of $[\text{RuCl}_2\text{P}(n\text{-Bu})_3(p\text{-cymene})]$ (13)

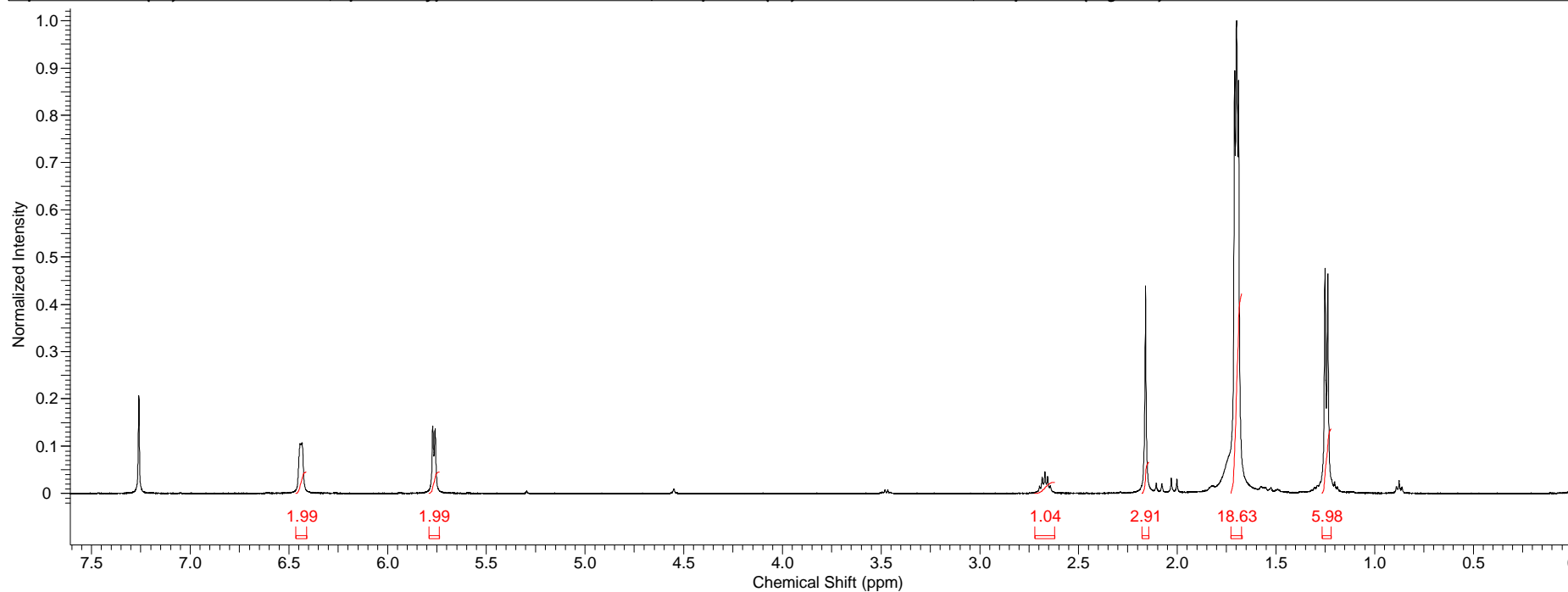
School of Chemistry Mass Spectrometry Service

Comment		Operator	Tanya						
Sample Name	jdaf33_37913	Acquisition Date	10/07/2011 15:48:02						
Analysis Name	D:\Data\stuartwarriner\chmslw\jdaf33_37913_1-D,7_01_13955.d								
Method	xxx.m								
Instrument	micrOTOF	Source Type	ESI	Ion Polarity	Positive	Scan Begin	50 m/z	Scan End	1000 m/z



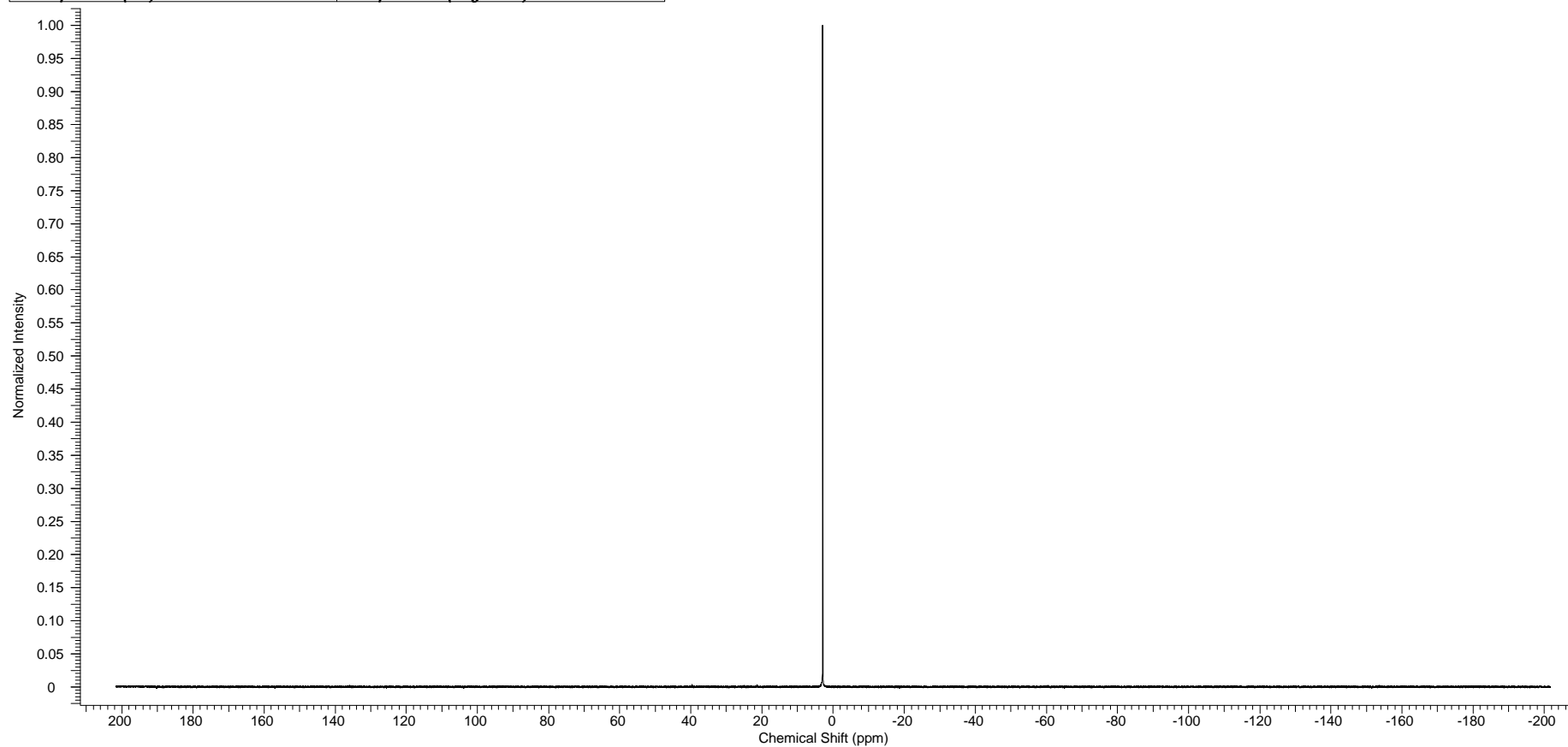
APPENDIX 14 – ¹H NMR spectrum of [RuCl(P(CH₃)₃)₂(*p*-cymene)]SbF₆ (14) in CDCl₃

Acquisition Time (sec)	2.5166	Comment	Full Name - Joel Fonseca Room No. - 1.29 Sample - jdaf28	Date	17 Jun 2011 15:28:16		
Date Stamp	17 Jun 2011 15:28:16		File Name	F:\Leeds Spectra\jdaf28\10\PDATA\1\1r			
Frequency (MHz)	500.23	Nucleus	1H	Number of Transients	32	Origin	avance500
Original Points Count	16384	Owner	nmr	Points Count	32768	Pulse Sequence	zg30
Receiver Gain	256.00	SW(cyclical) (Hz)	6510.42	Solvent	CHLOROFORM-d		
Spectrum Offset (Hz)	2734.1233	Spectrum Type	STANDARD	Sweep Width (Hz)	6510.22	Temperature (degree C)	25.500



APPENDIX 14.1 – $^{31}\text{P}\{^1\text{H}\}$ NMR spectrum of $[\text{RuCl}(\text{P}(\text{CH}_3)_3)_2(\textit{p}\text{-cymene})]\text{SbF}_6$ (14) in CDCl_3

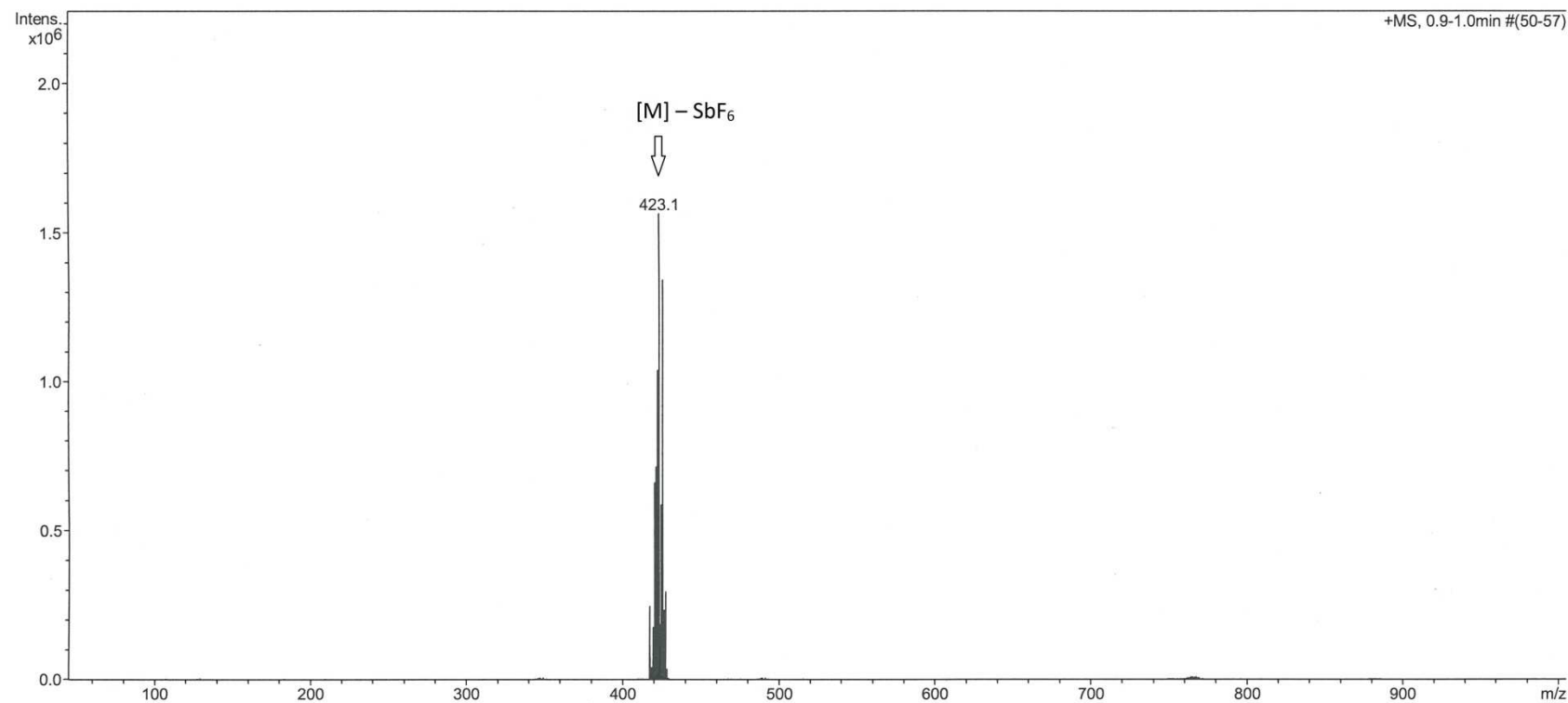
Acquisition Time (sec)	0.6685	Comment	Name- Joel Fonseca Room No- 1.29 Sample- jdaf28_new_31P		
Date	05 Aug 2011 12:12:00	Date Stamp	05 Aug 2011 12:12:00		
File Name	F:\Leeds Spectra\jdaf28_new_31P\10\PDATA\1\1r	Frequency (MHz)	121.49	Nucleus	31P
Number of Transients	160	Origin	spect	Original Points Count	32768
Points Count	65536	Pulse Sequence	zpgq30	Receiver Gain	2050.00
Solvent	CHLOROFORM-d	Spectrum Offset (Hz)	-0.0039	SW(cyclical) (Hz)	49019.61
Sweep Width (Hz)	49018.86	Temperature (degree C)	27.021	Spectrum Type	STANDARD



APPENDIX 14.2 – Mass spectrum of [RuCl(P(CH₃)₃)₂(*p*-cymene)]SbF₆ (14)

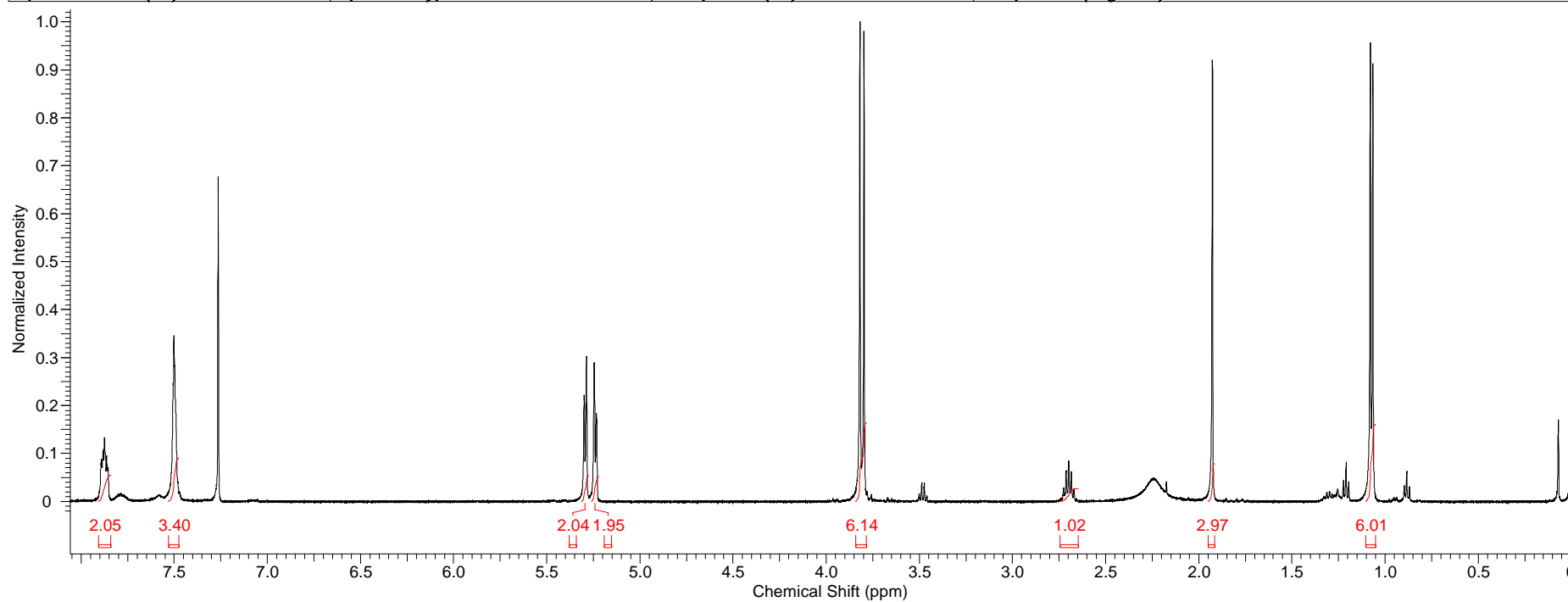
School of Chemistry Mass Spectrometry Service

Comment	jda-28	Operator	Tanya
Sample Name	114167	Acquisition Date	20/06/2011 17:12:58
Analysis Name	D:\Data\June2011\114167_1-B,6_01_13777.d		
Method	anneke 50-1000 lc.m		
Instrument	micrOTOF	Source Type	ESI
		Ion Polarity	Positive
		Scan Begin	50 m/z
		Scan End	1000 m/z



APPENDIX 15 – ¹H NMR spectrum of [RuCl₂PhP(OCH₃)₂(*p*-cymene)] (15) in CDCl₃

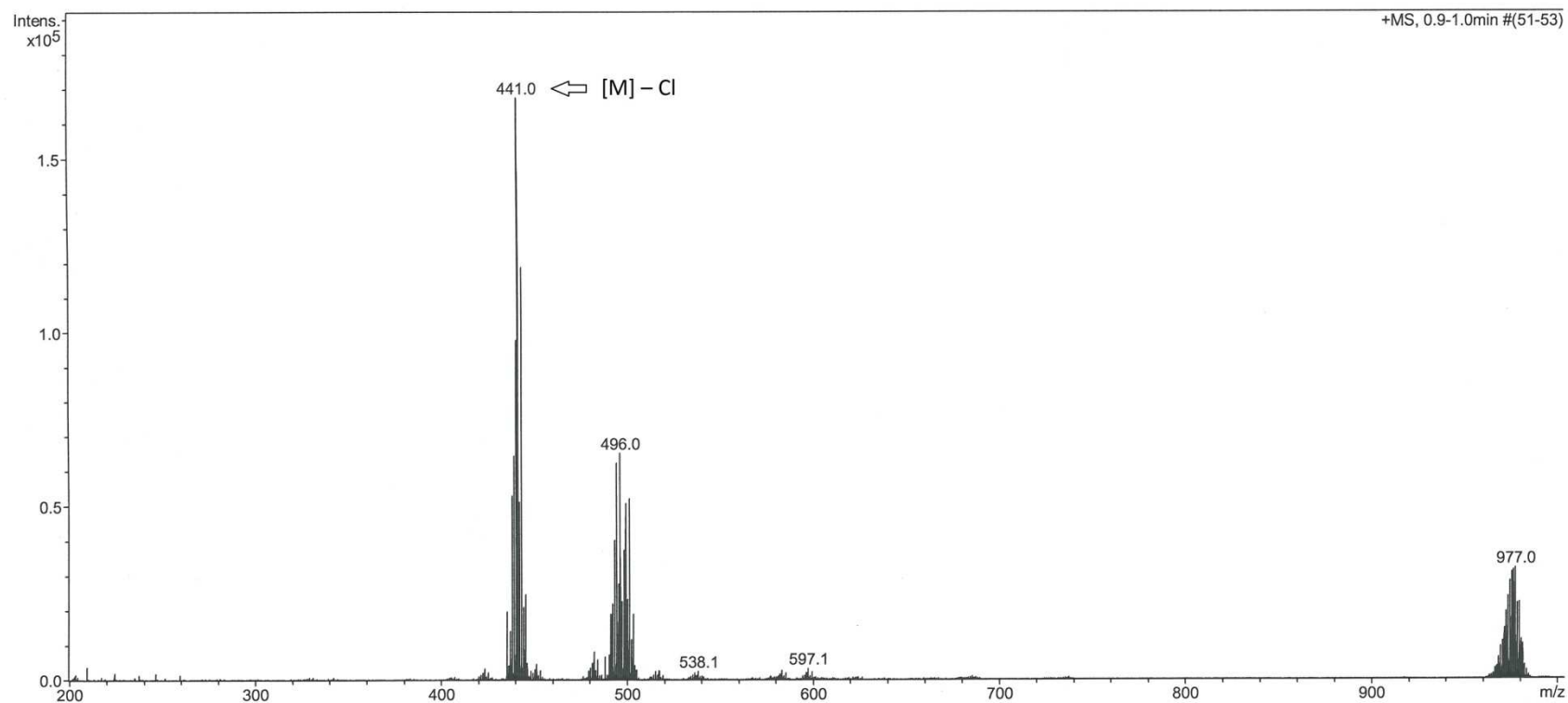
Acquisition Time (sec)	2.5166	Comment	Full Name - Joel Fonseca Room No. - 1.29 Sample - jdaf30	Date	17 Jun 2011 15:17:36		
Date Stamp	17 Jun 2011 15:17:36		File Name	F:\Leeds Spectra\jdaf30\10\PDATA\1\1r			
Frequency (MHz)	500.23	Nucleus	1H	Number of Transients	32	Origin	avance500
Original Points Count	16384	Owner	nmr	Points Count	32768	Pulse Sequence	zg30
Receiver Gain	574.70	SW(cyclical) (Hz)	6510.42	Solvent	CHLOROFORM-d		
Spectrum Offset (Hz)	2736.2866	Spectrum Type	STANDARD	Sweep Width (Hz)	6510.22	Temperature (degree C)	25.500



APPENDIX 15.1 – Mass spectrum of [RuCl₂PhP(OCH₃)₂(*p*-cymene)] (15)

School of Chemistry Mass Spectrometry Service

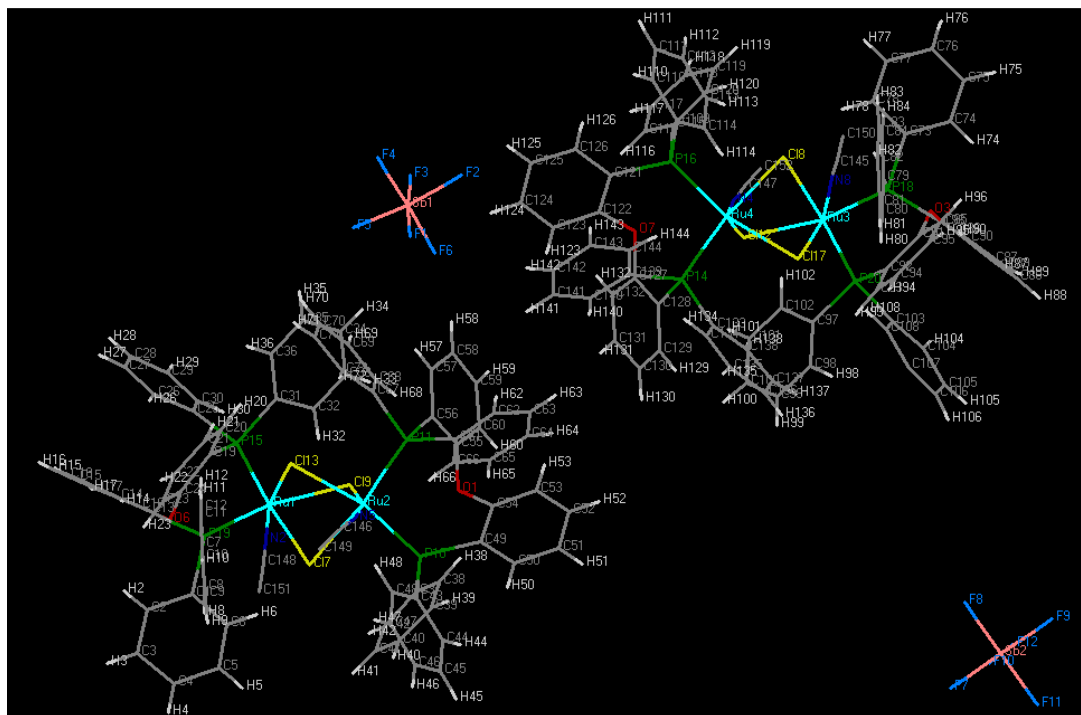
Comment	jda-30	Operator	Tanya						
Sample Name	114168	Acquisition Date	20/06/2011 17:18:06						
Analysis Name	D:\Data\June2011\114168_1-B,7_01_13778.d								
Method	anneke 50-1000 lc.m								
Instrument	micrOTOF	Source Type	ESI	Ion Polarity	Positive	Scan Begin	50 m/z	Scan End	1000 m/z



APPENDIX 16 – [Ru₂Cl₃(DPEPhos)₂(CH₃CN)₂]SbF₆ (8) Crystal Data

Formula	C ₁₅₂ H ₁₁₁ Cl ₆ F ₁₂ N ₄ O ₄ P ₈ Ru ₄ Sb ₂	
Formula weight	3393.69	
Size	0.22 x 0.15 x 0.07 mm	
Crystal morphology	Brown Fragment	
Temperature	150(2) K	
Wavelength	0.71073 Å [Mo-K _α]	
Crystal system	Monoclinic	
Space group	P2 ₁ /c	
Unit cell dimensions	$a = 27.319(3) \text{ \AA}$	$\alpha = 90^\circ$
	$b = 18.239(2) \text{ \AA}$	$\beta = 96.207(6)^\circ$
	$c = 33.008(4) \text{ \AA}$	$\gamma = 90^\circ$
Volume	16351(3) Å ³	
Z	4	
Density (calculated)	1.379 Mg/m ³	
Absorption coefficient	0.925 mm ⁻¹	
F(000)	6764	
Data collection range	$1.34 \leq \theta \leq 30.34^\circ$	
Index ranges	$-38 \leq h \leq 35, -25 \leq k \leq 24, -43 \leq l \leq 46$	
Reflections collected	329686	
Independent reflections	48605 [$R(\text{int}) = 0.1824$]	
Observed reflections	19785 [$I > 2\sigma(I)$]	
Absorption correction	multi-scan	
Max. and min. transmission	0.9374 and 0.8195	
Refinement method	Full	
Data / restraints / parameters	48605 / 0 / 1720	
Goodness of fit	1.033	
Final <i>R</i> indices [$I > 2\sigma(I)$]	$R_1 = 0.1029, wR_2 = 0.2845$	
<i>R</i> indices (all data)	$R_1 = 0.2466, wR_2 = 0.375$	
Largest diff. peak and hole	5.371 and -2.638 e.Å ⁻³	

APPENDIX 17 – Labelled molecular structure of $[\text{Ru}_2\text{Cl}_3(\text{DPEPhos})_2(\text{CH}_3\text{CN})_2]\text{SbF}_6$ (8)

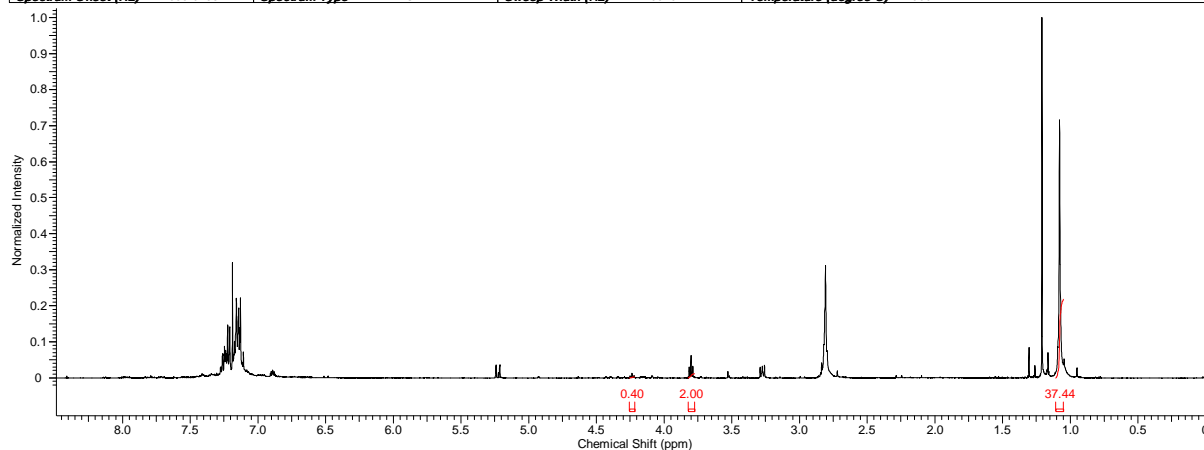


APPENDIX 18 – Selected Bond Lengths (Å) and Angles (deg) for $[\text{Ru}_2\text{Cl}_3(\text{DPEPhos})_2(\text{CH}_3\text{CN})_2]\text{SbF}_6$ (8) obtained by X-ray crystallography.

Bond Distances			
Ru(1)-P(15)	2.326(3)	Ru(1)-Cl(7)	2.513(2)
Ru(1)-P(19)	2.304(3)	Ru(1)-Cl(9)	2.520(2)
Ru(2)-P(10)	2.318(3)	Ru(1)-Cl(13)	2.428(3)
Ru(2)-P(11)	2.318(3)	Ru(2)-Cl(7)	2.492(2)
Ru(1)-N(2)	2.007(5)	Ru(2)-Cl(9)	2.418(2)
Ru(2)-N(5)	2.020(5)	Ru(2)-Cl(13)	2.497(2)
Bond Angles			
P(15)-Ru(1)-Cl(7)	174.74(9)	P(19)-Ru(1)-Cl(13)	98.81(9)
P(15)-Ru(1)-Cl(9)	97.07(8)	N(2)-Ru(1)-Cl(7)	94.05(14)
P(15)-Ru(1)-Cl(13)	95.25(9)	N(2)-Ru(1)-Cl(9)	89.89(14)
P(19)-Ru(1)-Cl(7)	86.07(8)	N(2)-Ru(1)-Cl(13)	168.56(14)
P(19)-Ru(1)-Cl(9)	165.97(9)		

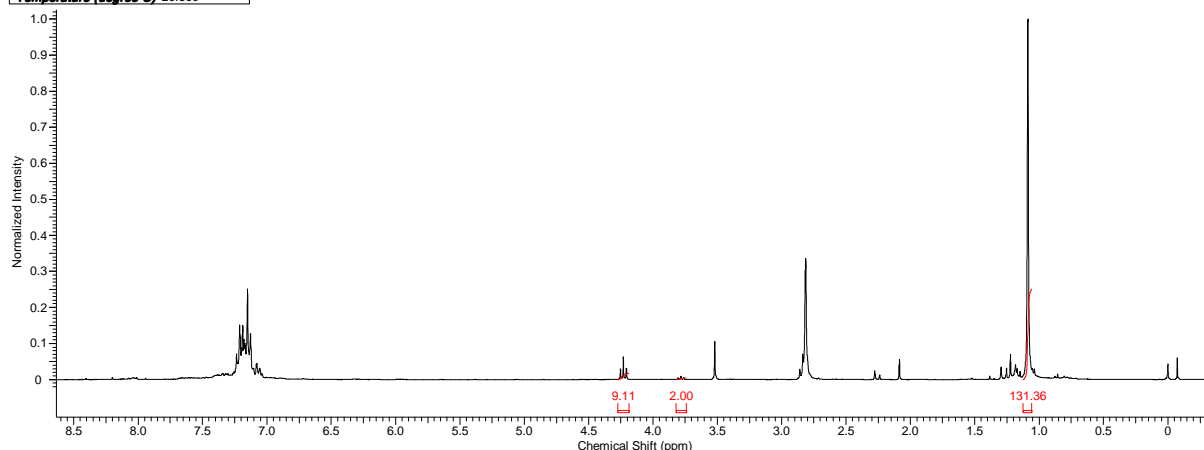
APPENDIX 19 – ¹H NMR spectrum of the product from the N-alkylation of *t*-butylamine using [RuCl₂(*p*-cymene)]₂ (1)-dppf as pre-catalyst (S/C=20), in CDCl₃

Acquisition Time (sec)	2.5166	Comment	Full Name Joel Fonseca Room No. 1.29 Sample idaf8.4	Date	02 Mar 2011 12:22:24		
Date Stamp	02 Mar 2011 12:22:24		File Name	F:\Leeds Spectra\idaf8.4\10\PDATA\111r			
Frequency (MHz)	500.23	Nucleus	¹ H	Number of Transients	32	Origin	avance500
Original Points Count	16384	Owner	nmr	Points Count	32768	Pulse Sequence	zg30
Receiver Gain	128.00	SW(cyclical) (Hz)	6510.42	Solvent	CHLOROFORM-d		
Spectrum Offset (Hz)	2699.6753	Spectrum Type	STANDARD	Sweep Width (Hz)	6510.22	Temperature (degree C)	27.000



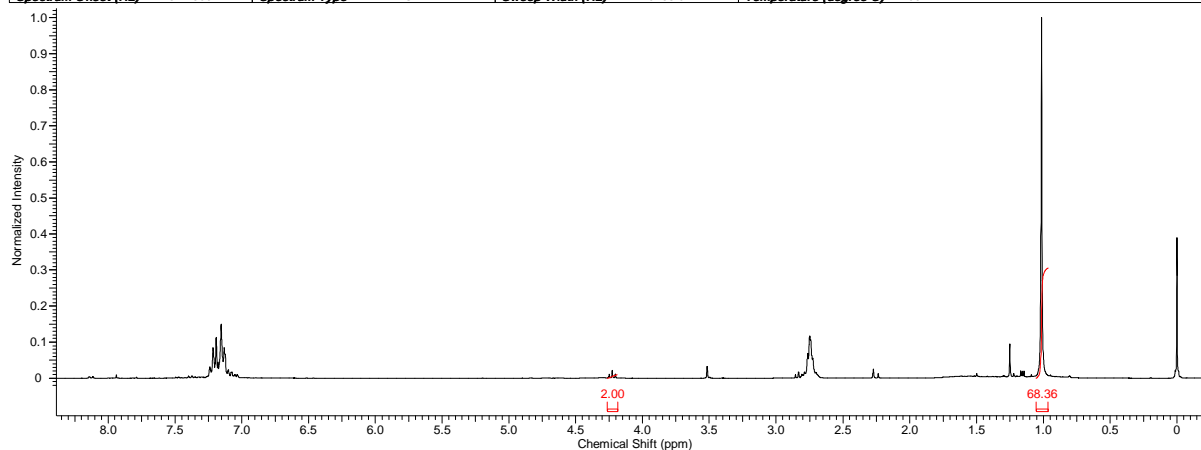
APPENDIX 20 – ¹H NMR spectrum of the product from the N-alkylation of *t*-butylamine using [RuCl₂(*p*-cymene)]₂ (1)-DPEPhos as pre-catalyst (S/C=20), in CDCl₃

Acquisition Time (sec)	5.2953	Comment	Name- Joel Fonseca Room No- 1.29 Sample- idaf23	Date	13 Jul 2011 12:26:56				
Date Stamp	13 Jul 2011 12:26:56		File Name	F:\Leeds Spectra\idaf23\10\PDATA\111r	Frequency (MHz)	300.13			
Nucleus	¹ H	Number of Transients	32	Origin	spect	Original Points Count	32768	Owner	nmr
Points Count	65536	Pulse Sequence	zg30	Receiver Gain	57.00	SW(cyclical) (Hz)	6188.12		
Solvent	CHLOROFORM-d	Spectrum Offset (Hz)	1822.6038	Spectrum Type	STANDARD	Sweep Width (Hz)	6188.02		
Temperature (degree C)	26.860								



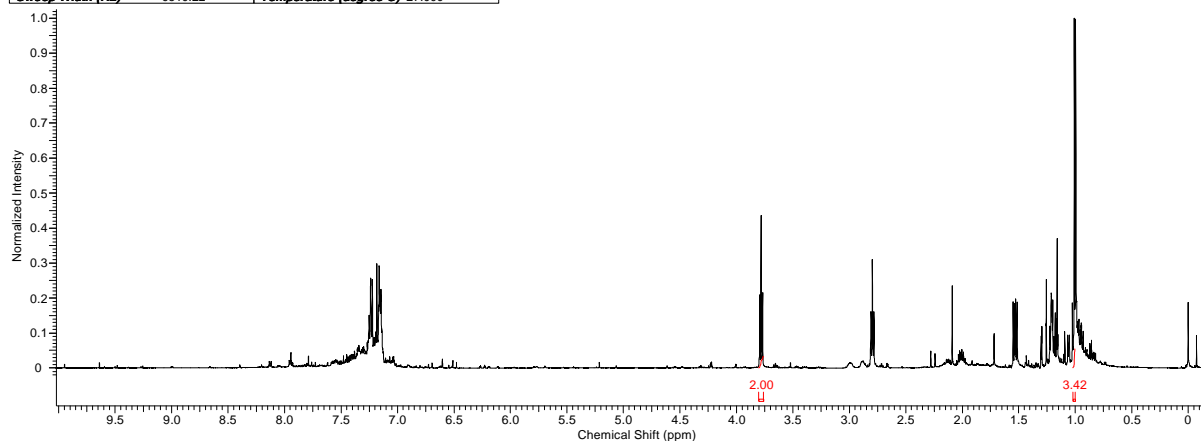
APPENDIX 21 – ¹H NMR spectrum of the product from the N-alkylation of *t*-butylamine using [RuCl₂(*p*-cymene)]₂ (1)-dippf as pre-catalyst (S/C=20), in CDCl₃

Acquisition Time (sec)	5.2953	Comment	Name- Joel Fonseca Room No- 1.29 Sample- idaf77	Date	05 Aug 2011 11:35:44
Date Stamp	05 Aug 2011 11:35:44	File Name	F:\Leeds Spectra\idaf77\idaf7710\PDATA\111r	Number of Transients	32
Frequency (MHz)	300.13	Nucleus	1H	Origin	spect
Original Points Count	32768	Owner	nmr	Points Count	65536
Receiver Gain	40.30	SW(cyclical) (Hz)	6188.12	Solvent	CHLOROFORM-d
Spectrum Offset (Hz)	1822.8661	Spectrum Type	STANDARD	Sweep Width (Hz)	6188.02
				Temperature (degree C)	27.037



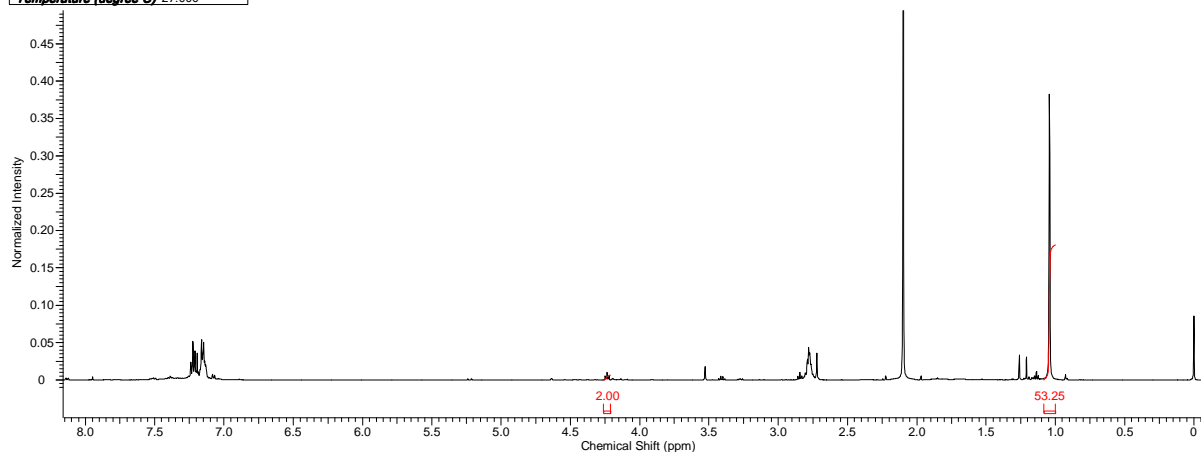
APPENDIX 22 – ¹H NMR spectrum of the product from the N-alkylation of *t*-butylamine using [RuCl₂(*p*-cymene)]₂ (1)-P(*i*-Bu)₃ as pre-catalyst (S/C=20), in CDCl₃

Acquisition Time (sec)	2.5166	Comment	Full Name - Joel Fonseca Room No. - 1.29 Sample - idaf42	Date Stamp	04 Jul 2011 12:56:48
Date	04 Jul 2011 12:56:48	File Name	F:\Leeds Spectra\idaf42\10\PDATA\111r	Frequency (MHz)	500.23
File Name	F:\Leeds Spectra\idaf42\10\PDATA\111r	Nucleus	1H	Number of Transients	32
Number of Transients	32	Origin	avance500	Original Points Count	16384
Points Count	32768	Pulse Sequence	zg30	Receiver Gain	28.50
Solvent	CHLOROFORM-d	SW(cyclical) (Hz)	6510.42	Spectrum Offset (Hz)	2695.7134
Sweep Width (Hz)	6510.22	Spectrum Type	STANDARD	Temperature (degree C)	27.000



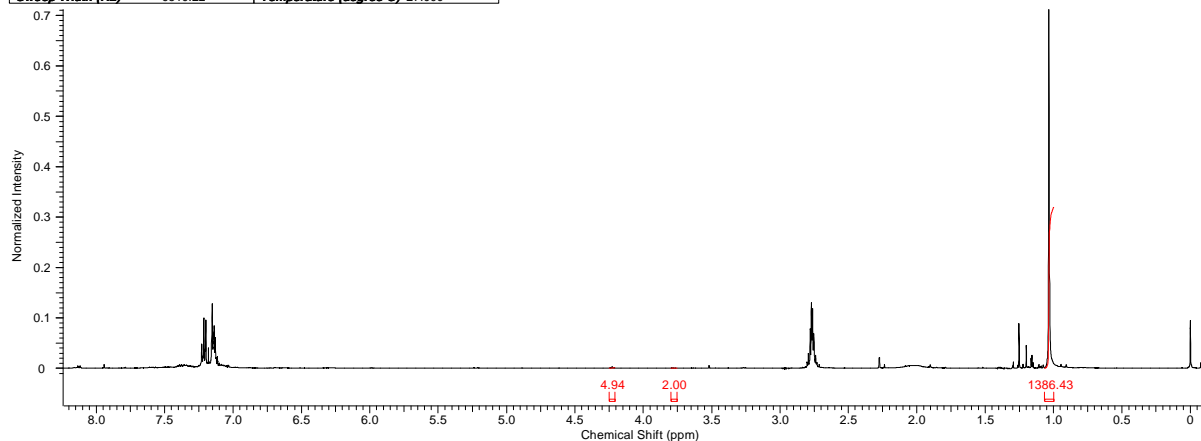
APPENDIX 23 – ¹H NMR spectrum of the product from the N-alkylation of *t*-butylamine using [RuI₂(*p*-cymene)]₂ (2)-dppf as pre-catalyst (S/C=20), in CDCl₃

Acquisition Time (sec)	1.1698	Comment	Full Name Joel Fonseca Room No. 1.29 Sample jdaf9	Date	13 Jan 2011 10:35:44						
Date Stamp	13 Jan 2011 10:35:44	File Name	F:\Leeds Spectra\jdaf9\10\fid	Frequency (MHz)	500.23						
Nucleus	¹ H	Number of Transients	32	Origin	avance500	Original Points Count	8192	Owner	gen		
Points Count	8192	Pulse Sequence	zg30	Receiver Gain	80.60	SW(cyclical) (Hz)	7002.80	Spectrum Type	STANDARD	Sweep Width (Hz)	7001.95
Solvent	CHLOROFORM-d	Spectrum Offset (Hz)	2691.4453	Temperature (degree C)	27.000						

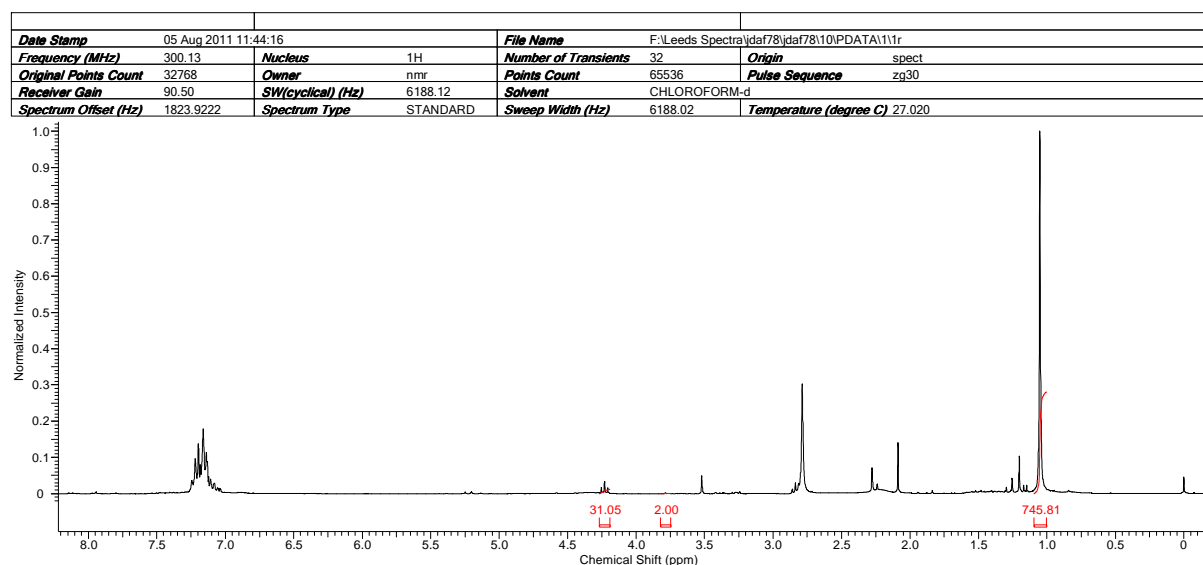


APPENDIX 24 – ¹H NMR spectrum of the product from the N-alkylation of *t*-butylamine using [RuI₂(*p*-cymene)]₂ (2)-DPEPhos as pre-catalyst (S/C=20), in CDCl₃

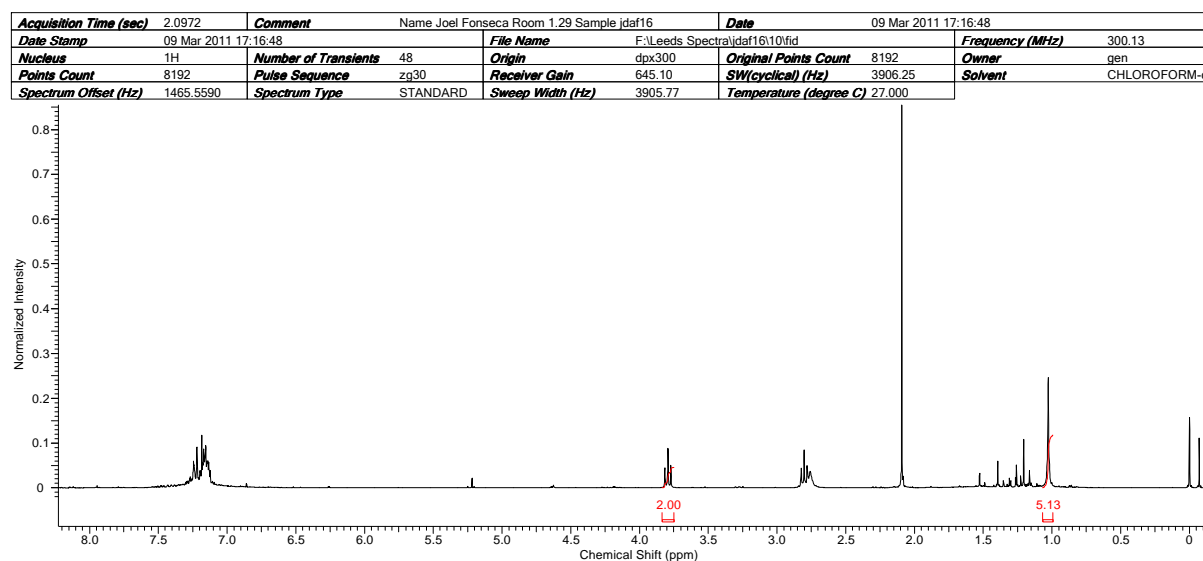
Acquisition Time (sec)	2.5166	Comment	Full Name - Joel Fonseca Room No. - 1.29 Sample - jdaf43	Date Stamp	04 Jul 2011 21:05:20		
Date	04 Jul 2011 21:05:20	File Name	F:\Leeds Spectra\jdaf43\10\PDATA\11\tr	Frequency (MHz)	500.23	Nucleus	¹ H
Number of Transients	32	Origin	avance500	Original Points Count	16384	Owner	nmr
Points Count	32768	Pulse Sequence	zg30	Receiver Gain	25.40	SW(cyclical) (Hz)	6510.42
Solvent	CHLOROFORM-d	Spectrum Offset (Hz)	2694.1929	Spectrum Type	STANDARD		
Sweep Width (Hz)	6510.22	Temperature (degree C)	27.000				



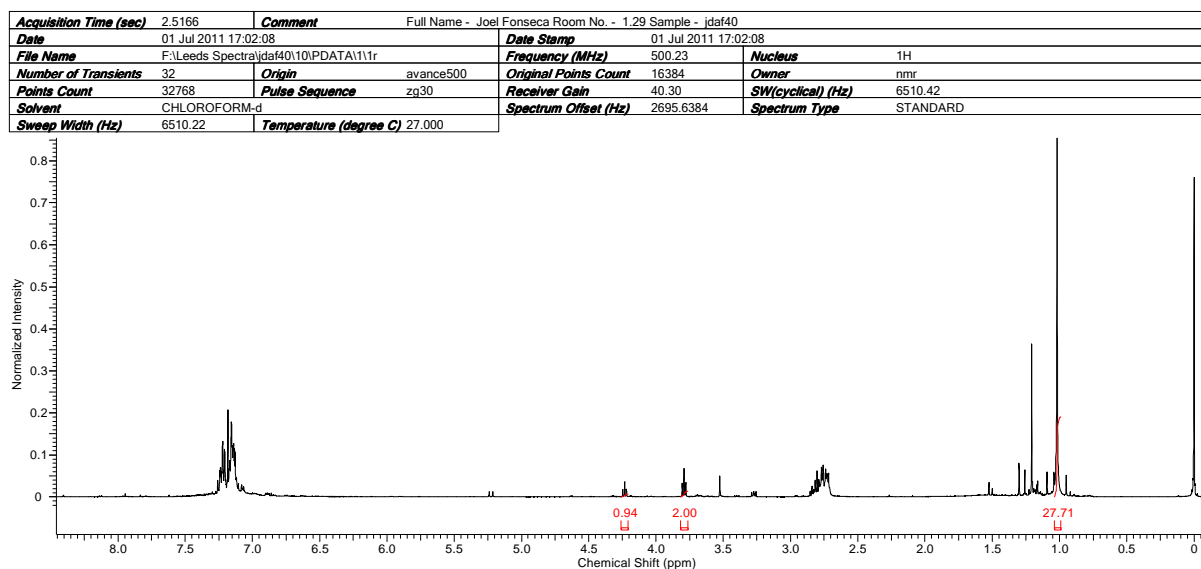
APPENDIX 25 – ¹H NMR spectrum of the product from the N-alkylation of *t*-butylamine using [RuI₂(*p*-cymene)]₂ (2)-dippf as pre-catalyst (S/C=20), in CDCl₃



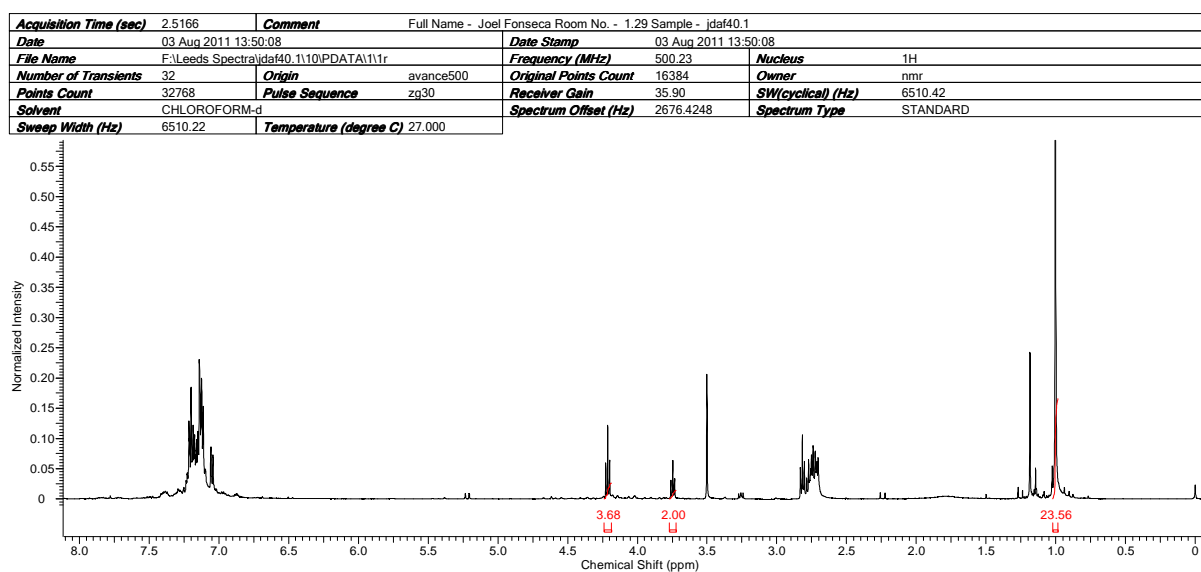
APPENDIX 26 – ¹H NMR spectrum of the product from the N-alkylation of *t*-butylamine using [RuCl(dppf)(*p*-cymene)]SbF₆ (4) as pre-catalyst (S/C=40), in CDCl₃



APPENDIX 27 – ¹H NMR spectrum of the product from the N-alkylation of *t*-butylamine using [RuCl(dppf)(*p*-cymene)]BF₄ (6) as pre-catalyst (S/C=40), in CDCl₃

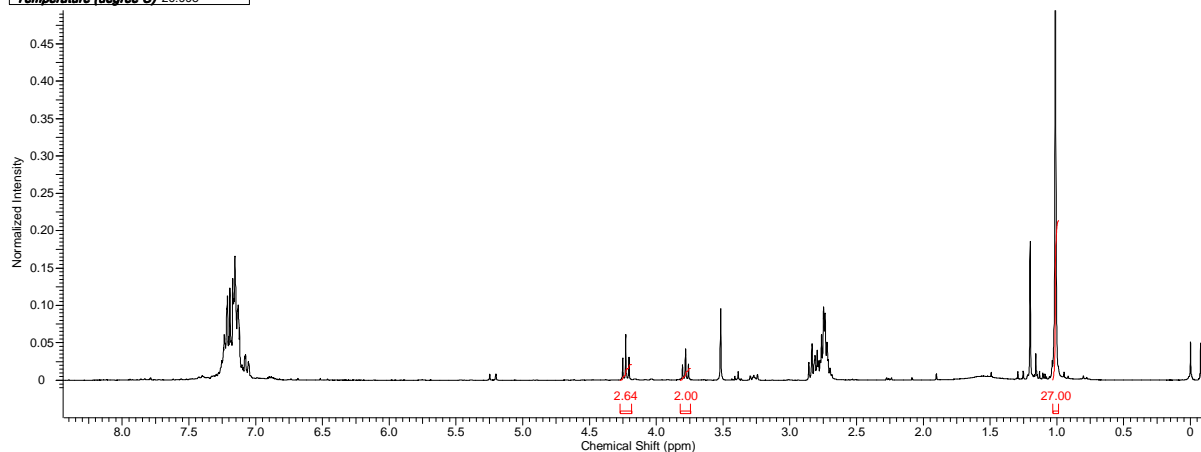


APPENDIX 28 – ¹H NMR spectrum of the product from the N-alkylation of *t*-butylamine using [RuCl(dppf)(*p*-cymene)]BF₄ (6) as pre-catalyst (S/C=20), in CDCl₃



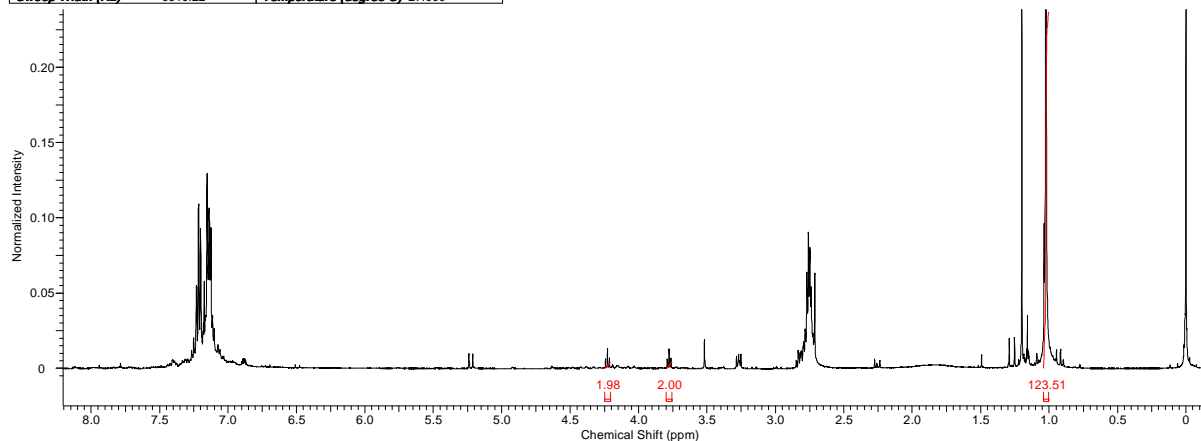
APPENDIX 29 – ¹H NMR spectrum of the product from the N-alkylation of *t*-butylamine using [RuCl(dppf)(*p*-cymene)]Cl (7) as pre-catalyst (S/C=40), in CDCl₃

Acquisition Time (sec)	5.2953	Comment	Name- Joel Fonseca Room No- 1.29 Sample- jdaf47	Date	07 Jul 2011 18:33:52				
Date Stamp	07 Jul 2011 18:33:52	File Name	F:\Leeds Spectra\jdaf47\10\PDATA\111r	Frequency (MHz)	300.13				
Nucleus	¹ H	Number of Transients	32	Origin	spect	Original Points Count	32768	Owner	nmr
Points Count	65536	Pulse Sequence	zg30	Receiver Gain	90.50	SW(cyclical) (Hz)	6188.12		
Solvent	CHLOROFORM-d	Spectrum Offset (Hz)	1821.2781	Spectrum Type	STANDARD	Sweep Width (Hz)	6188.02		
Temperature (degree C)	26.993								



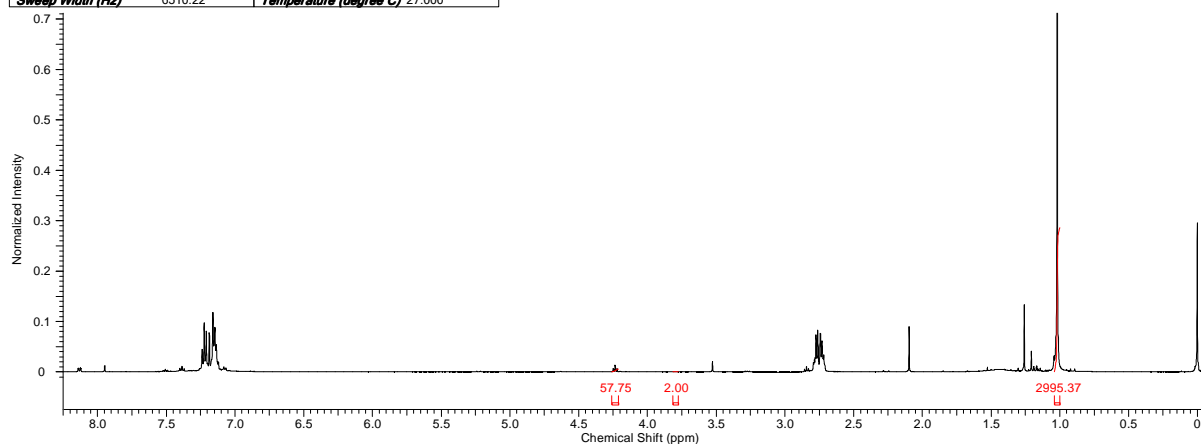
APPENDIX 30 – ¹H NMR spectrum of the product from the N-alkylation of *t*-butylamine using [RuCl(dppf)(*p*-cymene)]Cl (7) as pre-catalyst (S/C=20), in CDCl₃

Acquisition Time (sec)	2.5166	Comment	Full Name - Joel Fonseca Room No. - 1.29 Sample - idaf47.2	Date Stamp	03 Aug 2011 14:00:48		
Date	03 Aug 2011 14:00:48	File Name	F:\Leeds Spectra\jdaf47\2\10\PDATA\111r	Frequency (MHz)	500.23	Nucleus	¹ H
Number of Transients	32	Origin	avance500	Original Points Count	16384	Owner	nmr
Points Count	32768	Pulse Sequence	zg30	Receiver Gain	40.30	SW(cyclical) (Hz)	6510.42
Solvent	CHLOROFORM-d	Spectrum Offset (Hz)	2692.0771	Spectrum Type	STANDARD		
Sweep Width (Hz)	6510.22	Temperature (degree C)	27.000				



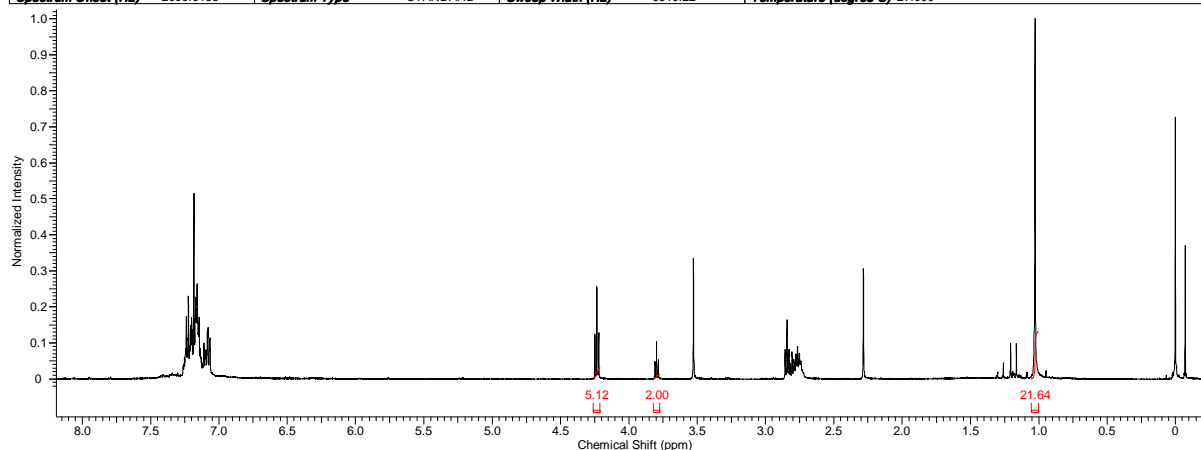
APPENDIX 31 – ¹H NMR spectrum of the product from the N-alkylation of *t*-butylamine using [Ru(dppf)(*p*-cymene)]SbF₆ (5) as pre-catalyst (S/C=40), in CDCl₃

Acquisition Time (sec)	2.5166	Comment	Full Name - Joel Fonseca Room No. - 1.29 Sample - jdaf38				
Date	01 Jul 2011 22:28:32	Date Stamp	01 Jul 2011 22:28:32				
File Name	F:\Leeds Spectra\jdaf38\10\PDATA\111r	Frequency (MHz)	500.23	Nucleus	1H		
Number of Transients	32	Origin	avance500	Original Points Count	16384	Owner	nmr
Points Count	32768	Pulse Sequence	zg30	Receiver Gain	35.90	SW(cyclical) (Hz)	6510.42
Solvent	CHLOROFORM-d	Spectrum Offset (Hz)	2698.0342	Spectrum Type	STANDARD		
Sweep Width (Hz)	6510.22	Temperature (degree C)	27.000				



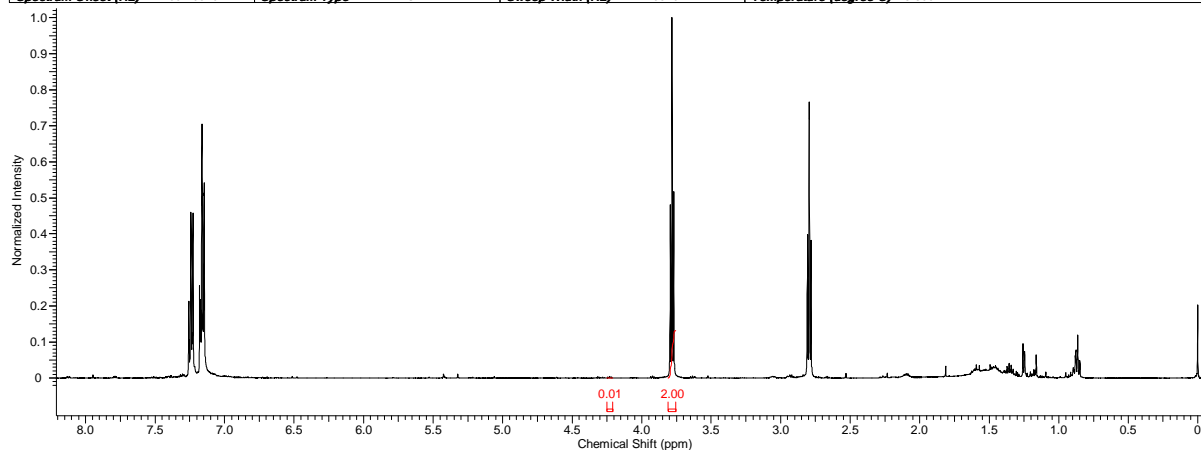
APPENDIX 32 – ¹H NMR spectrum of the product from the N-alkylation of *t*-butylamine using [Ru₂Cl₃(DPEPhos)₂(CH₃CN)₂]SbF₆ (8) as pre-catalyst (S/C=40), in CDCl₃

Acquisition Time (sec)	2.5166	Comment	Full Name - Joel Fonseca Room No. - 1.29 Sample - jdaf50		Date	14 Jul 2011 19:03:44	
Date Stamp	14 Jul 2011 19:03:44	File Name	F:\Leeds Spectra\jdaf50\10\PDATA\111r				
Frequency (MHz)	500.23	Nucleus	1H	Number of Transients	32	Origin	avance500
Original Points Count	16384	Owner	nmr	Points Count	32768	Pulse Sequence	zg30
Receiver Gain	228.10	SW(cyclical) (Hz)	6510.42	Solvent	CHLOROFORM-d		
Spectrum Offset (Hz)	2695.6133	Spectrum Type	STANDARD	Sweep Width (Hz)	6510.22	Temperature (degree C)	27.000



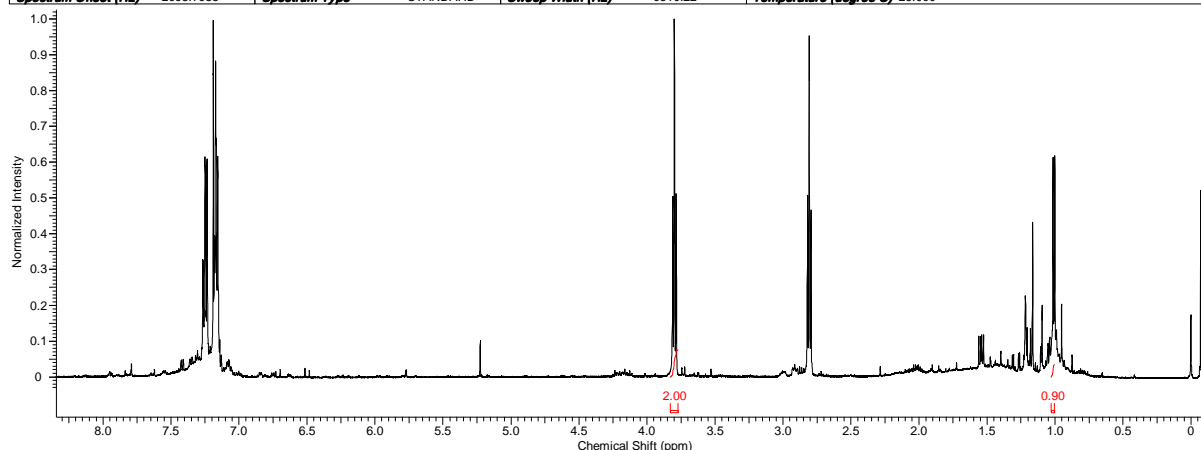
APPENDIX 33 – ¹H NMR spectrum of the product from the N-alkylation of *t*-butylamine using [Ru(P(*n*-Bu)₃)₂(*p*-cymene)]SbF₆ (10) as pre-catalyst (S/C=40), in CDCl₃

Acquisition Time (sec)	2.5166	Comment	Full Name - Joel Fonseca Room No. - 1.29 Sample - jdaf34	Date	28 Jun 2011 18:08:16
Date Stamp	28 Jun 2011 18:08:16		File Name	F:\Leeds Spectra\jdaf34\10\PDATA\111r	
Frequency (MHz)	500.23	Nucleus	¹ H	Number of Transients	32
Original Points Count	16384	Owner	nmr	Points Count	32768
Receiver Gain	90.50	SW(cyclical) (Hz)	6510.42	Solvent	CHLOROFORM-d
Spectrum Offset (Hz)	2694.6929	Spectrum Type	STANDARD	Sweep Width (Hz)	6510.22
				Temperature (degree C)	23.800

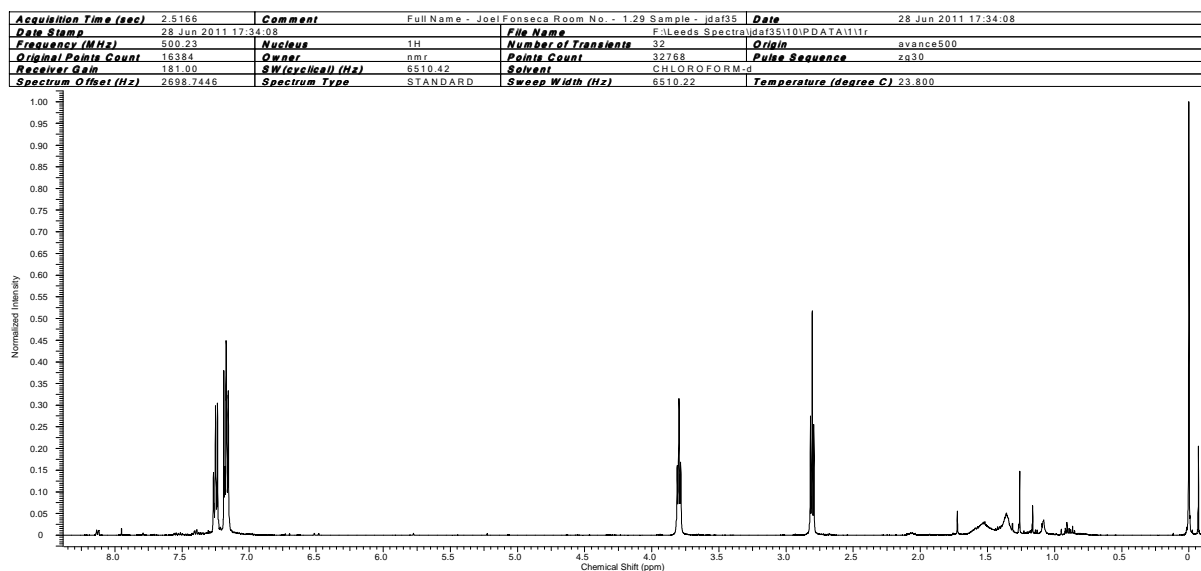


APPENDIX 34 – ¹H NMR spectrum of the product from the N-alkylation of *t*-butylamine using [RuCl(P(*i*-Bu)₃)₂(*p*-cymene)]SbF₆ (11) as pre-catalyst (S/C=40), in CDCl₃

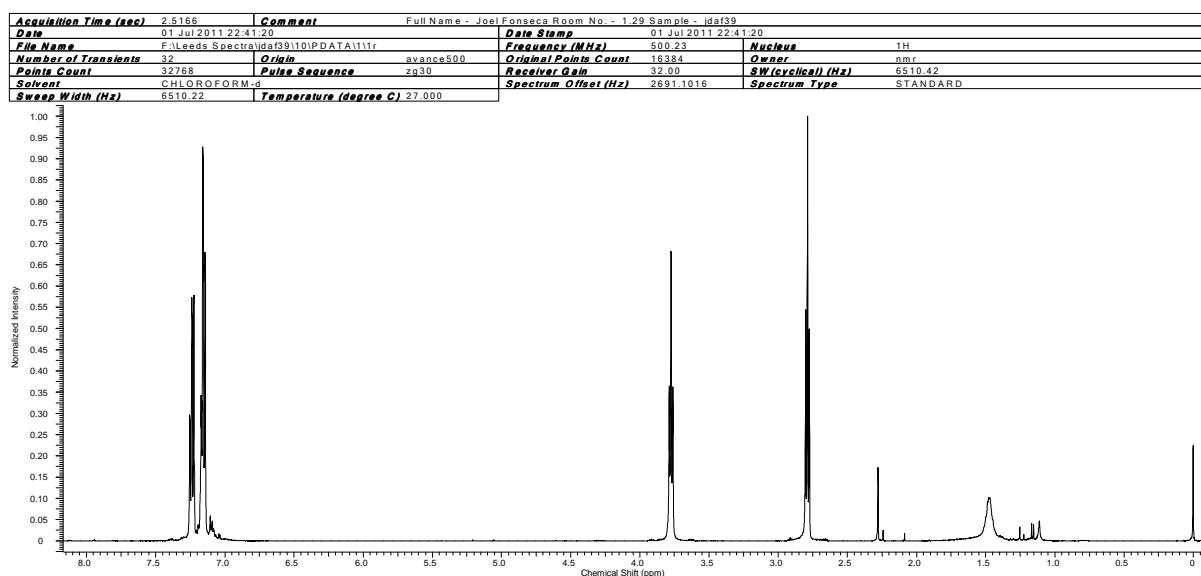
Acquisition Time (sec)	2.5166	Comment	Full Name - Joel Fonseca Room No. - 1.29 Sample - idaf32	Date	23 Jun 2011 16:38:40
Date Stamp	23 Jun 2011 16:38:40		File Name	F:\Leeds Spectra\idaf32\10\PDATA\111r	
Frequency (MHz)	500.23	Nucleus	¹ H	Number of Transients	32
Original Points Count	16384	Owner	nmr	Points Count	32768
Receiver Gain	228.10	SW(cyclical) (Hz)	6510.42	Solvent	CHLOROFORM-d
Spectrum Offset (Hz)	2698.7988	Spectrum Type	STANDARD	Sweep Width (Hz)	6510.22
				Temperature (degree C)	25.000



APPENDIX 35 – ¹H NMR spectrum of the product from the N-alkylation of *t*-butylamine using [RuCl₂(P(*n*-Bu)₃)₂(*p*-cymene)] (13) as pre-catalyst (S/C=40), in CDCl₃

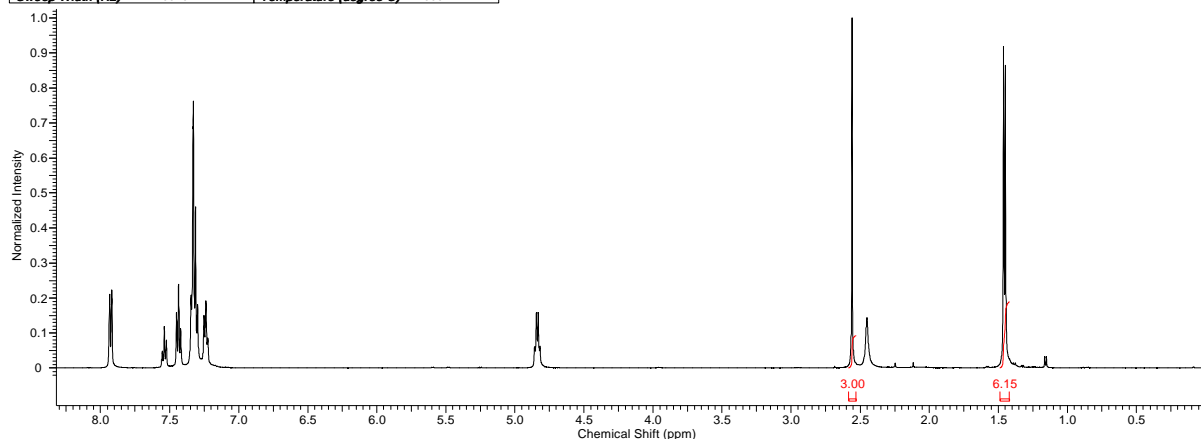


APPENDIX 36 – ¹H NMR spectrum of the product from the N-alkylation of *t*-butylamine using [RuCl(P(CH₃)₃)₂(*p*-cymene)]SbF₆ (14) as pre-catalyst (S/C=40), in CDCl₃



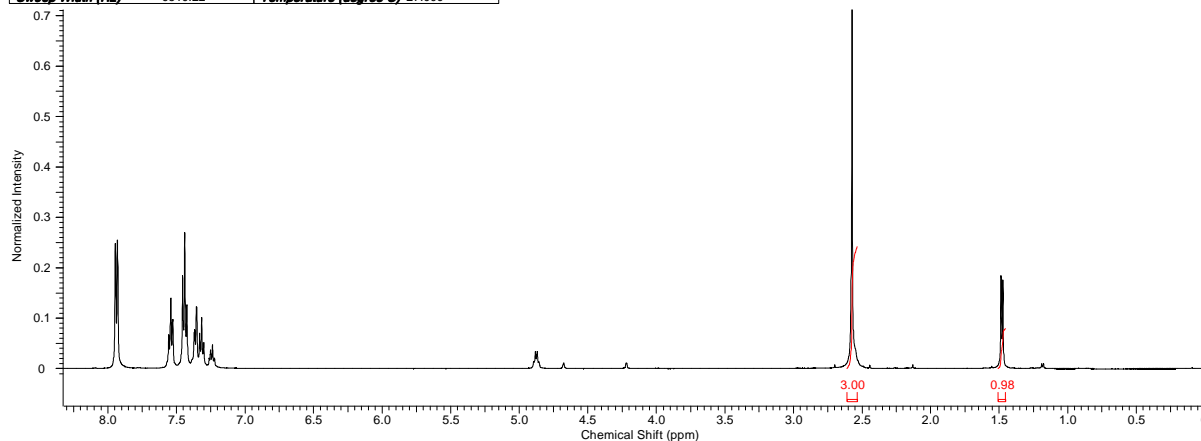
APPENDIX 37 – ¹H NMR spectrum of the product from the reduction of acetophenone using [RuCl₂(*p*-cymene)]₂ (1) as pre-catalyst, in CDCl₃

Acquisition Time (sec)	2.5166	Comment	Full Name - Joel Fonseca Room No. - 1.29 Sample - jdaf59		
Date	22 Jul 2011 21:43:44	Date Stamp	22 Jul 2011 21:43:44		
File Name	F:\Leeds Spectra\jdaf59\10\PDATA\11r	Frequency (MHz)	500.23	Nucleus	1H
Number of Transients	32	Origin	avance500	Owner	nmr
Points Count	32768	Pulse Sequence	zg30	Receiver Gain	35.90
Solvent	CHLOROFORM-d	Spectrum Offset (Hz)	2721.8958	SW(cyclical) (Hz)	6510.42
Sweep Width (Hz)	6510.22	Temperature (degree C)	27.000	Spectrum Type	STANDARD

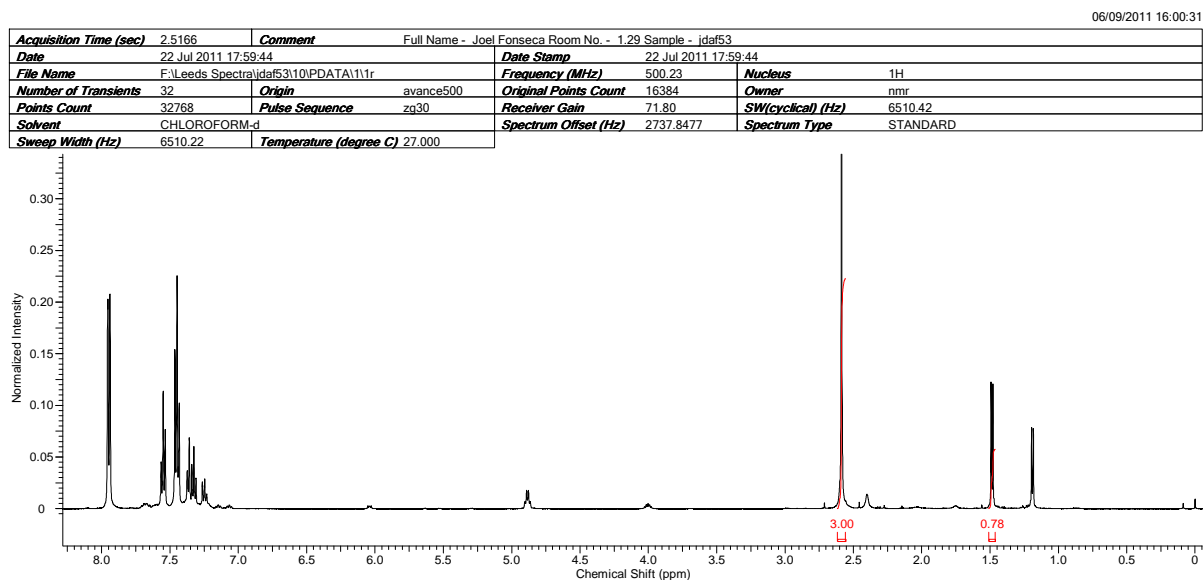


APPENDIX 38 – ¹H NMR spectrum of the product from the reduction of acetophenone using [RuCl₂(*p*-cymene)]₂ (1)-dppf as pre-catalyst, in CDCl₃

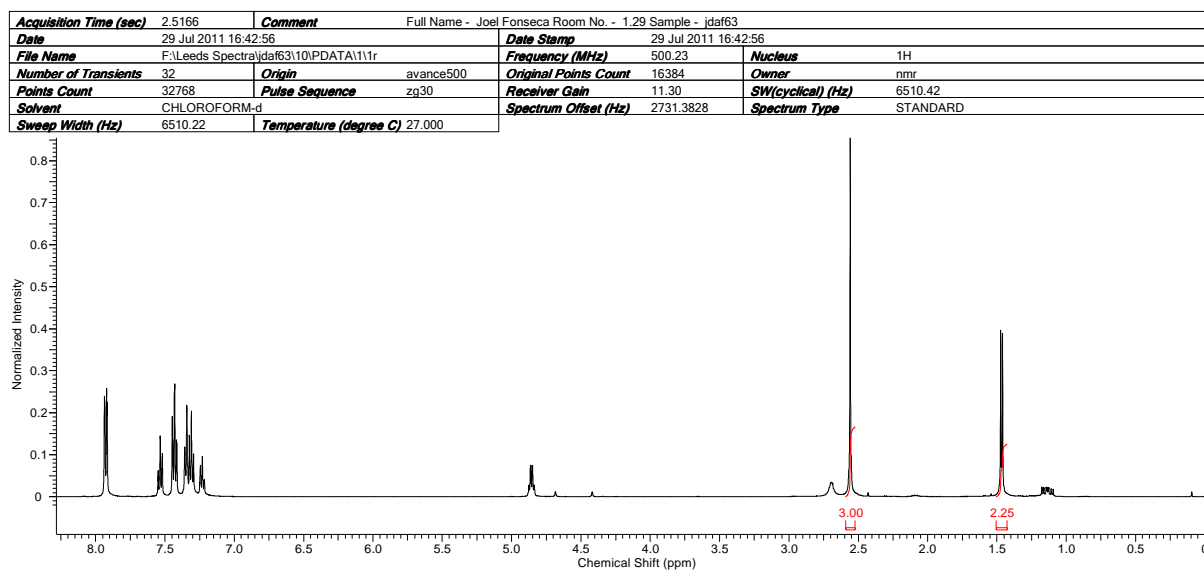
Acquisition Time (sec)	2.5166	Comment	Full Name - Joel Fonseca Room No. - 1.29 Sample - jdaf54		
Date	22 Jul 2011 18:10:24	Date Stamp	22 Jul 2011 18:10:24		
File Name	F:\Leeds Spectra\jdaf54\10\PDATA\11r	Frequency (MHz)	500.23	Nucleus	1H
Number of Transients	32	Origin	avance500	Owner	nmr
Points Count	32768	Pulse Sequence	zg30	Receiver Gain	35.90
Solvent	CHLOROFORM-d	Spectrum Offset (Hz)	2736.3616	SW(cyclical) (Hz)	6510.42
Sweep Width (Hz)	6510.22	Temperature (degree C)	27.000	Spectrum Type	STANDARD



APPENDIX 39 – ¹H NMR spectrum of the product from the reduction of acetophenone using [RuCl₂(*p*-cymene)]₂ (1)-DPEPhos as pre-catalyst, in CDCl₃

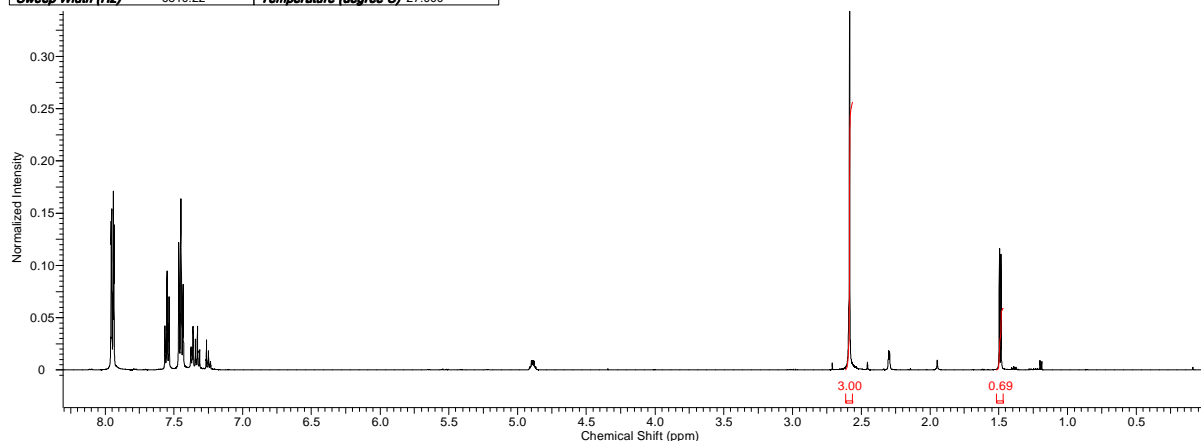


APPENDIX 40 – ¹H NMR spectrum of the product from the reduction of acetophenone using [RuCl₂(*p*-cymene)]₂ (1)-dippf as pre-catalyst, in CDCl₃



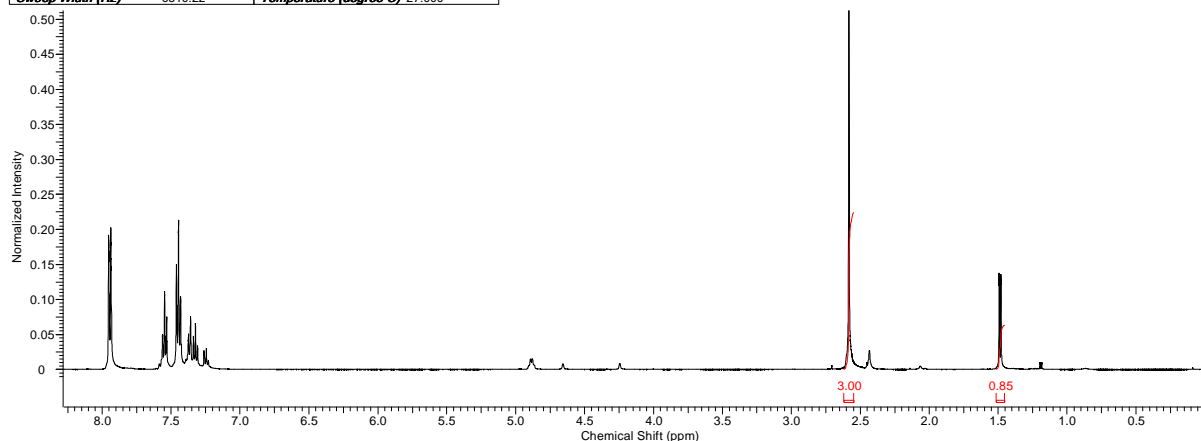
APPENDIX 41 – ¹H NMR spectrum of the product from the reduction of acetophenone using [Ru₂(*p*-cymene)]₂ (2) as pre-catalyst, in CDCl₃

Acquisition Time (sec)	2.5166	Comment	Full Name - Joel Fonseca Room No. - 1.29 Sample - jdaf60		
Date	22 Jul 2011 22:05:04	Date Stamp	22 Jul 2011 22:05:04		
File Name	F:\Leeds Spectra\jdaf60\10\PDATA\1\1r	Frequency (MHz)	500.23	Nucleus	1H
Number of Transients	32	Origin	avance500	Owner	nmr
Points Count	32768	Pulse Sequence	zg30	Receiver Gain	71.80
Solvent	CHLOROFORM-d	Spectrum Offset (Hz)	2737.0022	SW(cyclical) (Hz)	6510.42
Sweep Width (Hz)	6510.22	Temperature (degree C)	27.000		

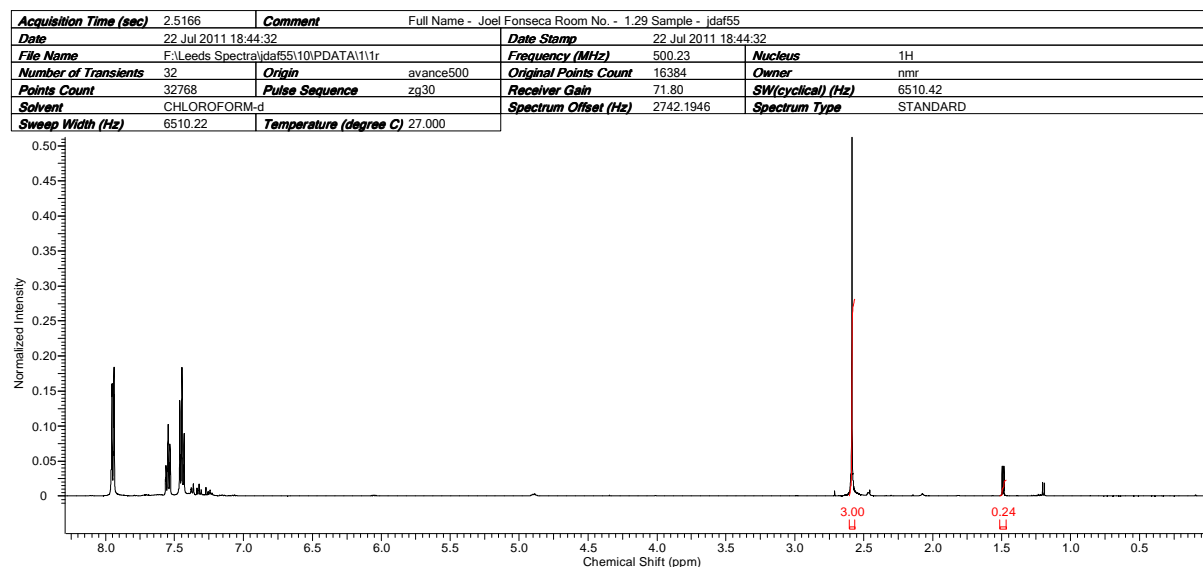


APPENDIX 42 – ¹H NMR spectrum of the product from the reduction of acetophenone using [Ru₂(*p*-cymene)]₂-dppf as pre-catalyst, in CDCl₃

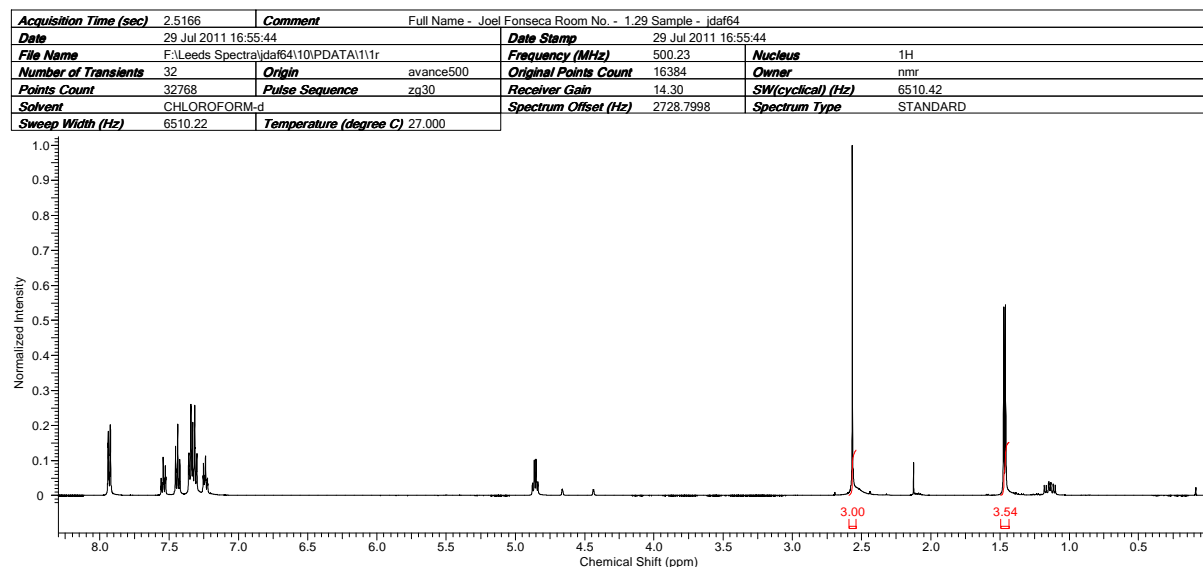
Acquisition Time (sec)	2.5166	Comment	Full Name - Joel Fonseca Room No. - 1.29 Sample - jdaf56		
Date	22 Jul 2011 19:33:36	Date Stamp	22 Jul 2011 19:33:36		
File Name	F:\Leeds Spectra\jdaf56\10\PDATA\1\1r	Frequency (MHz)	500.23	Nucleus	1H
Number of Transients	32	Origin	avance500	Owner	nmr
Points Count	32768	Pulse Sequence	zg30	Receiver Gain	71.80
Solvent	CHLOROFORM-d	Spectrum Offset (Hz)	2736.8821	SW(cyclical) (Hz)	6510.42
Sweep Width (Hz)	6510.22	Temperature (degree C)	27.000		



APPENDIX 43 – ¹H NMR spectrum of the product from the reduction of acetophenone using [RuI₂(*p*-cymene)]₂ (2)-DPEPhos as pre-catalyst, in CDCl₃



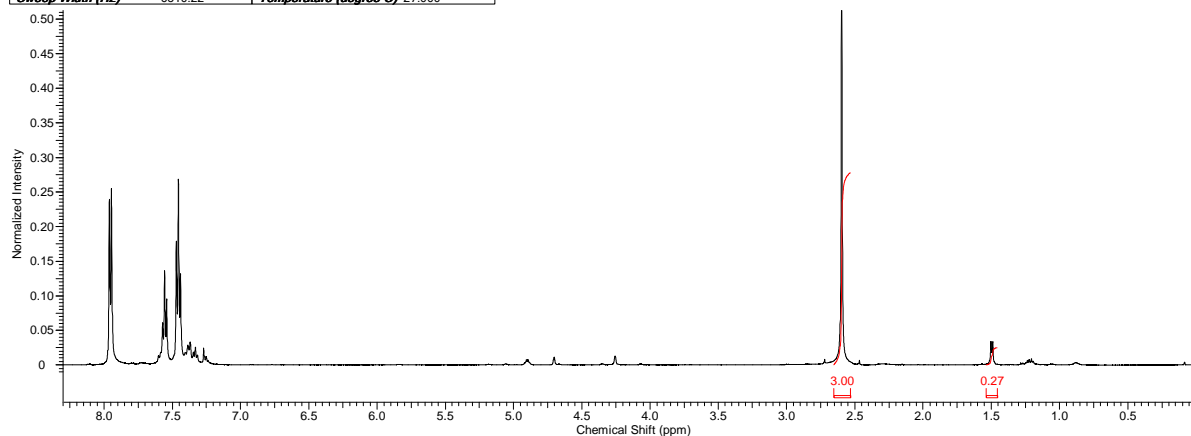
APPENDIX 44 – ¹H NMR spectrum of the product from the reduction of acetophenone using [RuI₂(*p*-cymene)]₂ (2)-dippf as pre-catalyst, in CDCl₃



APPENDIX 45 – ¹H NMR spectrum of the product from the reduction of acetophenone using [RuCl(dppf)(*p*-cymene)]Cl (7) as pre-catalyst, in CDCl₃

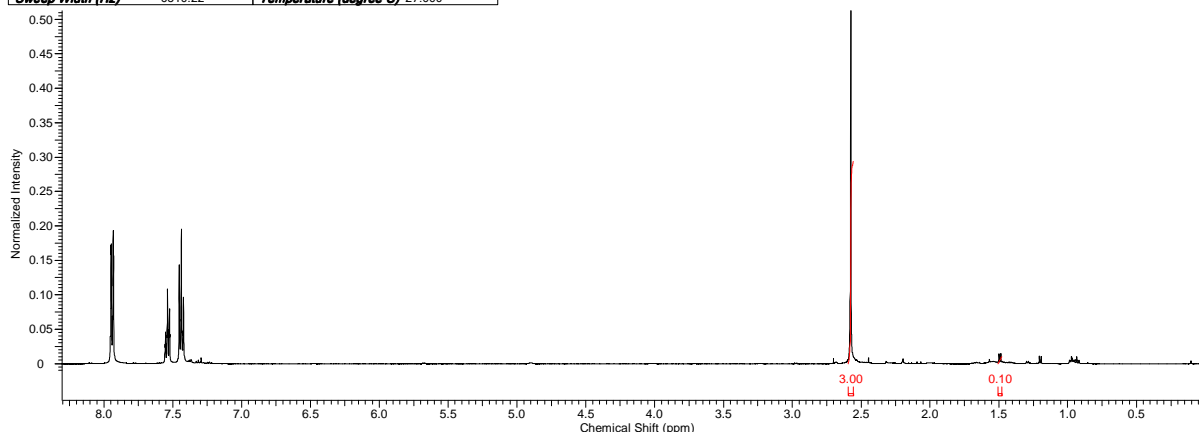
06/09/2011 18:43:13

Acquisition Time (sec)	2.5166	Comment	Full Name - Joel Fonseca Room No. - 1.29 Sample - idaf57	Date Stamp	22 Jul 2011 20:14:08		
Date	22 Jul 2011 20:14:08	File Name	F:\Leeds Spectra\idaf57\10\PDATA\111r	Frequency (MHz)	500.23	Nucleus	¹ H
Number of Transients	32	Origin	avance500	Original Points Count	16384	Owner	nmr
Points Count	32768	Pulse Sequence	zg30	Receiver Gain	71.80	SW(cyclical) (Hz)	6510.42
Solvent	CHLOROFORM-d	Spectrum Offset (Hz)	2740.3235	Spectrum Type	STANDARD		
Sweep Width (Hz)	6510.22	Temperature (degree C)	27.000				



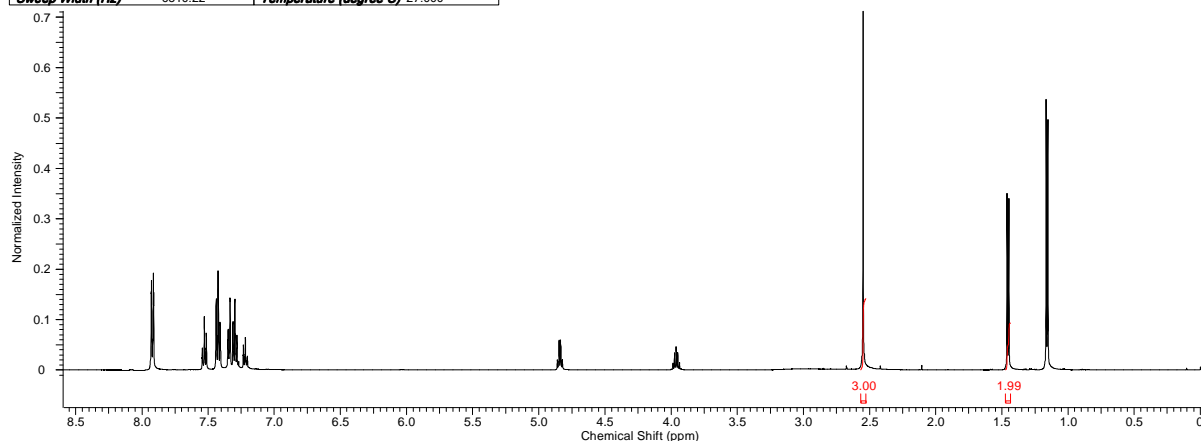
APPENDIX 46 – ¹H NMR spectrum of the product from the reduction of acetophenone using [RuI(P(*n*-Bu)₃)₂(*p*-cymene)]SbF₆ (10) as pre-catalyst, in CDCl₃

Acquisition Time (sec)	2.5166	Comment	Full Name - Joel Fonseca Room No. - 1.29 Sample - idaf58	Date Stamp	22 Jul 2011 21:30:56		
Date	22 Jul 2011 21:30:56	File Name	F:\Leeds Spectra\idaf58\10\PDATA\111r	Frequency (MHz)	500.23	Nucleus	¹ H
Number of Transients	32	Origin	avance500	Original Points Count	16384	Owner	nmr
Points Count	32768	Pulse Sequence	zg30	Receiver Gain	71.80	SW(cyclical) (Hz)	6510.42
Solvent	CHLOROFORM-d	Spectrum Offset (Hz)	2752.8691	Spectrum Type	STANDARD		
Sweep Width (Hz)	6510.22	Temperature (degree C)	27.000				



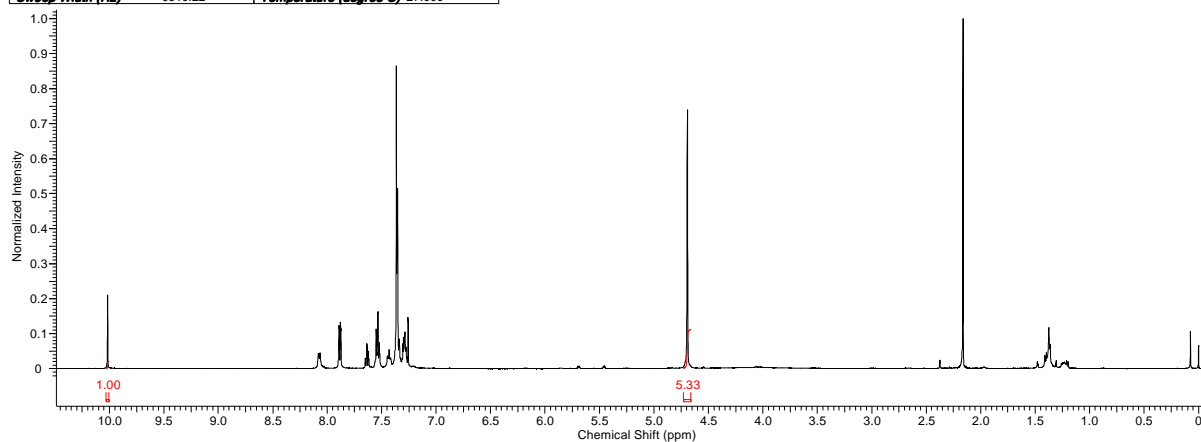
APPENDIX 47 – ¹H NMR spectrum of the product from the reduction of acetophenone using [Ru₂Cl₃(DPEPhos)₂(CH₃CN)₂]SbF₆ (8) as pre-catalyst, in CDCl₃

Acquisition Time (sec)	2.5166	Comment	Full Name - Joel Fonseca Room No. - 1.29 Sample - idaf52		
Date	22 Jul 2011 17:46:56	Date Stamp	22 Jul 2011 17:46:56		
File Name	F:\Leeds Spectra\idaf52\10\PDATA\1\1r	Frequency (MHz)	500.23	Nucleus	1H
Number of Transients	32	Origin	avance500	Owner	nmr
Points Count	32768	Pulse Sequence	zg30	Receiver Gain	22.60
Solvent	CHLOROFORM-d	Spectrum Offset (Hz)	2740.5139	SW(cyclical) (Hz)	6510.42
Sweep Width (Hz)	6510.22	Temperature (degree C)	27.000	Spectrum Type	STANDARD



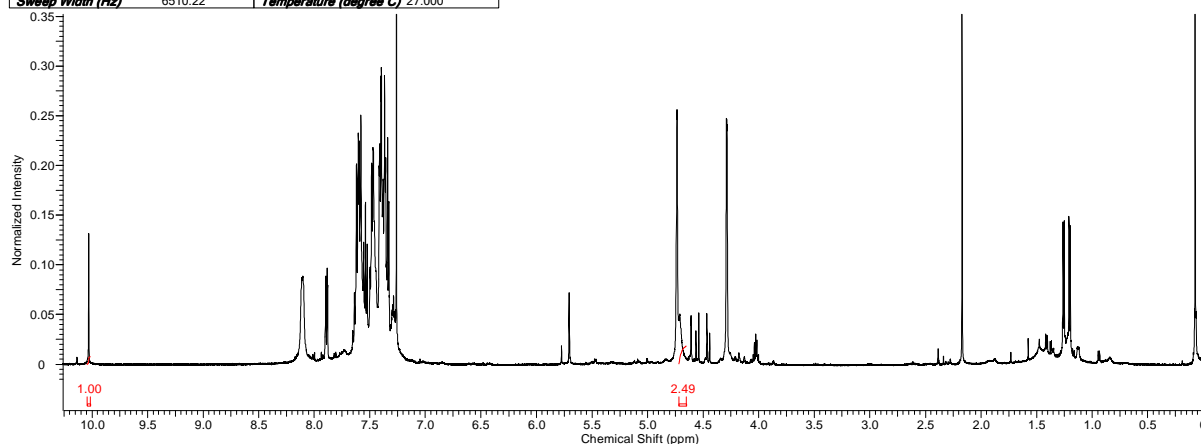
APPENDIX 48 – ¹H NMR spectrum of the product from the reduction of benzaldehyde using [RuCl₂(*p*-cymene)]₂ (1) as pre-catalyst, in CDCl₃

Acquisition Time (sec)	2.5166	Comment	Full Name - Joel Fonseca Room No. - 1.29 Sample - idaf72		
Date	29 Jul 2011 20:31:12	Date Stamp	29 Jul 2011 20:31:12		
File Name	F:\Leeds Spectra\idaf72\10\PDATA\1\1r	Frequency (MHz)	500.23	Nucleus	1H
Number of Transients	32	Origin	avance500	Owner	nmr
Points Count	32768	Pulse Sequence	zg30	Receiver Gain	35.90
Solvent	CHLOROFORM-d	Spectrum Offset (Hz)	2734.1643	SW(cyclical) (Hz)	6510.42
Sweep Width (Hz)	6510.22	Temperature (degree C)	27.000	Spectrum Type	STANDARD



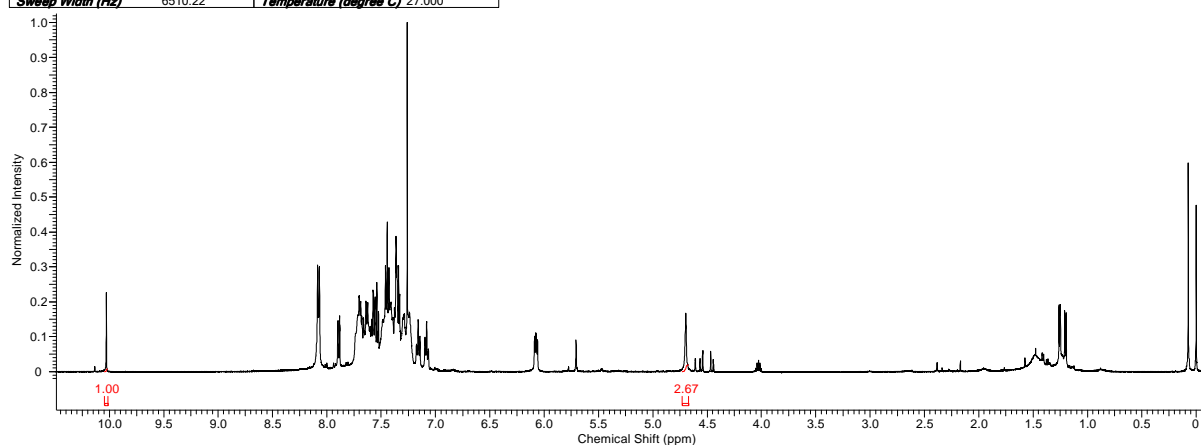
APPENDIX 49 – ¹H NMR spectrum of the product from the reduction of benzaldehyde using [RuCl₂(*p*-cymene)]₂ (1)-dppf as pre-catalyst, in CDCl₃

Acquisition Time (sec)	2.5166	Comment	Full Name - Joel Fonseca Room No. - 1.29 Sample - jdaf67		
Date	29 Jul 2011 17:57:36	Date Stamp	29 Jul 2011 17:57:36		
File Name	F:\Leeds Spectra\jdaf67\10\PDATA\1\1r	Frequency (MHz)	500.23	Nucleus	1H
Number of Transients	32	Origin	avance500	Owner	nmr
Points Count	32768	Pulse Sequence	zg30	Receiver Gain	71.80
Solvent	CHLOROFORM-d	Spectrum Offset (Hz)	2735.1577	SW(cyclical) (Hz)	6510.42
Sweep Width (Hz)	6510.22	Temperature (degree C)	27.000	Spectrum Type	STANDARD



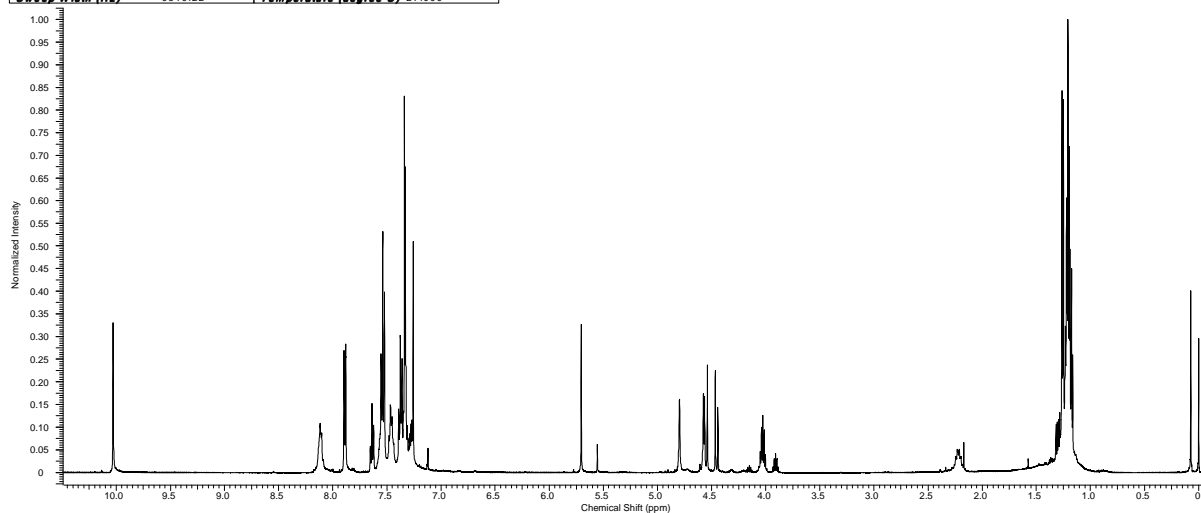
APPENDIX 50 – ¹H NMR spectrum of the product from the reduction of benzaldehyde using [RuCl₂(*p*-cymene)]₂ (1)-DPEPhos as pre-catalyst, in CDCl₃

Acquisition Time (sec)	2.5166	Comment	Full Name - Joel Fonseca Room No. - 1.29 Sample - jdaf66		
Date	29 Jul 2011 17:46:56	Date Stamp	29 Jul 2011 17:46:56		
File Name	F:\Leeds Spectra\jdaf66\10\PDATA\1\1r	Frequency (MHz)	500.23	Nucleus	1H
Number of Transients	32	Origin	avance500	Owner	nmr
Points Count	32768	Pulse Sequence	zg30	Receiver Gain	71.80
Solvent	CHLOROFORM-d	Spectrum Offset (Hz)	2734.9590	SW(cyclical) (Hz)	6510.42
Sweep Width (Hz)	6510.22	Temperature (degree C)	27.000	Spectrum Type	STANDARD



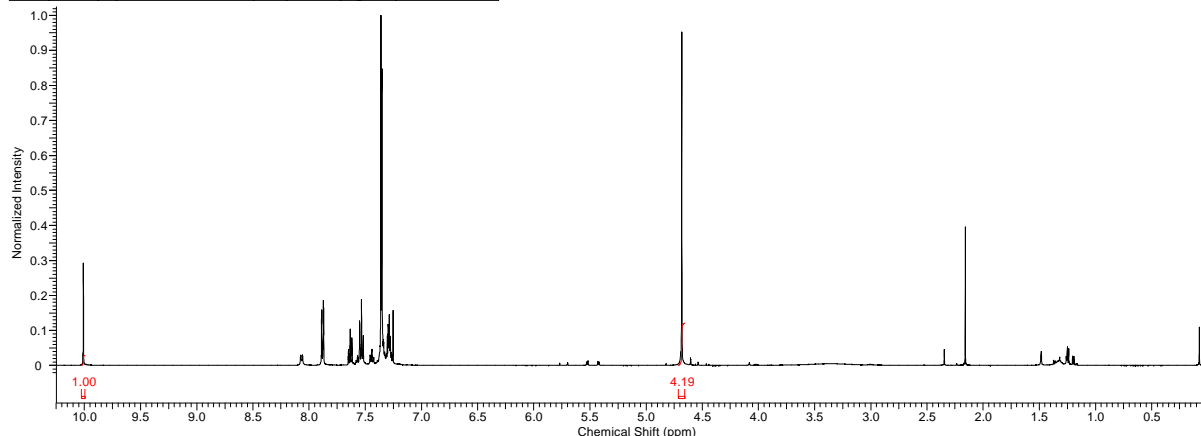
APPENDIX 51 – ¹H NMR spectrum of the product from the reduction of benzaldehyde using [RuCl₂(*p*-cymene)]₂ (1)-dippf as pre-catalyst, in CDCl₃

Acquisition Time (sec)	2.5166	Comment	Full Name - Joel Fonseca Room No. - 1.29 Sample - idaf74		
Date	29 Jul 2011 20:41:52	Date Stamp	29 Jul 2011 20:41:52		
File Name	F:\Leeds Spectra\idaf74\10\PDATA\1\1tr	Frequency (MHz)	500.23	Nucleus	1H
Number of Transients	32	Origin	avance500	Original Points Count	16384
Points Count	32768	Pulse Sequence	zg30	Receiver Gain	40.30
Solvent	CHLOROFORM-d	Spectrum Offset (Hz)	2734.1643	SW (cyclical) (Hz)	6510.42
Sweep Width (Hz)	6510.22	Temperature (degree C)	27.000	Spectrum Type	STANDARD



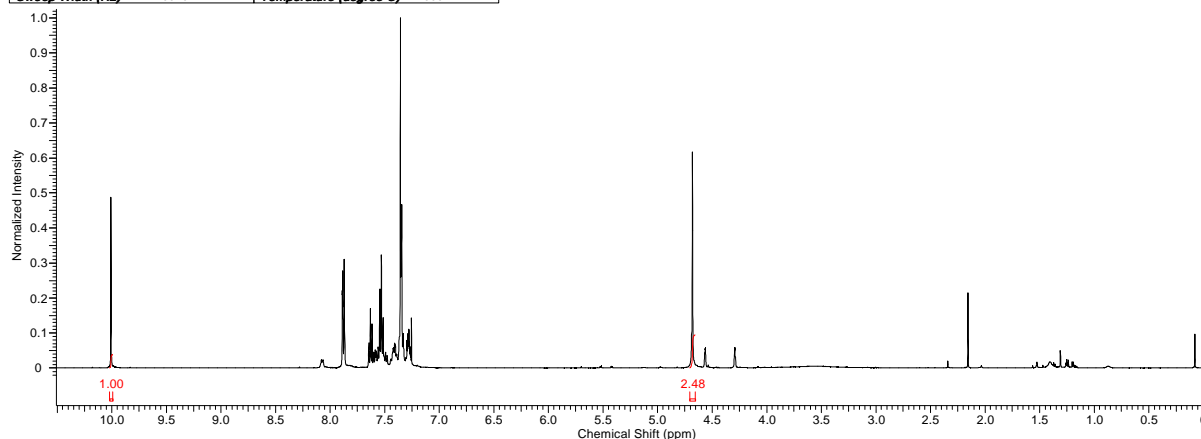
APPENDIX 52 – ¹H NMR spectrum of the product from the reduction of benzaldehyde using [RuI₂(*p*-cymene)]₂ (2) as pre-catalyst, in CDCl₃

Acquisition Time (sec)	2.5166	Comment	Full Name - Joel Fonseca Room No. - 1.29 Sample - idaf73		
Date	29 Jul 2011 22:37:04	Date Stamp	29 Jul 2011 22:37:04		
File Name	F:\Leeds Spectra\idaf73\10\PDATA\1\1tr	Frequency (MHz)	500.23	Nucleus	1H
Number of Transients	32	Origin	avance500	Original Points Count	16384
Points Count	32768	Pulse Sequence	zg30	Receiver Gain	35.90
Solvent	CHLOROFORM-d	Spectrum Offset (Hz)	2732.1775	SW (cyclical) (Hz)	6510.42
Sweep Width (Hz)	6510.22	Temperature (degree C)	27.000	Spectrum Type	STANDARD



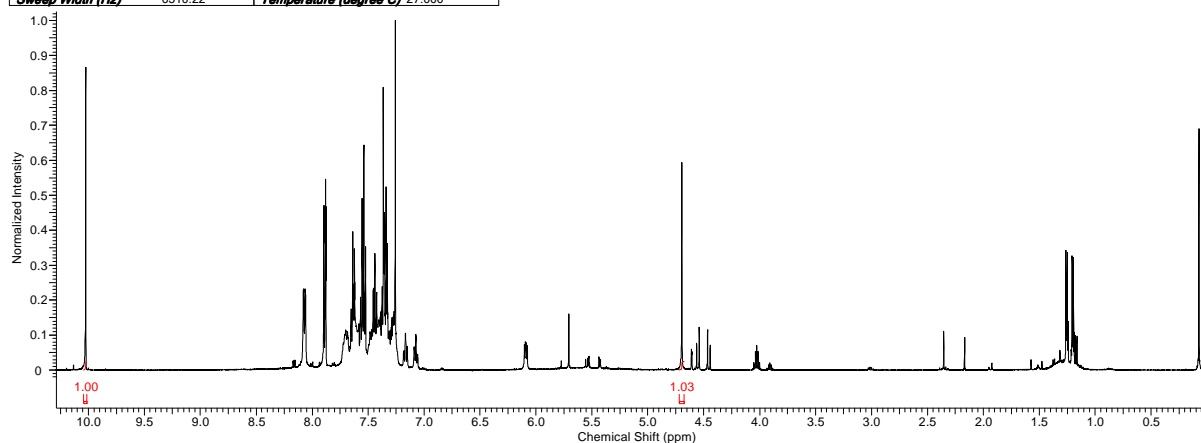
APPENDIX 53 – ¹H NMR spectrum of the product from the reduction of benzaldehyde using [Ru₂(*p*-cymene)]₂ (2)-dppf as pre-catalyst, in CDCl₃

Acquisition Time (sec)	2.5166	Comment	Full Name - Joel Fonseca Room No. - 1.29 Sample - jdaf69		
Date	29 Jul 2011 18:21:04	Date Stamp	29 Jul 2011 18:21:04		
File Name	F:\Leeds Spectra\jdaf69\10\PDATA\11r	Frequency (MHz)	500.23	Nucleus	1H
Number of Transients	32	Origin	avance500	Owner	nmr
Points Count	32768	Pulse Sequence	zg30	Receiver Gain	32.00
Solvent	CHLOROFORM-d	Spectrum Offset (Hz)	2732.7734	SW(cyclical) (Hz)	6510.42
Sweep Width (Hz)	6510.22	Temperature (degree C)	27.000	Spectrum Type	STANDARD



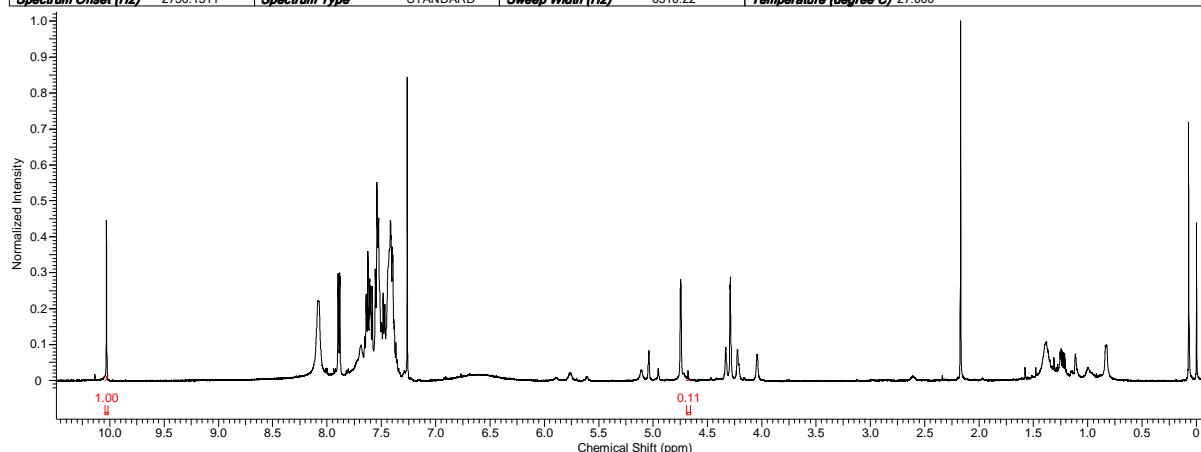
APPENDIX 54 – ¹H NMR spectrum of the product from the reduction of benzaldehyde using [Ru₂(*p*-cymene)]₂ (2)-DPEPhos as pre-catalyst, in CDCl₃

Acquisition Time (sec)	2.5166	Comment	Full Name - Joel Fonseca Room No. - 1.29 Sample - jdaf68		
Date	29 Jul 2011 18:10:24	Date Stamp	29 Jul 2011 18:10:24		
File Name	F:\Leeds Spectra\jdaf68\10\PDATA\11r	Frequency (MHz)	500.23	Nucleus	1H
Number of Transients	32	Origin	avance500	Owner	nmr
Points Count	32768	Pulse Sequence	zg30	Receiver Gain	71.80
Solvent	CHLOROFORM-d	Spectrum Offset (Hz)	2734.3630	SW(cyclical) (Hz)	6510.42
Sweep Width (Hz)	6510.22	Temperature (degree C)	27.000	Spectrum Type	STANDARD



APPENDIX 55 – ¹H NMR spectrum of the product from the reduction of benzaldehyde using [RuCl(dppf)(*p*-cymene)]Cl (7) as pre-catalyst, in CDCl₃

Acquisition Time (sec)	2.5166	Comment	Full Name - Joel Fonseca Room No. - 1.29 Sample - jda70		Date	29 Jul 2011 20:09:52	
Date Stamp	29 Jul 2011 20:09:52	File Name	F:\Leeds Spectra\jda70\10\PDATA\11r				
Frequency (MHz)	500.23	Nucleus	1H	Number of Transients	32	Origin	avance500
Original Points Count	16384	Owner	nmr	Points Count	32768	Pulse Sequence	zg30
Receiver Gain	114.00	SW(cyclical) (Hz)	6510.42	Solvent	CHLOROFORM-d		
Spectrum Offset (Hz)	2736.1511	Spectrum Type	STANDARD	Sweep Width (Hz)	6510.22	Temperature (degree C)	27.000



APPENDIX 56 – ¹H NMR spectrum of the product from the reduction of benzaldehyde using [RuI(P(*n*-Bu)₃)₂(*p*-cymene)]SbF₆ (10) as pre-catalyst, in CDCl₃

Acquisition Time (sec)	2.5166	Comment	Full Name - Joel Fonseca Room No. - 1.29 Sample - jda71				
Date	29 Jul 2011 20:20:32	Date Stamp	29 Jul 2011 20:20:32				
File Name	F:\Leeds Spectra\jda71\10\PDATA\11r	Frequency (MHz)	500.23	Nucleus	1H		
Number of Transients	32	Origin	avance500	Original Points Count	16384	Owner	nmr
Points Count	32768	Pulse Sequence	zg30	Receiver Gain	71.80	SW(cyclical) (Hz)	6510.42
Solvent	CHLOROFORM-d	Spectrum Offset (Hz)	2738.9326	Spectrum Type	STANDARD		
Sweep Width (Hz)	6510.22	Temperature (degree C)	27.000				

